Spin-Probe Studies. I. Applications to Latexes and Micelle Characterization

GARY PAUL RABOLD, *Radiochemistry Research Laboratory,*
The Dow Chemical Company, Midland, Michigan 48640

Synopsis

The interaction of sodium dodecyl sulfate (NaDS) with styrene–butadiene latexes was investigated by application of the recently developed spin-probe technique. It is possible by this method to detect the presence of micelles in a latex reasonably quantitatively. The effective surface area occupied per molecule of soap was calculated to be 53 Å². Differences in purity can readily be detected for several NaDS samples. The less pure samples show a lower critical micelle concentration (CMC) and a significantly more ordered micelle structure. The addition of hexane to NaDS solutions above the CMC leads to a greater immobilization of the spin probe. This is interpreted as reflecting a tighter packing of the soap molecules. The addition of ethanol, acetic acid, and acrylic acid leads to a looser association of the probe with the micelles. The micelles catalyze the decomposition of the nitroxide probe in the presence of organic acids. The aggregation of sodium deoxycholate was also conveniently followed by the spin-probe method.

INTRODUCTION

The spin-label technique was first introduced by McConnell and co-workers[1] in 1965. It has since been applied to a wide variety of problems, concerned mostly with biological macromolecules, where questions of binding and of conformational changes have been of interest.[2-4] The essence of the technique is that one is able to study the motion of a free radical in its microscopic environment by electron spin resonance (ESR) spectroscopy. Those free radicals which have proved most suitable for such use are organic nitroxides which have the essential moiety (I) in their overall structures. The nitroxide group possesses the paramagnetism

I
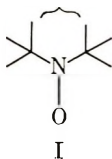
which enables one to employ ESR, while the adjacent *gem*-dimethyl substituents confer an extremely high degree of stability upon the molecule. The list of nitroxides reported in the literature is rapidly increasing, as different areas of application necessitate specific syntheses.

The calculated relation between the molecular motion of the nitroxide and the shape of its ESR spectrum has been treated in detail in the literature.[2–6] For our purposes it is sufficient to note that under the proper conditions one may calculate the value of τ_c, the rotational correlation time. The value of τ_c can be thought of as the time required for the nitroxide to rotate through an angle of one radian. Equations (1) and (2) are abbreviated expressions of the more detailed equations for calculating the rotational correlation time.[1, 3–5] The ESR spectrum usually consists of three lines. W_0 is a linewidth measure and h_1, h_0, and h_{-1} are the measured

$$\tau_c = W_0[(h_0/h_1)^{1/2} - (h_0/h_{-1})^{1/2}]C \tag{1}$$

$$\tau_c = W_0[(h_0/h_1)^{1/2} + (h_0/h_{-1})^{1/2} - 2]C' \tag{2}$$

amplitudes of each of the three lines. The values of C and C' are characteristic of the nitroxide and the particular experimental conditions employed. We repeat here that we are looking at the tumbling of a nitroxide on its microscopic environment and are studying the manner in which changes in the environment can bring about changes in the tumbling motion of the nitroxide.
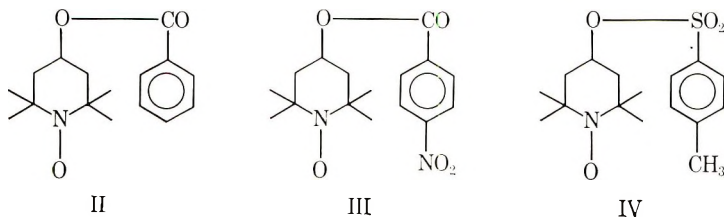
Griffith and co-workers have recently demonstrated that one may conveniently study solutions of micelles by the spin-label technique.[3] In particular they were able to obtain a good measure of the critical micelle concentration (CMC).

We report herein our observations on the behavior of certain soaps and also on soap/latex interactions. Strictly speaking, we are using the nitroxide as a probe in our experiments, not as a label, and the experiments should therefore be referred to as spin probing.

EXPERIMENTAL

Materials

The nitroxide (II), 2,2,6,6-tetramethyl-4-hydroxypiperidine-1-oxyl benzoate (BzONO), has been previously described in the literature.[7] Nitroxides III and IV were prepared in a similar manner from the nitroxide alcohol and the corresponding acid chlorides. Compounds III and IV had melting points of 144.5–145.5°C and 113.5–115.5°C (uncorrected), respec-

tively. The composition of the latexes employed is given in the specific sections relating to their use. They were synthesized by laboratories

within The Dow Chemical Company. The soaps used are all samples of sodium dodecyl sulfate (NaDS) of various degrees of purity. They are (lauryl alcohol content in parentheses): Dupont's Duponol WAQE (ca. 1.3%), Alcolac Chemical's Sipex SB-D (ca. 2%), Alcolac Chemical's Sipon WD (ca. 0.15%), and Eastman Kodak's NaDS, which has a low impurity level. Sodium deoxycholate was obtained from Sigma Chemicals and was used without further purification.

Methods

A Varian V4502 X-band spectrometer was used to obtain the ESR spectra. The Fieldial was initially calibrated with a gaussmeter and subsequent corrected readings were taken directly from the Fieldial. The power saturation studies made use of the attenuator calibration chart supplied by the manufacturer. For the micelle studies a nitroxide concentration of ca. $2 \times 10^{-5} M$ was used. In the latex studies it was necessary to go to solutions which were nominally ca. $10^{-3} M$ in nitroxide because of the broadness of the lines.

RESULTS

Figure 1 shows the ESR spectra one obtains for BzONO dissolved in water and in 0.30% EK-NaDS. It can be seen that the relative amplitudes of the three peaks vary in the two situations. The peak-to-peak width of the central line is broadened by about 0.25 gauss, and the widths of the other two lines are also correspondingly broader.

In Figure 2 we compare the results of a spin-probe determination of the CMC of four different samples of NaDS by using the method of Griffith
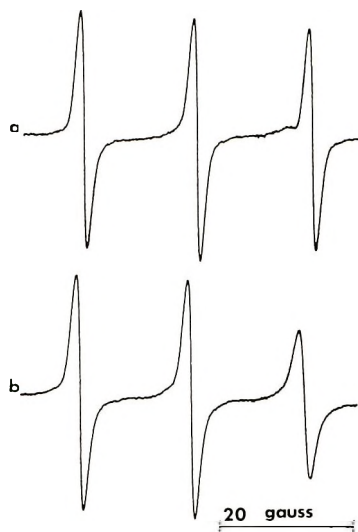

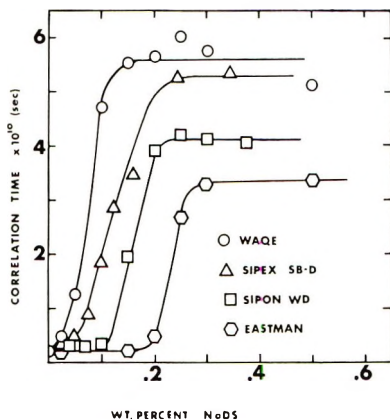Fig. 1. ESR spectra of BzONO in (a) water and (b) 0.3% EK-NaDS.

Fig. 2. Rotational correlation time of BzONO vs. % NaDS for several soaps.

and co-workers.[3]   The tendency is for the CMC to decrease as the impurity levels increase.   The less pure samples not only display a lower CMC, but also have a larger value for the rotational correlation time.

Referring to the EK-NaDS results, the initial flat part of the curve corresponds to a mixture which contains BzONO and the soap in true solution.   The plateau reached at 0.3% soap corresponds to a solution of micelles which contain solubilized BzONO in their hydrocarbon interior. The intermediate region corresponds to the transition from free soap to micelles.

Other closely related nitroxides show behavior similar to BzONO.   Thus nitroxide IV in WAQE and nitroxide III in EK-NaDS give curves which are virtually superimposable on their respective counterparts in Figure 2.

An ESR determination of the distribution coefficient of BzONO in equilibrium with water and hexane at room temperature gives a value $K = 1.22 \times 10^4$, where $K = $ (BzONO solubility in hexane)/(BzONO solubility in water).

The addition of hexane to a 3.0% aqueous solution of WAQE containing BzONO leads to a greater immobilization of the spin probe, as shown in Figure 3.   As the molar ratio of hexane to soap is increased, the rotational correlation time also increases.   At a hydrocarbon/WAQE ratio of about 12, the degree of immobilization is maximized.   At the higher hexane levels examined the degree of immobilization remains fairly constant.   It requires more than 24 hr for an equilibrium value of τ_c to be attained, indicating that the reorganization of the micelle structure is a rather slow process. The values reported here are equilibrium values.

The effects of acrylic acid, acetic acid, and ethanol were also noted. With WAQE in a 1% aqueous solution of acrylic acid the CMC is essentially unchanged, but the value of the rotational correlation time is lowered considerably, as is shown in Figure 4.   A similar change in the rotational correlation time is observed when acetic acid is substituted for acrylic acid. The nitroxide is fairly unstable under these conditions, disappearing com-
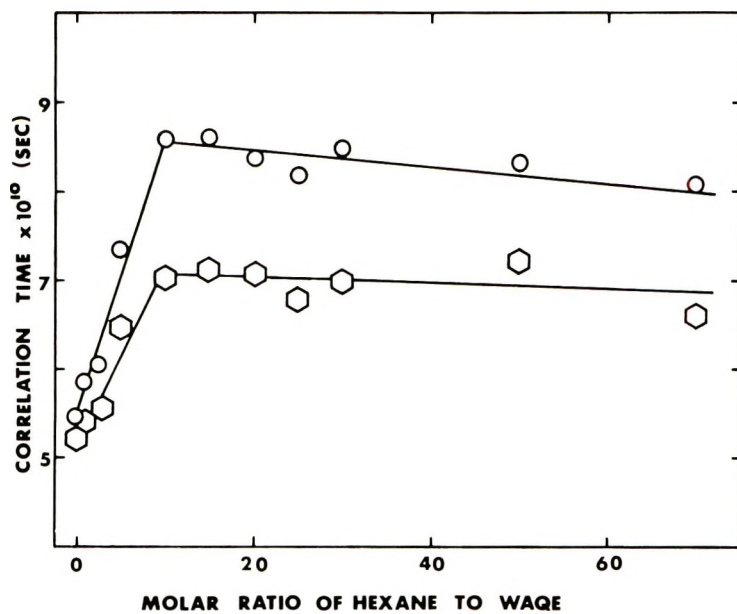
Fig. 3. Rotational correlation time of BzONO vs. the molar ratio of hexane to WAQE, (WAQE ca. 3.0%):   (upper curve) calculated from eq. (1); (lower curve) from eq. (2).
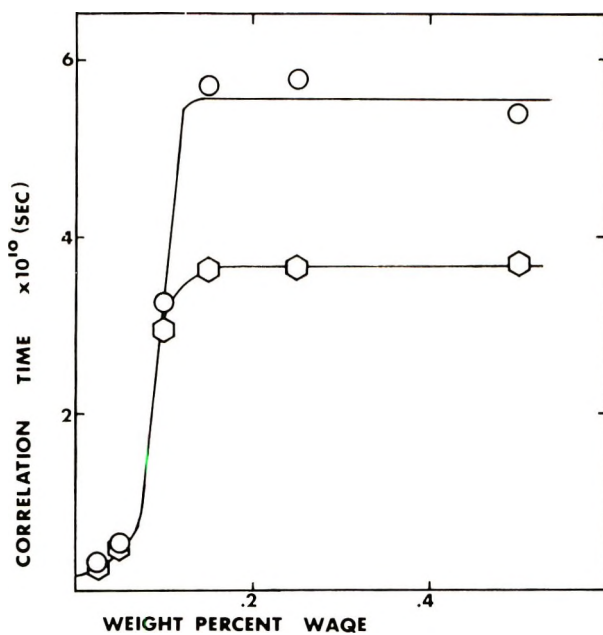

Fig. 4. Rotational correlation time of (upper curve) BzONO in water and (lower curve) BzONO in 1% aqueous acrylic acid vs. % WAQE.

pletely, as monitored by ESR, after 24 hr.   It should be noted that BzONO is quite stable in soap solutions alone and in acetic acid solutions of all concentrations.   The rotational correlation time of BzONO in EK-NaDS is decreased by the addition of 5% by weight of ethanol and the CMC is not appreciably changed.   The break in the curve, however, at the lower soap concentrations is not nearly as sharp as it is in the absence of ethanol.

Sodium Deoxycholate Aggregation

Although it is by no means correct to call the sodium deoxycholate (NaDC) aggregates micelles, the phenomenon studied is, nevertheless, quite similar to that with NaDS, namely, the association of lipophilic molecules in an aqueous serum.[8]   Figure 5 is a plot of the rotational
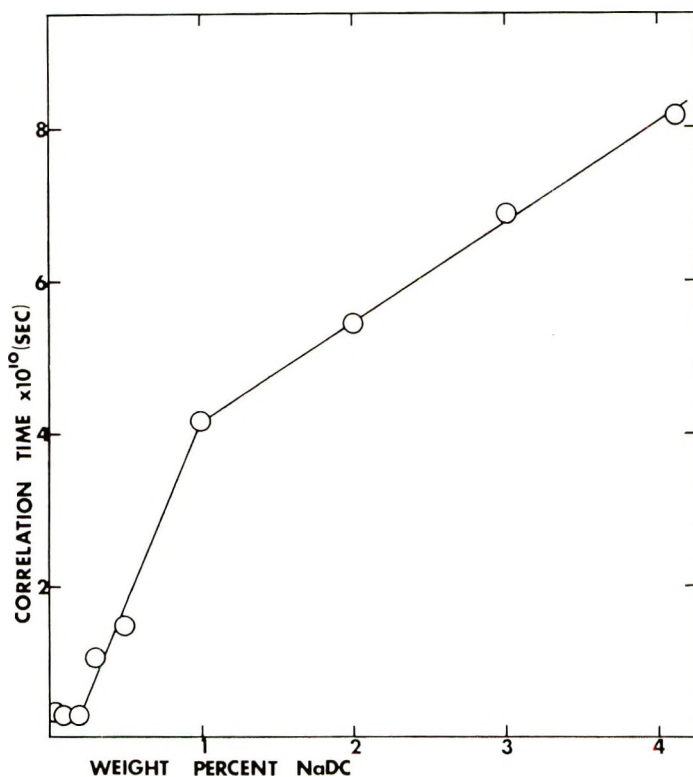
Fig. 5. Rotational correlation time of BzONO vs. % sodium deoxycholate.

correlation time of BzONO in aqueous NaDC solutions as a function of the NaDC content.   Below ca. 0.2 wt-% NaDC there is no significant change in the value of τ_c.   Over the region 0.2–1.0 wt-% NaDC, the slope of the curve changes fairly abruptly, and above the 1.0% level, the slope remains constant at a lower value than the slope in the 0.2–1.0% range.

Latex Studies

Among the latexes examined we have done the most work on SB-62. The compositions of all the styrene–butadiene latexes used are listed in

TABLE I
Compositions of the Styrene–Butadiene Latexes Employed[a]

Identification	Styrene content, %	Approximate particle diameter, Å
SB-62	62	1900
MC-745	62	1090
MC-747	52	1150
MC-762	42	1130

[a] All formulations contain 1.0% WAQE.

Table I.   The ESR spectra of BzONO in SB-62 under different conditions are shown in Figure 6.   The spectrum of Figure 6a is that of BzONO in a stock solution of SB-62 at 52% solids, and that of Figure 6c is of BzONO
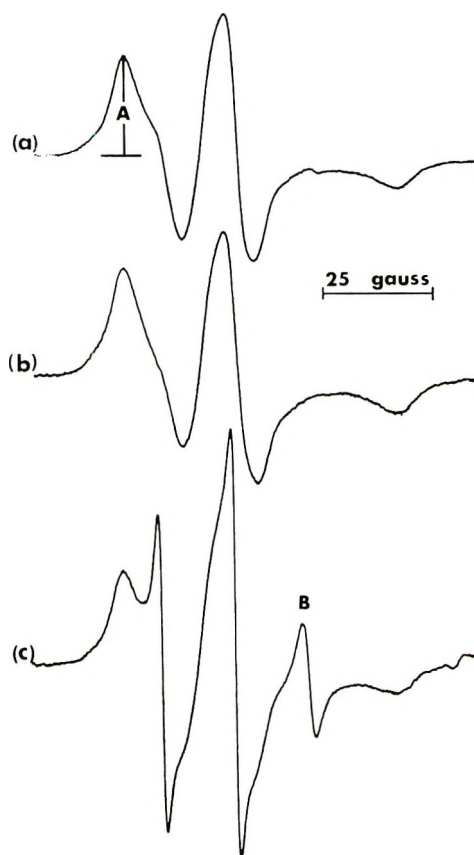

Fig. 6. ESR spectra of BzONO in (a) SB-62 latex, (b) SB-62 film, and (c) SB-62 latex with WAQE micelles present.
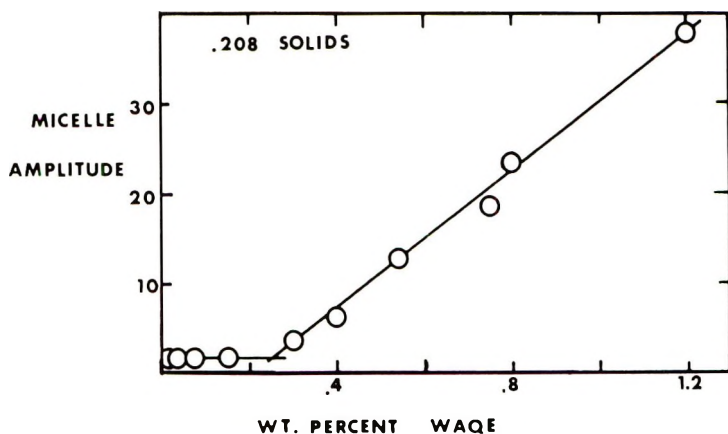
Fig. 7. Titration of SB-62 with WAQE. Amplitude of the ESR micelle peak vs. % WAQE added.
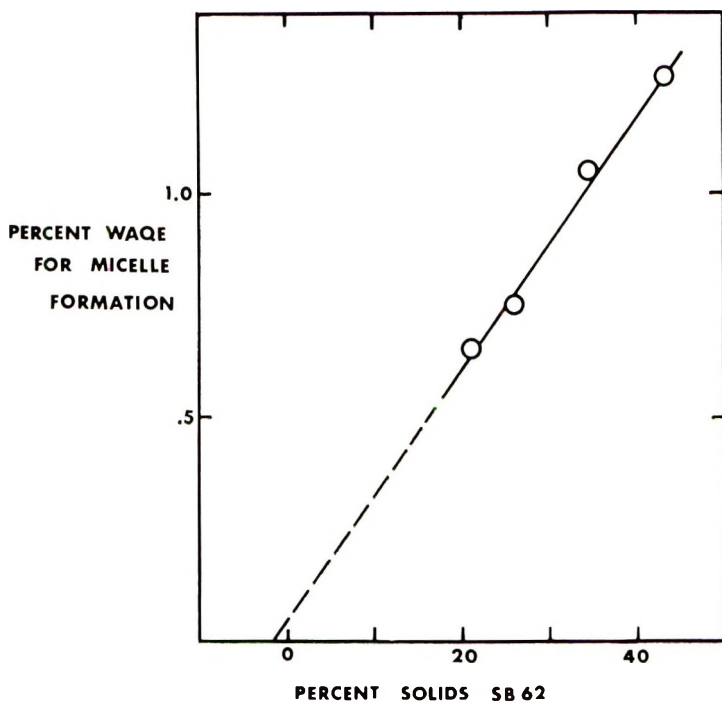
Fig. 8. Plot of % WAQE required for micelle formation vs. % SB-62 solids.

in SB-62 with sufficient added WAQE to have micelles present in the solution. The former spectrum will be referred to as the latex spectrum, and the low-field peak labeled A will be referred to as the latex peak. The spectrum of Figure 1b will be referred to as the micelle spectrum and the high-field peak labeled B will be designated as the micelle peak. This high-field micelle peak is clearly visible in spectrum 6c. It must be empha-

sized that this terminology is used only for convenience; it refers to the spectra and the peaks of the spin probe solubilized in the latex and the micelle, respectively. Spectra indistinguishable from that of Figure 6c are obtained when BzONO is dissolved in the other three latexes listed in Table I. When films of these BzONO-doped latexes are cast and allowed to dry, the ESR spectra are all identical at room temperature. The spectrum shown in Figure 6b is obtained from a film cast from SB-62. At higher temperatures the spectra differ from each other in a regular manner. This interesting aspect will be the subject of a separate publication. Figure 7 is a plot of the data obtained from the titration of BzONO-doped SB-62 with WAQE, where the amplitude of the micelle peak is plotted against the soap concentration. At low soap levels the amplitude of the micelle peak remains constant and low. At the higher levels of WAQE the micelle peak height increases linearly. Titrations were run at four different levels of latex solids (20.8, 26.0, 34.6, and 43.3%) and similar plots to that of Figure 7 were obtained in all cases. Figure 8 is a plot of the total soap present in the system at the point of intersection of the two lines versus the latex per cent solids. The least-squares y intercept is at 0.50% WAQE.

Power Saturation

The line shapes of the ESR spectra are sensitive not only to their molecular motion but also to the levels of microwave power used for detection.
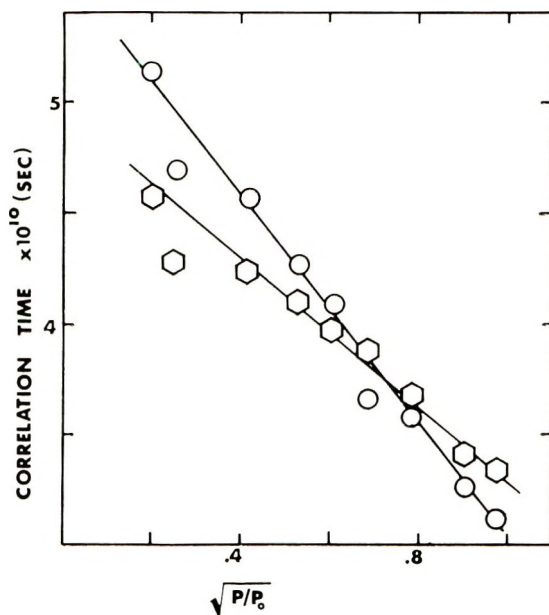

Fig. 9. Rotational correlation time of BzONO in 0.5% EK-NaDS vs. square root of (P/P_0), where P = attenuated microwave power, P_0 = unattenuated power: (○) calculated from eq. (1); (⬡) calculated from eq. (2).

This is illustrated in Figure 9, which is a plot of the rotational correlation time for BzONO in 0.5% EK-NaDS versus $(P/P_0)^{1/2}$, where P is the attenuated microwave power and P_0 is the unattenuated power. Here $\tau_c^{(1)}$ and $\tau_c^{(2)}$ were calculated from eqs. (1) and (2).

DISCUSSION

NaDS Micelles

Adequate explanations have been advanced[3] for spectra of the type shown in Figure 1. Griffith et al. have convincingly demonstrated that the nitroxide is strongly associated with the hydrocarbon portion of the micelle. The rotational correlation time calculated from the spectra of Figure 1 are 3×10^{-11} sec for the spin probe in water and 3.4×10^{-10} sec for the probe in EK-NaDS micelles.

Turning our attention first to the EK-NaDS curve of Figure 2, the values of τ_c on the portion of the curve with a nonzero slope can correspond to two distinct physical situations. One possibility is that the nitroxide is completely dissolved in the micelles which exist above the CMC, which is 0.20 wt-%. In this case, the value for τ_c would reflect the presence of different micelle structures up to the plateau at about 0.30% NaDS. The second possibility is that the probe is distributed between the aqueous serum and the micelles, in which case the calculated τ_c would really be an "effective" τ_c, that is, a weighted average of the contributions from each environment. Our results strongly support this latter case for the following reason. To a first approximation one may draw an anology between the distribution of the spin probe between the serum and the micelles in the aqueous soap solution and the distribution of the same probe between a hydrocarbon and water in contact with each other. The measured distribution coefficient for BzONO for the immiscible solvent pair hexane–water is 1.22×10^4. Using this value to obtain the distribution of the probe between the water and the micelles, one can then calculate values for τ_c in the 0.20–0.30% soap region which are in excellent agreement with the measured values.

In the previous study[3] it was reported that there was no difference observed between the behavior of the commercial and the laboratory samples of NaDS. Both samples gave curves which are quite similar to what we have observed with EK-NaDS (cf. Fig. 2). It is extremely interesting in our case that the less pure samples of NaDS not only display a lower CMC, but also show a tighter micelle structure as reflected by the higher plateau values of τ_c. In speaking of a tighter micelle structure we are referring to the motional restrictions the micelles impose on the solubilized spin probe. The major organic impurity in our soap samples is lauryl alcohol. Becher has commented on the role of impurities such as lauryl alcohol in enhancing the stability of emulsions by strengthening the hydrocarbon-to-water interfacial film.[10] It would appear from our results that the micelle struc-

ture is affected in the same manner as is the emulsion interfacial film. It is possible that the alcohol acts to decrease polar endgroup repulsion, which could then lead to a more ordered array of the hydrocarbon chains.

The change which the ESR spectrum of the spin probe undergoes when hexane is added to a 3.0% aqueous solution of WAQE is somewhat surprising. The generally accepted working model for the molecular structure of an emulsion is of a radial distribution of the soap and synergistic impurities about the hydrocarbon or oily liquid core.[11] Based on this we anticipated that as we added a hydrocarbon to the aqueous BzONO-doped soap solution the solubilized hydrocarbon would allow the spin probe a greater degree of rotational freedom up to the point where the nitroxide would be nearly completely dissolved in the central hydrocarbon core of the soap-coated sphere. Such was not the case. As can be seen from Figure 3, the rotational correlation time of the spin probe becomes larger as the ratio of hexane to soap increases up to a molar ratio of about 12. It shows no further change as the hexane to soap ratio is increased right up to the point where phase separation is evident. The increase in the rotational correlation time as hexane is added can be explained if the spin probe remains associated with the hydrocarbon portion of the soap molecules and is not significantly dissolved in the inner liquid region. In this case, the greater degree of molecular orientation of the surface film, which has been proposed by Shulman and Cockbain,[11] would strongly hinder the spin probe's molecular motion. Although this interpretation is in accord with the hypothesis of a more highly organized outer film, it is nevertheless puzzling in one respect. It is not clear why the spin probe should be preferentially soluble in the surface layer of soap molecules rather than in the hexane interior. Simple calculations show that the spherical inner liquid core would have a minimum diameter several times the diameter of the spin probe. Therefore if the nitroxide were in the interior of the emulsion droplet, it would be readily apparent from the ESR spectrum.

The addition of the more polar molecules, acrylic acid, acetic acid, and ethanol, to the soap solutions has an effect unlike the nonpolar hexane. In all cases the apparent rotational correlation time is considerably lower, indicating that a less ordered micelle structure exists under these conditions. Again, the term "less ordered" refers to the decreased ability of the micelle to hinder the molecular tumbling of the solubilized nitroxide. Interestingly, the CMC is essentially unchanged. Figure 4 shows the results for BzONO-doped WAQE solutions in 1% aqueous acrylic acid. The plateau value of the rotational correlation time decreases by about 40% in this case compared to the acid free case. While the mode of action of these polar molecules is not known one possibility is suggested here. The solvation of the sulfate end of the soap chains by these relatively bulky polar organic molecules could make it more difficult for the hydrocarbon chains to form as organized a structure as they otherwise do.

The instability of the nitroxide in soap solutions containing acrylic or acetic acids is interesting in view of the fact that the spin probe is quite

stable in soap solutions alone, and in acetic acid solutions ranging from 1% aqueous to glacial. How this reaction occurs is not known at present, but one cannot overlook the possibility that the micelle functions as a catalytic surface and provides an active site where the nitroxide and the acid may come together to react. NaDS has been shown to exhibit catalytic behavior in a large number of instances.[12]

Sodium Deoxycholate Aggregation

It is well documented that NaDC forms molecular aggregates in aqueous solution.[8] These aggregates produce an increased viscosity which is thixotropic in nature. Under certain conditions it is possible to draw out helical microfibrils from these solutions. We felt that it should be possible to follow the NaDC aggregation by the use of a spin probe just as was done with the NaDS micelles. This would require, of course, that the aggregates which form are able to bind the nitroxide. The curve of Figure 5 indicates that this requirement is fulfilled and that as the NaDC molecular aggregates form, the nitroxide probe does associate with it very strongly. Below about 0.2% NaDC the unchanged value of the nitroxide rotational correlation time indicates that there is no significant degree of association of the NaDC molecules. In the 0.2–1.0% region, the fairly rapid rise in τ_c shows that the probe is now in a microscopic environment which hinders its molecular motion. The same is also true above 1.0%, but the rate of change of τ_c is not as great. On drawing an analogy between the NaDC aggregation and the NaDS micellization, the broadness of the concentration range on the maximum slope portion of the curve implies either that there is not a unique stoichiometry to the aggregate formed or that the stoichiometry is quite low.[13] From the x-ray data of Bonamico and Giacomello on some crystalline choleic acids[14] one can estimate the radius of a 2:1 deoxycholic acid:BzONO complex to be not less than 10Å. Using the Stokes law relation[15]

$$\tau_c = (4\pi\eta a^3)/3kT \tag{3}$$

one calculates a rotational correlation time of 1.0×10^{-9} sec for a nitroxide complexed with two NaDC molecules. In eq. (3) η is the solvent viscosity and a is the particle radius. Previous workers have shown that correlation times calculated by the Stokes law relation are about twice as large as the values obtained from direct ESR measurements,[3] and we would therefore expect a value of about 5×10^{-10} sec for the complex with a 10 Å radius. As can be seen from Figure 5 the probe does not have a correlation time of this magnitude until the NaDC is present at about the 2.0% level. This is well past the 0.2% NaDC level where association of the probe with the bile acid is evident. It is thus clear that the probe forms a fairly loose association with the NaDC aggregates. The change in slope of the curve of Figure 5 beyond the 2.0% level, where the NaDC aggregates probably exist in a helical chain structure,[8] may reflect the smaller effect that an increased molecular weight and chain length has on local chain structure

and motions. The steady increase in the correlation time is in interesting contrast with NaDS, where the correlation time remains constant at soap concentrations appreciably above the CMC.

Latex Studies

A problem arose where it was necessary to detect micelles in a latex. It seemed that the spin-probe technique would prove useful in this area and, indeed, it showed itself to be of quite broad applicability.

The spectrum of Figure 6a is of BzONO in SB-62. This is to be contrasted with the spectra of Figure 1. The much broader latex spectrum is indicative of a rotational correlation time at least three orders of magnitude greater than that associated with the micelle spectrum. There is superimposed on the pure latex spectrum a less than 0.1% contribution from a more free species, which can be seen as an inflection on the low-field latex peak, A, and as a separate peak between the middle- and high-field latex peaks. These are more clearly indicated in Figure 6c. This more mobile species has a rotational correlation time very nearly equal to that of BzONO in a NaDS micelle. This does not necessarily mean that it is in a micelle, since there may be other ways it can associate with the latex polymer particles. It is clear, however, that greater than 99.9% of the spin probe is intimately associated with the polymer particles. It is most likely that the nitroxide is solubilized in the interior of the latex particle, since our evidence points against it being on the surface. Thus if a film is cast and allowed to dry completely the ESR spectrum of the probe-doped solid polymer is identical to that of the original latex, with the exception of the complete absence of the 0.1% contribution from the more mobile species. This latter spectrum is shown in Figure 6b. If the probe in the latex were associated with the surface of the polymer particles one would expect to see a change in the ESR spectrum as the particles coalesced. No such change was observed with SB-62 nor with the other three latexes of Table I.

If one adds sufficient WAQE to the probe-doped latex the spectrum of Figure 6c is obtained. This spectrum is the resultant of the superposition of a latex spectrum and a micelle spectrum. In this situation where the nitroxide is distributed between the polymer particles and the micelles, the ESR spectrum clearly reflects the two environments. Fortunately, the latex peak A and the micelle peak B are nonoverlapping, permitting a straightforward analysis. Thus, at a low soap/polymer ratio the amplitude of the micelle peak is a direct measure of the micelle concentration (see Appendix I). Titration of a stock sample of SB-62 with WAQE gives the results shown in Figure 7. The amplitude of the micelle peak remains very small and constant up to about 0.25% added WAQE. From that point on the amplitude of the micelle peak increases linearly. The amount of soap present initially was 0.40%, so at the 20.8% solids level it can be seen that there are essentially no micelles present below 0.65% WAQE. Similarly, at other levels of polymer solids we have calculated the soap

levels below which there are no appreciable quantities of micelles in solution. The graph of Figure 8 shows the results. This can be interpreted in terms of a saturation surface coverage of the polymer particles by the soap molecules. When the saturation point is reached, the soap molecules are then able to reach the solution concentration necessary for micelle formation. The intercept of 0.05% WAQE required for micelle formation at zero polymer solids should equal the CMC. The agreement of this value with the value obtained by direct measurements is quite good.

Assuming that the soap forms a monolayer on the polymer surface, it is possible from these data to calculate an effective surface area occupied by each soap molecule. The range of particle sizes for SB-62 is 1 800–2 000 Å. The calculated values for the effective surface coverage per molecule of soap is 51 Å^2 and 55 Å^2 based on polymer particle diameters of 2 000 and 1 800 Å, respectively. The details of these calculations are in Appendix II.

APPENDIX I

Calculation of the Expected Distribution of BzONO Between Polymer Particles and Micelles in the Same Solution

Let $K = (a/x)/(b/y)$

where $a/x = a$ grams BzONO per x grams latex and $b/y = b$ grams BzONO per y grams micelles.

$$a/b = K(x/y). \ a + b = c$$
$$b = cy/(y + Kx)$$

For the latex and micelle mixture we assume

$$K \geqslant 1$$

Then for $x >> y$

$$b = (cy)/(Kx).$$

Thus, when the latex solids are present in sufficient excess over the micelles, the micelle ESR peak is a direct measure of the micelle concentration.

APPENDIX II

Calculation of the Effective Surface Area of WAQE on SB-62

Using the data of Figure 8 one calculates that 0.5 g polymer solids requires 0.0141 g of WAQE for complete coverage. The particle size distribution for SB-62 is 1 800–2 000 Å.

For the 1 800 Å particle size,

$$A = 4 \pi r^2 = 1.01 \times 10^{-9} \ cm^2/particle$$
$$V = {}^4/_3 \pi r^3 = 3.02 \times 10^{-15} \ cm^3/particle$$

Grams per particle:

$(3.02 \times 10^{-15} \text{ cm}^3/\text{particle})(1.03 \text{ g/cm}^3) = 3.11 \times 10^{-15} \text{ g/particle}$

Particles per 0.5 g:

$(5 \times 10^{-1} \text{ g})/(3.11 \times 10^{-15} \text{ g/particle}) = 1.61 \times 10^{14} \text{ particles}$

Total area per 0.5 g:

$(1.01 \times 10^{-9} \text{ cm}^2/\text{particle})(1.61 \times 10^{14} \text{ particles}) = 1.62 \times 10^5 \text{ cm}^2$

Total WAQE required per 0.5 g polymer solids:

$(N)(1.41 \times 10^{-2} \text{ g})/(2.88 \times 10^2 \text{ g/mole}) = 2.95 \times 10^{19} \text{ molecules}$

Effective area occupied per soap molecule:

$(1.62 \times 10^5 \text{ cm}^2 \times 10^{16} \text{ Å}^2/\text{cm}^2)/(2.95 \times 10^{19} \text{ particles}) = 55 \text{ Å}^2/\text{molecule}$

A similar calculation based on a $2\,000$ Å diameter gives a value of 51 Å^2/molecule WAQE.

References

1. T. J. Stone, T. Buckman, P. L. Nordio, and H. M. McConnell, *Proc. Nat. Acad. Sci. U. S.*, **54**, 1010 (1965).

2. L. Stryer and O. H. Griffith, *Proc. Nat. Acad. Sci. U. S.*, **54**, 1785 (1965).

3. A. S. Waggoner, O. H. Griffith, and C. R. Christensen, *Proc. Nat. Acad. Sci. U. S.*, **57**, 1198 (1967).

4. M. D. Barratt, D. K. Green, and D. Chapman, *Biochem. Biophys. Acta.* **152**, 20 (1968).

5. D. Kivelson, *J. Chem. Phys.*, **33**, 1094 (1960).

6. N. Edelstein, A. Kwok, and A. H. Maki, *J. Chem. Phys.*, **41**, 179 (1964).

7. E. G. Rozantsev, V. A. Golubev, and M. B. Neiman, *Bull. Acad. Sci. USSR*, **1965**, 379.

8. D. M. Blow and A. Rich, *J. Amer. Chem. Soc.*, **82**, 3566 (1960).

9. G. P. Rabold, *J. Polym. Sci. A-1*, this issue.

10. P. Becher, Emulsions: Theory and Practice, 2nd ed., ACS Monograph No. 162, American Chemical Society, Washington, D. C., 1965, pp. 104–110 and references therein.

11. J. H. Shulman and E. G. Cockbain, *Trans. Faraday Soc.*, **36**, 651 (1940).

12. R. B. Dunlap and E. H. Cordes, *J. Amer. Chem. Soc.*, **90**, 4395 (1968).

13. A. E. Alexander and P. Johnson, *Colloid Science*, Vol. 2, Oxford, 1949, pp. 670–75.

14. M. Bonamico and G. Giacomello, *Gazz. Chim. Ital.*, **92**, 647 (1962).

15. G. E. Pake, *Paramagnetic Resonance*, Benjamin, New York, 1962, Chap. 5.

Spin-Probe Studies. II. Applications to Polymer Characterization

GARY PAUL RABOLD, *Radiochemistry Research Laboratory, The Dow Chemical Company, Midland, Michigan 48640*

Synopsis

The spin-probe technique has been employed to study interactions between several small organic nitroxides and host polymers in which they are dissolved. By this method one is able to study the mobility of the dissolved molecule in its microscopic environment using electron spin resonance spectroscopy. The behavior of one nitroxide has been examined in twelve different polymers and copolymers. An ESR line shape parameter has been correlated with T_m and T_g. In addition, energy barriers for the rotation of the dissolved nitroxides in the polymers have been calculated. They range from 7.8 to 18 kcal/mole, depending on the structure of the nitroxide and the polymer. Similar experiments in a hydrocarbon solvent afford a rotational energy barrier of 3.8 kcal/mole.

INTRODUCTION

In recent years a great deal of attention has been focused on the relation between the macroscopic behavior and properties of polymers and the microscopic molecular motions of the polymer chains. Prominent among those methods which have been found to be useful in such studies are differential thermal analysis, dynamic mechanical testing, and nuclear magnetic resonance. In a review article Boyer describes the application of these methods to questions of molecular motions in polymers.[1] The three methods mentioned above all have the common feature that they involve making a direct measurement on the system being studied. A second approach to studies of polymer behavior would be to use a suitable molecular probe, some measurable parameter of which responds to the molecular motions of the host polymer. We have attempted to use such an indirect method by the application of the spin-probe technique,[2] and we present some of our results in this report.

THEORY

The spin-probe technique is based on the response of the line shape of the ESR spectrum of a suitable paramagnetic probe to its molecular motion. The probes used to date have all been members of the class of paramagnetic compounds known as nitroxides. Comprehensive treatments of the motional dependence of the ESR line shapes for nitroxides have appeared in
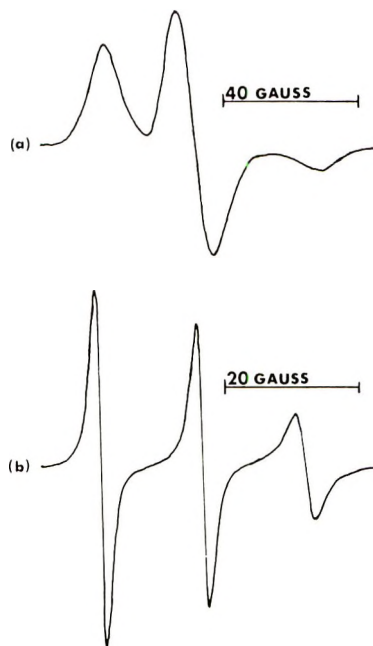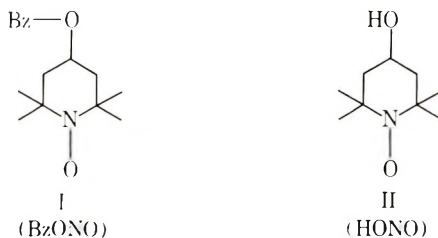
1203

Fig. 1. ESR spectra of BzONO in polyethylene (IIX 116) (a) at −180°C, and (b) at +80°C. The external field increases from left to right.

the literature.[3,4] Typical ESR spectra for nitroxide I under two different conditions are shown in Figure 1.

Spectrum 1a, of BzONO in high-density polyethylene at −180°C, is characteristic of a slowly tumbling nitroxide in an environment which restricts its tumbling frequency to the order of $< 10^5$ to 10^6 Hz. Spectrum 1b, of BzONO in high density polyethylene at +80°C, is indicative of a much less restrictive environment and a reorientational frequency of 10^9 Hz can be calculated, where this frequency is defined as the reciprocal of the rotational or reorientational correlation time. The rotational frequencies which can be examined by the present method fall in the range 10^6–10^{11} Hz. The rotational frequencies which can be measured with a fair degree of confidence are in the approximate range 5×10^8–5×10^{10} Hz. Values for the correlation time (τ_c) are calculated from eqs. (1) and (2).

$$\tau_c{}^{(1)} = W_0[(h_0/h_1)^{1/2} - (h_0/h_{-1})^{1/2}]C \qquad (1)$$

$$\tau_c{}^{(2)} = W_0[(h_0/h_1)^{1/2} + (h_0/h_{-1})^{1/2} - 2]C' \qquad (2)$$

Figure 1b is used as a representative example; W_0 is the peak to peak linewidth of the center line, h_1, h_0, and h_{-1} are the peak to peak amplitudes of the low-, middle-, and high-field peaks, and C and C' are constants which are characteristic of the g and hyperfine tensor anisotropies and of the particular experimental conditions.[3] The value of τ_c can be thought of as the time required for the nitroxide to rotate through an angle of one radian.

The experiment that is carried out is to make a solid solution, about 100 ppm, of the nitroxide probe in a polymer and then to study the response of the dissolved nitroxide's ESR spectrum with temperature. The rationale is that the motion of the nitroxide will reflect the motion of the chain segments of the host polymer. It is assumed that a rigid polymer matrix will impose more severe motional restrictions on the dissolved probe than will a flexible polymer.

EXPERIMENTAL

Materials

The nitroxides I (2,2,6,6-tetramethyl-4-hydroxypiperidine-1-oxyl benzoate), II (2,2,6,6-tetramethyl-4-hydroxypiperidine-1-oxyl), and III (2,2,5,5-tetramethyl-3-carbamido pyrroline-1-oxyl) have been described previously in the literature.[5,6] Details on the latexes are given in Table I. The polyethylenes used were low density (0.921 g/cm³) and high density (0.964 g/cm³). Both the poly(vinyl chloride) and the polystyrene were latexes obtained from within The Dow Chemical Company.

TABLE I
Composition of the Styrene–Butadiene Latexes Employed

Identification	Styrene, %	WAQE, wt. %
SB-62	62	1
MC-745	62	1
SB-57	57	1
MC-747	52	1
MC-762	42	1

Methods

ESR spectra were recorded with a Varian V4502 X-band spectrometer using 100 KHz field modulation. In some cases enhanced resolution was obtained by using a field modulation line sharpener which is described by Glarum.[7] Varian's standard variable temperature accessory was employed for temperature control. A calibration of the variable temperature unit showed it to be accurate to within one degree. Samples were allowed to equilibrate for a minimum of 3 min for each 10°C change in temperature

(the manufacturer's recommendation is 7 min/100°C change). Power
saturation studies utilized the attenuator calibration chart supplied by the
manufacturer. Most spectra were run under conditions where power
saturation effects were negligible.

Samples of the nitroxide probes in polyethylene and in polypropylene
were prepared by blending weighed amounts of the probe into the polymer
near its melting point by the hot roll/cold roll technique. The nitroxide
was introduced into polystyrene, poly(vinyl chloride), and the various
copolymers by adding it to the corresponding latexes and casting films
which were then allowed to dry. It has been shown previously that the
nitroxide is solubilized by the polymer.[2] In all cases the nitroxide was
less than 0.01% by weight of the polymer mixture.

RESULTS

The ESR spectra of BzONO in high-density polyethylene and in poly-
(vinyl chloride) are shown in Figures 2 and 3, respectively. These spectra
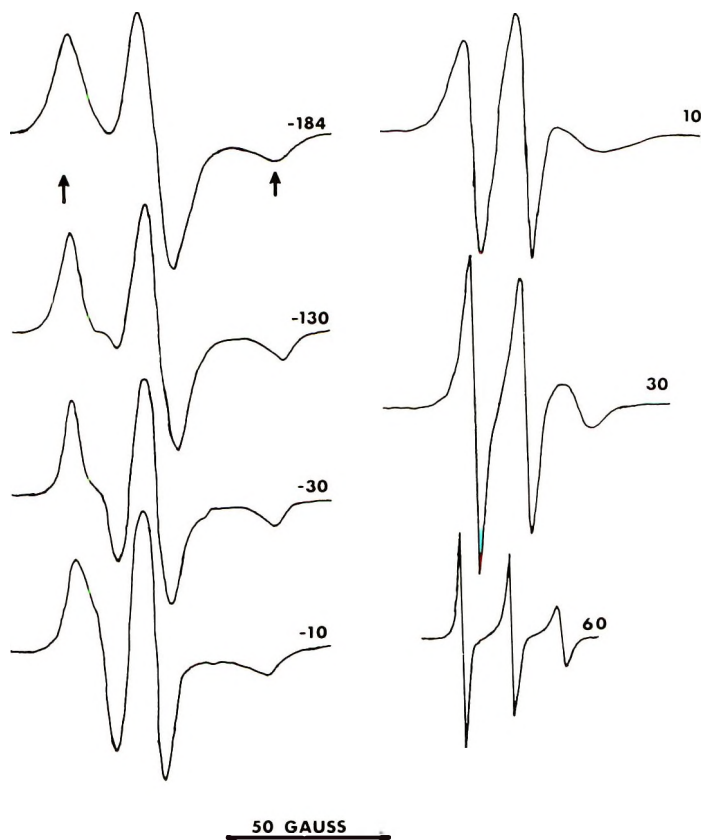

Fig. 2. ESR spectra of BzONO in polyethylene (HX 116) at the indicated temperatures (deg. C).
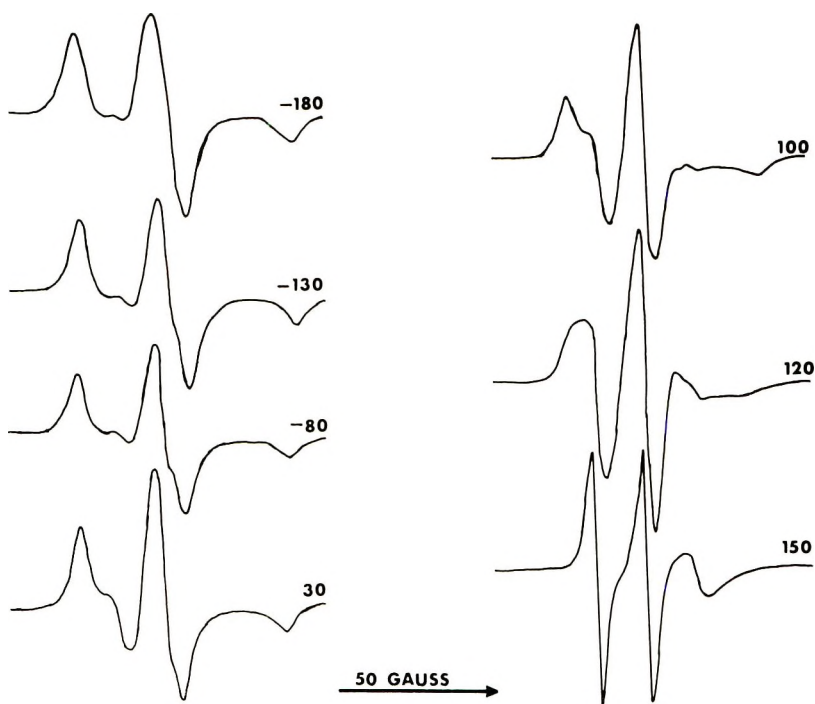
Fig. 3. ESR spectra of BzONO in poly(vinyl chloride) at the indicated temperatures.

are representative of those obtained from all of the BzONO doped polymers. At the lower temperatures the spectra are dominated by the broad, asymmetric triplet which is characteristic of a high degree of nitroxide immobilization.[4,8] In some samples there are contributions from a second, less hindered species, superimposed on the more dominant broad spectrum. As the temperature is raised the spectrum slowly narrows. Ultimately, when the melting temperature of the host polymer is approached the ESR spectrum is essentially that of the nitroxide in a low molecular weight liquid hydrocarbon. Similar temperature studies were made using HONO as the probe. Figure 4 shows the variation of the ESR spectra with temperature for HONO in poly(vinyl chloride). The greater degree of resolution in these spectra is the result of employing the field modulation line sharpener. The superposition of the broad and the narrow spectra is much more clearly seen.

The data for the several polymers can be plotted as ΔW versus temperature, where ΔW is the peak to peak separation of the two extrema. Such curves all show a fairly sharp break considerably below T_m. The position and sharpness of the break depends both on the particular nitroxide used and on the composition of the host polymer. Curves for BzONO and HONO in high-density polyethylene, polypropylene, poly(vinyl chloride), and polystyrene are shown in Figures 5, 6, 7, and 8, respectively. The difference in the approximate points of inflection for the BzONO and
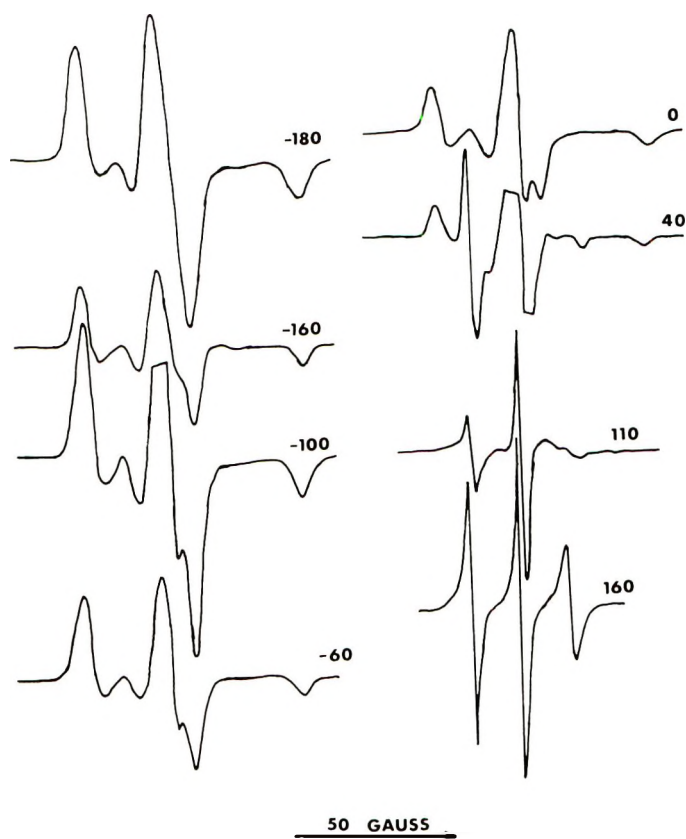
Fig. 4. ESR spectra of HONO in poly(vinyl chloride) at the indicated temperatures. The field modulation line sharpener was used to obtain enhanced resolution. The center lines at −100°C and at 40°C are truncated for clarity.
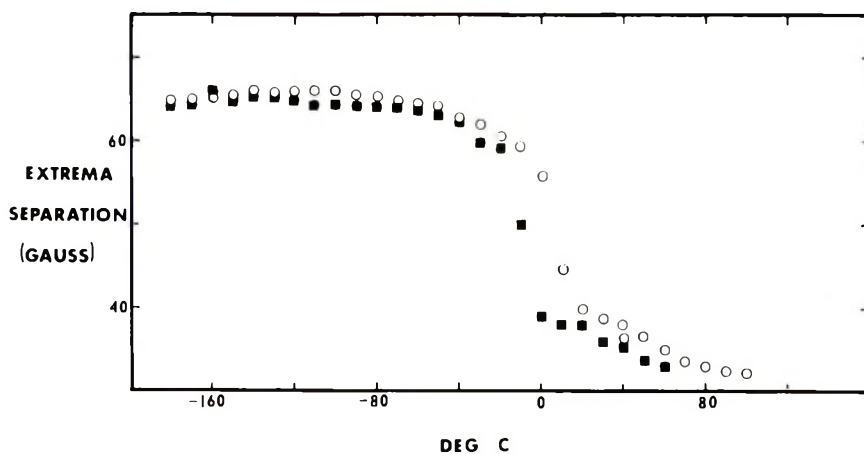

Fig. 5. Plots of extrema separation vs. temperature in the ESR spectra of (○) BzONO and (■) HONO in polyethylene.
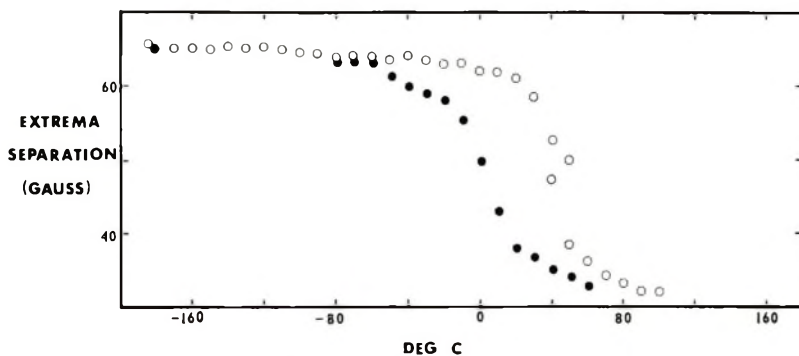
Fig. 6. Plots of extrema separation vs. temperature in the ESR spectra of (○) BzONO
and (●) HONO in polypropylene.
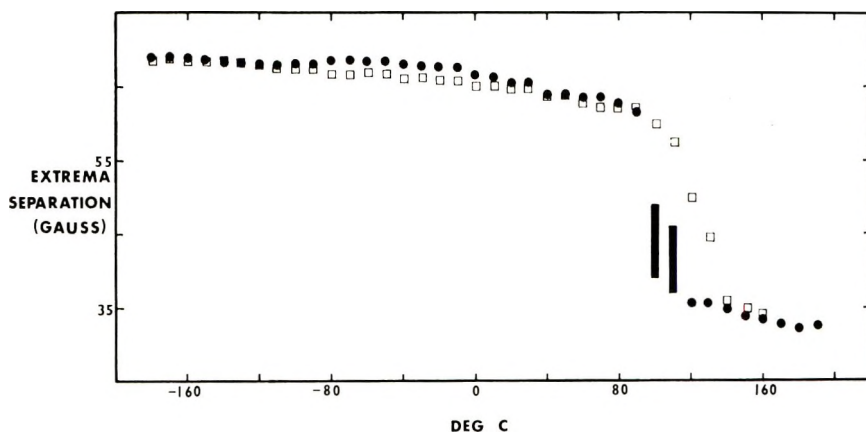
Fig. 7. Plots of extrema separation vs. temperature in the ESR spectra of (□) BzONO
and (●,▬) HONO in poly(vinyl chloride).

HONO curves for high-density polyethylene is nearly the same as that for
poly(vinyl chloride), while the difference for polypropylene is somewhat
larger, and that for polystyrene is considerably greater. Figure 9 shows
similar plots over a more limited temperature range for BzONO in the
styrene–butadiene copolymers MC-762, MC-747, and MC-745. As the
ratio of styrene to butadiene increases the inflection point is shifted to
higher temperatures.

As will be discussed below, there is a temperature region where the rate
of tumbling can be calculated with a good degree of confidence. For most
of the polymers the data from this region gives excellent straight line fits
for plots of ln(rotational frequency) versus $1/°K$, where the rotational
frequency is defined as the reciprocal of the rotational correlation time.
The slope of such a plot affords a value for the rotational activation energy
of the nitroxide in the polymer. One such plot is shown in Figure 10,
which is for BzONO in polypropylene. A summary of the results of the

Fig. 8. Plots of extrema separation vs. temperature in the ESR spectra of (○) BzONO and (■) HONO in polystyrene.

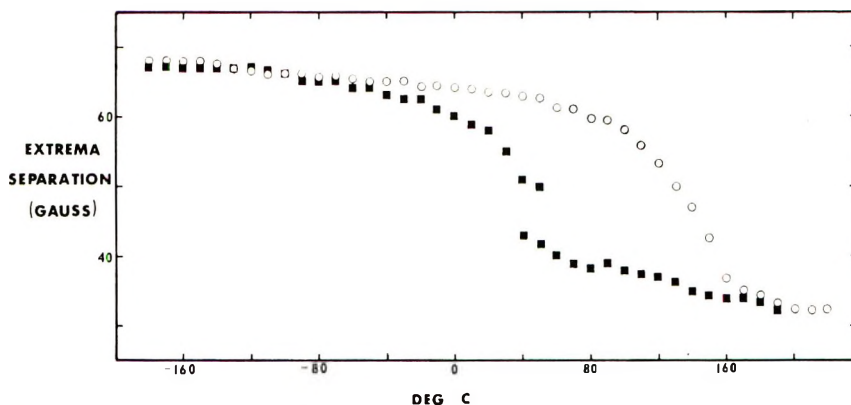Arrhenius plots is included in Table II. Such a treatment was not possible in the cases of polystyrene and poly(vinyl chloride), since the nitroxide was unstable at the higher temperatures these polymers required.

The ESR spectra of the nitroxides in the polymer matrices are decidedly sensitive to the incident microwave power levels. Figure 11 shows plots of the reciprocal of the correlation time as a function of the incident power for BzONO in polyethylene at three different temperatures. For most of the results discussed in this report the incident power was such that it did not appreciably alter the line shapes.

TABLE II
Summary of Experimental Results

Polymer	Activation energy, kcal/mole[a]	T_m, °C[b] BzONO	T_m, °C[b] HONO
MC-762	11.1	39	
MC-747	11.7	52	
SB-57	12.3	47	
SB-62	13.7	62	
MC-745	14.0	65	
SB-62[c]	12.6		
Polyethylene (low-density)	11.0	4	
Polyethylene (high-density)	11.0	5	−10
Polypropylene	12.3	42	1
Ethylene–propylene, 50/50	10.5	16	
Ethylene–propylene, 75/25	9.6		
Ethylene–propylene, 75/25[d]	7.6		
Polystyrene	18.3	130	45
Poly(vinyl chloride)		120	98

[a] Estimated to be reliable to ± 0.2 kcal/mole.

[b] Temperature at which the extrema separation is 50 gauss.

[c] Nitroxide III used as the probe.

[d] HONO used as the probe.

The styrene–butadiene copolymers showed a limiting value of ⁓1.3 gauss for the linewidth of the M=O line for dissolved BzONO, whereas the BzONO M=O linewidth had a limiting value of ⁓1.6 gauss when poly-
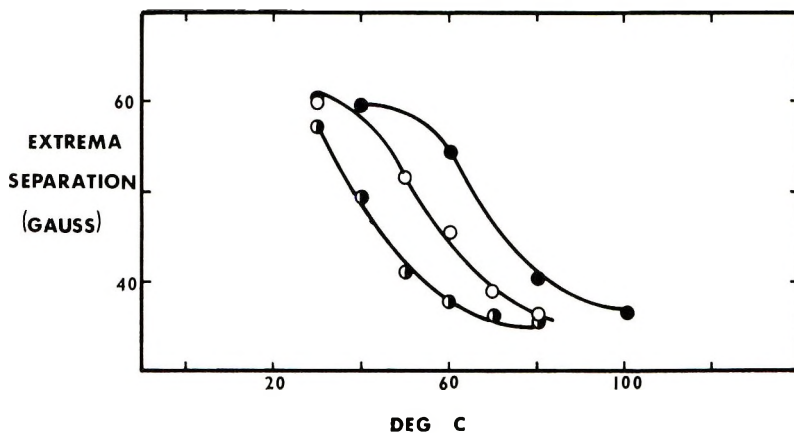
Fig. 9. Plots of extrema separation vs. temperature in the ESR spectra of (●) BzONO in MC-745, (○) MC-747, and (◑) MC-762.
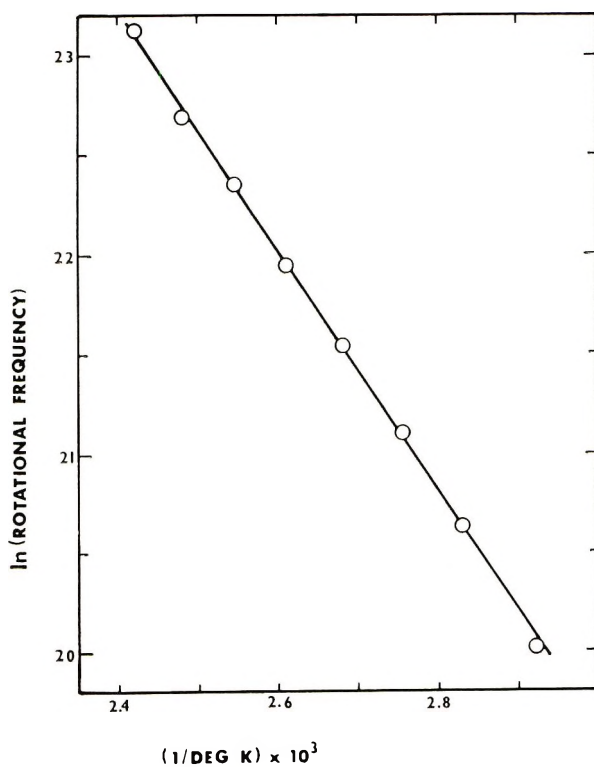
Fig. 10. Arrhenius plot for BzONO in polypropylene. The rotational frequency is defined as the reciprocal of the rotational correlation time.
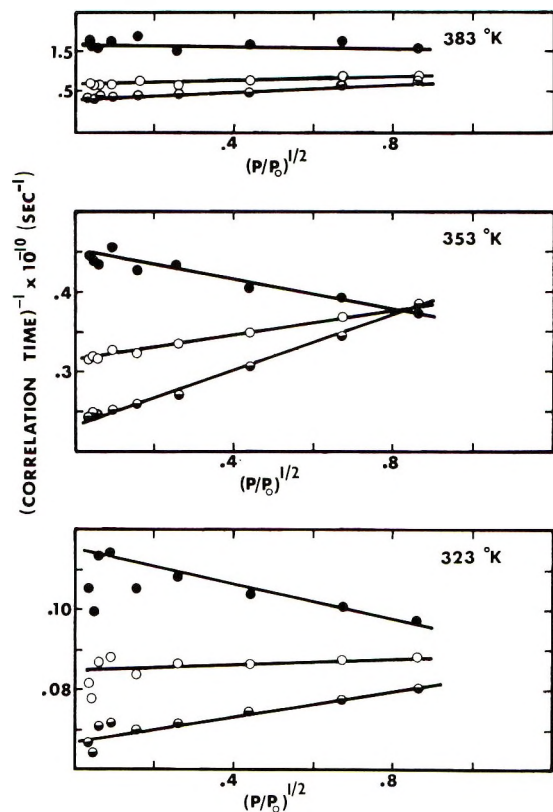
Fig. 11. Plots of (correlation time)$^{-1} \times 10^{-10}$ vs. $(P/P_0)^{1/2}$ for BzONO in polyethylene, where P_0 = unattenuated microwave power: (●) $1/\tau_c^{(2)}$; (◐) $1/\tau_c^{(1)}$; (○) $1/\tau_c^{(av)}$.
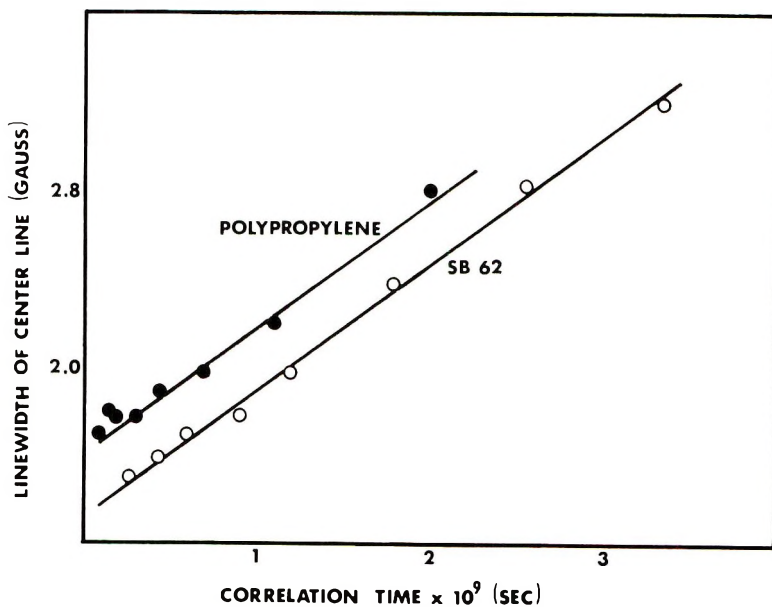
Fig. 12. Plots of linewidth (M = 0) vs. correlation time for BzONO in polypropylene and in SB-62.
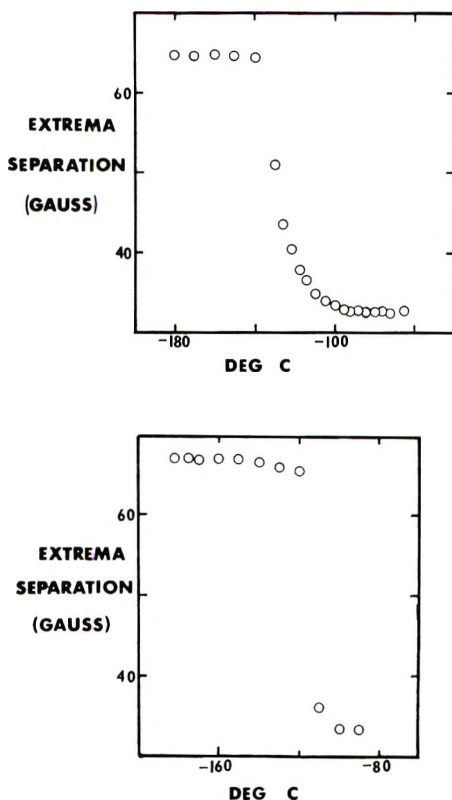
Fig. 13. Plots of the extrema separation vs. temperature for BzONO in hydrocarbon solvents: (upper curve) methylcyclohexane; (lower curve) 1:1 mixture of toluene and cyclohexane.

ethylene or polypropylene served as the host polymer. These limiting values were obtained from plots of the linewidth versus the correlation time as in Figure 12.

As a point of reference, the ESR spectra of BzONO in methylcyclohexane and in a 1:1 mixture of toluene and cyclohexane were run as a function of temperature. Plots of the separation of the outermost lines of their ESR spectra versus temperature are shown in Figure 13. The break in the curve for the toluene/cyclohexane mixture is much more sharp than that for methylcyclohexane. The break in both curves is much sharper than for any of the similar plots for BzONO in the polymers.

DISCUSSION

A discussion of the results should be prefaced by a few general remarks. The measurements afford information about the steric interactions between a small molecule and the chain segments of its host polymer. Kosfeld has discussed this general problem earlier in a paper on plasticized polystyrene,[9] in which he suggests a microscopic model of the polymer–plasticizer system.

In his model Kosfeld proposes that at and below T_g there exist submicroscopic cavities in which a plasticizer molecule may possess a liquid-like mobility, although no quantitative relation was suggested between the relative sizes of the cavity and the plasticizer. Our results in general conform with the above model. Thus the spectrum for BzONO in polyethylene at $-130°C$, shown in Figure 2, points to the onset of molecular motion well below T_g. As a convenient point of reference we have arbitrarily defined T_w as that temperature at which the extrema separation is equal to 50 gauss. This is approximately the point of maximum slope on the plots of extrema separation versus temperature, and it corresponds to a tumbling frequency of about 10^8 Hz. The 10°C spectrum of Figure 2 is representative of those obtained at T_w when the nitroxide environments are all quite similar. It is not possible to assign a definite site within the polymer matrix to the probe at a given temperature, say T_w, but it is reasonable to assume that there are submicroscopic cavities which allow the nitroxide this high degree of rotational mobility. There is reason to believe that there may be correlations between the extrema separation versus temperature plots and loss peaks observed by mechanical spectroscopy. The evidence is not sufficiently strong at present, however, to justify an extension of the discussion to this possibility.

It will be noted from Figure 3 (100, 120°C) and Figure 4 (-180 to 110°C) that the spectra reflect two nitroxide environments. This was clearly manifested in the spectra of both BzONO and HONO in several of the polymers. We are unable to make specific assignments regarding these environments, but it appears that there is not a continuous distribution of cavity sizes within the polymer matrix, but rather that there are at least two discrete narrow distributions of cavity sizes present under those conditions mentioned above.

At this stage such variables as molecular weight and tacticity have not been examined. Neither have we looked closely for effects brought about by the rate of experimental variation of the temperature, or similar facets of a given sample's history. It is possible, therefore, that some of the scatter in the results could be accounted for by a proper consideration of some of these variables. Nevertheless, as will be seen below, the trends in the experimental results are sufficiently distinct to allow firm conclusions to be drawn. In the case of the latexes it is assumed that the probe is dissolved in the pure polymer, and that the emulsifier effect is negligible. This is based on the mechanism of latex particle coalescence put forth by Vanderhoff, wherein it is proposed that the emulsifier is exuded to the surface of the polymer film.[10]

Polyethylene

Both a high-density (0.964 g/cm³) and a low-density (0.921 g/cm³) sample of polyethylene were examined. Figure 2 shows the ESR spectra of BzONO in the high density polyethylene over a wide temperature range. The arrows below the $-184°C$ curve point to the high- and low-field

extrema, whose separation should be equal to $2A$ for a completely frozen random sample of nitroxide where A is the magnitude of the hyperfine splitting resulting from the orientation of the nitroxide axis parallel to the external magnetic field. A plot of the extrema separation versus temperature is shown in Figure 5 for BzONO and HONO in high-density polyethylene. Nearly superimposable curves are obtained for these same two nitroxide probes in the low-density sample of polyethylene. For BzONO and HONO in polyethylene the values for T_w are 5 and $-10°C$, respectively. Since the 50 gauss extrema separation for the respective values of T_w implies that the nitroxide moiety in each probe molecule is tumbling in the host polymer at the same frequency, it is apparent that at $-10°C$ the smaller HONO has the same degree of motional freedom as does BzONO at 5°C.

There is a second aspect of the temperature dependent spectral changes which is of considerable interest. Inspection of the -30 and $-10°$ spectra of Figure 2 shows that each is a superposition of two spectra, one corresponding to the probe in a restrictive environment and one corresponding to the probe in a looser structural network. This is quite similar to what we showed earlier for BzONO distributed between the polymer and the micelle phases in a latex.[2] In the present case it is possible that the two environments reflect contributions from the probe in those regions of the polymer where crankshaft chain motion is occurring and from other regions where lower frequency chain motion is dominant.

The spectra of BzONO in polyethylene near the polymer's melting point are amenable to a reliable calculation of the rotational correlation time. If we define the rotational frequency as the reciprocal of the correlation time and assume that the tumbling of the probe in the host polymer can be treated as a typical rate process, we can then obtain an estimate of the energy barrier to rotation by plotting the natural logarithm of rotation frequency versus $1/°K$. For both the high-density and the low-density samples of polyethylene we have obtained activation energy values which are essentially identical, 11.0 ± 0.2 kcal/mole based on $\tau_c^{(2)}$ and 10.7 ± 0.2 kcal/mole based on $\tau_c^{(av)}$. For the remainder of the discussion we shall refer to activation energy values based on $\tau_c^{(2)}$. Our results are in quite close agreement to those reported by Strukov and Rozantesev[11] for the nitroxide IV in polyethylene. They obtained a value of 10.7 kcal/mole for IV in a low-density (0.918 g/cm³) polyethylene and a value of 10.4 kcal/mole for IV in a high-density (0.950 g/cm³) polyethylene, based on $\tau_c^{(2)}$.

III   IV
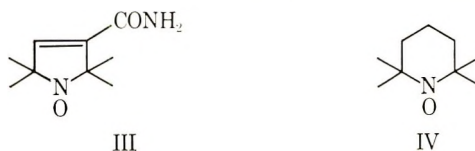
The close agreement would imply that the measured activation energy is primarily a function of the polymer and not of the particular probe used.

This is borne out in one instance below, but is not supported in a second case. More experiments with nitroxides of various sizes will help to clear up this point.

Figure 11 depicts the dependence of the results of the correlation time calculations on the microwave power levels employed. Although the results shown are for BzONO in the low-density polyethylene, similar results were obtained with all the samples for which the correlation time could be calculated. From a pragmatic standpoint, the near constancy of the values of $\tau_c^{(av)}$ justify its introduction as a measure of the nitroxide's molecular motion.

When the tumbling frequency of the nitroxide probe increases the linewidths all tend to narrow, due to an averaging out of the g-factor and hyperfine anisotropies. It is interesting that the limiting linewidth for the M=O line (i.e., center line of Figure 1) is about 1.65 gauss for BzONO in the polyethylene and the polypropylene samples, but is about 1.35 gauss for the styrene–butadiene copolymers (Fig. 12). In the previous paper (2) the linewidth for BzONO in a sodium dodecyl sulfate micelle was shown to be 1.40 gauss, suggesting that its limiting value would be similar to those of the styrene–butadiene latexes. One explanation of this apparent discrepancy is that the motion of the probe in the polyethylene and polypropylene host is not entirely isotropic. This could arise from the high degree of orientation which might exist between the chains of the polyethylene and polypropylene samples, an orientation which might not be present in the styrene/butadiene copolymers. The limiting linewidth (M=O) for BzONO in the ethylene–propylene copolymers listed in Table I is about 1.55 gauss. It is known that the lines of nitroxides in hydrocarbon solvents can be narrowed by removing the dissolved oxygen. With BzONO in polyethylene we were able to decrease the linewidth about 5% by pumping on the sample during the measurements. The oxygen broadening is not large enough, however, to account for the differences mentioned above.

Polypropylene

The variations of the ESR spectra for BzONO and for HONO in polypropylene are quite similar to those for BzONO in polyethylene (cf. Fig. 2). As with polyethylene, there is evidence for a small fraction of the probe being in a mobile environment. Again, as with polyethylene, the smaller HONO has a larger fraction in the looser areas of the polymer. Figure 6 is a plot of the extrema separation versus temperature for BzONO and HONO in polypropylene. These two probes have values of 42 and 1°C, respectively, for T_w, each being somewhat higher than the corresponding values for the same nitroxides in polyethylene.

A calculation of E_a, the rotational energy barrier for BzONO in polypropylene, affords a value of 12.3 ± .2 kcal/mole, which is significantly higher than the corresponding value for BzONO in polyethylene. An Arrhenius plot for BzONO in polypropylene is shown in Figure 10. We

are not able to draw any firm conclusions at this point concerning the physical basis of the higher energy barrier.   It could be due either to a more rigid chain structure or to the steric effect of the pendant methyl groups.

Ethylene–Propylene Copolymers

We have examined the behavior of BzONO and HONO in two ethylene–propylene copolymers, whose compositions are 50 and 75% ethylene. From a plot of the extrema separation versus temperature one obtains a value of $T_w = 16°C$ for BzONO in the 50:50 ethylene–propylene copolymer, which lies between the values for this nitroxide in polyethylene or polypropylene.   In the 50:50 ethylene–propylene sample the spectra display the two polymer environments which were mentioned above for the polyethylene and polypropylene results.

The values of E_a for BzONO in the 50% and in the 75% ethylene copolymers are 10.5 and 9.6 kcal/mole, respectively.   HONO in the 75% ethylene copolymer gives a value of 7.6 kcal/mole.   The results for BzONO are
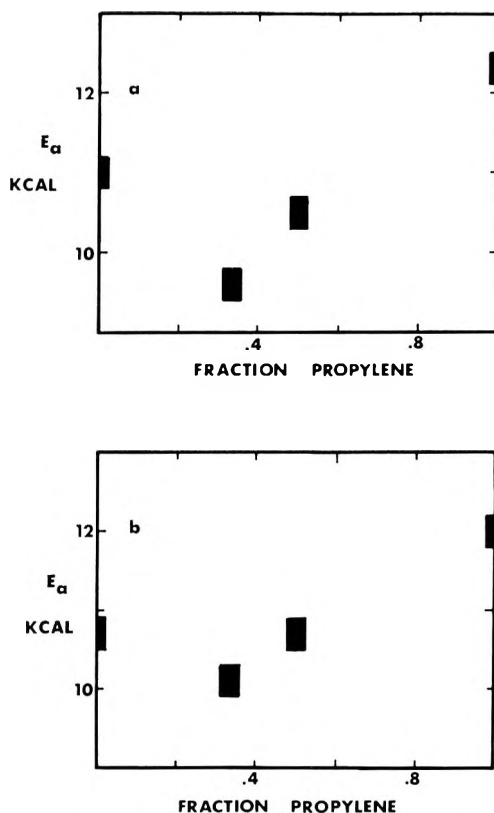

Fig. 14. Plots of the rotational activation energy E_a vs. polymer composition for BzONO in the ethylene–propylene copolymers and in the corresponding homopolymers: (a) based on $\tau_c^{(av)}$; (b) based on $\tau_c^{(2)}$.

shown in Figure 14, where the activation energy is plotted as a function of the polymer composition. There is a minimum in the curve at a propylene fraction of 0.33. It is interesting to compare this with the NMR results of Kontos and Slichter[12] and the mechanical measurements of Turley[13] where minima are obtained at the same propylene content. The lower energy barrier undoubtedly reflects a minimum in the content of ordered structural regions in the copolymer.

The activation energy value of 7.6 kcal/mole for HONO in the 75% ethylene copolymer is 2 kcal/mole less than for BzONO in the same polymer. This is in contrast to the results with BzONO and nitroxide IV in polyethylene, where only a 0.5 kcal/mole difference was observed. The actual physical significance of the calculated activation energies will remain somewhat clouded until one can determine what sort of an interplay there is between the polymer structure and the probe structure. Nevertheless, it is clear that it is not the polymer structure alone that determines the activation energy value which is obtained.

Polystyrene

The ESR spectra of polystyrene containing BzONO, and HONO show a temperature variation which is similar to the results obtained with polyethylene and polypropylene. With both probes there is evidence of two microscopic polymer environments which differ with respect to the degree of their motional restrictions. The plot shown in Figure 8, which is the variation of the extrema separation versus temperature for BzONO and HONO in polystyrene, differs from the similar plots for polyethylene and polypropylene in that the changes in the separation occur over a wider temperature range for polystyrene than is the case for the latter two polymers. It is most likely that this reflects a higher energy barrier to rotation which polystyrene offers the nitroxides. In the polystyrene sample derived from the latex the BzONO was unstable in the temperature region necessary to measure rotational correlation times for an activation energy calculation. However, using a polystyrene sample obtained from solution polymerization we were able to go to temperatures as high as 200°C without any noticeable nitroxide decomposition. The activation energy obtained from this sample is 18.3 kcal/mole. It should be pointed out that extrema separation versus temperature plots for both samples are essentially the same.

With polystyrene the difference between the values of T_w for HONO and for BzONO is larger than it is for any of the other polymers. If we assume that a cavity must exist in which the nitroxide can rotate we can draw certain conclusions about the changes that take place in the polymer as it is heated. The data from Figure 8 shows that cavities which are large enough to allow HONO to undergo rapid rotation are present at about 40°C. This is about 100°C below the temperature at which the cavities are large enough to allow BzONO to undergo the same degree of rotation. If the mode of nitroxide entrapment is similar for each of the polymers,

then it can be concluded that the loosening of the polystyrene matrix occurs over a wider temperature range than for the other polymers examined. This is supported by a comparison of the coefficients of expansion for polystyrene and polyethylene where that for polystyrene is smaller.

Poly(vinyl Chloride)

The ESR spectra of BzONO and of HONO in poly(vinyl chloride) over a wide temperature range are shown in Figures 3 and 4, respectively. It was not possible to obtain results above 190°C because the nitroxide was completely reacted at higher temperatures. This is most likely due to reaction of the nitroxide with decomposition products of the poly(vinyl chloride).

The feature which is most notable in these spectra is that they very clearly reflect the presence of two environments in which the nitroxide is situated. The more mobile nitroxide fraction is present in detectable amounts well below the glass transition temperature. The presence of the more mobile fraction is much more clearly seen with HONO as the probe, as is shown in Figure 4. These spectra were obtained by using the field modulation line sharpener described by Glarum.[7] The resolution is greater than what would ordinarily be obtained and the linewidths recorded are narrower than the actual linewidths. We have not attempted to make a quantitative estimate of the relative amounts of the probe in each particular type of environment for two reasons. First, such calculations would be extremely tedious and time-consuming. Second, and more important, one would need the distribution coefficient of the probe between the two regions, and it is not easily seen how such a number could be obtained.

The poly(vinyl chloride) data have been plotted in Figure 8 as the extrema separation versus temperature, as was done with the other polymers. It should be noted that these plots do not describe everything that is taking place with respect to the motion of the nitroxide. They pertain only to the behavior of the less mobile fraction, since it is this fraction which has the largest separation between its outermost lines. It is reasonable to assume, therefore, that such a plot is descriptive of the more ordered regions of the polymer matrix. This would also hold, of course, for the other polymers examined above. The break in the curve for BzONO in poly(vinyl chloride) is of about the same degree of sharpness as is observed for the polyethylene and polypropylene curves, and is sharper than was the case for the polystyrene curve. Also, the difference in T_w for the BzONO and HONO curves is about 25°C, which is quite similar to the polyethylene and polypropylene results. We shall discuss these figures in more detail below.

Styrene–Butadiene Copolymers

The composition of the styrene–butadiene copolymers is listed in Table I. They vary over the limited range of 42–62% styrene. We have plotted
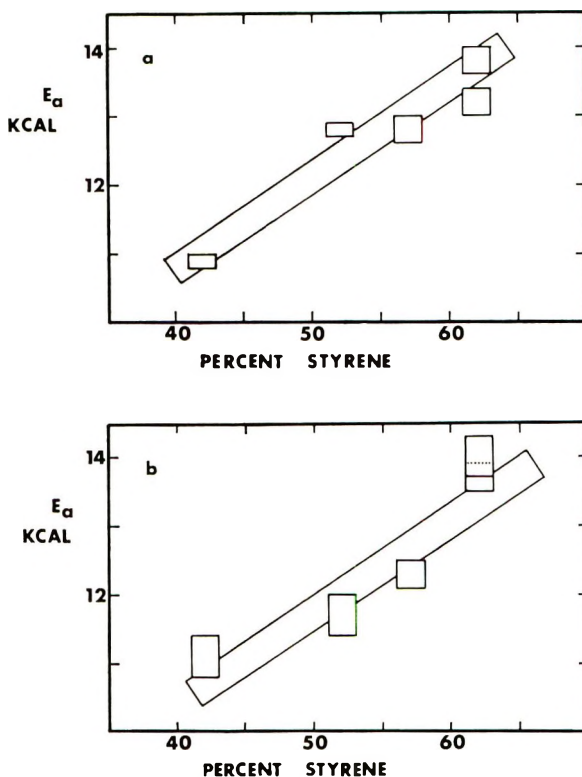
Fig. 15. Plots of the rotational activation energy E_a vs. polymer composition for BzONO in the styrene–butadiene copolymers of Table I: (a) based on $\tau_c^{(av)}$; (b) based on $\tau_c^{(2)}$.

the temperature variation of the extrema separation for three of the styrene–butadiene copolymers with styrene contents of 42, 52, and 62% in Figure 9. The curves for the copolymers which are higher in styrene are shifted toward higher temperatures, indicating that at a given temperature the nitroxide probe has less rotational mobility in these copolymers. This is also shown by an examination of the rotational energy barriers for BzONO in each of these copolymers listed in Table II. These values for the rotational activation energy were calculated from the slopes of the Arrhenius plots. The values of E_a for each of the styrene–butadiene copolymers, taken from Table II, are plotted in Figure 15 as a function of the per cent styrene. While there is considerable scatter in the points, the trend is quite clear. If it is valid to extrapolate the data of Figure 15 to pure polystyrene one obtains a value of 18 kcal/mole for the rotational activation energy of BzONO in polystyrene. This is in agreement with the value of 18.3 kcal/mole obtained from measurements on the polystyrene homopolymer.

As with the other polymers, there is evidence from the ESR spectra for the presence of two microscopic environments in which the probe is situated.

The contribution from the more mobile fraction is very much smaller than that from the more hindered fraction, and its relative amount in the styrene/butadiene copolymers is also much lower than the corresponding amount in poly(vinyl chloride).

We have measured the energy barrier to motion for nitroxide III in SB-62, which has 62% styrene, and have obtained a value of 12.6 ± 0.2 kcal/mole which is to be compared with 13.7 ± 0.2 kcal/mole for BzONO in this same polymer.

Hydrocarbon Solvents

It is of interest to compare the results mentioned above with the results of similar experiments in hydrocarbon solvents. Figure 13 shows the plots of the extrema separation versus temperature for BzONO in methylcyclohexane and in a 1:1 mixture of toluene and cyclohexane. The curve for methylcyclohexane is not as sharp as that for the toluene–cyclohexane mixture, but is much more sharp than those curves for the polymers. The methylcyclohexane forms a glasslike structure when rapidly cooled to −180°C. For the first half hour in this temperature region the spectra are remarkably similar to those for the probe-doped polymers. They clearly indicate the presence of two environments in the methylcyclohexane. At this temperature the solvent is about 10°K above its reported T_g of 85°K.[14] After standing at these low temperatures for about $1/2$ hr the narrow lines of the spectrum broaden until just a single environment is visible. This change very likely reflects a relaxation of the stresses which were frozen into the solvent during its rapid cooling. We hope to discuss this aspect of the relaxation of frozen solvents at a later date. The plot of Figure 13 is on the stress-free solution. We do not dwell on the results from the toluene/cyclohexane mixture but merely point out that the shape of its curve in Figure 13 probably reflects a solid–liquid transition rather than a glass–liquid transition.

An Arrhenius plot of the data for BzONO in methylcyclohexane yields a value of 3.8 ± 0.2 kcal/mole for the energy barrier to rotation. This is about three times lower than the values for this same nitroxide in polyethylene and polypropylene. The value is about twice as large as the rotational energy barrier for a methyl group in poly(methyl methacrylate).[15]

General Considerations

From the results and discussion above it is apparent that the spin-probe technique can be applied quite profitably to a study of molecular motions in polymeric materials. The data obtained cannot only be correlated well with known parameters of the polymers, but they can also yield a new parameter, the activation energy for the rotation of a guest molecule in a host polymer. This measure of the rotational energy barrier should be directly applicable to studies of plasticized polymers and also to questions relating to the behavior of antioxidants. In addition to these areas, one is also able to determine from the ESR line shape that a particular material,
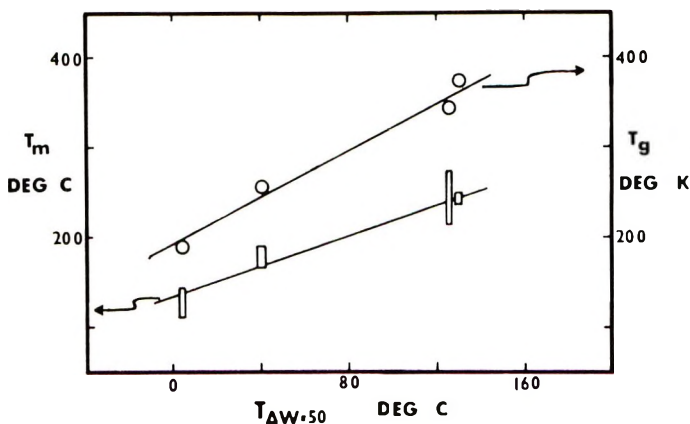
Fig. 16. Plots of (□) T_m and (○) T_g vs. T_w for polyethylene, polypropylene, poly-(vinyl chloride), and polystyrene. Note that units of T_m are degrees Centigrade and those of T_g are in degrees Kelvin. The lines are therefore vertically offset.

in this case the nitroxide probe, is not only uniformly dispersed throughout the polymer matrix, but that it is in true solution.

An example of the correlation of the data from the spin-probe experiments with known parameters of the polymers examined is presented in Figure 16. This is a plot of T_m and T_g versus T_w. The T_m and T_g data were taken from the *Polymer Handbook*,[16] and all values reported there are included in the points on the graph. We do not at present have a physical model to describe the polymer–probe interactions, but it does appear that one can use T_w and the slope of the lines of Figure 16 to obtain reliable values for T_m and T_g. Since T_w appears between T_m and T_g it might be more desirable to measure T_w in cases where T_m or T_g appear at inconveniently high or low temperatures. The difference between the values of T_w for HONO and BzONO in each of the polymers can serve as a secondary measure of the rate of expansion of polymer with temperature. The larger ΔT_w is, the lower will the rate of expansion of the polymer be.

References

1. R. F. Boyer, *Rubber Revs.*, **36**, 1303 (1963).

2. G. P. Rabold, *J. Polym. Sci. A-1*, this issue.

3. D. Kivelson, *J. Chem. Phys.*, **33**, 1094 (1960).

4. T. J. Stone, T. Buckman, P. L. Nordio, and H. M. McConnell, *Proc. Nat. Acad. Sci. U. S.*, **54**, 1010 (1965).

5. E. G. Rozantsev, V. A. Golubev, and M. B. Neiman, *Bull. Acad. Sci. USSR*, **1965,** 379.

6. R. Briere, H. Lemaire, and A. Rassat, *Bull. Soc. Chim. France*, **1965,** 3273.

7. S. H. Glarum, *Rev. Sci. Instr.*, **36,** 771 (1965).

8. M. S. Itzkowitz, *J. Phys. Chem.*, **46,** 3048 (1967).

9. R. Kosfeld, *Plasticization and Plasticizer Processes (Adv. Chem. Ser.*, No. 48), American Chemical Society, Washington, D. C. (1964).

10. J. W. Vanderhoff, paper presented at 2nd Symposium of the Annual Great Lakes Conferences on Polymer and Colloid Science, Northwood Institute Campus, Midland, Michigan, June, 1968.

11. V. B. Strukov and E. G. Rozantsev, *Vysokomol. Soedin. A*, **10,** 626 (1968).

12. E. G. Kontos and W. P. Slichter, *J. Polym. Sci.*, **61,** 61 (1962).

13. Private communication to R. F. Boyer (See p. 1371 of ref. 1). S. Turley

14. B. Wunderlich, *J. Phys. Chem.*, **64,** 1052 (1960).

15. K. Bergmann and K. Nawotki, *Molecular Relaxation Processes*, Chemical Society Special Publication No. 20, Academic Press, New York, 1966.

16. *Polymer Handbook*, J. Bandrup and E. H. Immergut, editors, Interscience, New York, 1966.

Selective Reactivities and Accessibilities of the Hydroxyl Groups in Cotton Cellulose Based on Equilibrium Data from a Reversible Chemical Reaction*

V. O. CIRINO, A. L. BULLOCK, and S. P. ROWLAND,
Southern Regional Research Laboratory, Agricultural Research Service, U. S. Department of Agriculture, New Orleans, Louisiana 70119

Synopsis

In order to determine the relative equilibrium constants for reactions of the hydroxyl groups at C_2, C_3, and C_6 of the D-glucopyranosyl units, methyl vinyl sulfone was reacted with cellulose dissolved in benzyltrimethylammonium hydroxide. The reaction was carried to constancy in distribution of substituents between the 2-0- and 6-0-positions. The distributions of substituents in the D-glucopyranosyl units were measured by gas-liquid chromatographic analysis of the products from hydrolysis of the modified cellulose. Relative equilibrium constants were then evaluated, assuming complete accessibility of all three types of hydroxyl groups of the cellulose in solution. For determination of the relative accessibilities of the individual types of hydroxyl groups in heterogeneous reactions of cotton cellulose with methyl vinyl sulfone, the reactions were carried to equilibrium distributions in media of various normalities of sodium hydroxide (i.e., media of various swelling strength). The distributions of substituents in the D-glucopyranosyl units were measured. From these values and the ratio of equilibrium constants, the relative accessibilities of the hydroxyl groups at C_2 versus those at C_6 were calculated. Apparent accessibilities of the hydroxyl groups at C_2 are approximately double those at C_6 when the reaction is carried out in $1N$ sodium hydroxide and about triple those at C_6 when the reaction is carried out in $0.5N$ sodium hydroxide.

INTRODUCTION

Chemical reactions of cellulose have generally been interpreted to occur with the hydroxyl groups of chain segments in regions of imperfect lateral order.[1] The concept of Marchessault and Howsmon,[2] which pictures these regions ranging progressively from near perfect order to complete disorder (laterally), has often been adopted as a part of the larger concept such as the fringed micelle theory of the microstructure of cellulose.[3]

An increasing disparity of physical data with this type of picture of the microstructure of cellulose has developed over the past several years, the data being rather more indicative of a fringed fibril structure (i.e., lower

---

* Presented at the 24th Annual Southwest Regional Meeting of the American Chemical Society, Austin, Texas, December 4–6, 1968.

order only in the fringed regions of the fibrils[4]) or a paracrystalline fibril structure (low order in imperfections in an otherwise crystalline structure).[5] The latter case requires accessible hydroxyl groups to be those on the surfaces of elementary fibrillar structures. Recently, Jeffries et al.[6] interpreted the distribution of substituents introduced into the D-glucopyranosyl units of cotton cellulose from repeated methylations with dimethyl sulfate and $2N$ sodium hydroxide to be consistent with a rapid reaction occurring on the surfaces of elementary fibrils together with a slower reaction resulting from penetration to hydroxyl groups beneath these surfaces. At the extrapolated point which represented completion of the rapid stage of the reaction, 56% of the D-glucopyranosyl units were without substituents, i.e., inaccessible to the reagent. This degree of inaccessibility is essentially that to be expected from the reaction on surfaces of elementary fibrils having dimensions (from electron microscopy) of ca. 50 Å by 50–100 Å and having a rectangular cross section consisting of 8 D-glucopyranosyl units on one side and 12 units on another. More recently, Wade et al.[7] have shown that the selectivity of reaction of 2-chloroethyldiethylamine at the hydroxyl group at C_2 of the D-glucopyranosyl unit of cotton cellulose increases as the normality of the sodium hydroxide (catalyst) is decreased from $4N$ (borderline mercerizing) to $1N$ to a nonaqueous system in which the base is insoluble. On the basis of these results, it was considered probable that heterogeneous reactions of cellulose which are conducted in media which are weaker swelling agents than mercerizing caustic take place on the surfaces of the microstructural units of the cotton cellulose fiber.

The work described here was undertaken with the twofold objective: (a) to test the simple method of Touzinsky[8] for estimating the distribution of substituents in the D-glucopyranosyl units of cellulose from a reversible reaction carried to equilibrium in a mercerizing medium and (b) to utilize a modification of his mathematical approach on data from reactions in various nonmercerizing media to obtain measures of accessibilities under these conditions of reaction. It soon became evident that with the reagent of our choice, i.e., methyl vinyl sulfone, the relative reactivities of the hydroxyl groups at C_2, C_3, and C_6 in the D-glucopyranosyl units were dependent upon the degree of substitution;[9] it now appears quite general that a substituent in the 2-0-position activates the hydroxyl group at C_3 by a factor of ca. 2–4.[10] Further, it became impossible to attain the same distribution of substituents at equilibrium in nonmercerizing media as in mercerizing media. This dilemma is discussed in this report; the selective reactivities which have been encountered in these reactions of fibrous cotton in aqueous media of various swelling strengths are pertinent to selective accessibilities of the hydroxyl groups at C_2 and, we believe, to the further evidence that reactions of cotton cellulose may be limited to surfaces of microstructural units or to controlled penetration into the structural units depending upon the swelling strength of the medium employed for the reaction.

EXPERIMENTAL

Materials

The cotton cellulose (desized, scoured, bleached, 80 × 80 print cloth weighing 3.3 oz/yd) was reduced to the form of (1) chopped fibers (chopped in a Wiley mill to pass a 20-mesh screen) and (2) decrystallized cotton cellulose (ball-milled 30 min in a vibratory mill[11]). Reagents were used as received from the following sources: methyl vinyl sulfone (K&K Laboratories, Inc.); trimethylchlorosilane (General Electric Co.); hexamethyldisilizane (Peninsular Chemresearch); acid-washed dimethyldichlorosilane-treated Chromosorb G, 100–120 mesh (Johns-Manville Corp.); QF-1 liquid phase (Wilkens Instrument and Research, Inc.); benzyltrimethylammonium hydroxide (aqueous, 40% Triton B) (Miles Laboratories, Inc.); Aerosol OT (American Cyanamid Co.).

Gas–Liquid Chromatography

The gas chromatograph was an F&M Model 1609 unit equipped with a flame ionization detector. The column was prepared from 3% QF-1 on Chromosorb G in stainless steel tubing 0.25 in. in outside diameter and 5.5 ft long.

Methylsulfonylethyl Celluloses

Homogeneous Reaction with Chopped Fibers (A). Chopped fibers [2 g 0.0123 mole calculated as anhydroglucose units (AGU)] were wet with distilled water (14.10 g, containing 0.04% Aerosol OT) and added to aqueous benzyltrimethylammonium hydroxide (45.10 g of 63% solution). The mixture was stirred under an atmosphere of nitrogen until a solution resulted. The benzyltrimethylammonium hydroxide of 63% concentration was prepared from 40% material by evaporation on a rotary evaporator while immersed in a water bath at 40°C. Sodium hydroxide (11.22 g of a 19.8% solution, 0.0555 mole) was added to the dissolved cellulose. The solution was stirred at 4°C under nitrogen. Methyl vinyl sulfone (11.26 g, 0.106 mole, about a threefold excess over hydroxyl groups) was added and stirring was continued. Samples were removed at 10-min, 30-min, 3-hr, 24-hr, and 48-hr reaction times, and the samples were neutralized with dilute acetic acid; methanol was added to facilitate filtering. The insoluble material was removed by filtration and washed several times with methanol–water (1:1) then with methanol and finally allowed to air-equilibrate.

Homogeneous Reaction with Ball-Milled Cotton (B). Sodium hydroxide (11.2 g of 40% solution, 0.112 mole) was added to 4 g (0.0247 mole of AGU) of ball-milled cotton, which had been wet with 28.1 g water (containing 0.04% Aerosol OT) and dissolved in an aqueous solution of benzyltrimethylammonium hydroxide (115.48 g. of 55.5% solution). The solution was stirred under an atmosphere of nitrogen and maintained at

6-8°C. Methyl vinyl sulfone (22.53 g, 0.213 mole, ca. threefold excess over hydroxyl groups) was added and stirring was continued. Samples were withdrawn at reaction times of 19 min, 60 min, 12 hr, 32 hr, and 48 hr. The reaction mixtures were neutralized with dilute acid and isolated as described above.

Homogeneous Reaction of Ball-Milled Cotton with Higher Concentrations of Methyl Vinyl Sulfone (C). Sodium hydroxide (3.05 g of a 24.6% solution, 0.0188 mole) was added to ball-milled cotton (1 g, 0.0062 mole of AGU) which had been wet with 7.05 g water (containing 0.04% Acrosol OT) and dissolved in aqueous benzyltrimethylammonium hydroxide (24.9 g of 55% solution). Methyl vinyl sulfone (9.8 g, 0.0925 mole, ca. fivefold excess over hydroxyl groups) was added. The reaction was stirred under an atmosphere of nitrogen and maintained at 10-11°C. Samples were withdrawn at 48 and 72 hr. The samples were neutralized with dilute acetic acid and isolated as described above.

In another experiment (D), a reaction was conducted under the same conditions as (C) except that the ball-milled cotton (wet with water containing Aerosol OT) was dissolved in 20.9 g. of 65% benzyltrimethylammonium hydroxide (aqueous solution) and a 7.5-fold excess of methyl vinyl sulfone (14.3 g., 0.135 mole) was added. The mixture was stirred under an atmosphere of nitrogen and maintained at 10-11°C. Samples were withdrawn, neutralized, and isolated as described above.

Heterogeneous Reaction of Fibrous Cotton to Determine Equilibrium Conditions (E). Chopped fibers (4 g, 0.0247 mole of AGU) were dispersed in 120 ml of 0.5N sodium hydroxide solution (0.060 mole) at room temperature for 30 min. Methyl vinyl sulfone (38 g, 0.358 mole) was added with stirring. The reaction was continued with agitation for periods of 17 min, 64 min, 5 hr, 22 hr, 46 hr, and 70 hr. At the end of each period ca. 1/6 of the reaction mixture was withdrawn and neutralized with dilute acetic acid. The samples were washed with distilled water until the wash water was free of salts. The samples were then allowed to air-equilibrate.

Heterogeneous Reactions of Fibrous Cotton (F). Samples of chopped fibers (1 g, 0.0062 mole of AGU) were dispersed in 30 ml of sodium hydroxide solution (0.5, 1.0, 2.0, or 4.0N) at room temperature for 30 min. Methyl vinyl sulfone (9.5 g, 0.0896 mole) was added with stirring. The reactions were continued until equilibrium was reached (one series for 48 hr and a second series for 72 hr). At the end of the reaction periods the samples were neutralized and isolated as described above.

Hydrolysis of Methylsulfonylethyl Celluloses and Estimation of the Distribution of Substituents

Samples of the methylsulfonylethyl celluloses were dissolved in 72% sulfuric acid and hydrolyzed according to the method of Rowland et al.[12] The acid was neutralized with barium hydroxide, filtered, and the filtrate freeze-dried to a solid mixture of glucose and O-methylsulfonylethyl-D-

glucopyranoses. Trimethylsilyl ethers[13] of the dry hydrolyzates were prepared and analyzed for the ratio of the 2-0-, 3-0-, and 6-0-mono (methylsulfonylethyl)-D-glucopyranoses by gas–liquid chromatography[12] (isothermal at 220°C and 50 psig on a QF-1 column).

RESULTS

The general course of a reaction of methyl vinyl sulfone with cellulose is that in which the degree of substitution increases rapidly, passes through a maximum, and decreases progressively to zero as the reagent in the aqueous medium is depleted by side reactions (i.e., formation of 2-hydroxyethyl methyl sulfone and bis[2-(methylsulfonyl) ethyl] ether).[14] The relationship between degree of substitution and duration of reaction is illustrated in curves A and B of Figure 1 for reactions of cotton cellulose of conventional molecular weight (curve A, chopped fibers) and of reduced molecular weight (curve B, ball-milled cellulose) dissolved in benzyltrimethylammonium hydroxide at 4–8°C. The differences here appear to be due to the fact that the cellulose of conventional molecular weight (DP ca. 3500) was present to some extent as dispersed gel particles while the ball-milled cellulose (DP ca. 500) was present in true solution.

The ratio of substitution in the 2-0-position to that in the 6-0-position of the monosubstituted D-glycopyranosyl units is plotted in Figure 2 (Curve AB) as a function of the duration of the reactions described above. It is evident that this ratio decreases and approaches a constant value as extended time is allowed for reaction within the cellulose to reach equilibrium
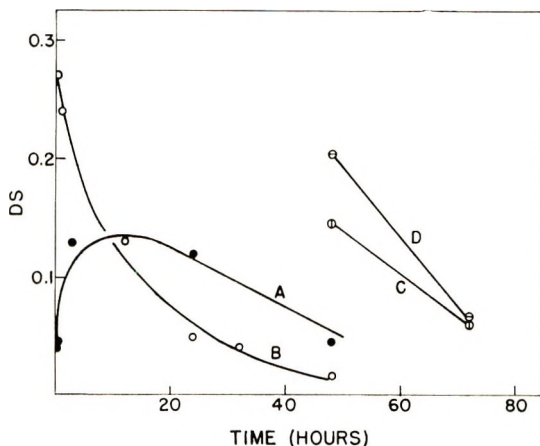
Fig. 1. Variation in degree of substitution (DS) with reaction time in the homogeneous reactions of methyl vinyl sulfone with cellulose: (A) chopped fibers dissolved in benzyltrimethylammonium hydroxide, 3-fold excess methyl vinyl sulfone; (B) ball-milled cotton dissolved in benzyltrimethylammonium hydroxide, 3-fold excess methyl vinyl sulfone; (C) ball-milled cotton dissolved in benzyltrimethylammonium hydroxide, 5-fold excess methyl vinyl sulfone; (D) ball-milled cotton dissolved in benzyltrimethylammonium hydroxide, 7.5-fold excess methyl vinyl sulfone.

distribution between these two positions.   In order to extend the data in Figure 2 beyond the 48-hr limit of reactions represented by curves A and B in Figure 1, reactions similar to that of curve B were conducted with higher concentrations of methyl vinyl sulfone; the results, which are shown in Figure 1 as curves C and D, provide the smooth extension of
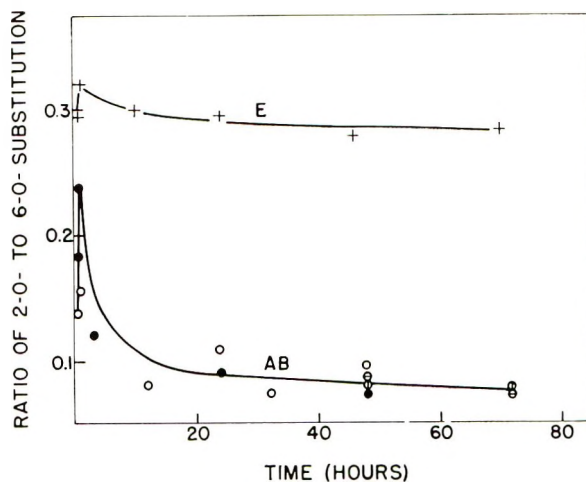
Fig. 2. Variation in 2-0-/6-0-substitution with reaction time in reactions of methyl vinyl sulfone with cellulose: AB homogeneous reactions; (E) heterogeneous reaction in 0.5N sodium hydroxide.

curve AB in Figure 2 to 72 hr.   The scatter of points in curve AB of Figure 2 is substantially broader than our normal experience in the measurement of the ratio of substitution in the 2-0- to 6-0-position; it appears to be related to the medium for this reaction.

Heterogeneous reactions of methyl vinyl sulfone with cotton cellulose were conducted in the presence of solutions of sodium hydroxide of various

TABLE I

Ratio of 2-0- to 6-0-Substitution in Cotton Cellulose as a Result of
Reactions Conducted in Alkaline Media of Various Swelling Strengths

Medium	Ratio of 2-0- to 6-0-substitution		
	At 48 hr	At 72 hr	Average
Homogeneous solution in benzyltri- methylammonium hydroxide	0.083	0.078	0.08
4N Sodium hydroxide (mercerizing strength)	0.101	0.092	0.10
2N Sodium hydroxide (nonmercerizing)	0.120	0.100	0.11
1N Sodium hydroxide	0.178	0.167	0.17
0.5N Sodium hydroxide	0.27	0.268	0.27
0.1N Sodium hydroxide	No reaction		

concentrations. The change of the ratio of substitution in the 2-0- to 6-0-position throughout the reaction of methyl vinyl sulfone with fibrous cellulose in $0.5N$ sodium hydroxide is shown in Figure 2 (curve E). Equilibrium distribution of substituents among the various types of hydroxyl groups was complete at 48 hr of reaction. The results at these steady states of distribution of substituents between the 2-0- and 6-0-positions for the reactions conducted in various concentrations of sodium hydroxide are listed in Table I (together with results for the reactions conducted in solution in benzyltrimethylammonium hydroxide) in descending order of (potential) swelling strength for cellulose. The $4N$ sodium hydroxide (13.9% solution) is a borderline mercerizing medium for cellulose at $25°C$; the lower concentrations are below mercerizing strength and can only be estimated to have swelling effects in the order listed.[15] It is significant that the ratio of substitution at the 2-0- and 6-0-positions increased progressively from top to bottom of the table: i.e., as the estimated swelling strength of the medium decreased.

It is interesting that the reactions in the more concentrated solutions of sodium hydroxide showed patterns of reaction similar to that of curve A of Figure 1. On the other hand, the reaction in $0.5N$ sodium hydroxide proceeded rapidly to a degree of substitution of approximately 0.15 and maintained a similar level at 48 and 72 hr of reaction. Thus, the side reactions of the methyl vinyl sulfone occur to much smaller extent in the dilute solutions.

Changes in the ratio of substitution at the 3-0- to 6-0-positions with variation in reaction media are subject to considerable uncertainty. Constancy in this ratio was observed in products from 48-hr and 72-hr reaction periods in the cases involving fibrous cellulose in heterogeneous reactions. On the other hand, constancy was not realized in the case of homogeneous reactions in benzyltrimethylammonium hydroxide. Only a tentative explanation can be offered at this time: i.e., that the slow reverse reaction at the 3-0-position is significantly slower than the rate at which the overall equilibrium is upset by the consumption of methyl vinyl sulfone in side reactions in this medium. Qualitatively, the significance of the side reactions appears to decrease from reaction in homogeneous solution in benzyltrimethylammonium hydroxide to heterogeneous reactions in $4N$, $2N$, $1N$, and $0.5N$ sodium hydroxide. The ratios of 3-0- to 6-0-substitution observed for reactions in the various media are: 0.22/1.00 rather arbitrarily, 0.17/1.00, 0.07/1.00, 0.05/1.00, and 0.08/1.00 for benzyltrimethylammonium hydroxide solution and for $4N$, $2N$, $1N$, and $0.5N$ sodium hydroxide media, respectively.

DISCUSSION

The reversible reaction of methyl vinyl sulfone with the hydroxyl groups at C_2, C_3, and C_6 of the D-glucopyranosyl units may be abbreviated as shown in eq. (1) where CellOH designates cellulosic hydroxyl groups, R

designates reagent (methyl vinyl sulfone), and CellORH designates the
0-[2-(methylsulfonyl)ethyl]cellulose resulting from the reaction.

$$CellOH + R \rightleftharpoons CellORH \tag{1}$$

For each type of hydroxyl group (as indicated by the subscript), the
expression of the equilibrium constant, K, is as shown below:

$$K_2 = \frac{a_{CellORH_{(2)}}}{a_{CellOH_{(2)}}a_R} = \frac{[CellORH_{(2)}]}{[CellOH_{(2)}][R]}\frac{\gamma_{CellORH_{(2)}}}{\gamma_{CellOH_{(2)}}\gamma_R} \tag{2}$$

The activity for each species (designated by a) is the product of the con-
centration of that species (in brackets) and an activity coefficient γ, the
latter being referred most commonly to the standard state of infinite dilu-
tion of the solute.[16] For equilibrium measurements involving dilute solu-
tions, it is often possible to obtain adequate accuracy by replacing the
activities with concentrations: i.e., the activity coefficients are unity.

It is assumed that in solutions of cellulose the hydroxyl groups are
equally accessible at C_2 and C_6, i.e., $[CellOH_{(2)}] = [CellOH_{(6)}]$. Since the
concentration (or activity) of the reagent, R, in equilibrium with the vari-
ous hydroxyl groups is one and the same, the ratio of the equilibrium
constant for the reaction at the hydroxyl group on C_2 to that for the
reaction at the hydroxyl group on C_6 becomes $[CellORH_{(2)}]/[CellORH_{(6)}]$.*
At low degrees of substitution this is the ratio of substituents in the mono-
substituted D-glucopyranosyl units. The value of K_2/K_6 determined from
the reactions in homogeneous solutions in benzyltrimethylammonium
hydroxide is 0.08 (see Table I).

In the case of reactions of fibrous cellulose, it is well known that only a
fraction of the total hydroxyl groups is accessible; thus, the concentrations
of hydroxyl groups at C_2 and at C_6 which are available to the reagent are
unknown. Furthermore, the chemical reaction may involve surfaces, and
the diffusion of the reagent to the surfaces or the diffusion of byproducts
away from the surfaces may be rate controlling. However, in neither case
is the thermodynamic statement of equilibrium violated, since both the
forward and reverse reactions depend on the surface area in the same way;
this factor cancels out when the two rates are equated at equilibrium.[17]

To express the equilibrium constant for reactions involving fibrous cellu-
lose in a heterogeneous phase, it is useful to express the activity of each
species as the product of three factors: the activity of the reference state,
Γ; a factor expressing concentration (in brackets); and the activity co-
efficient, γ, which again expresses the deviation from ideal solution behav-

---

* This same expression, i.e., $K_2/K_6 = CellORH_{(2)}/CellORH_{(6)}$, results when the right
side of equation (2) is divided by a corresponding expression for the reaction at the
hydroxyl group on C_6. It then follows that the activity coefficients for $CellORH_{(2)}$ and
$CellORH_{(6)}$ may be considered to be essentially equal, if not identical; the same applies
to the activity coefficients for $CellOH_{(2)}$ and $CellOH_{(6)}$.

ior.[18]   When the expression for the equilibrium constant for reaction of the hydroxyl group at C_2, as indicated in eq. (3), is divided by

$$K_2 = \frac{\Gamma_{CellORH_{(2)}}}{\Gamma_{CellOH_{(2)}}\Gamma_R} \frac{[CellORH_{(2)}]}{[CellOH_{(2)}][R]} \frac{\gamma_{CellORH_{(2)}}}{\gamma_{CellOH_{(2)}}\gamma_R} \qquad (3)$$

a corresponding expression for the equilibrium constant for reaction of the hydroxyl group at C_6, the ratio of the two equilibrium constants may be reduced to eq. (4).   This simplification is based on the equivalency

$$K_2/K_6 = \frac{[CellORH_{(2)}]}{[CellORH_{(6)}]} \frac{[CellOH_{(6)}]}{[CellOH_{(2)}]} \qquad (4)$$

of the reference states and on the reasonable assumption or approximation that the activity coefficients of the different types of hydroxyl groups in
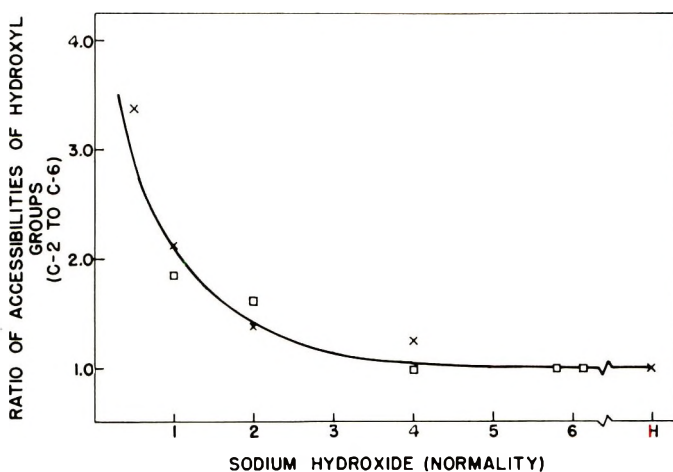
Fig. 3. Comparison of relative accessibilities of hydroxyl groups on C_2 and C_6 from a nonreversible reaction and a reversible reaction with normality of sodium hydroxide (H = homogeneous reactions in benzyltrimethylammonium hydroxide):   (×) relative accessibilities from reactions of methyl vinyl sulfone; (□) relative accessibilities based on reactions of 2-chloroethyldiethylamine.[7]

the "solid solution" are equal and that the same is true for the individual types of substitution products.   The rearrangement of eq. (4) to the form shown in eq. (5) provides an expression for evaluating the ratio

$$\frac{[CellOH_{(2)}]}{[CellOH_{(6)}]} = \frac{K_6}{K_2} \frac{[CellORH_{(2)}]}{[CellORH_{(6)}]} = \frac{1}{0.08} \frac{[CellORH_{(2)}]}{[CellORH_{(6)}]} \qquad (5)$$

of accessible hydroxyl groups at C_2 to those at C_6.   The ratio of equilibrium constants is known from the equilibrium data for the reaction in homogeneous solution and, again, $[CellORH_{(2)}]/[CellORH_{(6)}]$, at low degree of

substitution is the ratio of substituents in the 2-0- and 6-0-positions of the monosubstituted D-glucopyranosyl units. Thus, the apparent accessibility of the hydroxyl groups at C_2 relative to those at C_6 is obtained by dividing the value of [CellORH$_{(2)}$]/[CellORH$_{(6)}$] listed in Table I by 0.08. The quotients are plotted in Figure 3 in relation to the normality of the solution of sodium hydroxide employed for the reaction of methyl vinyl sulfone. The ($\times$) symbols represent data from the reactions of methyl vinyl sulfone, whereas the square symbols refer to data of Wade et al.[7] from the reactions of 2-chloroethyldiethylamine. The published data on the latter reaction have been divided by the value of the ratio of the 2-0- to 6-0-substitution obtained from reactions in mercerizing media (i.e., 1.25) in order to put them on a basis similar to that employed for data from the methyl vinyl sulfone reaction.

The experimental scatter of data points in Figure 3 may be due in large part to the fact that there are inherent differences (of necessity) in the way the reactions have been carried out. It should be noted that the base is diluted with different reagents in each case and that the order in which the cellulose has been contacted with the components of the total reaction medium has also been different.

It is rather remarkable that data from a nonreversible reaction (i.e., with 2-chloroethyldiethylamine) at the outset of reaction and from a reversible reaction (i.e., with methyl vinyl sulfone) carried to steady state or equilibrium distribution of substituents yield generally similar indication of selective reactivities of the hydroxyl groups at C_2 and C_6. It is evident that the selective reactivities or apparent accessibilities of the hydroxyl groups of the fibrous cellulose change in a very similar manner for the two different types of reactions as the base strength of the reaction medium is altered. The confirmation between the two different reactions is considered indication that the effect is one of general and basic significance. It is well known that cotton cellulose swells to increasing extents in aqueous solutions of sodium hydroxide as the concentration of the base is increased.[15] The obvious possibility that changes in the selective reactivities or apparent accessibilities are due solely to different extents of penetration of reagent into the fibrous cellulose must be tempered by the consideration that other factors may also be operative. It must be emphasized that the activity coefficients of the hydroxyl groups at C_2 and C_6 have been assumed to be equal in the various media of reaction. Thus, inequalities or changes in the activity coefficients which actually occur from one to another reaction medium will be reflected in the foregoing selective reactivities or apparent accessibilities of the hydroxyl groups at C_2 and C_6. This is the subject of other studies.

References

1. J. Honeyman, *Recent Advances in the Chemistry of Cellulose and Starch*, Heywood, London, 1959, pp. 147–185.

2. R. H. Marchessault and J. A. Howsmon, *Text. Res. J.*, **27**, 30 (1957).

3. J. W. S. Hearle and R. H. Peters, *Fiber Structure*, Butterworth, London, 1963, pp. 212–213.

4. J. W. S. Hearle, *J. Polym. Sci.*, **28**, 432 (1958).

5. R. Hosemann, *Polymer*, **2–3**, 349 (1961–1962).

6. R. Jeffries, J. G. Roberts, and R. N. Robinson, *Text. Res. J.*, **38**, 234 (1968).

7. C. P. Wade, E. J. Roberts, and S. P. Rowland, *J. Polymer Sci. B*, **6**, 673 (1968).

8. G. F. Touzinsky, *J. Org. Chem.*, **30**, 426 (1965).

9. V. O. Cirino, A. L. Bullock, and S. P. Rowland, *Anal. Chem.*, **40**, 396 (1968).

10. S. P. Rowland, E. J. Roberts, A. L. Bullock, V. O. Cirino, C. P. Wade, and M. A. F. Brannan, *Text. Res. J.*, **38** (1968).

11. A. L. Bullock, S. P. Rowland, and V. O. Cirino, *Text. Res. J.*, **38** (1968).

12. S. P. Rowland. V. O. Cirino, and A. L. Bullock, *Can. J. Chem.*, **44**, 1051 (1966).

13. C. C. Sweeley, R. Bentley. M. Maketa, and W. W. Wells, *J. Amer. Chem. Soc.*, **85**, 2497 (1963).

14. S. P. Rowland, A. L. Bullock, V. O. Cirino, and C. P. Wade, *Can. J. Chem.*, **46**, 451 (1968).

15. J. O. Warwicker, *J. Polym. Sci. A-1*, **5**, 2579 (1967).

16. A. A. Frost and R. G. Pearson. *Kinetics and Mechanism*, 2nd ed., Wiley, New York, 1961, p. 127.

17. A. W. Adamson, *Physical Chemistry of Surfaces*, Interscience, New York, 1960, p. 284.

18. G. N. Lewis and M. Randall, revised by K. S. Pitzer and L. Brewer, *Thermodynamics*, 2nd ed., McGraw-Hill, New York, 1961. p. 250.

Free-Radical-Induced Polymerization of Epoxides in the Presence of Maleic Anhydride

SOHEI SUGA and HAJIME AOYAMA, *Department of Industrial Chemistry, Faculty of Technology, Kanazawa University, Kanazawa, Japan*

Synopsis

The free-radical-induced reactions of cyclohexene oxide in the presence of maleic anhydride have been found to lead to polyether in presence of AIBN and to a mixture of polyether, ester, and maleic anhydride adduct of polyether with di-*tert*-butyl peroxide (DTBP), the amounts of the mixture components depending on the concentration of DTBP and the temperature. Analogous reactions in the presence of succinic anhydride lead to no polyether. The obtained polyether has no hydroxyl group. The reaction appears to consist of three different steps, radical initiation, cationic propagation, and radical termination.

INTRODUCTION

The free-radical-induced polymerization of epoxides has been studied extensively. For example, propylene oxide is scarcely polymerized in the presence of di-*tert*-butyl peroxide (DTBP)[1] or ultraviolet light[2] as the initiator. Styrene oxide[3] affords polymer having a molecular weight of ca. 1 500–2 000 with DTBP. Conant and Peterson[4] observed that in the presence of benzoyl peroxide, cyclohexene oxide (CHO) was polymerized to a viscous liquid with difficulty, even under severe conditions. Lenzi and Mele[5] reported that it can be polymerized to give a solid amorphous polymer by ionizing radiation (γ-ray). From these studies the preparation of polyether of high molecular weight from epoxides by free-radical polymerization seems practically impossible. The free-radical-induced reactions of epoxides with 1-octene[1,2,6] and of tetrahydrofuran with maleic anhydride (MAH)[7,8] lead to 1:1 adducts. These studies prompted us to prepare a succinic derivative by the free-radical-induced reaction of CHO with MAH. However, this reaction proceeded in an unexpected way. Thus, when initiated by AIBN, polymerization of CHO was markedly accelerated to produce polyether exclusively with recovery of most of the MAH, while by the initiation with DTBP a mixture of ester and MAH adduct of polyether were obtained, in addition to polyether.

The present paper is concerned with a detailed study of the polymerization of CHO.

EXPERIMENTAL

Materials

Cyclohexene oxide (CHO) was prepared according to the method of Guss and Rosenthal[9] and distilled before use (bp 129–130°C, n_D^{20} 1.4526). Commercial grade maleic anhydride (MAH) was purified by vacuum sublimation (bp 93–94°C/23 mm Hg). Succinic anhydride was purified by recrystallization from ethanol (mp 119–120°C). Di-*tert*-butyl peroxide (DTBP) was purified by vacuum distillation (bp 45–46°C/76 mm Hg). α,α'-Azobisisobutyronitrile (AIBN) was the purest grade commercially available and used without further purification. All other reagents were purified according to standard procedures.

Procedure

AIBN-Induced Polymerization of CHO. Polymerization was carried out at 60°C in a sealed glass ampoule (diameter 20 mm, length 200 mm), charged with appropriate amounts of reactants in benzene and flushed with nitrogen. The tubes were immediately chilled in a Dry Ice–ethanol bath to stop polymerization. All volatile materials were removed *in vacuo*, and a large amount of methanol was poured into the residue. The precipitated polymer (I) was washed thoroughly to remove unchanged CHO, remaining MAH, and a small amount of poly(MAH), if any, then filtered and dried *in vacuo*.

DTBP-Induced Polymerization of CHO. Polymerization was carried out as described above at 150°C. All volatile materials were removed *in vacuo*, and the residue was separated into petroleum ether-soluble (II), water-soluble (MAH), and insoluble parts (III), in order. After petroleum ether was removed *in vacuo*, II was washed with a large amount of methanol to remove CHO and MAH. III was saponified with 10% sodium hydroxide for 1 hr and then acidified with concentrated hydrochloric acid. The precipitate was filtered, washed with distilled water till free of chloride ion, dried, and separated into petroleum ether-soluble (IV) and -insoluble parts (V).

Free-Radical-Induced Reaction of CHO in the Presence of Succinic Anhydride. A solution of 0.05 mole of CHO, 0.05 mole of succinic anhydride and 5×10^{-4} mole of radical initiator in 0.15 mole of benzene was charged in a glass ampoule as described above. The experiments with AIBN or DTBP were carried out for 5 hr at 60°C or 150°C, respectively. All volatile materials were removed *in vacuo*, and succinic anhydride was separated off by the addition of petroleum ether. No polyether was isolated from the petroleum ether solution.

Analytical Methods

For analysis of polymer, I and II were purified further by reprecipitation from chloroform solution with a large amount of methanol. Viscosity

measurements of benzene solution of polyether were performed in an Ostwald viscometer at 30°C. Molecular weight of polyether was determined by the cryoscopic method in cyclohexane. Acid equivalent measurements of V were carried out by the following procedure. The polymer (V) was dissolved in warm 0.1N sodium hydroxide, and excess alkali was titrated with 0.1N hydrochloric acid, thymolphthalein being used as indicator.

RESULTS

AIBN-Induced Polymerization of CHO

Polymer I obtained by AIBN-induced polymerization of CHO in the presence of MAH was a white powder melting at 87–92°C and was soluble in hydrocarbons and ether and insoluble in ethanol and acetone. Analytical data show fairly good agreement with the calculated value for $(CHO)_n$.

ANAL. Calcd for poly (CHO): C, 73.46%; H, 10.20%. Found: C, 71.44%; H, 10.93%.

The infrared spectrum (Fig. 1) exhibited characteristic bands at 1 085 cm^{-1} (ether) and at 2 925, 2 858, and 1 450 cm^{-1} (methylene). It seems clear that polymer I has the polyether structure derived from CHO.

The effect of the concentration of CHO on polymerization is shown in Figure 2. Polymerization of CHO rarely occurred in the absence of radical initiator at 60°C without coloration. In the presence of radical initiator,
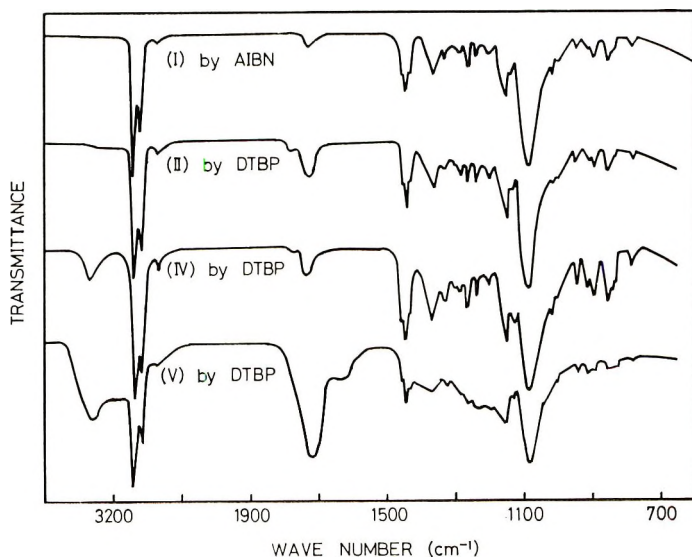
Fig. 1. Infrared spectra of polymers obtained by the free-radical-induced polymerization of CHO in the presence of MAH.

Fig. 2. AIBN-induced polymerization of CHO at different concentration of CHO in the presence of MAH in benzene at 60°C. (○) [CHO] = 20 mole-%; (×) [CHO] = 40 mole-%; (△) [CHO] = 60 mole-%; (□) [CHO] = 80 mole-%, (●) [CHO] = 20 mole-%, no radical initiator (based on the total amount of reaction mixture); [MAH] = 20 mole-%, [AIBN] = 0.2 mole-%.
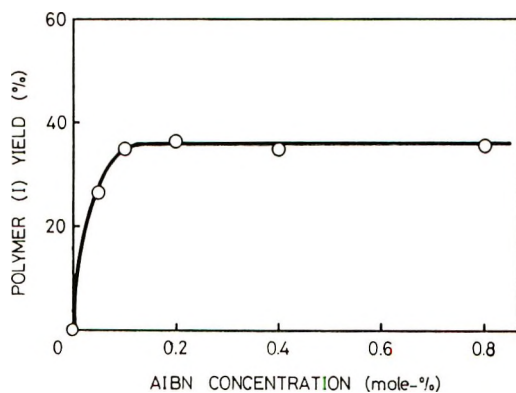
Fig. 3. Effect of the concentration of AIBN on polymerization of CHO in benzene at 60°C for 15 hr; [CHO] = 20 mole-%, [MAH] = 20 mole-%, based on the total amount of reaction mixture.
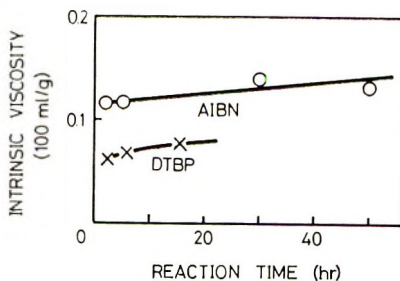
Fig. 4. Relation between reaction time and intrinsic viscosity of polyether at 30°C in benzene. Polymers obtained under the following reaction conditions: [CHO] = 40 mole-%, [MAH] = 20 mole-%, [radical intiator] = 0.2 mole-%.

the rate of polymerization increased with increasing concentration of CHO, while the reacting mixture turned yellow brown.

The yield of I increased with increasing concentration of AIBN up to 0.1 mole-%, and remained constant above that concentration (Fig. 3).

The intrinsic viscosity of I was in the range of 0.11–0.14 as shown in Figure 4.   The molecular weight of I was estimated to be 6 000–10 000 from these values in comparison with the literature[5] and determined to be about 6 000 by the cryoscopic method in cyclohexane.

DTBP-Induced Polymerization of CHO

Polymers IV and V, in addition to II, were obtained by DTBP-induced polymerization of CHO in the presence of MAH; this result is different from that of AIBN-induced polymerization described above.   The reacting mixture became reddish brown with increasing reaction time, similar to the case of AIBN-induced polymerization.

The infrared spectra of II and IV are essentially identical with that of I, except that IV has a hydroxyl band at 3 440 cm^{-1} (Fig. 1).   IV seems to be formed from the ester of polyether by saponification.
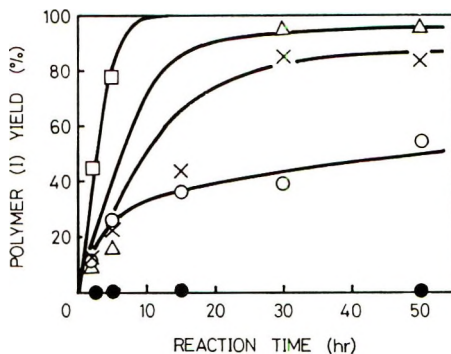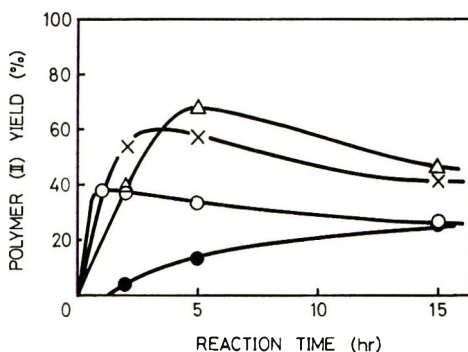

Fig. 5. DTBP-induced polymerization of CHO at different concentrations of CHO in the presence of MAH in benzene at 150°C: (○) [CHO] = 20 mole-%, (×) [CHO] = 40 mole-%, (△) [CHO] = 60 mole-%; (●) [CHO] = 20 mole-%, no radical initiator. [MAH] = 20 mole-%, [DTBP] = 0.2 mole-%.
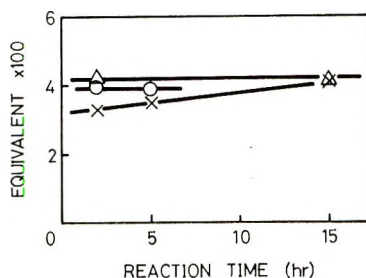
Fig. 6. Acid equivalent of polymer: V obtained under the following conditions: (○) [CHO] = 20 mole-%, (×) [CHO] = 40 mole-%, (△) [CHO] = 60 mole-%; [MAH] = 20 mole-%, [DTBP] = 0.2 mole-%.

At 150°C polyether was formed in low yield even in the absence of radical initiator; the yield increased with reaction time (Fig. 5). When DTBP was used, the yield of II increased through a maximum with reaction time and was related to the concentration of CHO. Consequently, the radical initiator was effective in accelerating the polymerization of CHO at the early stage.

The intrinsic viscosity of II (Fig. 4) was in the range of 0.06–0.09, being about half that of I, and the molecular weight of II was about 2 000–3 000 by the cryoscopic method in cyclohexane.

Polymer V was soluble in ether, acetone, and aqueous alkali and insoluble in hydrocarbons. The infrared spectrum of V (Fig. 1) exhibits characteristic bands at 1 085 cm^{-1} (ether), at 1 720 cm^{-1} (carbonyl), and at 3440 cm^{-1} (hydroxyl). The intensity of the carbonyl band of V did not vary, even after several alkali treatments followed by acidification. V seems to be
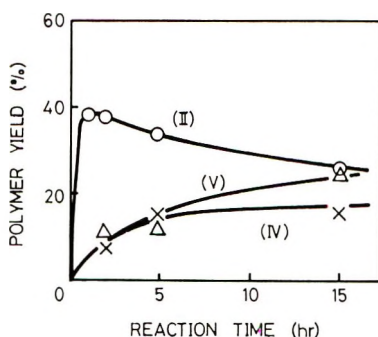
Fig. 7. DTBP-induced polymerization of CHO in benzene at 150°C. [CHO] = 20 mole-%, [MAH] = 20 mole-%, [DTBP] = 0.2 mole-%, based on the total amount of reaction mixture. Yield is based on the amount of CHO.
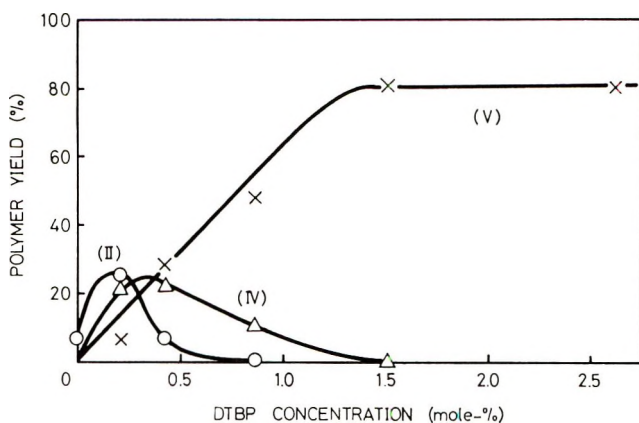
Fig. 8. Effect of the concentration of DTBP on polymerization of CHO in benzene at 150°C for 5 hr. [CHO] = 20 mole-%, [MAH] = 20 mole-%, based on the total amount of reaction mixture. Yield is based on the amount of CHO.

the adduct of polyether to the double bond of MAH. The acid equivalent of V was about 400 and was independent of the reaction time and the mole ratio of reactants (Fig. 6); therefore V appears to be composed of CHO and MAH in 7:1 mole ratio.

The yield of each polymer (II, IV, and V) was followed with reaction time and the concentration of DTBP as shown in Figures 7 and 8. As shown in Figure 8, II and IV were produced within an appropriate concentration range of DTBP and vanished above 1.5 mole-% of DTBP.

## Free-Radical-Induced Reaction of CHO in the Presence of Succinic Anhydride

Analogous reactions in the presence of succinic anhydride instead of MAH led to no polymer of CHO, suggesting that the double bond of MAH and radical initiator play an important part in polymerization of CHO.

DISCUSSIONS

Recently, Okamura and co-workers[10-12] reported that cyclic ethers such as trioxane are easily polymerized in the presence of MAH by radical initiators. It was considered that the free radical formed from cyclic ether by hydrogen abstraction and MAH form a charge transfer complex which initiates polymerization of cyclic ether. This view seems partly to elucidate the formation of our polyether. A further detailed proposed mechanism will be discussed below.

The fact that polymerization of CHO rarely occurs even in the presence of MAH without radical initiator except at high temperature suggests that abstraction of a hydrogen atom from CHO by radical initiator plays an important role in the initial step in polymerization. Previously, Gritter[13] reported that in DTBP-induced reaction of CHO, abstraction of a hydrogen atom occurs mainly in the position alpha to the oxygen atom, as shown in eq. (1).*

$$
\text{(structure)} \xrightarrow[-H\cdot]{\text{Radical initiator}} \text{(structure)} \tag{1}
$$
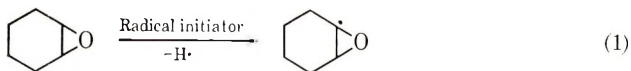
Polymerization of CHO occurs easily in the presence of MAH only on addition of a small amount of radical initiator. Consequently, it is presumed that, owing to the strong electron-accepting property of MAH, electron transfer between MAH and the free radical formed from CHO by abstraction of a hydrogen atom may lead to the formation of a cationic complex, which may initiate cationic polymerization [eq. (2)].

*In the case of AIBN, the initiating radical is probably formed by reaction of a small amount of O_2 present with the radicals from AIBN, i.e.,

$$
\text{CH}_3\text{—}\underset{\underset{\text{CN}}{|}}{\overset{\overset{\text{CH}_3}{|}}{\text{C}}}\text{—O—O}\cdot
$$
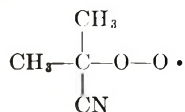
In the infrared spectra of I and II the appearance of a weak carbonyl band reveals that the polymers contain a cyclohexanonyl end group, which may be ascribed to the formation of the cationic complex [eq. (3)]. The absence of the hydroxyl group in the polyethers (I and II) indicates that, in the propagation step, preferential attack occurs on the oxygen atom rather than on the ring carbon atom of epoxide. On the other hand, it has been reported that in the radical process[1,3,6] an attack on the ring carbon atom occurs to give a hydroxyl end group. Therefore, the fact that the attack the oxygen atom occurs indicates that cationic propagation may occur as shown in eq. (4).

$$\text{(cyclohexene oxide radical cation)} + MAH \rightleftarrows \left[\text{(epoxide)}^{\oplus}\right]\left[MAH\cdot^{\ominus}\right] \quad (2)$$

$$\rightarrow \left[\text{(cyclohexanone cation)}^{\oplus}\right]\left[MAH\cdot^{\ominus}\right] \quad (3)$$

$$\xrightarrow{n(CHO)} \left[\text{VI}\right]\left[MAH\cdot^{\ominus}\right] \quad (4)$$

VI

$$\rightleftarrows \text{VII} \quad + \quad MAH \quad (5)$$

VII

$$VI \rightarrow \quad \text{---}O\text{---}C(\!=\!O)\text{---}C\cdot(\!=\!O),\ CH\!=\!CH \quad (6)$$

VIII

$$VII \quad \begin{cases} +H\cdot \rightarrow \text{---}O\text{---(ring)} & \text{I, II} \quad (7) \\ \xrightarrow{n(MAH)} +H\cdot \rightarrow \text{---}O\text{---(ring)}\left(CH\!-\!CH(C\!=\!O\ O\ C\!=\!O)\right)_n\!-\!H & \text{V} \quad (8) \end{cases}$$

I, II

V
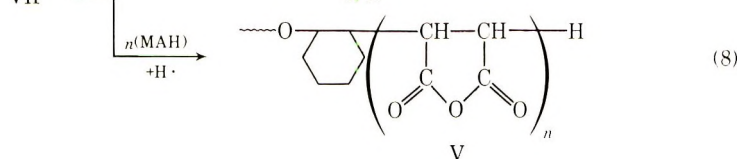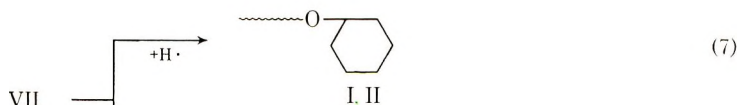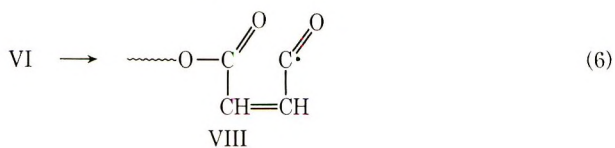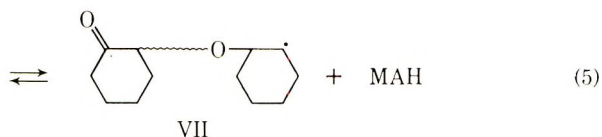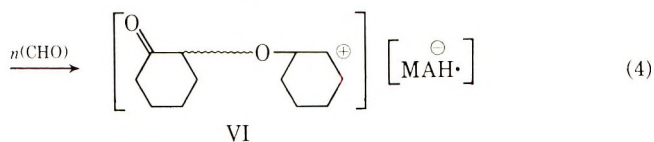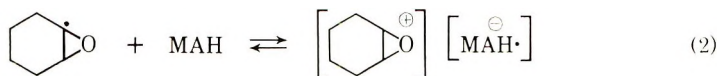
The formation of IV and V suggests that polymer–cation complex (VI) and polymer radical (VII) may exist. As shown in eq. (6), at high temperatures, the polymer–cation VI may attack the oxygen atom of the counter-anion-radical (anion-radical of MAH) to give the ester IV. But the acid component of the ester was not investigated further, since radical VIII is

considered to be highly reactive, and therefore the subsequent termination product may be complex. VII may attack the double bond of MAH to give V [eq. (8)] or may abstract a hydrogen atom to form I or II [eq. (7)]. The facts that V forms easily at high temperature and that the molecular weight of I obtained with AIBN is higher than that of II obtained with DTBP indicate that an equilibrium between VI and VII may exist, as shown in eq. (5), and have a tendency to proceed to the right at high temperature. At high concentration of DTBP the polyether is scarcely obtained, the MAH adduct of polyether being the only product. These facts show that owing to the increase of radical initiator, a free radical formed from the terminated polyether by another hydrogen abstraction may attack further the double bond of MAH to give MAH adduct.

Our results are explained by a cationic mechanism at low temperature. However, at high temperature, both the cationic and radical mechanisms operate, since the addition of polymer radical to MAH is subsequent to the radical-induced cationic polymerization.

These reactions appear to consist of three different steps, radical initiation, cationic propagation, and radical termination.

References

1. T. J. Wallace and R. J. Gritter, *Tetrahedron*, **19**, 657 (1963).
2. R. J. Gritter and E. C. Sabatino, *J. Org. Chem.*, **29**, 1965 (1964).
3. A. Oku, M. Okano and R. Oda, *Bull. Chem. Soc. Japan*, **37**, 570 (1964).
4. J. B. Conant and W. R. Peterson, *J. Amer. Chem. Soc.*, **54**, 628 (1932).
5. D. Cordishi, M. Lenzi, and A. Mele, *J. Polym. Sci. A*, **3**, 3421 (1965).
6. T. J. Wallace and R. J. Gritter, *J. Org. Chem.*, **26**, 282 (1961).
7. R. L. Jacobs and G. G. Ecke, *J. Org. Chem.*, **28**, 3036 (1963).
8. A. Ledwith and M. Sambhi, *J. Chem. Soc. B*, **1966**, 670.
9. C. O. Guss and R. Rosenthal, *J. Amer. Chem. Soc.*, **77**, 2549 (1955).
10. K. Takakura, K. Kayashi, and S. Okamura, *J. Polym. Sci. B*, **2**, 861 (1964).
11. K. Takakura, K. Hayashi, and S. Okamura, *J. Polym. Sci. A-1*, **4**, 1731 (1966).
12. K. Takakura, K. Hayashi, and S. Okamura, *J. Polym. Sci. A-1*, **4**, 1747 (1966).
13. E. C. Sabatino and R. J. Gritter, *J. Org. Chem.*, **28**, 3427 (1963).

Radiation Chemical Studies of Protein Reactions: Effect of Irradiation Liquid Containing Aromatic Hydrocarbons and pH on Viscosity

MIZUHO NISIZAWA, *Department of Chemistry,
Defense Academy, Yokosuka, Japan*

Synopsis

When protein is irradiated by γ-rays from a ^{60}Co source in various liquids containing aromatic hydrocarbons, such as benzene, naphthalene, and phenanthrene, the effect of the radiation varies with the irradiation liquids containing aromatic hydrocarbons. An empirical equation for the viscosity change was obtained. Protein irradiated by γ-rays from a ^{60}Co source in air showed the effect of pH on protein reactions. An empirical equation for the viscosity change was obtained.

INTRODUCTION

It is well known that macromolecules are more stable to radiation on mixing aromatic hydrocarbons with the macromolecules,[1] and also that on increasing the pH the viscosity of protein in urea solution increases.[2] Since the effect of irradiation liquid containing aromatic hydrocarbons and the effect of pH on protein reactions are problems of general interest, it was therefore considered desirable to study them.

The denaturation of protein by urea was selected as the protein reaction, since it was described in previous papers.[3–5] The determination can be followed conveniently by measuring the reduced viscosity of the solutions.

EXPERIMENTAL

Materials

Albumin and urea used in this work were commercial materials produced by the Kanto Chemical Co., Inc.

Carbon tetrachloride was a commercial material produced by the Kanto Chemical Co., Inc.

Benzene, naphthalene, and phenanthrene used were commercial materials produced by Wako Pure Chemical Industries, Ltd., Kanto Chemical Co., Inc., and Junsei Pure Chemical Co., Ltd., respectively.

Sodium hydroxide and boric acid used were commercial materials produced by the Kanto Chemical Co., Inc.

Phosphoric acid and acetic acid used were commercial materials produced by Nippon Rikagakuyakuhin Kabushikikaisha and Ieda Pure Chemical Ltd., respectively.

Apparatus and Procedure

The irradiation was from a 300 Ci ^{60}Co source. The dose rate in this experiment was 1.7×10^3 r/hr.

In the studies of effect of irradiation liquid, the solid albumin was put into each irradiation bottle and the bottles were filled with irradiation liquid (carbon tetrachloride) containing various amounts of benzene, naphthalene, or phenanthrene. The irradiation was carried out at the room temperature. The irradiated solid albumin was cleaned with fresh carbon tetrachloride, dried at 30°C under vacuum, powdered, dissolved with distilled water, and mixed with urea solution; the viscosity was then measured.[3]

In the pH studies the solid albumin (powder) was irradiated at room temperature. The irradiated albumin was dissolved with distilled water and mixed with urea–buffer mixtures; the viscosity was then measured.[3]
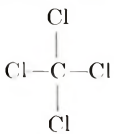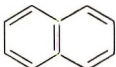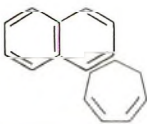
The pH values were measured with a glass electrode pH meter.

RESULTS

Effect of Irradiation Liquid

The change with time in reduced viscosity at 30°C of 3% albumin in 10M urea was measured after irradiation with γ-rays of the albumin in liquid containing small amounts of aromatic hydrocarbons.

TABLE I
Compounds Used in Irradiation Liquid for Solid Protein

Compound	Formula and structure	Resonance energy, kcal/mole
Carbon tetrachloride	CCl_4	0
Benzene	C_6H_6	39
Naphthalene	$C_{10}H_8$	61
Phenanthrene	$C_{14}H_{10}$	92
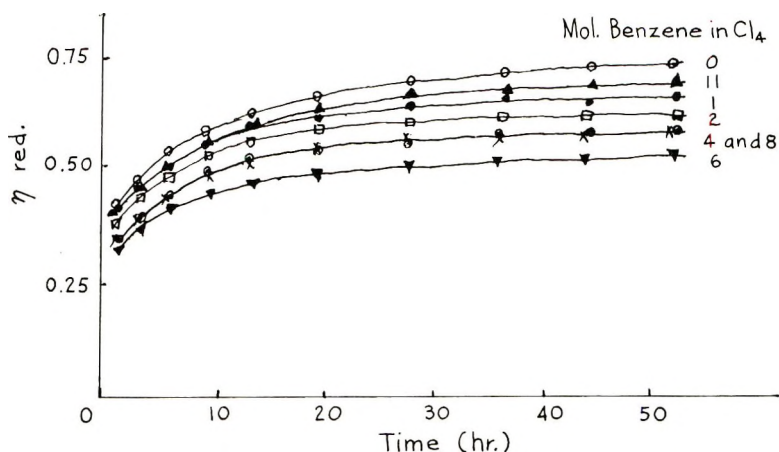
Fig. 1. Relationship of reduced viscosity to time in the presence of various amounts of benzene (in CCl_4): (○) none; (●) 1 mole; (□) 2 moles; (◓) 4 mole; (▼) 6 moles; (×) 8 moles; (▲) 11 moles. Conditions: 3% albumin in $10M$ urea, 10^3 r, 30°C.
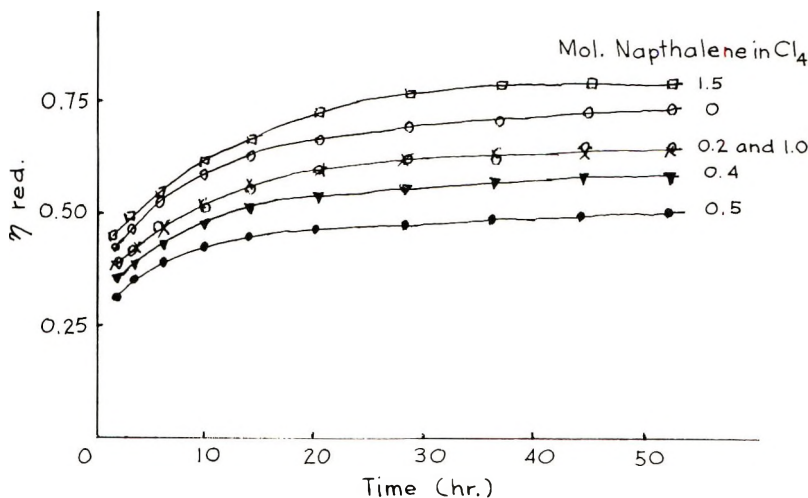
Fig. 2. Relationship of reduced viscosity to time in the presence of various amounts of naphthalene (in CCl_4): (○) none; (◓) 0.2 mole; (▼) 0.4 mole; (●) 0.5 mole; (×) 1.0 mole; (□) 1.5 mole. Conditions: 3% albumin in $10M$ urea, 10^3 r; 30°C.

The irradiation liquid was CCl_4 (because it is not a denaturant); the aromatic additives were benzene, naphthalene, and phenanthrene. Formulas, structures, and resonance energies are shown in Table I.

Experimental results are shown in Figures 1–3. From these it is clear that the reduced viscosity does not continue to increase, but approaches a limiting value. When the values of the reduced viscosity at infinite time in Figures 1–3 are plotted against the concentration of aromatic hydrocarbons, the relation shown in Figures 4–6 is obtained. With increasing

concentration of aromatic hydrocarbons, the reduced viscosity first de-
creases, reaches a minimum, and then increases; the minimum in the
reduced viscosity indicates the maximum effective protective effect for the
denaturation of protein.

Effect of pH

The change with time in reduced viscosity at 30°C of 3% albumin in
10M urea after irradiation by γ-rays in buffer solutions of various pH's
was studied.
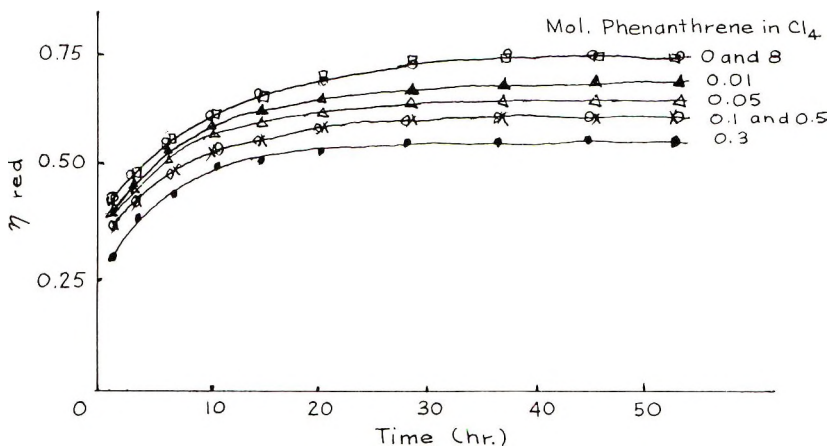
Fig. 3. Relationship of reduced viscosity to time in the presence of various amounts
of phenanthrene (in CCl$_4$): (⊖) none; (▲) 0.01 mole; (△) 0.05 mole; (×) 0.1 mole;
(○) 0.3 mole; (●) 0.5 mole; (□) 8 moles.   Conditions: 3% albumin in 10M urea, 10^3 r,
30°C.
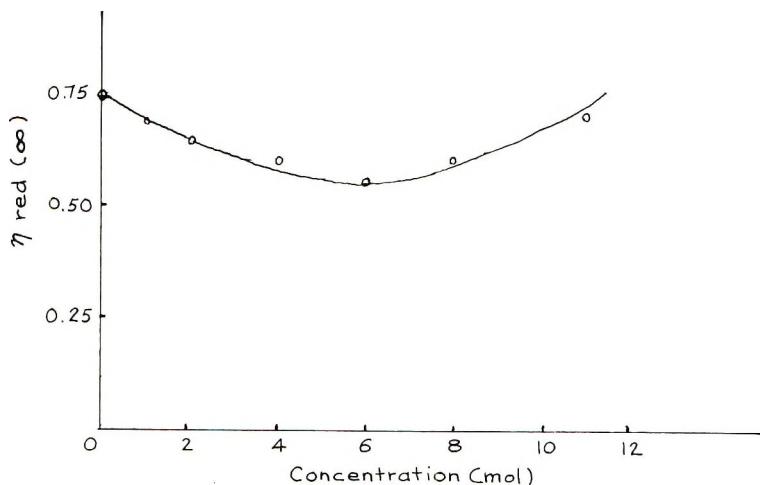
Fig. 4. Dependence of the protective effect on the concentration of benzene.   Condi-
tions: 3% albumin in 10M urea, 10^3 r, 30°C.

Experimental results are shown in Figure 7. It is clear that the reduced viscosity does not go up to an infinite value, but approaches a limiting value. When the values of the reduced viscosity at infinite time in
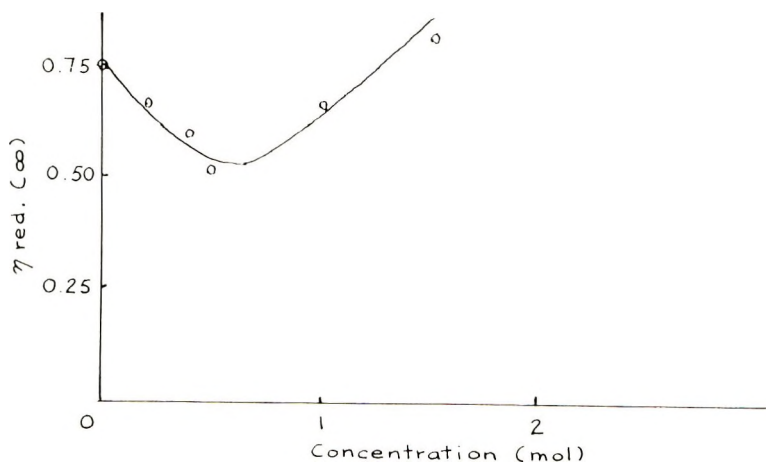
Fig. 5. Dependence of the protective effect on the concentration of naphthalene. Conditions: 3% albumin in 10M urea, 10³ r, 30°C.
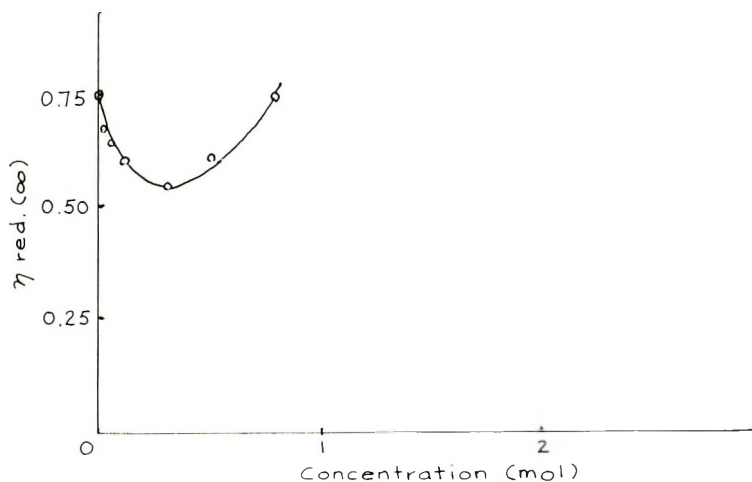
Fig. 6. Dependence of the protective effect on the concentration of phenanthrene. Conditions: 3% albumin in 10M urea, 10³ r, 30°C.

Figure 7 are plotted against the pH values, the relations shown in Figure 8 are obtained. With increasing pH the reduced viscosity at infinite time of the irradiated albumin in urea increases. This increase shows the effect of pH on the denaturation of the irradiated protein.
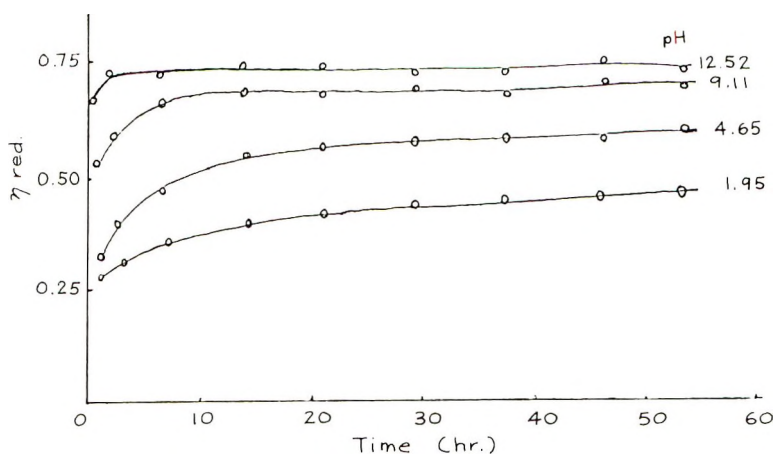
Fig. 7. Relationship of reduced viscosity to time at different pH's. Conditions: 3% albumin, in 10.M urea, 10^3 r, 30°C.
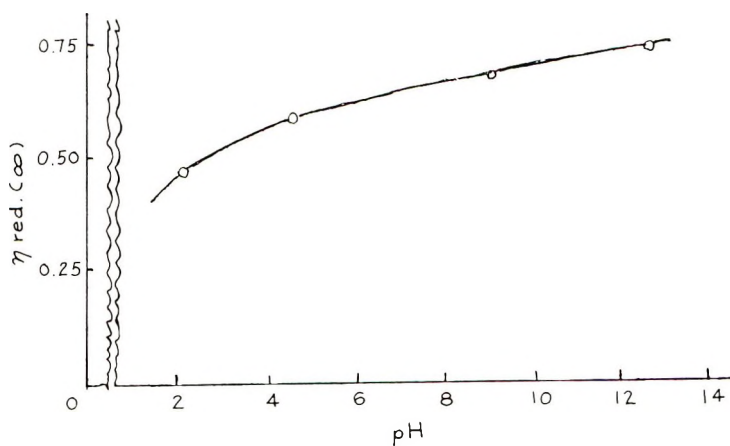
Fig. 8. Reduced viscosity as a function of pH. Conditions: 3% albumin in 10.M urea, 10^3 r, 30°C.

DISCUSSION

As stated above, it is known that macromolecules can be made more stable to radiation by mixing aromatic hydrocarbons with the macromolecules[1] and also that on increasing the pH the viscosity of protein in urea solution increases.[2]

A discussion of the effect of irradiation liquid containing aromatic hydrocarbons and of pH in a protein reaction follows. The protein reaction is estimated from the change in viscosity as shown in Figures 1–8.

The relation between the viscosity change and the concentration of aromatic hydrocarbons is related to that between the protein reaction and protective reaction. When the concentration of protein and urea and

radiation dose are constant, a change in the concentration of aromatic hydrocarbons results in a change of activation required for denaturation reaction (Figs. 4–6). The reaction mechanism must, therefore, depend on the concentration of aromatic hydrocarbons. If the main processes for the protective action are assumed to be as shown in eqs. (1)–(4)

$$P{-}P \xrightarrow{h\nu} P* + P* \tag{1}$$

$$P* + P* \longrightarrow P{-}P + E_a \tag{2}$$

$$A + E_a \longrightarrow A* \tag{3}$$

$$A* \longrightarrow A + (E_a - E_r) \tag{4}$$

where P–P denotes the protein molecule, A is an aromatic hydrocarbon, E_a is the activation energy of the γ-rays, and E_r is the resonance energy of aromatic hydrocarbon, then the protective step is reaction (3), which means that the observed protective effect follows a parabolic curve versus the concentration of aromatic hydrocarbons. Therefore the response of albumin molecule to aromatic hydrocarbons may be determined by measuring the reduced viscosity.

If in the system X is the concentration of aromatic hydrocarbons, and a, b, and c are adjustable constants, then eq. (5) expresses the protective effect:

$$\eta_{red}(\infty) = aX^2 + bX + c \tag{5}$$

This formula agrees with the experimental data that describe the curves in Figures 4–6.

In the mechanism these aromatic hydrocarbons may be involved in energy loss by fluorescence from the electron system of the aromatic rings.

Second, the relation between the viscosity change and the pH change is related to swelling of protein molecule caused by the electrostatic repulsion associated with the increased net charge of the molecule activated by γ-rays. When the concentrations of protein and urea and the radiation dose are constant, the increase in the pH results in an increase of the viscosity change required for denaturation (see Fig. 7). The reaction mechanism must, therefore, depend on the pH. If the main processes for the effect of pH are assumed to be

$$P{-}P \xrightarrow{h\nu} P* + P* \tag{6}$$

$$P* \xrightarrow{OH^-} P \tag{7}$$

where P–P is the protein molecule, OH^- is a hydroxyl radical, then the rate-determining step is reaction (7), which means that the observed viscosity change is related to the pH value. Therefore the response of the albumin molecule to OH^- radical may be determined by measuring the reduced viscosity.

If in the system X is the concentration of the OH^- radical, and a, b, and k are adjustable constants, then eq. (8) expresses the effect of

$$\eta_{red}(\infty) = a(1 - e^{-kx}) + b \tag{8}$$

This formula agrees with the experimental data that describe the curve in Figure 8.

References

1. J. B. Gardner and G. Harper, *J. Appl. Polym. Sci.*, **9**, 1585 (1965).
2. H. K. Frensdorff, M. T. Watson, and W. Kauzman, *J. Amer. Chem. Soc.*, **75**, 5157 (1953).
3. M. Nisizawa, *J. Appl. Polym. Sci.*, **12**, 321 (1968).
4. M. Nisizawa, *J. Appl. Polym. Sci.*, **12**, 1781 (1968).
5. M. Nisizawa, *J. Appl. Polym. Sci.*, **12**, 2183 (1968).

Polymerization of Vinyl Chloride

S. ENOMOTO, *Kureha Chemical Industry Company,*
Tokyo Laboratory, Shinjuku-ku, Tokyo, Japan

Synopsis

Polymerization of vinyl chloride (VC) was studied. Natural evolution of HCl from VC occurred in the polymerization. VC, VC-αd_1, VC-$\beta,\beta d_2$ and VC-d_3 were used to study the reactivities of the hydrogen atoms in the polymerization and the β-hydrogen atoms contributed to the chain transfer. Chemical and physical methods were used to observe irregular structures, such as branching, double bonds, and head-to-head or tail-to-tail addition, and also to confirm the relation between conversion and the irregular structures.

INTRODUCTION

Polymerization of vinyl chloride (VC) has been studied by many investigators. A rate increase with conversion was observed in the bulk polymerization.[1a] Mickely et al.[2] reported that the high reactivity of the growing radical accelerated the rate of polymerization and the rate depended on the surface area of the precipitated particle.[2] Jones and Melville[3] detected butadiene in the polymerization and explained the chain-transfer reaction by the following mechanism of eqs. (1) and (2).

$$CH_2{=}CHCl + CH_2{=}CHCl \rightarrow CH_2{-}CHCl_2 + CH_2{=}CH\cdot \qquad (1)$$

$$CH_2{=}CH\cdot + CH{=}CH_2 \rightarrow CH_2{=}CH{-}CH{=}CH_2 \qquad (2)$$
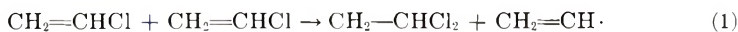
Lím and Kolinsky[4] carried out the polymerization in 2,4-dichloropentane and 2,4,6-trichloroheptane to determine the chain-transfer constant by the usual kinetic theory based on the assumption of a stationary state. The model polymers swelled the produced polymer and facilitated the mobility of the monomer; however, the observed value of the chain transfer was rather low, and it was concluded that the value in heterogenous system would be less than the value obtained in approximately homogenous system.[4] Methyl methacrylate, acrylic esters, and acrylonitrile showed a similar gel effect.[1b] These effects could be explained on the basis of an occlusion theory, and ESR proved the presence of substantial amounts of radicals occluded in the polymers.[5-8] However, this method was not successful in the detection of a trapped radical in the polymerization of VC. It was also interesting that the degree of polymerization depended rather on temperature of polymerization than concentration of catalyst.[9a]

Bier and Krämer discussed the formation of double bonds and branching on the basis of the kinetics of VC polymerization.[10] Cotman hydrogenated

poly(vinyl chloride) (PVC) to polyethylene with $LiAlH_4$ to study the branching by infrared spectroscopy.[11] Nakajima et al.[12] reported that the amount of branching was reduced by lowering the temperature of polymerization.[12] Boccato et al.[13] investigated the same problem in detail with respect to the mechanism of branch formation during polymerization.[13] Ultraviolet spectroscopy and visible spectroscopy were available to determine the polyene structure of the thermally degraded polymer, but these methods did not give us any information about the type of unconjugated double bonds which were expected to be present in the degraded polymer. Branching and the double bonds would be less stable to heat treatment than regular structures.

Asahina and Onozuka studied heat stabilities of model compounds which contained branching, double bonds, or both.[14] A lowering of pH was observed in the suspension polymerization, and this increased with increasing conversion. It was found that VC peroxide which was prepared by addition of oxygen to VC decomposed to acidic substances in presence of water; thus it was suggested that the decrease in pH was due to such a reaction with VC peroxide formed with oxygen which was contained in VC and water or from peroxide catalyst.[9b]

Enomoto and Asahina previously studied the mechanism of VC addition by use of partially or completely deuterated monomers and infrared spectroscopy.[15] The same technique and mass spectrometry have been applied to the study of the polymerization of VC in this report.

EXPERIMENTAL

Preparation and Purification of Materials

The deuterated monomers used in this study were $CH_2{=}CDCl$, $CD_2{=}CHCl$, and $CD_2{=}CDCl$. Their preparations and purities were described in detail previously.[16] After drying the monomer with $CaCl_2$ in the gaseous state, it was charged into a glass ampoule connected to a vacuum line in the liquid state. Freezing and thawing *in vacuo* was repeated four times to remove traces of air completely. Water was distilled after refluxing with $AgNO_3$ and was redistilled with NaOH under a stream of nitrogen to remove CO_2. The purified water in a vessel containing the catalyst and methyl cellulose (stabilizer) was degassed *in vacuo* by the same method as the monomer, and the purified monomer was added to the vessel *in vacuo*. The prepared 2,4,6-trichloroheptane was also degassed before addition of the purified monomer.

Detection of HCl Produced in Polymerization

Suspension Polymerization. Lauroyl peroxide and azobisisobutyronitrile were used to confirm the effect of peroxide on the lowering of pH, The purified $CH_2{=}CHCl$ was sealed into several glass ampoules containing purified water, initiator, and methyl cellulose. They were immersed

in a bath at 50°C and mechanically shaken. The polymerization was stopped at various intervals and the pH of the water was measured by a pH meter in a dry box filled with highly purified argon.

Bulk Polymerization. Bulk polymerization of CH_2=CHCl was carried out to ascertain the effect of water. The purified monomer was charged into an autoclave containing lauroyl peroxide *in vacuo* at −78°C. A trace of the charged monomer was sealed into a small gas cell from the autoclave through a vacuum line before and after polymerization at its boiling point.

Reactivities of Hydrogen Atoms of VC in Polymerization

In order to study differences in the reactivities of the α and β hydrogens in the polymerization, rates of polymerization and degrees of polymerization were observed with CH_2=CHCl, CH_2=CDCl (VC-αd_1), CD_2=CHCl (VC-$\beta,\beta d_2$) and CD_2=CDCl (VC-d_3). The reaction was carried out by the suspension polymerization method described above. The ratio of monomer to water was 1:2 (by weight), the concentration of catalyst (lauroyl peroxide) was 0.1 wt-% (based on monomer), the concentration of commercial poly(vinyl alcohol) was 0.5% wt-% (based on water), and the temperature of polymerization was 58°C.

Polymerization of VC-d_3 in 2,4,6-Trichloroheptane

Lím and Kolinsky polymerized VC in 2,4,6-trichloroheptane to measure the constant of chain transfer kinetically, but they did not prove the addition of the monomer to the model polymer experimentally. Pure PVC-d_3 should not have any CH stretching mode in its infrared spectrum. The polymerization of VC-d_3 was carried out in 2,4,6-trichloroheptane to obtain a direct evidence. The feed ratio of VC-d_3 to the model polymer was 0.5, and 0.1 mole-% of azobisisobutyronitrile (based on monomer) was used as a catalyst. The temperature was 55°C, the time was 48 hr, and the conversion was 50%. The polymer was dissolved in tetrahydrofuran and precipitated three times with methanol to remove the occluded model polymer completely. The inherent viscosity and the infrared spectrum were observed after drying the purified polymer at 60°C *in vacuo*. The degree of polymerization was 203.5. Similar polymerizations at different feed ratios were carried out to measure the constant of the chain transfer, but the conversions were less than 3%.

Detection of Double Bonds

Asahina and Onozuka pointed out the double bond initiated thermal degradation of poly(vinyl chloride).[14] Infrared spectroscopy could not show the presence of double bonds in the undegraded polymer because of their quite low content. Some spectral change could be expected in the infrared spectrum of the low molecular polymer, and CS_2 was used to extract this fraction from the commercial polymer at room temperature. The extracted solution was evaporated by vacuum distillation without heating to avoid structural changes, and then the residue was purified by repeated

precipitation with tetrahydrofuran and methanol. The dried polymer was a white powder. This white powder was also brominated in CCl_4 at room temperature.

Thermal Degradation of PVC-αd_1

PVC-αd_1 was degraded thermally to observe the possibility of evolution of DCl. The pressure of HCl in a gas cell was proportional to the band at 2940 cm^{-1} in the infrared spectrum and the infrared absorption band of DCl at 2110 cm^{-1} had the same relation. A 2-g portion of the polymer was filled into a small glass ampoule which was attached to a gas cell with NaCl windows through a glass tube. The whole system was connected to a vacuum line to dry the polymer *in vacuo* (10^{-5} mm Hg) at room temperature for 24 hr. The connecting part was sealed to keep the system *in vacuo* and the ampoule was immersed in a bath at 180°C to degrade the polymer. The infrared spectrum of the gas evolved from the thermally degraded polymer was observed. The intensity of the DCl evolved during initial degradation was very weak. Mass spectroscopy was also used to analyze the evolved gas. Aliquots of the evolved gas were collected into a small glass ampoule by cooling with liquid nitrogen every half hour for the mass spectroscopic analysis.

Thermal Degradation of Poly(vinyl Chloride) Prepared with Combination of VC and VC-d_3

The branching and the double bonds were expected to initiate the thermal degradation of poly(vinyl chloride). These structures might be produced by the attack of radicals such as those derived from the decomposing catalyst or the growing chains on the polymer chains during the polymerization. The polymer formed at the initial stage of polymerization was thought to receive a prolonged attack as compared with the polymer formed at the later stage. However, the relative heat stabilities were not certain, and two series of suspension polymerizations, e.g., VC + VC-d_3 and VC-d_3 + VC, were carried out to evaluate this point. The first monomer of each pair was polymerized at 55°C in an autoclave equipped with a stirrer until the conversion reached about 50%, when the residual monomer was recovered completely through a stainless steel pipe into an evacuated vessel immersed in a liquid nitrogen bath. Then an equal amount of the second monomer was added to the autoclave under stirring. This added monomer diffused completely into the polymerized particles and did not separate if the agitation was stopped. The temperature of the autoclave was kept at 0°C to prevent polymerization during the recovery of the first monomer and refilling procedures, and then the temperature was raised to 55°C and polymerization continued up to a certain predetermined conversion. If the second monomer was identical to the first one and the total time of both polymerizations was equal to that of a single monomer addition, there was no difference with regard to the degrees of polymerization and the conversions. If the second monomer was

different from the first one, particular care was required to control the time of polymerization in order to adjust for the isotope effect. The compositions of the deuterated polymer were determined by infrared spectroscopy and the infrared spectroscopic method was applied to observe the HCl and the DCl evolving from the polymers during their thermal degradation at 180°C.

DISCUSSION

Table I shows the decrease of pH in the suspension polymerization. The pH of the mixture with only methyl cellulose was lower than that of pure water and this tendency increased with heating time. However, the mixture with only VC showed a far lower value. No difference with regard to lowering the pH was observed between azobisisobutyronitrile and lauroyl peroxide. In spite of complete removal of oxygen from the suspension polymerization system, the pH decrease was more marked with increasing conversion, and the pH at high conversion was of the same order of that of a heated VC–water mixture. Obviously, the previously proposed mechanism by which water decomposed the peroxide structure —CH$_2$CHCl—O—O—CH$_2$CHCl— to yield acidic substances[9b] does not seem to play the main role in the lowering of the pH. Evolution of HCl in the bulk polymerization is observed by analysis of mass spectroscopy. VC is split into HCl$^+$ and CHCH$^+$, and the evolved HCl is expressed by the relative intensity based on the HCl$^+$ fragments obtained from VC before polymerization. Table II shows that HCl was evolved in the bulk polymerization and that the amount increased with the time of polymerization. Slight hydrolysis of VC and a trace of thermal degradation of the formed polymer may be involved in lowering the pH in the polymerization.

TABLE I
Lowering of pH in Suspension Polymerization

No.	CH$_2$=CHCl/H$_2$O (weight ratio)	Methyl cellulose, %[a]	Catalyst, %[b]	Polymerization time, hr	Conversion, %	pH
1	0	0	0	0	0	6.7
2	0	0.05	—	—	—	5.3
3	0	"	—	30	—	4.0–4.05
4	1/4	—	—	30	---	3.5
5	"	0.05	AIBN, 0.1	8	2k,5	4.0–4.05
6	"	"	"	12	45.6	4.0–4.02
7	"	"	"	18	87.0	4.0
8	"	"	"	24	89.0	3.9
9	"	"	LPO, 0.1	15	31.0	4.3
10	"	"		20	54.0	4.2
11	"	"		30	88.7	3.9

[a] Concentration based on water.

[b] AIBN = azobisisobutyronitrile; LPO = lauroyl peroxide; concentrations are based on monomer.

TABLE II
Analysis of HCl⁺ in Bulk Polymerization[a]

No.	Polymerization time, hr	Relative intensities[b]		
		$^{36}HCl^+$	$^{38}HCl^+$	Mean
12	5	1.06	1.08	1.07
13	15	1.10	1.10	1.10

[a] Catalyst LPO, 0.2% (based on monomer).

[b] Relative intensity $= I_t/I_0$, where I_0 is intensity of HCl⁺ fragment from VC before polymerization and I_t is that from residual VC after polymerization for time t.

Figures 1 and 2 show the effects of deuterium substitution in the monomer on the rate of polymerization and the degree of polymerization. Bartlett and Tate[17] reported that the deuteration of allyl acetate ($CH_2=CHCD_2OCOCH_3$) doubled both values and that the isotopic effect prevented the transfer reaction. The same effect was observed in the polymerization with the various deuterated vinyl chlorides; however, the two kinds of hydrogen atoms showed different effects. The deuteration of the α-hydrogen atom prompted the rate of polymerization to change in the order, VC-d_3 > VC-αd_1 = VC-$\beta,\beta d_2$ > VC. On the other hand the β-deuterium atom increased the degree of polymerization extraordinarily in the order, VC-d_3 > VC-$\beta,\beta d_2$ > VC = VC-αd_1. This marked effect cannot be explained without assuming that the β-hydrogen atom is more active than the α-hydrogen atom or the chlorine atom in the transfer reaction, because the transfer reaction is the most important factor which determines the degree of polymerization in the polymerization with a fixed concentration of catalyst. The dominant role of the α-hydrogen atom in the rate of
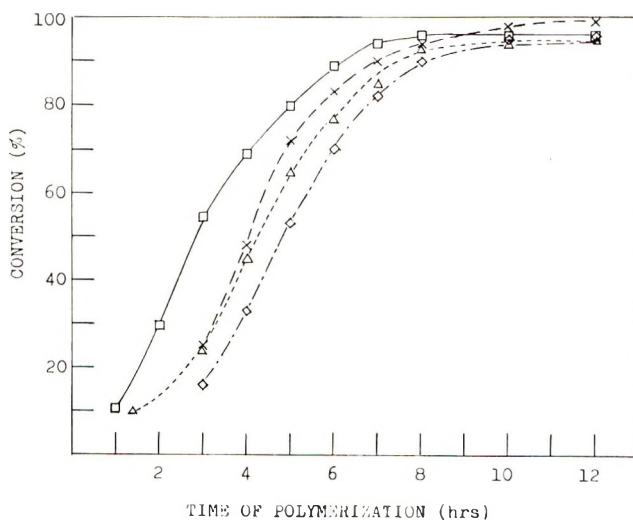
Fig. 1. Relations between time of polymerization and conversion in polymerizations of VC and its deuterated monomers: ($\Diamond$) $CH_2=CHCl$; ($\times$) $CH_2=CDCl$; ($\triangle$) $CD_2=CHCl$; ($\square$) $CD_2=CDCl$.

polymerization is not explained satisfactorily at present because this atom is not active in increasing the degree of polymerization. However, the effect of the β-hydrogen atom must be taken into account, as the rate of VC-αd_1 is not so much different from that of VC-$\beta,\beta d_2$.

Figure 3 shows the result of polymerization of VC-d_3 in 2,4,6-trichloroheptane. The two strong CH-stretching modes of 2,4,6-trichloroheptane appeared in the infrared spectrum of the purified PVC-d_3 which was polymerized in 2,4,6-trichloroheptane, and this fact is experimental evidence
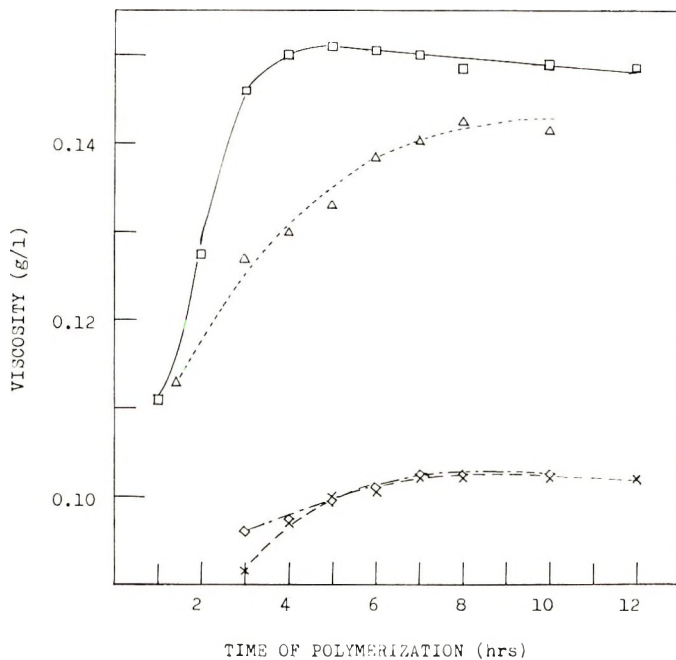
Fig. 2. Relations between time of polymerization and degree of polymerization in polymerization of VC and its deuterated monomers: ($\Diamond$) CH$_2$=CHCl; ($\times$) CH$_2$=CDCl; ($\triangle$) CD$_2$=CHCl; ($\square$) CD$_2$=CDCl.

of the addition of VC to the polymer. The transfer constant at 55°C, from eq. (3), was 9.8×10^{-4}.

$$1/P = (1 + \lambda)/2(k_t + k_p^2)(R_p/M^2) + C_M + C_S(S/M). \qquad (3)$$

As shown in Figure 4, three weak bands appeared at 800, 753, and 740 cm^{-1} in the infrared spectrum of the low molecular weight PVC extracted from a commercial PVC. The bands at 800 and 740 cm^{-1} disappeared on bromination of the polymer, and they may be assigned to the CH out-of-plane modes of the double bonds. In spite of the uncertainty, this spectral change suggests that PVC has two kinds of double bond. The band at 800 cm^{-1} is probably due to the double bond at the chain end and the other band corresponds to an inner double bond.
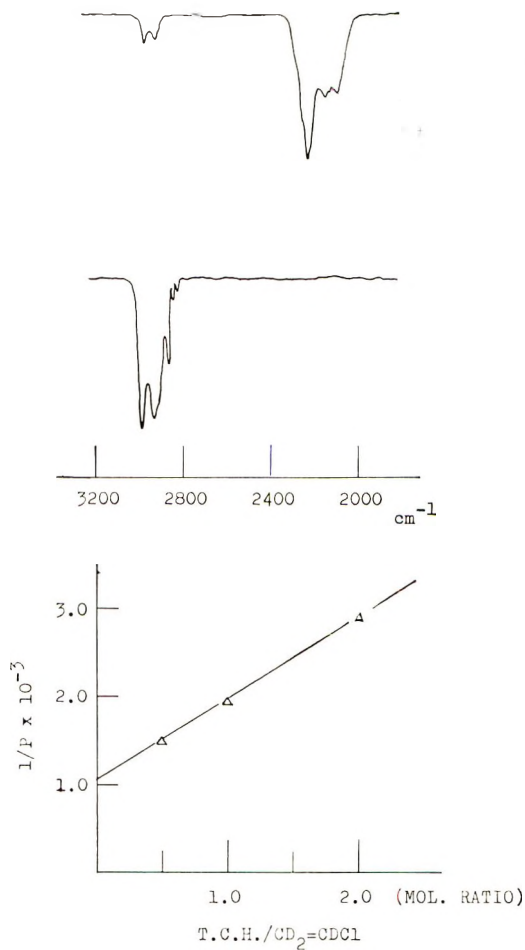
Fig. 3. Polymerization of VC-d_3 in 2,4,6-trichloroheptane (TCH): (top) infrared spectrum of PVC-d_3 prepared in absence of TCH; (middle) infrared spectrum of PVC-d_3 prepared in TCH solution; (bottom) relation between $1/P$ and TCH/VC-d_3 mole ratio in the polymerization.
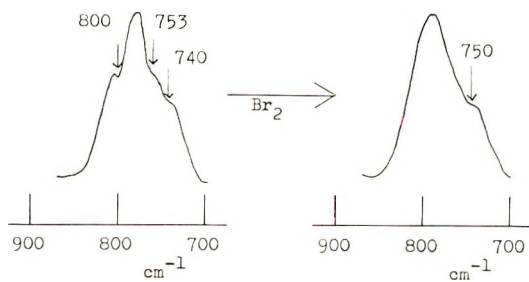
Fig. 4. Infrared spectral change of low molecular weight PVC by bromination.

Figure 5 shows the pressures of evolved gases in the thermal degradation of PVC-αd_1. This monomer was prepared by the reactions summarized in eqs. (4) and (5), and its purity was confirmed by infrared spectroscopy

$$CH_2{=}CCl_2 + DBr \rightarrow CH_2Br{-}CDCl_2 \tag{4}$$

$$CH_2Br{-}CDCl_2 + Zn \rightarrow CH_2{=}CDCl + ZnBrCl \tag{5}$$
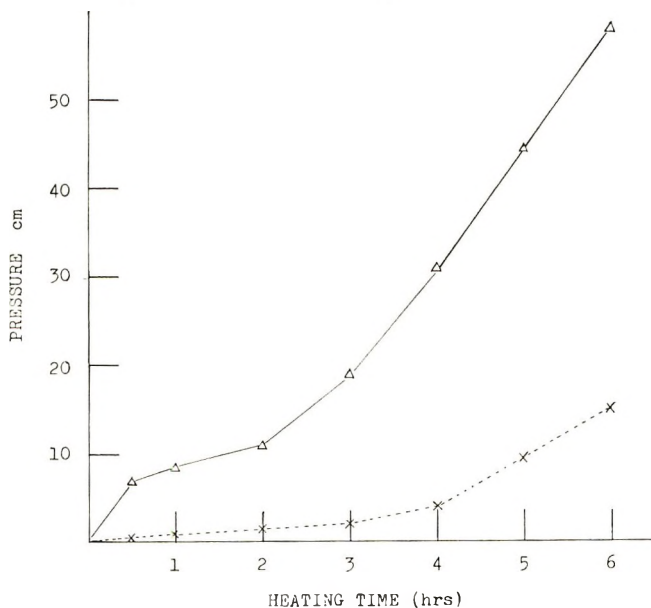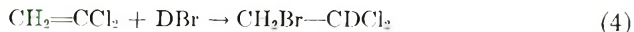
Fig. 5. Relation between pressures of evolved gases and heating time in thermal degradation of PVC-αd_1: ($\triangle$) HCl; ($\times$) DCl.
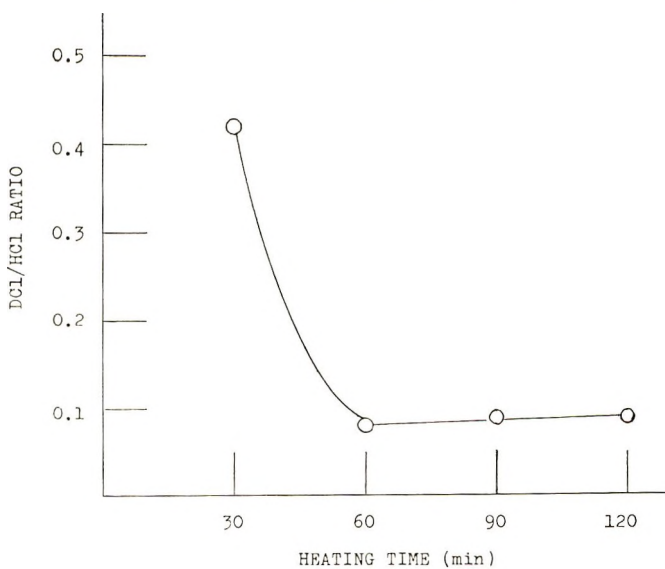
Fig. 6. Relation between DCl/HCl ratio and heating time in thermal degradation of PVC-αd_1.
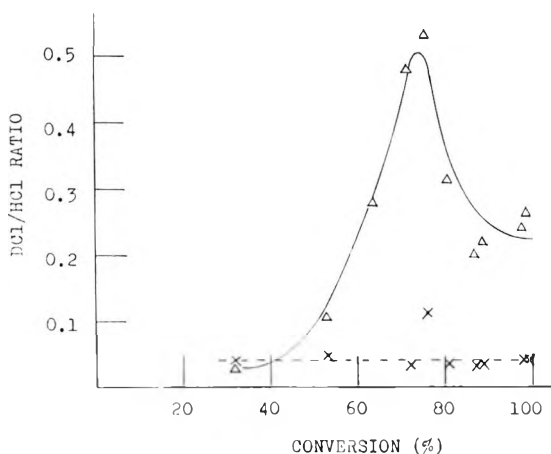
Fig. 7. Relation between DCl/HCl ratio and conversion in thermal degradation of PVC-αd_1:   ($\triangle$) 0–30 min;   ($\times$) 30–60 min.

and high-resolution NMR spectroscopy. It was pure $CH_2=CDCl$, and no trace of $CH_D=CHCl$ was observed in its spectrum.[16]   Splitting out of HCl was expected only in the initial thermal degradation of the PVC-αd_1 because of the structure of the monomer and of the absence of crosslinks; however, DCl was also evolved, even with the very first degradation.   The mass spectroscopic data of the evolved gas are shown in Figure 6; the ratio of the DCl to the HCl evolved within the initial half hour was rather large and remained unchanged with heating time.   No crosslinking could be found in this initial degradation product, which dissolved completely in tetrahydrofuran.   This abnormal dehydrochlorination is probably due to some abnormal additions occurring in the polymerization.   The evolution of DCl in the later stage is caused by the intermolecular dehydrochlorination, and the ratio was constant.   Figure 7 shows that the abnormal degradation also depended on the conversion.   The initial ratio increased with the conversion, its maximum value being reached at around 70% conversion; then the value decreased slowly.   This omission seemed to be like the variations of the rate of polymerization and the degree of polymerization.   As it is impossible to expect the initial splitting of DCl from the usual structure formed by head-to-tail addition, $-CH_2CDClCH_2-CDCl-$, some abnormal structures

$$-CH_2CDClCDClCH_2- \text{ and } -CH_2CD-CH_2CDCl-$$
$$| $$
$$CDClCH_2CDCl-$$
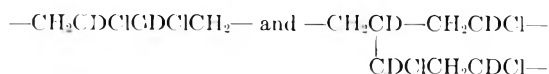
are probably formed; it may be reasonable to anticipate these abnormal additions in the polymerization of VC.

   Table III shows results for typical polymerizations with combination of VC and VC-d_3.

   The formation of branches and double bonds and some abnormal additions in the polymerization of VC are supported by the spectroscopic meth-

TABLE III
Polymerizations with (VC + VC-d_3) and (VC-d_4 + VC)[a]

No.	First polymerization			Second polymerization		Total conversion, %	PVC/PVC-d_3 ratio	Molecular weight
	Monomer	Time, hr	Conversion, %	Monomer	Time			
14	VC	4.70	42.5	VC-d_3	11.25	90.5	51.3/48.7	1270
15	VC-d_3	2.50	49.2	VC	13.50	80.9	60.9/39.1	1400
16	VC	5.00	50.3					

[a] Monomer:water = 1:2; catalyst, lauroyl peroxide, 0.3 wt-%; suspension agent, commercial PVA, 0.15 wt-% based on water.

ods described above. It seems probable that these formations are stimulated by the chain-transfer activity of the β-hydrogen atom. These structures are less heat-stable than the regular head-to-tail bond. Thus, thermal degradation of the polymer prepared with combination of VC and VC-d_3 is a convenient method to study the relation between the less stable structures and conversion. The samples used for this experiment are listed in Table III, and Figure 8 shows the result of their thermal
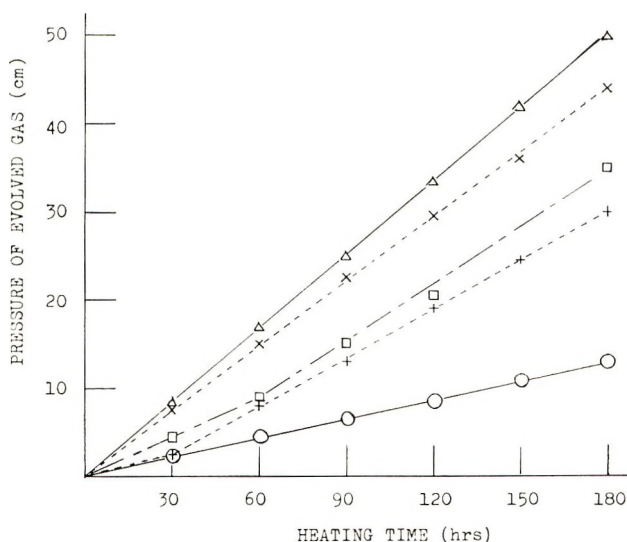
Fig. 8. Thermal degradation of PVC: ($\times$) HCl, sample 14; (+) DCl, sample 14; ($\triangle$) HCl, sample 15; ($\bigcirc$) DCl, sample 15; ($\square$) HCl, sample 16.

degradations. As the samples were mixtures of PVC and PVC-d_3, both HCl and DCl evolved from the original polymer. Therefore, the observed pressures were corrected to their values based on the corresponding pure polymer. Sample 16 of 50% conversion showed the lowest evolution of HCl. Sample 14, where VC was polymerized first, was intermediate; the highest evolution of HCl was found with sample 15, where VC was added as the second monomer. The polymer formed in the initial stage

is more stable than that formed at the later stage, but the initially formed polymer becomes less stable when it is kept in the field of polymerization until high conversion is reached. The same phenomenon is observed in the evolution of DCl from PVC-d_3 however, the amount of DCl evolved is far less than that of HCl and the PVC-d_3 of samples 14 and 15 are more stable than the undeuterated PVC of both samples. The denaturation of the initially formed polymer is probably due to attack by radicals, such as growing chains and catalyst fragments, on the polymer resulting in the formation of some unstable structures at higher conversion.

The polymer formed in the later stage is less stable than the polymer which is formed in the initial stage and is kept within the field of polymerization during the polymerization. This experimental fact is not explained satisfactorily, but it seems to be related to the monomer concentration in a polymer–monomer particle. The rate of the polymerization decreases gradually above about 50% conversion in the suspension polymerization. A relatively ideal polymerization probably proceeds in the particle because the monomer swells the particle and moves easily between the polymer chains during the initial stage; however, the mobility is decreased and the remaining monomer polymerizes locally in the particle as the conversion increases and the particle becomes rigid. This local polymerization yields less stable polymer.

From the above one might conclude that the high transfer ability of the β-hydrogen atom and the tail-to-tail addition result in some abnormal structures (branches and double bonds) which cause the formation of HCl and containing consequently result in a decrease of the pH during the polymerization. The present study should present some insights into the complicated polymerization of vinyl chloride, but there are still problems left which require further clarifications.

References

1. C. H. Bamford, W. G. Barb, A. D. Jenkins, and P. F. Onyon, *The Kinetics of Vinyl Polymerization by Radical Mechanisms*, Butterworths, London, 1958, (a) p. 117; (b) pp. 76, 82, 104.

2. H. S. Mickely, A. S. Michaels, and A. L. Moores, *J. Polym. Sci.*, **60**, 121 (1962).

3. T. T. Jones and H. W. Melville, *Proc. Roy. Soc.* (London), **A187**, 19 (1944).

4 D. Lím and M. Kolinsky, *J. Polym. Sci.*, **53**, 173 (1961).

5. C. H. Bamford, D. J. E. Ingram, A. D. Jenkins, and M. C. R. Symons, *Nature*, **175**, 894 (1955).

6. J. F. Gibson, D. J. E. Ingram, M. C. R. Symons, and M. G. Townsend, *Trans. Faraday Soc.*, **53**, 914 (1957).

7. D. J. E. Ingram, M. C. R. Symons, and M. G. Townsend, *Trans. Faraday Soc.*, **54**, 409 (1958).

8. H. Fischer, *Z. Naturforsch.*, **B19**, 866 (1964).

9. *Kinki Kagaku Kogyo-kai* [*Poly(vinyl Chloride)—Its Chemistry and Industry*], Asakura Schoten, Tokyo, 1961, (a) p. 73; (b) p. 82.

10. G. Bier and M. Krämer, *Kunststoffe*, **46**, 498 (1956).

11. J. D. Cotman, *J. Amer. Chem. Soc.*, **77**, 2790 (1955).

12. A. Nakajima, H. Hamada, and S. Hayashi, *Makromol. Chem.*, **95**, 52 (1966).

13. G. Boccato, A. Rigo, G. Talamini, and F. Zillio-Grandi, *Makromol. Chem.*, **108**, 218 (1967).

14. M. Asahina and M. Onozuka, *J. Polym. Sci. A*, **2**, 3503 (1965).

15. S. Enomoto and M. Asahina, *J. Polym. Sci. A-1*, **4**, 1373 (1966).

16. S. Enomoto and M. Asahina, *J. Mol. Spectry.*, **19**, 117 (1966).

17. P. D. Bartlett and F. A. Tate, *J. Amer. Chem. Soc.*, **75**, 91 (1953).

Electron-Transfer Polymers. XXXIX.
Redox Polymers based on Duroquinonyl Glycol

NOBUO NAKABAYASHI,* GERHARD WEGNER,† and HAROLD
G. CASSIDY, *Sterling Chemistry Laboratory,*
Yale University, New Haven, Connecticut 06520

Synopsis

Redox polyurethanes, polyesters, and alternate copolyurethanes and copolycarbonates from two kinds of benzoquinonyl glycol were prepared based on 2-(duroquinonyl)-propan-1,3-diol. The oxidized polymer is stable. When the fully reduced polymer in solution is exposed to air the durohydroquinonyl residues are oxidized to the quinone form while the less substituted hydroquinonyl glycol residues remain stable in the reduced form. There is thus prepared polymer with oxidized and reduced groups alternating along the chain.

Redox polyesters,[1] polyurethanes,[2] and polycarbonates[3] based on benzo-quinonyl glycols[4] have been reported as part of our continuing study of oxidation-reduction polymers. In all of these, the redox group has two hydrogens on the ring. Experience has shown the desirability of replacing these with methyl in order to improve stability toward oxidation. Furthermore, in these polymers the redox group has been part of the polymer chain, so that as it is oxidized or reduced the chain must change in length.[5] It was therefore decided to prepare polymer with fully substituted redox groups which would be pendant to the main chain. The redox monomer that seems most suitable is 2-(duroquinonyl)-propan-1, 3-diol (Du).[6] It is prepared from trimethylhydroquinone [eq. (1)] and is very stable. In the presence of pyridine, polyesters (E) could be prepared by reacting Du with terephthaloyl chloride (T) or isophthaloyl chloride (I), or sebacoyl chloride. The first two were obtained as yellow powders; the last (not studied further) as viscous yellow oil. By use of dibutyltin diacetate catalyst in dry THF, polyurethanes (U) were obtained by condensing Du with methylene-bis(4-phenylisocyanate) (M) or hexamethylenediisocyanate (H). They were both obtained as yellow powders.

These quinoid polymers are very stable. In contrast, when reduced with dithionite, or sodium borohydride, or by catalytic hydrogenation, they

---

* Present address: Institute for Medical and Dental Engineering, Tokyo Medical and Dental University, Kanda, Tokyo, Japan.

† Present address: Laboratory for the Physics of High Polymers, Institute for Physical Chemistry, University of Mainz, Mainz, Germany.

$$(1)$$

(Du)
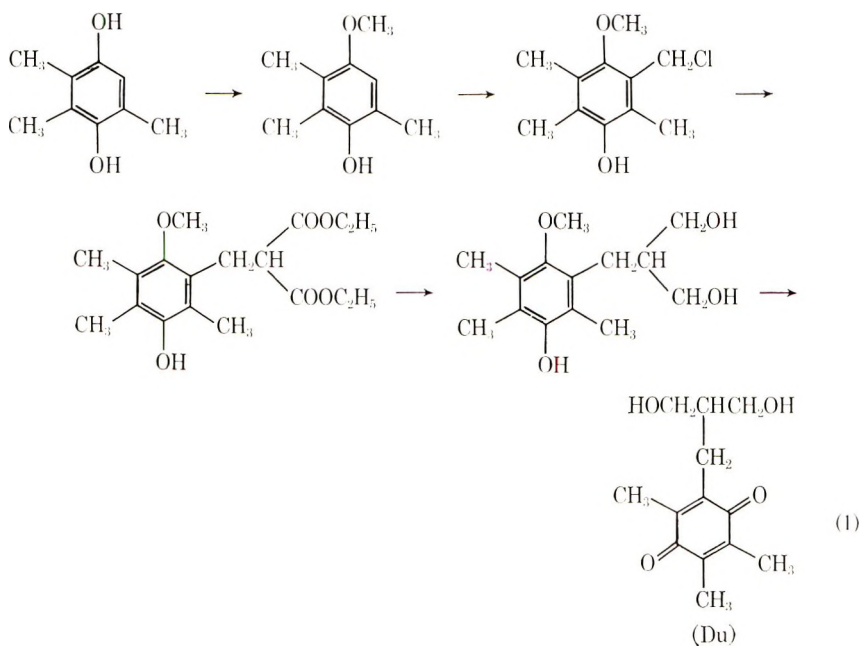
are immediately oxidized upon exposure to air. They are best preserved in the yellow oxidized form.

With two types of monomers available, namely Du and the benzo-quinonyl glycols 2,5-bis(2′-hydroxyethyl)-1,4-benzoquinone[4] (Et) and 2,5-bis(3′-hydroxypropyl)-1,4-benzoquinone[4] (Pr), it seemed of interest to prepare polymers containing the two functions (which have quite different
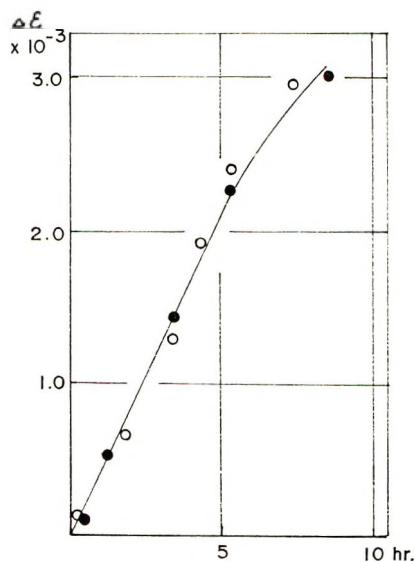
Fig. 1. Relation between increase of quinoid extinction coefficients with time: (●) $\Delta\epsilon$ of U-HDuEt at 262–263 mμ; (○) $\Delta\epsilon$ of U-HDu at 264 mμ.

Du + 2 OCN—R—NCO ⟶

OCNRNHCOOCH₂CHCH₂OCONHRNCO + Et ⟶

$$\left[-OCH_2CH_2 - \text{(quinone)} - CH_2CH_2OCONHRNHCOOCH_2CHCH_2OCONHRNHCO - \right] \quad (2)$$

U-H-DuEt
U-M-DuEt

U-H-DuEt: R = —(CH₂)₆—
U-H-DuEt: R = —C₆H₄—CH₂—C₆H₄— (both *para*)
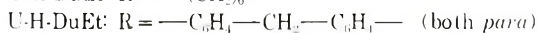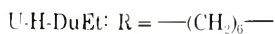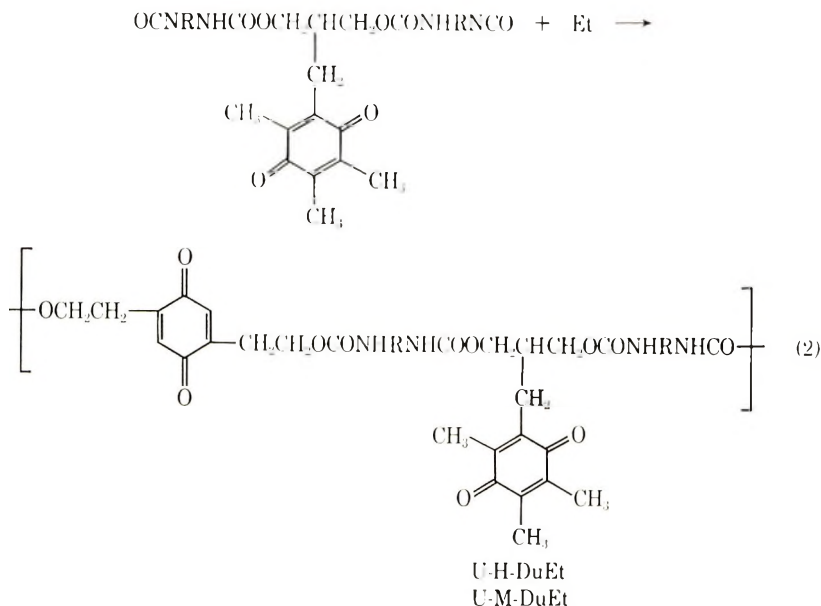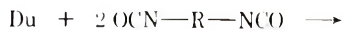
midpoint potentials) arranged alternately along the chain [eq. (2)]. It might be possible, then, to obtain polymer with alternate oxidized and reduced portions on the same chain, with consequent interesting charge transfer and other properties.

Accordingly, alternate copolyurethanes were prepared according to eq. (2) by reaction through M or H. Alternate copolycarbonate (C) was prepared according to eq. (3) from the bischloroformate of Du by condensa-

Du + 2 COCl₂ ⟶ ClCOOCH₂CHCH₂OCOCl + Et ⟶

$$\left[-OCH_2CH_2 - \text{(quinone)} - CH_2CH_2OCOCH_2CHCH_2OC - \right] \quad (3)$$

C-DuEt
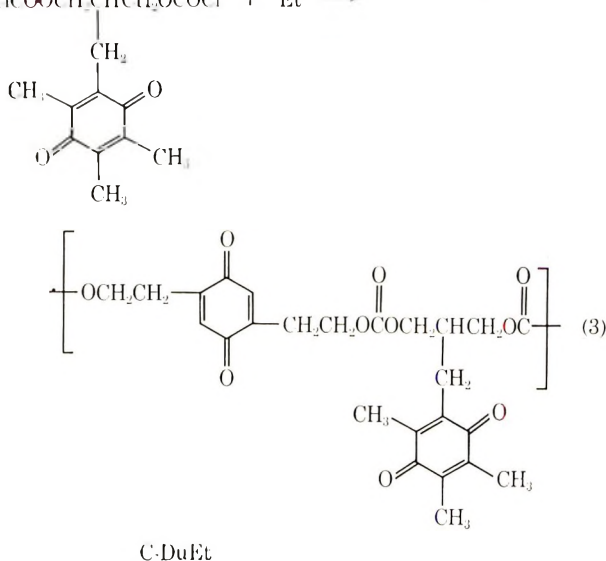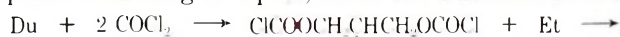
tion with Et in dry THF containing pyridine. All of these copolymers could be reduced. The data for oxidized and reduced forms (where obtainable) are collected in Table I. The spectral data for the reduced forms of

TABLE I
Summary of Measurement of Polymers

Polymer[a]	State	η_{sp}/c, dl/g[b]	Ultraviolet data[c]		Infrared data, cm^{-1}[d]	
			λ_{max}, mμ	$\epsilon \times 10^{-3}$	Quinone	Urethane or ester
E-T-Du	Ox	0.06	253	26.0	1640	1720, 1265
	Red	0.10	292	4.8	—	—
E-I-Du	Ox	0.04	262	14.7	1640	1720, 1234
	Red	0.08	292	3.3	—	—
U-H-Du	Ox	0.10	264	24.8	1640	1710, 1535, 1250
	Red	0.15	291	4.2	—	—
U-M-Du	Ox	0.20[e]	251	57.0	1639	1726, 1709, 1530, 1218
U-H-DuEt	Ox	0.11	262	30.3	1659, 1648, 1640	1704, 1536, 1250
	Red	0.12	295	7.6	—	—
U-M-DuEt	Ox	0.12	252	84.5	1648 (broad)	1730, 1710, 1535, 1217
U-M-DuPr	Ox	0.13	252	84.0	1650 (broad)	1730, 1710, 1538, 1220
C-DuEt	Ox	—	260	30.1	1645 (broad)	1750, 1250
	Red	—	290	12.0	—	—

[a] E = polyester; T = from terephthaloyl chloride; Du = 2(duroquinonyl) propan-1,3-diol; I = from isophthaloyl chloride; U = polyurethane; M = methylenebis(4-phenylisocyanate); H = hexamethylenediisocyanate; Et = 2,5-bis(2'-hydroxyethyl)-1,4-benzoquinone; Pr = 2,5-bis(3'-hydroxypropyl)-1,4-benzoquinone; C = polycarbonate. DuEt and DuPr mean alternate copolymer.

[b] η_{sp}/c: concentration of polymer solutions 0.50 g/100 ml in THF containing 5% water.

[c] Spectra taken in THF containing 5% water; the extinction coefficient is based on the repeating unit.

[d] Spectra were taken as film.

[e] In dry dimethylacetamide at 25°C.

TABLE II
Elementary Analysis of Polymers

Polymer	Formula	Calcd			Found		
		C, %	H, %	N, %	C, %	H, %	N, %
E-TDu	$(C_{21}H_{20}O_6)_n$	68.47	5.47	—	68.18	5.52	—
E-TDu	$(C_{21}H_{20}O_6)_n$	68.47	5.47	—	68.21	5.51	—
U-HDu	$(C_{24}H_{30}N_2O_6)_n$	62.05	7.44	6.89	61.80	7.33	6.79
U-MDu	$(C_{28}H_{28}N_2O_6)_n$	68.84	5.78	5.74	68.77	5.98	5.63
U-HDuEt	$(C_{42}H_{60}N_4O_{12})_n$	62.05	7.44	6.89	62.20	7.33	6.74
U-MDuEt	$(C_{53}H_{50}N_4O_{12})_n$	68.08	5.39	5.99	67.91	6.04	5.38
U-MDuPr	$(C_{55}H_{54}N_4O_{12})_n$	68.59	5.65	5.82	68.34	6.11	5.52
C-DuEt	$(C_{25}H_{26}O_{10})_n$	61.72	5.39	—	61.54	5.42	—

some of the polymers could not be obtained; where they were obtained this was accomplished in a special optical cell under hydrogen. Elementary analyses are given in Table II.

The fully reduced copolymers are colorless in solution, but extremely sensitive to air oxidation. To prepare the half-oxidized copolyurethane U-HDuEt it suffices to transfer a solution of the reduced polymer to the optical cell and allow air present above the liquid in the sealed cell to react with it. Absorption at 295 mμ falls while that 262–263 mμ rises as the durohydroquinonyl functional groups are oxidized to the quinoid form (Fig. 1). In experiments of this kind a stable state is reached with λ_{max}-262 mμ, ϵ-21.0 $\times$ 10^3, corresponding to the value of oxidized U-HDu. A shoulder at λ_{max}-295 mμ, ϵ-4.0 $\times$ 10^3, corresponds to reduced U-H Et. This indicates that the durohydroquinonyl residues in the HDu part are oxidized, while the less substituted hydroquinonyl groups of the glycol part (HEt) remain reduced. This state is stable in air for at least 150 hr. When the polymer is precipitated it appears as a red powder. We would have needed more material than we had available to measure this new presumably quinhydrone-like absorption. When the copolymer is fully oxidized it is yellow. The potential of the half-oxidized copolymer was found to be high, even in the presence of detergent.[7]

It was observed that the molar extinction coefficients of the copolyurethanes are close to additive functions of the individual polyurethanes. Thus U-MDu (57.0 $\times$ 10^3); + U-M Et (18.5 $\times$ 10^3) corresponds to U-M DuEt (84.5 $\times$ 10^3); U-M Du (57.0 $\times$ 10^3) + U-MPr (21.2 $\times$ 10^3) corresponds to U-M DuPr (84.0 $\times$ 10^5); U-H Du (24.8 $\times$ 10^3) + U-H Et (11.0 $\times$ 10^3) corresponds to U-H DuEt (30.3 $\times$ 10^3); and reduced U-H Du (4.2 $\times$ 10^3) + reduced U-H Et (3.9 $\times$ 10^3) corresponds to reduced U-H DuEt (7.6 $\times$ 10^3). This would seem to imply no marked electronic interaction between the separated species.

Viscosity numbers, as is commonly found,[1,2] are higher for the reduced than the oxidized forms, and upon reoxidation return to the original value for the oxidized form. This is an indication that the linkages are stable to oxidation and reduction under the employed conditions. There is no evidence of viscosity obstruction that interchain quinhydrone formation (with weak crosslinking) would produce if it were present.

EXPERIMENTAL

Materials. The benzoquinones Du, Et, and Pr were recrystallized just before use. Du is very stable. The diisocyanates M and H were purified by vacuum distillation. The acid chlorides T and I were recrystallized from *n*-hexane. THF was dried over sodium and distilled; pyridine was dried over barium oxide and distilled.

Polyester E-TDu. In 10.0 ml dry THF were dissolved 0.2349 g T and 0.2743 g Du. The solution was cooled in ice water, and 0.35 ml pyridine was added with stirring. The stirred mixture was allowed to come to room temperature, and after about 2 hr the mixture was poured

into water. The yellow precipitate was collected, dried *in vacuo*, and dissolved in THF. This solution was poured into ether; the yellow precipitate was gathered, and the treatment repeated. The yield was essentially quantitative.

Polyurethane U-MDuPr. M (0.4603 g) and Du (0.2187 g) were dissolved in dry THF. To the stirred mixture was added a drop of dibutyltin diacetate (Eastman, used without purification). (Amines are not suitable catalysts with these redox monomers[4].) After an hour at 25°C, 0.2061 g Pr was added to the mixture, and the polymerization was allowed to take place over a 2-hr period at the same temperature. The viscous mass was treated with alcohol to destroy any terminal isocyanate groups, and poured into *n*-hexane. Yellow flakes precipitated, were collected, dissolved in dimethylacetamide, and reprecipitated by pouring into a mixture of THF and *n*-hexane. The yield was 0.85 g.

Polycarbonate C-DuEt. About 5 ml of phosgene was collected from a Dry Ice condenser in a flask cooled in an ice–salt mixture. To it, a solution of 0.2371 g Du in 10 ml dry THF was added gradually. The mixture was then allowed to come to room temperature. After about 4 hr at room temperature all volatile material had evaporated. The red, viscous oil was dissolved in dry THF containing 0.1956 g Et. The mixture was cooled in an ice bath, and polycondensation was initiated by addition of 0.30 ml dry pyridine. Water was then poured into the mixture and a gummy material was collected and dried. This was taken up in THF and precipitated as dark yellow powder by pouring the solution into *n*-hexane. The yield was 0.30 g.

Reduction of Polymers. Copolymers containing reduced Du residues are not stable in air. Reduction was carried out by palladium on charcoal in 95% THF. The amount of hydrogen taken up was between 10 and 20% more than that required for the polymer alone. After reaction the catalyst was separated, and the solution was used directly for ultraviolet and viscosity measurements.

References

1. G. Wegner, N. Nakabayashi, and H. G. Cassidy, *J. Polym. Sci. B*, **6**, 97 (1968).
2. G. Wegner, N. Nakabayashi, and H. G. Cassidy, *J. Polym. Sci. A-1*, in press.
3. G. Wegner, N. Nakabayashi, S. Duncan, and H. G. Cassidy, *J. Polym. Sci. A-1*, submitted.
4. G. Wegner, N. Nakabayashi, and H. G. Cassidy, *J. Org. Chem.*, **32**, 3155 (1967).
5. H. G. Cassidy and K. Kun, *Oxidation-Reduction Polymers (Redox Polymers)*, Interscience, New York, 1965.
6. N. Nakabayashi, G. Wegner, and H. G. Cassidy, *J. Org. Chem.*, **33**, 2539 (1968).
7. N. Nakabayashi, G. Wegner, and H. G. Cassidy, *J. Polymer Sci. A-1*, in press.

Received October 16, 1968

Electron-Transfer Polymers. XL. Redox Polyamides

NOBUO NAKABAYASHI* and HAROLD G. CASSIDY,

Department of Chemistry, Yale University, New Haven, Connecticut 06520

Synopsis

By condensing a hydroquinone bis-lactone of 1,4-dihydroxybenzene-2,5-bis(ethyl-2'-carboxylic acid) with diamines such as hexamethylene diamine, piperazine, 4-amino-ethylpiperidine, or 1,3-di-(4'-piperidinyl) propane, redox polyamides can be prepared. The lactone functions protect the hydroxyl groups until the polymerization occurs at which point, due to the opening of the lactone rings, free hydroquinone hydroxyls appear. The resulting polymer is oxidizable. When the oxidized polymer is reduced the viscosity is higher than that of the original reduced polymer.
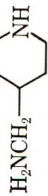
The earliest synthetic redox polyamide was produced by Harwood and Cassidy,[1] who had considerable difficulty in removing hydroquinone-protecting acetyl groups from the initial product of polymerization without damaging the main chain. In the present work we bring together the polycondensation of bis-lactone with diamine, reported by Iwakura and co-workers,[2] and the concept of a redox monomer containing two lactone rings that involve hydroquinone hydroxyls. When polycondensation is carried out, the hydroxyl groups released are those of the redox function, so that redox polyamide immediately results.
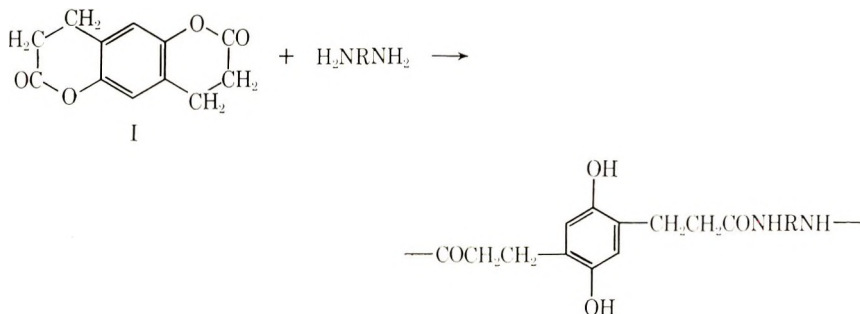
The monomer, 3H, 4H, 8H, 9H-benzo [1,2-b: 4,5-b'] dipyran-2,7-dione (1), the bis-lactone of hydroquinone-2,5-bis(ethyl-2'-carboxylic acid), was prepared by heating the acid[3,4] at 250–280°C without catalyst or solvent, preferably *in vacuo*. Polycondensation was carried out as reported,[2] with the use of hexamethylenediamine, piperazine, 4-aminomethylpiperidine, or

* Present address: Institute for Medical and Dental Engineering, Tokyo Medical and Dental University, Tokyo, Japan.

TABLE I
Data for Reduced and Oxidized Forms of Redox Polyamides

Diamine	Form[a]	η_{sp}/c, dl/g[b]	Softening temp, °C	Ultraviolet data[c] λ_{max}, mμ	$\epsilon \times 10^{-3}$	OH (NH), cm^{-1}	Infrared data[d] Amide, cm^{-1}	Quinone, cm^{-1}
H₂N(CH₂)₆NH₂	Red	0.18	200	294	3.7	3287	1630, 1550	—
H₂NCH₂–[cyclohexyl]–NH	Red	0.14		295	4.8	3287	1630, 1550 (small)	—
	Ox			262	13.6	3200 (NH)	1630, 1550	1650
HN–[cyclohexyl]–(CH₂)₃–[cyclohexyl]–NH	Red	0.12	170	293	~4.1	3190	1629, 1609	—
	Ox			262	12.8	—	1613	1650
Comparison amine n-C₄H₉NH₂	Red			294	4.1	3310	1636, 1560	—
	Ox					3331 (NH)	(1652), 1540	1652

[a] Red-reduced form of redox polyamide or comparison diamide; Ox = oxidized form.

[b] At 25°C, concentration = 0.50 g/100 ml dimethyl acetamide.

[c] In formic acid.

[d] In the case of polymer, film cast on plate; of comparison compound, KBr disk.

1,3-di-(4'-piperidinyl)propane as diamines. A small excess of I was used in order to place lactone groups at the ends of the chains. This is in order to avoid possible crosslinking which might occur on oxidation if there were a terminal amino group in the presence of benzoquinone. It appeared that crosslinking nevertheless occurred (see below). For comparison purposes, hydroquinone-2,5-bis(ethyl-2'-n-butylamide) was prepared from I and n-butylamine.

The polymers were white to light brown powdery flakes. All except that from piperazine were soluble in dimethylacetamide (DMAc), dimethylformamide (DMF), and formic acid. The piperazine polymer was soluble only in hot solvents. When the first two polymers in Table I were dissolved in concentrated sulfuric acid in the cold, spectral changes occurred— possibly associated with sulfonation of the hydroquinone residues. The oxidation of the polymers was carried out with the stoichiometric amount of ceric ammonium nitrate in DMAc. The yellow polymers so obtained were precipitated by addition of water. They were soluble in the same solvents as the reduced forms except for the hexamethylenediamine polymer which required hot solvents. Re-reduction could be carried out by dithionite or hydrogenation over palladium on charcoal. Optical and viscosity properties of the polymers are gathered in Table I.

It appeared that during the sequence of reactions from original reduced form to oxidized form and back to re-reduced form some crosslinking or other side-reaction occurred, because the viscosity of the recovered reduced form was higher than that of the original polyamide polymer.

EXPERIMENTAL

The monomer I. Into a sublimation apparatus was placed 2.0 g (0.079 mole) hydroquinone-2,5-bis-(ethyl-2'-carboxylic acid).[3] This was evacuated to 2 mm Hg and held at 250–280°C. White needles of sublimate, mp 290–292°C (1.5 g, 87%) were obtained. When crystallized from acetonitrile, these yielded a product that melted at 294–295°C.

ANAL. Calcd for $C_{12}H_{10}O_4$: C, 66.05%; H, 4.62%. Found: C, 65.86%; H, 4.51%.

The infrared spectrum (KBr disk) showed ester absorption bands at 1 740, 1 271, 1 181, 1 154 cm^{-1}, and no hydroxyl or carboxylic acid bands. When I was reduced with lithium aluminum hydride, hydroquinone-2,5-bis(propanol-3')[3] was obtained in 60% yield.

Typical Polycondensation. In the polycondensation of I with hexamethylenediamine, 0.2044 g (1.763 mmole) of freshly distilled hexamethylenediamine and 0.3845 g (1.765 mmole) of I were dissolved in 15 ml dry DMAc. The mixture was stirred and heated to 70°C. After 1 hr the temperature was allowed to fall to 50°C. The total heating time was 5.5 hr. After evaporation of DMAc *in vacuo*, the viscous solution was poured into water. A quantitative yield of flaky material was collected.

It was purified by twice repeated solution in DMAc and reprecipitation with water. A final yield of 0.44 g (75%) was obtained.

ANAL. Calcd for $(C_{18}H_{26}N_2O_4)_n$: C, 64.65%; H, 7.84%; N, 8.38%. Found: C, 64.44%; H, 7.88%; N, 8.86%.

Calculated and found nitrogen values for the three other polyamides were, respectively, for 4-aminomethylpiperidine, 8.43, 8.58%; for 1,3-di(4'-piperidinyl)propane, 6.54, 6.19%; and from piperazine, 9.21, 8.93%.

The polymer with piperazine was very insoluble, and the analysis is the only measurement obtained on it.

Hydroquinone-2,5-bis(ethyl-2'-*n*-butylamide). Monomer I (0.44 g) and *n*-butylamine (0.29 g) were stirred in 10.0 ml dry DMAc at room temperature. After 2 hr, when the butylamine odor had disappeared, DMAc was removed *in vacuo* at 60–70°C. and the residue was recrystallized from acetonitrile. White plates, mp 201–203°C, were obtained in a yield of 0.65 g (89%).

ANAL. Calcd for $C_{20}H_{32}N_2O_4$: C, 65.91%; H, 8.85%; N, 7.69%. Found: C, 66.13%; H, 8.92%; N, 7.53%.

References

1. H. J. Harwood, Jr. and H. G. Cassidy, *J. Amer. Chem. Soc.*, **79**, 4360 (1957).

2. Y. Iwakura, K. Hayashi, M. Shimizu, and T. Watanabe, *Makromol. Chem.*, **95,** 228 (1966).

3. G. Wegner, N. Nakabayashi, and H. G. Cassidy, *J. Org. Chem.*, **32,** 3155 (1967).

4. G. Wegner, N. Nakabayashi, and H. G. Cassidy, *J. Polym. Sci. B*, **6**, 97 (1968).

Effects of Substituents on Chain-Transfer Reactivities of p-Substituted Cumenes in Radical Polymerization of p-Substituted Styrenes

TADAHIRO YAMAMOTO* and TAKAYUKI OTSU, *Department of Applied Chemistry, Faculty of Engineering, Osaka City University, Sugimotocho, Sumiyoshi-ku, Osaka, Japan*

Synopsis

In order to study the effects of the substituents in both substrate and attacking radical on the chain-transfer reactivities of nuclear-substituted cumenes toward substituted polystyryl radicals, the polymerizations of p-substituted styrenes in the presence of p-substituted cumenes were carried out with α,α'-azobisisobutyronitrile as an initiator at 60°C, and their chain-transfer constants were determined. The relative chain transfer reactivities of p-substituted cumenes toward given p-substituted polystyryl radicals did not follow the Hammett equation, but were correlated with the modified Hammett equation, $\log(k/k_0) = \rho\sigma + \gamma E_R$, which was proposed by the present authors for evaluating the substituent effects in radical reactions. On the other hand, the relative reactivities of poly-(p-substituted styrene) radicals toward given p-substituted cumenes were correlated by the Hammett equation. Thus, it was concluded that the effects of the substituents in substrate cumene depended upon the contributions of both polar and resonance factors, while those in attacking polystyryl radical depended upon only a polar factor.

INTRODUCTION

A relationship between the structure and the reactivity in the reactions of a series of compounds toward a growing polymer radical is one of the interesting problems in the radical polymerization of vinyl monomers. Useful information to clarify this relationship is easily obtainable by studying the effects of substituents in both the compounds and the attacking radicals on copolymerization and chain-transfer reactivities.

In the previous papers, we studied the substituent effects on the reactivities in the chain-transfer reaction of nuclear-substituted cumenes toward the polystyryl,[1] poly(p-substituted styryl),[2] and poly(methyl methacrylate) radicals.[3] Similar substituent effects on the reactivities of a series of nuclear-substituted compounds such as toluenes,[4] acetophenones,[5] benzaldehydes,[6] dibenzoyl disulfides,[7] and diphenyl disulfides[8,9] toward attack by a particular polymer radical have been also investigated in our previous papers. However, previous investigations of the substituent effects in

* Present address: Himeji Institute of Technology, Idei, Himeji, Japan.

radical reactions have dealt exclusively with those in substrate, and there is little information regarding the substituent effects of attacking polymer radicals toward a definite substrate compound.   The purpose of the present study is to clarify not only the substituent effects in substrate but also those in the attacking radical.

The effect of the substituents on reactivities has been usually evaluated by the Hammett equation, eq. (1).

$$\log(k/k_0) = \rho\sigma, \text{ or } \rho\sigma^+ \qquad (1)$$

However the reactivities in radical reaction series are not always correlated with the Hammet σ or σ^+ constants of the substituents as those observed in many ionic reactions.   In the previous papers,[10,11] we have proposed the generalized Hammett equations, eq. (2), including the resonance term for evaluating the effect of the substituents in both radical and ionic reactions:

$$\log(k/k_0) = \rho\sigma + \gamma E_R \qquad (2)$$

where σ and E_R are polar and resonance substituent constants, and ρ and γ are reaction constants giving the susceptibilities of the polar and resonance effects caused by the substituents, respectively.   Recently, it has been found that the radical reaction series for over a hundred examples are fitted by eq.(2).[10]

In the present paper, the polymerizations of unsubstituted, p-methoxy, p-methyl, and p-chlorostyrenes in the presence of cumene and its p-substituted derivatives were carried out by using α,α'-azobisisobutyronitrile (AIBN) as an initiator at 60°C, and the chain-transfer constants were determined.   The effects of the substituents in both the substrate cumene and the attacking polystyryl radical on the chain transfer reactivities of these reactions are described and discussed on the basis of eq.(1) and eq.(2).

The p-substituents in styrene and cumene used in this study were as follows: for styrenes: CH_3O, CH_3, H, and Cl; for cumenes: CH_3O, t-C_4H_9, i-C_3H_7, H, Cl, Br, and CN.

EXPERIMENTAL

Materials

Styrene was used after purifying the commercial product. p-Chlorostyrene was prepared by the aluminum isopropoxide reduction of p-chloroacetophenone, followed by dehydration over potassium bisulfate according to the procedure of Brooks;[12] bp 53–54°C/3 mm Hg, $n_D^{20}1.5658$ (lit.[12] bp 52–53°C/3 mm Hg, $n_D^{20}1.5658$). p-Methylstyrene was prepared by acetylation of toluene, followed by Meerwein-Ponndorff reduction and then dehydration[13]; bp 54.5°C/11 mm Hg, $n_D^{16}1.5453$, (lit.[13] $n_D^{16.4}1.5446$). p-Methoxystyrene was synthesized by Grignard reaction of methylmagnesium bromide with anisaldehyde, followed by dehydration[14]; bp 45°C/0.5 mm Hg, $n_D^{20}1.5623$ (lit.[14] $n_D^{20}1.5622$).   Styrene and its derivatives were purified through distillation under reduced pressure before use.

The substituted cumenes except cumene were prepared by the methods reported previously,[1] and these materials were also purified by distillation before use. The other reagents were also used after purification by the usual method.

Polymerization Technique

Polymerizations were carried out in sealed glass tubes at 60°C under shaking. The required amount of benzene solution of cumenes was placed into a hard glass tube which contained given amounts of monomer and AIBN. This tube was degassed by the ordinary freezing and thawing technique and then sealed off under vacuum. After polymerization to below 10% conversion, the polymerization mixture was poured into a large amount of methanol to precipitate the polymer. The resulting polymer was filtered, washed with methanol, and then dried under vacuum.

Determinations of Average Degrees of Polymerization and Chain-Transfer Constants

The intrinsic viscosities $[\eta]$ of the resulting polymers were determined by using an Ubbelohde viscometer in benzene at 30°C. The number-average degree of polymerization $(\overline{P}_n)$ were then calculated from eqs. (3)–(6).

Polystyrene, 30°C:[15]
$$\log \overline{P}_n = 3.205 + 1.37 \log [\eta] \tag{3}$$

Poly-p-methoxystyrene, 30°C:[16]
$$\log \overline{P}_n = 3.472 + 1.43 \log [\eta] \tag{4}$$

Poly-p-methylstyrene, 25°C:[17]
$$\log \overline{P}_n = 3.312 + 1.42 \log [\eta] \tag{5}$$

Poly-p-chlorostyrene, 20°C:[18]
$$\log \overline{P}_n = 3.419 + 1.29 \log [\eta] \tag{6}$$

Chain-transfer constants (C) to cumenes toward given polymer radicals were calculated from the Mayo equation; eq. 7:

$$1/\overline{P}_n = (1/\overline{P}_{n0}) + C[S]/[M] \tag{7}$$

where [S] and [M] are the initial concentrations of cumene and monomer, respectively.

RESULTS AND DISCUSSION

The rates of polymerizations of these styrenes, whose concentrations were kept constant, were determined as a function of the concentration of cumenes to benzene used as diluent. The detailed results for determining chain-transfer constants of cumenes in polymerizations of unsubstituted,[1] p-methoxy-,[19] p-methyl-,[17] and p-chlorostyrenes[20] were described in previous papers. Since no appreciable retarding effect of all cumenes on the

TABLE I

Chain-Transfer Constants C of p-Y-Cumenes Toward p-X-Styrene Radicals at 60°C

Substituents in Cumenes Y	σ	E_R	$C \times 10^4$ with various substituents (X) in styrenes			
			H	p-Cl	p-CH$_3$	p-OCH$_3$
p-OCH$_3$	−0.268	0.11	3.23	3.86	3.27	3.40
p-t-C$_4$H$_9$	−0.197	0.03	3.46	3.52	3.59	3.64
p-i-C$_3$H$_7$	−0.15	0.03	3.30[a]	3.62[a]	3.67[a]	—
H	0.00	0.00	3.88	3.44	4.12	4.28
p-Cl	0.227	0.10	6.90	4.97	7.67	8.52
p-Br	0.232	0.12	7.57	5.71	9.23	11.8
p-CN	0.660	0.24	18.6	8.84	26.0	40.9

[a] Indicates the C value for one isopropyl group.

polymerization rates was observed, it was thought that accurate chain-transfer constants were obtained. Table I summarized the resulting chain transfer constants of the substituted cumenes toward attacks of various substituted polystyryl radicals at 60°C.

As is seen in Table I, the chain-transfer constants of the substituted cumenes are greater than those of unsubstituted cumene, regardless of the electron-attracting or -repelling character of the substituents. The plots according to eq.(1) are shown in Figure 1.

From Figure 1, it is observed that these plots do not give straight line relationships, but concave curves. Similar results were observed in chain-transfer reactivities of various other substrates[4–9] than cumene and in many radical reactions.[10]

Then, the plots of $\log(k/k_0) - \gamma E_R$ against Hammett σ constants of the
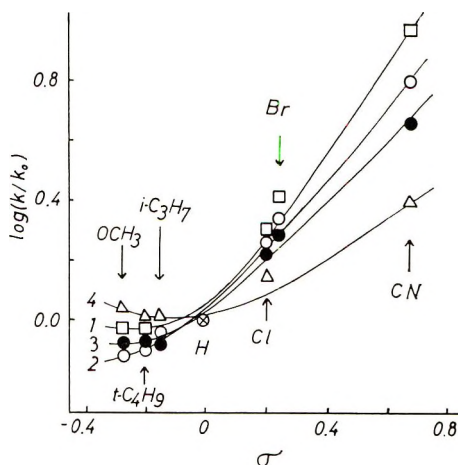
Fig. 1. Plots according to Hammett equation [eq. (1)] for the chain-transfer reactivities of p-substituted cumenes toward given poly(p-substituted styryl) radicals. Numbers refer to the same substituents in the polystyryl radical as indicated in Table II.
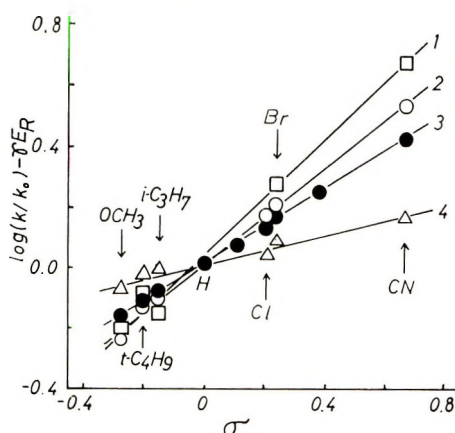
Fig. 2. Plots according to modified Hammett equation [eq. (8)]. Numbers refer to the same substituents in the polystyryl radical as indicated in Table II.

substituents according to eq. (8), which was derived from eq. (2) were attempted.

$$\log(k/k_0) - \gamma E_R = \rho\sigma \qquad (8)$$

The results are shown in Figure 2, from which linear relationships between $\log(k/k_0) - \gamma E_R$ and σ constants were found when the γ values were assumed to be about unity. These results strongly indicated that the reactivities of cumenes toward radicals were controlled by both polar and resonance effects caused by their substituents. The resulting ρ and γ values are listed in Table II.

It is expected that the ρ and γ values in eq. (2) depend on the structures (i.e., substituents) in both the substrate and the attacking polymer radical. From the ρ values in Table II, all of these chain-transfer reactions were observed to proceed nucleophilically, i.e., the chain-transfer reactivities of substituted cumenes toward these polymer radicals increased as electron-attracting substituents were introduced in the substrate cumene. It was also found that the ρ values changed widely and regularly with the substituents in the attacking polymer radical. The introduction of electron-attracting substituents in the attacking polystyryl radical decreased the ρ value as a result of a decrease in its nucleophilicity.

TABLE II

ρ and γ Values in the Application of Equation (2) for Chain-Transfer Reactivities of Cumenes Toward Given Radicals at 60°C

No.	Attacking radical	ρ	γ
1	Poly-p-methoxystyryl	+1.0	1.3
2	Poly-p-methylstyryl	+0.8	1.1
3	Polystyryl	+0.7	1.0
4	Poly-p-chlorostyryl	+0.2	1.0
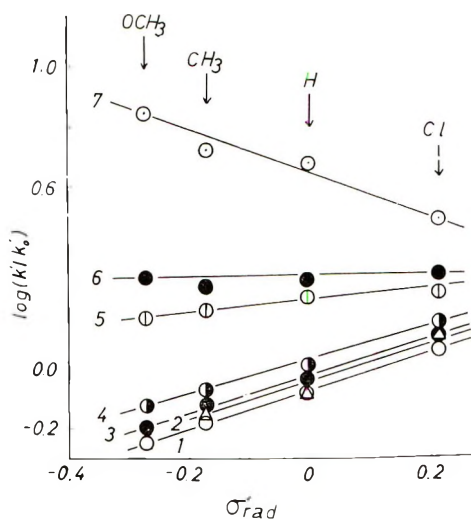
Fig. 3. Plots according to the Hammett equation [eq. (9)] for the chain-transfer reactivities of poly(p-substituted styrene) radicals toward given p-substituted cumenes. Numbers refer to the same substituents in p-substituted cumene as indicated in Table IV.

However, the resulting γ values in Table II were almost unchanged with the nature of the attacking polystyryl radicals in these reactions. Recently, the γ values were found to depend mainly on the principal structure of the radical produced from the substrate used.[4,6] These results were in contrast to those that the effect of the substituents in attacking polystyryl radicals toward γ values in given substituted cumenes were found to be zero (see Fig. 3).

The effect of the substituents in the attacking polystyryl radical toward given substrate cumenes was investigated by applying the Hammett equation (9):

$$\log(k'/k_0') = \rho\sigma_{\text{rad}} \tag{9}$$

TABLE III

Chain-Transfer Rate Constants k' of p-X-Substituted Polystyryl Radicals Toward Given p-Y-Substituted Cumenes

Y in cumene	$k' \times 10^4$ for various polystyryl radicals, mole/l -sec[a]			
	p-OCH$_3$	p-CH$_3$	H[b]	p-Cl
p-OCH$_3$	241	275	342	579
p-t-C$_4$H$_9$	258	326	367	528
p-i-C$_3$H$_7$	—	308	350	543
H	304	346	411	516
p-Cl	605	644	731	746
p-Br	838	775	802	857
p-CN	2904	2184	1932	1326

[a] Reported propagation rate constants for p-OCH$_3$, p-CH$_3$, H, and p-Cl styrenes were 71, 84, 106, and 150 mole/l -sec at 30°C.[21]

[b] Indicated k_0' values.

where k' and k_0' are chain-transfer rate constants of p-substituted and unsubstituted polystyryl radicals toward given cumenes, respectively (see footnote of Table III), and σ_{rad} is the Hammett constant for the substituents in the substituted polystyryl radical. The values of k' and k_0' were calculated from the reported rate constants for propagation of polymerizations of p-substituted styrenes[21] as shown in Table III.

The plots of $\log(k'/k'_0)$ with σ_{rad} are illustrated in Figure 3; all of these plots were found to satisfy straight-line relationships, indicating that the γ values in eq. (2) were zero, i.e., the resonance effect of the substituents in the attacking radical was not significant. One reason might be that the resulting radicals in the entire reaction series have the same structure. A similar result was reported by Imoto et al.[22] for the effect of the substituents on the copolymerization reactivities of p-substituted polystyryl radicals toward p-substituted styrenes.

The ρ values obtained from Figure 3 are shown in Table IV.

TABLE IV
ρ Values in Equation (9) Obtained from Figure 3

No.	Substituent in cumenes	ρ
1	p-OCH$_3$	$+0.68$
2	p-t-C$_4$H$_9$	$+0.55$
3	p-i-C$_3$H$_7$	$+0.50$
4	H	$+0.46$
5	p-Cl	$+0.10$
6	p-Br	$+0.04$
7	p-CN	-0.65

Table IV indicates that the ρ values also change regularly, depending on the polar nature of the substituents in the attacking polystyryl radical. Accordingly, it was concluded that the polar effects of the substituents in both the attacking radical and the substrate were significant for these chain-transfer reactions. However, the resonance effect of the substituents was considered to become important only for the reaction series giving radicals which have different substituents.

References

1. T. Yamamoto, Bull. Chem. Soc. Japan, **40**, 642 (1967).
2. T. Yamamoto and T. Otsu, J. Polym. Sci. B, **4**, 1039 (1966).
3. T. Yamamoto and T. Otsu, J. Polym. Sci. A-1, **6**, 49 (1968).
4. T. Yamamoto, S. Nakamura, M. Hasegawa, and T. Otsu, Kogyo Kagaku Zasshi, **72**, 727 (1969).
5. T. Yamamoto, M. Hasegawa, and T. Otsu, Bull. Chem. Soc. Japan, **41**, 2788 (1968).
6. T. Yamamoto and T. Otsu, Bull. Chem. Soc. Japan, in press.
7. K. Tsuda and T. Otsu, Bull. Chem. Soc. Japan, **39**, 2206 (1966).

8. T. Otsu, Y. Kinoshita, and M. Imoto, *Makromol. Chem.*, **73**, 225 (1964).

9. K. Tsuda, S. Kobayashi, and T. Otsu, *Bull. Chem. Soc. Japan*, **38**, 1517 (1965).

10. T. Otsu and T. Yamamoto, *J. Soc. Org. Synth. Chem. Japan*, **23**, 643 (1965).

11. T. Yamamoto and T. Otsu, *Chem. Ind.* (London), **1967**, 787.

12. L. A. Brooks, *J. Amer. Chem. Soc.*, **66**, 1295 (1944).

13. D. T. Mowry, *J. Amer. Chem. Soc.*, **68**, 1106 (1946).

14. C. Walling and K. B. Wolfstirn, *J. Amer. Chem. Soc.*, **69**, 852 (1947).

15. F. R. Mayo, R. A. Gregg, and M. S. Matheson, *J. Amer. Chem. Soc.*, **73**, 1691 (1951).

16. T. Alfrey, Jr., A. Bartovics, and H. Mark, *J. Amer. Chem. Soc.*, **65**, 2319 (1943).

17. T. Yamamoto, T. Otsu, and M. Imoto, *Kogyo Kagaku Zasshi*, **69**, 990 (1966).

18. N. Fuhrman and R. B. Mesrobian, *J. Amer. Chem. Soc.*, **76**, 3281 (1954).

19. T. Yamamoto and T. Otsu, *Kogyo Kagaku Zasshi*, **70**, 2403 (1967).

20. T. Yamamoto and T. Otsu, *Bull. Chem. Soc. Japan*, **40**, 2449 (1967).

21. M. Imoto, M. Kinoshita, and M. Nishigaki, *Makromol. Chem.*, **86**, 217 (1965).

22. M. Imoto, M. Kinoshita, and M. Nishigaki, *Makromol. Chem.*, **94**, 238 (1966).

Polymerization of β-Cyanopropionaldehyde.   IV. Polymerization by the Adducts of β-Cyanopropionaldehyde with Triethylaluminum

KAZUKIYO KOBAYASHI* and HIROSHI SUMITOMO, *Faculty of Agriculture, Nagoya University, Chikusa, Nagoya, Japan*

Synopsis

Adducts (X, Y, and Z) between triethylaluminum and β-cyanopropionaldehyde (CPA) have been prepared and characterized. It was found that an equimolar amount of triethylaluminum undergoes Grignard type addition reaction with aldehyde group of CPA to give aluminum alkoxide and that another equimolar quantity of triethylaluminum undergoes coordination with the nitrile group of CPA (adduct X, in which the molar ratio of CPA to aluminum is 1:2). The coordinated triethylaluminum in adduct X may be changed to aluminum alkoxide by the addition of further equimolar amount of CPA (adduct Y, molar ratio = 1:1); on the other hand, heating at 130°C affords mixtures of aluminum aldimine and aluminum ketenimine structures (adduct Z, molar ratio = 1:2). From the cryoscopic measurement, adduct Z may be regarded as a coordinated polymer joined through bridged structures I and II.
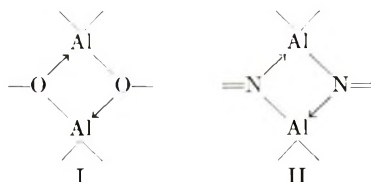
In the polymerization of CPA at −78°C, the stereoregularity of the resulting poly-(cyanoethyl)oxymethylene was found to increase in the order: X < triethylaluminum < Y < Z. The polymerizations with triethylaluminum, X, and Y are considered to be initiated by NCCH₂CH₂CH(C₂H₅)—O—Al(C₂H₅)₂. The degree of association of the species may influence the stereoregularity of the polymer.

INTRODUCTION

β-Cyanopropionaldehyde (CPA), having a polar nitrile group, is expected to exhibit characteristic polymerization behavior different from that of the common aliphatic or chlorinated aldehydes.

It was previously pointed out[1] that complex formation between the nitrile group of CPA and titanium makes a contribution to steric control in the polymerization of CPA with use of organoaluminum–titanium chloride complexes as initiators.

*On leave from the Department of Chemical Technology, Faculty of Engineering, Osaka University, Japan.

During the course of the subsequent investigation, some types of adducts of triethylaluminum with CPA have been prepared. It was found that the nitrile group, as well as the aldehyde group, of CPA participates in the reaction with triethylaluminum and that the resulting adducts can initiate the stereospecific polymerization of the monomer at low temperature. The present paper is concerned with the preparation of the adducts and the elucidation of the polymerization of CPA initiated by them, compared with the polymerization mechanism of acetaldehyde.

Preparation and Characterization of Adducts of
β-Cyanopropionaldehyde with Triethylaluminum

The preparation and purification of CPA and triethylaluminum have already been described.[1-3] The air- and moisture-sensitive adducts were prepared and examined in a glass apparatus and in a dry box filled with dry nitrogen. A solution of CPA in benzene was added dropwise with stirring to a solution of triethylaluminum (14.22 g, 0.1246 mole) in benzene (40 ml) on cooling at 0°C over 30–60 min. Addition of the solution of CPA (5.18 g, 0.0623 mole) in benzene (20 ml) gave adduct X, in which the molar ratio of CPA to triethylaluminum is 1:2. Adduct Y (molar ratio = 1:1) was obtained by further adding the same amount of CPA solution to X. The solvent was removed from X *in vacuo* and the residue was heated at 130°C for 30 min, leaving a brown, viscous liquid (adduct Z).

It is generally known[4] that the aldehyde group is susceptible to Grignard-type addition with organoaluminum compounds. For example, acetaldehyde was treated with triethylaluminum to give $(C_2H_5)_2AlOCH(CH_3)$-C_2H_5, which was hydrolyzed to *sec*-butanol.[5] The infrared absorption spectra of adducts X, Y, and Z were measured in benzene as shown in Figure 1. No band was observed in the region of carbonyl stretching in any of the spectra, but the vibration of C—O stretching was suggested by the appearance of a new absorption at 1040 cm^{-1} (9.62 μ). Hydrolysis of X and Y gave 4-hydroxyhexanenitrile (yield, 5.4 g from X and 11.0 from Y), which was confirmed by infrared- and NMR spectra. It may be reasonable to assume that the aldehyde group of CPA is converted to aluminum alkoxide by the reaction with triethylaluminum.

Noticeable variations of the absorption peak are also observed in the region around 2200 cm^{-1} in the infrared spectra shown in Figure 1. CPA originally exhibits nitrile absorption at 2250 cm^{-1} (4.44 μ).[2] The peak is found to shift to 2300 cm^{-1} (4.35 μ) in the infrared spectrum of adduct X. However, it returns to the original position of 2250 cm^{-1} in the spectrum of adduct Y. The characteristic shift of the nitrile stretching band to higher wave number is well known to be assignable to the coordination of the nitrile compounds with Lewis acids[1,6-8] or with organometallic compounds.[9-11] It may be concluded that in adduct X one equimolar amount of triethylaluminum reacted with aldehyde group of CPA to give aluminum alkoxide and that the second equimolar triethylaluminum underwent coordination with the nitrile group of CPA. The coordination bond,

which is considered to be weak and reversible, may be broken down by the approach of the new incoming aldehyde group. In this way the addition of another equimolar amount of CPA to adduct X may result in the formation of adduct Y.

The reaction mixture of CPA with triethylaluminum prepared in toluene at −78°C underwent ethanolysis at this temperature to give 4-hydroxy-
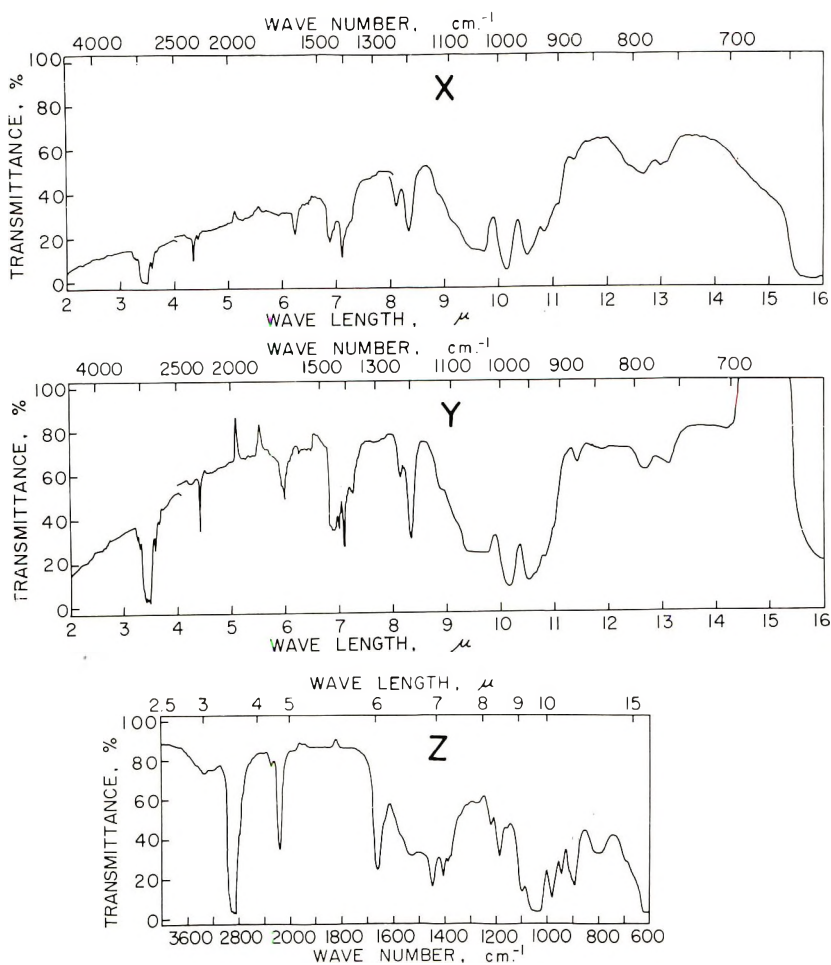
Fig. 1. Infrared absorption spectra of CPA–triethylaluminum adducts (in benzene, 10%).

hexanenitrile. This means that aluminum alkoxide can be formed even at −78°C.

Adducts X and Y are estimated to have a dimeric structure from the results of cryoscopic molecular weight measurements carried out in benzene under nitrogen (Table I). Bridged structures resulting from the coordination of oxygen to aluminum may be present in both adducts X and Y.

Adduct Z displayed characteristic absorption peaks at 1660 cm^{-1} (6.02 μ) and at 2160 cm^{-1} (4.63 μ), but no C$\equiv$N stretching vibration in the infrared spectrum.

The hydrolysis of Z yielded liquid product (6.1 g). The product (0.92 g) was treated with acidic 2,4-dinitrophenylhydrazine to give 2,4-dinitrophenylhydrazone (1.99 g) of 4-hydroxyhexanal, mp 127–129°C.

ANAL. Calcd. for C$_{12}$H$_{16}$N$_4$O$_5$: C, 48.65%; H, 5.44%; N, 18.91%. Found: C, 48.00%; H, 5.21%; N, 18.59%.

The molecular weight was determined to be 299 by vapor pressure osmometry (calcd. for C$_{12}$H$_{16}$N$_4$O$_5$, 296). The absorption maximum at 363 mμ (ϵ = 20 900) in ethanol in the visible absorption spectrum shifted to 435 mμ (ϵ = 14 400) and 540 mμ (ϵ = 7 000) on treatment with 0.25N ethanolic sodium hydroxide. Both peaks almost disappeared within 90 min after mixing. It is reported to be characteristic of 2,4-dinitrophenylhydrazone of aldehyde compounds.[12] The formation of 4-hydroxyhexanal indicates that adduct Z contains the aluminum aldimine unit, $-$CH$=$N$-$Al$<$, which can also be confirmed by the absorption at 1 660 cm^{-1} (6.02 μ) in the infrared spectrum.

Thermal rearrangement at 110–240°C of the coordinated compounds of nitriles with organoaluminums and organogalliums was studied in detail by Wade et al.[9–11] It was reported that in the trimethylaluminum and triphenylaluminum systems an organic group migrated from aluminum to the carbon of the nitrile to yield an aluminum ketimine structure. However, if the organic group was an alkyl group other than a methyl group, it separated as an olefin, leaving hydrogen to become attached to the nitrile carbon and to yield an aluminum aldimine structure.[9,10] The results are also supported by the fact that AlR$_3$ itself (where R is a higher alkyl other than methyl), on heating above 120°C, gives the corresponding olefin and AlR$_2$H,[13] which acts as a strong reducing agent toward nitrile, through the aldimine structure as an intermediate.[9,10] In the system of the present paper, although the possibility of the migration of an ethyl group might not be completely excluded, it is assumed that there is formed principally the aluminum aldimine structure, which affords the aldehyde on hydrolysis.

TABLE I

Cryoscopic Measurement of Molecular Weight of CPA–Triethylaluminum Adducts in Benzene

Adduct	Observed molecular weight	Degree of association
X	579	1.9
Y	441	2.2
Z	1346	4.8[a]

[a] The value was estimated from the average molecular weight of Z$_1$ and Z$_2$ units [Eq. (1)].
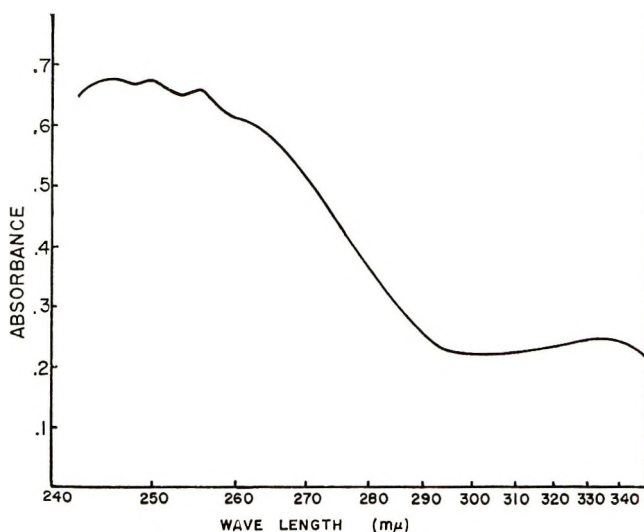
Fig. 2. Ultraviolet spectrum of adduct Z (in chloroform, 0.087 g/l.; path length, 1 cm).

On the other hand the ultraviolet spectrum of Z shown in Figure 2 shows absorption maxima around 255 and 338 mμ in chloroform solution. It is known that ketenimine compounds exhibit ultraviolet absorption maxima at these regions.[14,15] The ketenimine structure may also be confirmed by the strong absorption at 2 160 cm^{-1} (4.63 μ) in the infrared spectrum. Little is known about ketenimine formation through the reaction of organometallic compound with nitrile groups, except for the preparation of $(CH_3)_2Ga-N=C=CH_2$[11] and $(CH_3)_3SiCH=C=N-Si(CH_3)_3$.[16]

The evidence presented above indicates that the reaction of triethyl-aluminum with nitrile group of CPA at 130°C affords mainly mixtures of aluminum aldimine and aluminum ketenimine structures. The proportion of the two structures and the mechanism of their formation are still not clear. The analysis of gas liberated during the reaction would also be useful for the more quantitative discussion.

Adduct Z can be presumed to have not only the four-membered bridged structure I but also the structure II.[9-11]
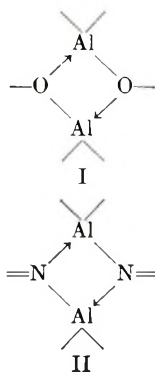
This seems to be supported by the fact that degree of association of adduct Z, as estimated cryoscopically, is 4.8 (Table I). It is interesting to note that Z may be regarded as a coordinated polymer, in which the bridged structures containing nitrogen and oxygen come out alternately to extend linearly.

The presumed reaction scheme and structures for the adducts are summarized in eq. (1). Further investigation to clarify the detailed structures of these compounds must be the subject of future research.

$$Z : \text{ mixture of } Z_1\text{- and } Z_2 \text{ unit} \tag{1}$$
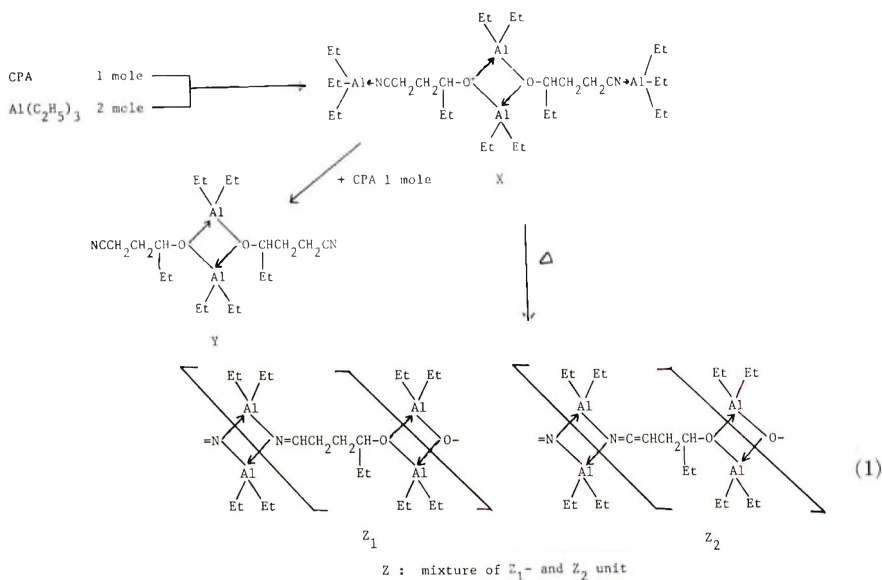
We have as yet very little information on the reaction of organometallic compounds with compounds having two or more reactive functional groups such as aldehyde and nitrile. Some possibility of the formation of a new type of linear coordinated polymer may be introduced here. The formation of ketenimine structure in the present reaction system as shown in Z is also noticeable.

Polymerization

The polymerization of CPA was carried out with the use of triethylaluminum, adduct X, Y, and Z as initiators in methylene chloride at $-78°C$. A solution of initiator in methylene chloride (10 g) was prepared in a glass tube, the aluminum content being maintained at 1% relative to monomer. A cold solution of CPA (10 g) in methylene chloride (10 g) was added on cooling at $-78°C$. After evacuation at liquid nitrogen temperature, the ampoule was sealed and then placed in a Dewar flask filled with solid carbon dioxide. The method of termination and elution fractionation and the measurement of the optical density ratio, D_{1258}/D_{1270}, of the resulting polymer were identical with those described previously.[1-3]

The results of polymerization of CPA are listed in Table II. Catalysts are arranged in order of decreasing polymer yield. The content of DMF-

TABLE II
The Results of Polymerization of CPA[a]

Catalyst	Total polymer		DMF-insoluble fraction	
	%	D_{1258}/D_{1270}	%	D_{1258}/D_{1270}
X	40.8	<1.0	8.9	1.30
$Al(C_2H_5)_3$	33.9	<1.0	33.6	1.53
Y	26.2	1.47	54.6	1.50
Z	8.1	1.50	69.3	1.56

[a] CPA, 10 g; aluminum content in catalyst, 1 mole-% (on monomer); solvent, methylene chloride, 20 g; −78°C; time, 1 day.

insoluble fraction is found to increase in the same order with decreasing polymer yield.

The unfractionated polymers prepared with X and triethylaluminum show values of D_{1258}/D_{1270} lower than unity. Adducts Y and Z afforded unfractionated polymer having a high optical density ratio, D_{1258}/D_{1270}, and little increase in the value was observed even after the fractionation with DMF. It was mentioned previously that the optical density ratio D_{1258}/D_{1270} increases with the stereoregularity of poly(cyanoethyl)oxymethylene.[1] The poly(cyanoethyl)oxymethylene prepared with adducts Y and Z may be thus considered to have a rather high and uniform stereoregularity, although X and triethylaluminum produce a larger amount of amorphous polymer. It may be concluded that the catalytic activity decreases in the order: X > triethylaluminum > Y > Z, and the stereoregularity of the resulting polymer increases in the reverse order: X < triethylaluminum < Y < Z.

It is clear that triethylaluminum, X, and Y are originally different from one another, but, as pointed out earlier, triethylaluminum and nitrilecoordinated triethylaluminum in X would react with the aldehyde group of CPA monomer newly added at −78°C to form aluminum alkoxide. This suggests that the addition of cold CPA monomer to catalyst solution of triethylaluminum, X, and Y may all afford the same molecular species, $NCCH_2CH_2CH(C_2H_5)—O—Al(C_2H_5)_2$, while the degrees of association are different.

Furukawa et al.[5,17,18] pointed out that the active species in the polymerization of acetaldehyde with use of triethylaluminum is aluminum alkoxide, $(C_2H_5)_2Al—O—CH(CH_3)C_2H_5$. It seems reasonable to assume that the aluminum alkoxide is also involved in the coordinated anionic polymerization of CPA. Though all polymerizations of CPA with triethylaluminum, X, and Y are probably induced by the same initiator, $NCCH_2CH_2CH(C_2H_5)—O—Al(C_2H_5)_2$, the polymer yield and stereoregularity do not agree. This may be explained by the concept that the stereoregularity of the resulting polymer depends upon the degree of association of the initiator. This concept was first proposed by Fujii et al.[5] It was suggested that an aluminum alkoxide having a dimeric structure yielded highly stereoregular polymer, while monomeric alkoxide, if it could

not form dimer owing to the solvation through aldehyde and nitrile, would exhibit little steric control.

The cryoscopic molecular weight measurements support a dimeric structure for adduct Y, which can carry out highly stereospecific polymerization of CPA. Adduct X consists of two kinds of aluminum components: one is an aluminum alkoxide which is also considered to be dimeric; the other is triethylaluminum coordinated to a nitrile group, and it would probably form monomeric aluminum alkoxide if mixed with CPA at low temperature. Therefore nearly equal amounts of dimeric and monomeric aluminum alkoxide may be derived from X. On the other hand, triethylaluminum was also found to make a steric contribution to the polymerization of CPA as effectively as adduct X. This may be due to the fact that triethylaluminum itself is dimeric.[4,19] If the reaction is assumed to take place, as it were, in the cage solvated through an amount of polar functional groups of the monomer, dimeric triethylaluminum would react with CPA to be ready to give dimeric aluminum alkoxide, while nitrile-coordinated triethylaluminum would give monomeric aluminum alkoxide.

Poly(cyanoethyl)oxymethylene of high stereoregularity was also obtained in the catalyst system with Z. Both Al—O and Al—N[20] species are assumed to be able to initiate the stereospecific polymerization of aldehyde, but which species exhibits effective steric control is a future problem. The length and rigidity of the catalyst species might also affect the steric control in the polymerization.

References

1. K. Kobayashi and H. Sumitomo, *J. Polym. Sci. A-1*, **7** (Apr., 1969).
2. H. Sumitomo and K. Kobayashi, *J. Polym. Sci. A-1*, **4**, 907 (1966).
3. H. Sumitomo and K. Kobayashi, *J. Polym. Sci. A-1*, **5**, 2247 (1967).
4. R. Köster and P. Binger, *Adv. Inorg. Chem. Radiochem.*, **7**, 263 (1965).
5. H. Fujii, I. Tsukuma, T. Saegusa, and J. Furukawa, *Makromol. Chem.*, **82**, 32 (1965).
6. H. J. Coerver and C. Curran, *J. Amer. Chem. Soc.*, **80**, 3522 (1958).
7. W. Gerrard, M. F. Lappert, H. Pyszora, and J. W. Wallis, *J. Chem. Soc.*, **1960**, 2182.
8. T. L. Brown and M. Kubota, *J. Amer. Chem. Soc.*, **83**, 4175 (1961).
9. J. E. Lloyd and K. Wade, *J. Chem. Soc.*, **1965**, 2662.
10. J. R. Jennings, J. E. Lloyd, and K. Wade, *J. Chem. Soc.*, **1965**, 5083.
11. J. R. Jennings and K. Wade, *J. Chem. Soc. Inorg. Phys. Theoret.*, **1967**, 1222.
12. L. A. Jones, J. C. Holmes, and R. B. Seligman, *Anal. Chem.*, **28**, 191 (1956).
13. K. Ziegler, *Angew. Chem.*, **68**, 721 (1956).
14. C. L. Stevens and J. C. French, *J. Amer. Chem. Soc.*, **75**, 657 (1953).
15. C. L. Stevens and R. J. Gasser, *J. Amer. Chem. Soc.*, **79**, 6057 (1957).
16. M. Prober, *J. Amer. Chem. Soc.*, **78**, 2274 (1956).
17. J. Furukawa, T. Saegusa, and H. Fujii, *Makromol. Chem.*, **44/46**, 398 (1961).
18. J. Furukawa, T. Saegusa, and H. Fujii, in *Macromolecular Chemistry (J. Polym. Sci. C*, **4**), M. Magst, Ed., Interscience, New York, 1963, p. 281.
19. G. E. Coates, *Organometallic Compounds*, 2nd ed., Methuen, London, 1960, p. 130.
20. H. Tani and N. Oguni, *J. Polym. Sci. B*, **3**, 123 (1965).

Polysiloxanes Having Aromatic Heterocyclic Units. I. Polydimethylsiloxane Benzimidazole Polymer

TOSHINARI NAKAJIMA and C. S. MARVEL, *Department of Chemistry, University of Arizona, Tucson, Arizona 85721*

Synopsis

A polymer containing dimethylsiloxane units (35) and benzimidazole units (1) has been prepared by the condensation of 3,3'-diaminobenzidine and an α,ω-bis-(γ-carboxy-n-propyl) polydimethylsiloxane. The new polymer has some rubbery properties, but it decomposes catastrophically at 400°C.

In a search for a thermally stable rubber material, the condensation of a polydimethylsiloxane with carboxyl end groups (I) with 3,3'-diamino-benzidine has been carried out. The polysiloxane contains approximately 35 dimethylsiloxane units. The benzimidazole polymer obtained (II),

$$HO_2C(CH_2)_3-\underset{\underset{CH_3}{|}}{\overset{\overset{CH_3}{|}}{Si}}\left[-O-\underset{\underset{CH_3}{|}}{\overset{\overset{CH_3}{|}}{Si}}\right]_n(CH_2)_4-CO_2H$$

I
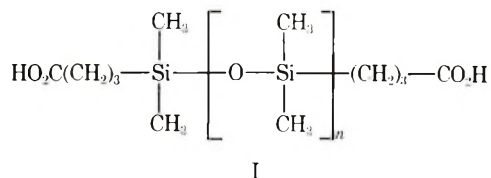
was a light tan-colored, rubbery material which did not melt completely until heated to 105–110°C. Various samples varied in inherent viscosity of 0.38 to 0.66 (0.5 g/100 ml THF at 30°C).

II
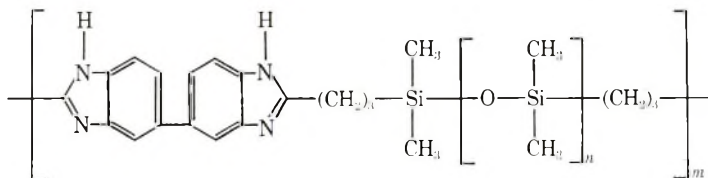
The conditions used in various condensations and the properties of individual samples of polymers are given in Table I. The best condition seemed to be heating at about 280°C. At 300°C, insoluble material seemed to form.

TABLE I
Polysiloxane–Benzimidazole Polymers

Run no.	Starting material	Reaction at 1 atm. pressure		Reaction at the reduced pressure (0.1 mm Hg)		Inherent viscosity η_{inh}[b]
		Temperature, °C	Time, hr	Temperature, °C	Time, hr	
E-1	I[a] + 3,3'-diamino-benzidine	240	14	300	1/2	0.38
E-2	I[a] + 3,3'-diamino-benzidine	200	2			
		200 → 250	1	255	2	0.28
E-3	Polymer E-2	230 → 265	1/6	280	1/3	0.47
E-4	Polymer E-2	260	2/3	280	1	0.66
E-5	I[a] + 3,3'-diamino-benzidine	220	17	—	—	0.21
E-6	Polymer E-5	—	—	300	1/2	0.32
E-7	Polymer E-5	—	—	270	1/2	0.53

[a] $\eta = 0.06$.
[b] 0.5 g/100 ml THF at 30°C.

The thermogravimetric analysis of the polysiloxane–benzimidazole polymer (E-4) is shown in Figure 1.

Attempts to make the diphenyl ester of the siloxane I through the acid chloride resulted in degradation of the siloxane. Attempts to equilibrate
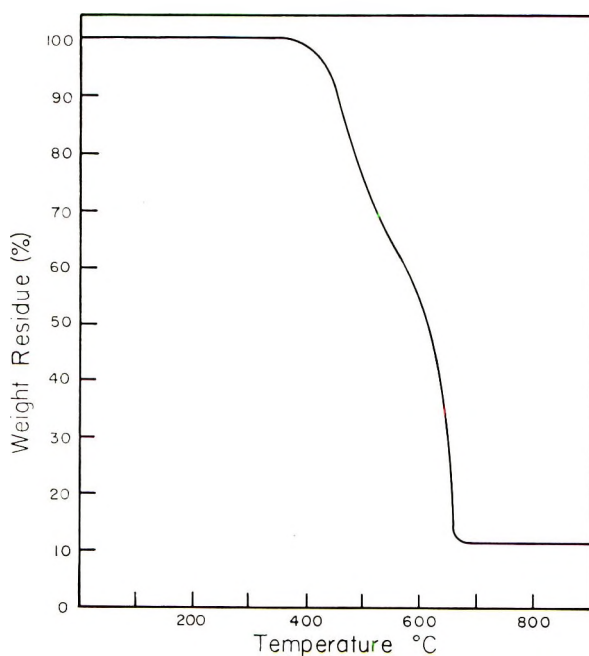
Fig. 1.   TGA curve for polydimethyl-siloxane with imidazole units.

diphenyl 5,5-tetramethyl-5,7-disiloxaneoxaundecanoate[1] with octamethyl-cyclooctasiloxane only resulted in partial hydrolysis of the ester.

The model compound III was prepared from the polysiloxane dicarboxylic acid and o-phenylenediamine. The polymeric diacid, I was prepared as previously described.[2]

III
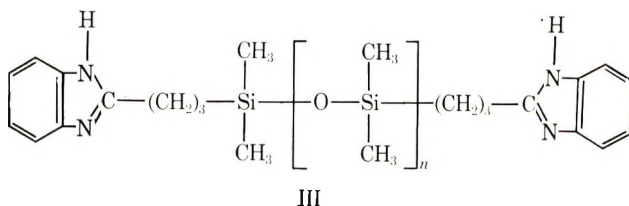
EXPERIMENTAL

Model Compound III. Under nitrogen atmosphere, compound I (0.662 g, 0.00022 mole) was heated with o-phenylenediamine (0.047 g, 0.00044 mole) at 220°C for 2 hr. The flask was then evacuated to 0.15 mm Hg and heated at 290°C for an additional $1/2$ hr to yield 0.360 g (52.6%) of product.

The infrared spectrum of compound III shows Si-CH$_3$ linkage (1 020 cm^{-1} and 1 100 cm^{-1}), and its ultraviolet spectrum showed λ_{max} at 277 and 283 mμ in ethanol.

ANAL. Calcd for C$_{96}$H$_{250}$O$_{37}$N$_4$Si$_{38}$: C, 37.0%; H, 8.03%; Si, 34.2%. Found: C, 32.86%; H, 8.57%; Si, 34.19%.

It will be noted that all carbon analyses are low, perhaps due to formation of some silicon carbide during the analysis. The other values check well.

Polysiloxane-Benzimidazole Polymer (II) (Run E, Table I). In a reaction tube fitted with nitrogen inlet and outlet, and a magnetic stirrer were placed 1.899 g. of α,ω-bis(γ-carboxy-n-propyl)dimethylpolysiloxane (I) ($\eta_{inh} = 0.06$) and 0.162 g of 3,3'-diaminobenzidine. The mixture was heated under nitrogen. After being heated at 120°C for 2 hr, the reaction tube was heated at the same temperature for 1 hr and at 300°C for additional 20 min. The reaction mixture was cooled, and ethyl alcohol was added to the reaction tube to give 1.500 g of cold alcohol insoluble rubbery material and 0.311 g of cold alcohol-soluble material. Tetrahydrofuran solution of the cold alcohol-insoluble part had an inherent viscosity of 0.38 at 30°C (0.5 g/100 ml).

ANAL. Calcd for (C$_{96}$H$_{248}$O$_{37}$N$_4$Si$_{38}$)$_n$: C, 37.1%; H, 7.97%; N, 1.80%; Si, 34.2%. Found: C, 33.04%; H, 8.18%; N, 1.81%; Si, 34.2%.

The infrared spectrum (film from tetrahydrofuran) of the polymer shows the presence of Si-O-Si linkage (1 020 and 1 100 cm^{-1}), Si-CH$_3$ linkage (800 and 1 255 cm^{-1}), and the ultraviolet spectrum of the polymer shows λ_{max} at 228, 277, 283, and 300 (shoulder) mμ in ethanol.

References

1. J. E. Mulvaney and C. S. Marvel, *J. Polym. Sci.*, **50**, 541 (1961).
2. K. Kojima, C. R. Gore, and C. S. Marvel, *J. Polym. Sci. A-1*, **4**, 2325 (1966).

Syntheses and Reactions of Functional Polymers. XLII.   Preparation and Use of Polymers Having N-Hydroxy-succinimide Unit in the Chain

MASAYASU AKIYAMA, MITSUAKI NARITA, and MAKOTO OKAWARA, *Research Laboratory of Resources Utilization, Tokyo Institute of Technology, Meguro-ku, Tokyo, Japan*

Synopsis

Styrene–maleic anhydride alternating copolymer was converted to N-hydroxymale-imide–styrene copolymer by reaction with hydroxylamine in pyridine at room temperature.   The conversion was more than 90%.   From this copolymer, N-acetoxy- or N-benzoyloxymaleimide–styrene copolymers were derived by action of acetic anhydride or benzoyl chloride in dimethylformamide at room temperature.   Acylation of several primary amines was carried out effectively by use of these N-acyloxyimide-styrene copolymers.   The reaction of the acetylated copolymer with diethylamine at room temperature afforded N-hydroxyimide copolymer.

INTRODUCTION

The utilization of functional polymers in organic syntheses can be classified into three major categories:[1] *(1)* as catalysts, *(2)* as supports, and *(3)* as chemical reagents.   Extensive studies of polymeric catalysts in enzyme model work[2] or of polymer supports in peptide[3] and nucleotide[4] syntheses have been made, and, in practical applications, ion exchange resins are widely used.   Except for these, few polymers have been utilized as chemical agents.   Fridkin used polymers carrying phenyl ester groups as acylating agents in oligopeptide syntheses.[5]   Similarly, a phenol–formaldehyde resin was used by Wieland[6] and a polycarbodiimide was tested as a polymeric condensing agent by Wolman.[7]   However, we have been working with various polymeric reagents since our earlier use of N-bromoimide polymers in bromination reactions.[8]

Polymeric agents because of their characteristic solubilities, might be used in some organic syntheses as a means of simplifying the procedures and obtaining products of high purity and good conversion.

The esters of N-hydroxysuccinimide, introduced by Anderson in peptide chemistry,[9] have been used frequently and found to be free from racemization during peptide bond formation.[10]   A polymer having the N-hydroxyimide structure in the chain was anticipated to retain the reactivity, and hence to be a good polymeric activator component for carboxylic acid group.   As an extension of our investigations, the preparation and use of

N-acyloxysuccinimide type polymers were undertaken in this paper.   A report along this line has recently appeared.[11]

RESULTS

Styrene–maleic anhydride copolymer with an anhydride content of 50 mole-% served as a starting material in the present synthesis. A series of polymer modifications was carried out as shown in eq. (1). Styrene–maleic anhydride copolymer(I) was converted to N-hydroxymaleamic acid and/or N-hydroxymaleimide–styrene copolymer (II′) by treatment with hydroxylamine in pyridine. The designation II was used for N-hydroxy-maleamic acid–styrene copolymer which was not obtained here. Cyclization with simultaneous acylation of II′ in dimethylformamide then produced N-acyloxymaleimide–styrene copolymers (III), from which N-hydroxymaleimide–styrene copolymer(IV) was obtained by treatment with diethylamine in dimethylformamide.
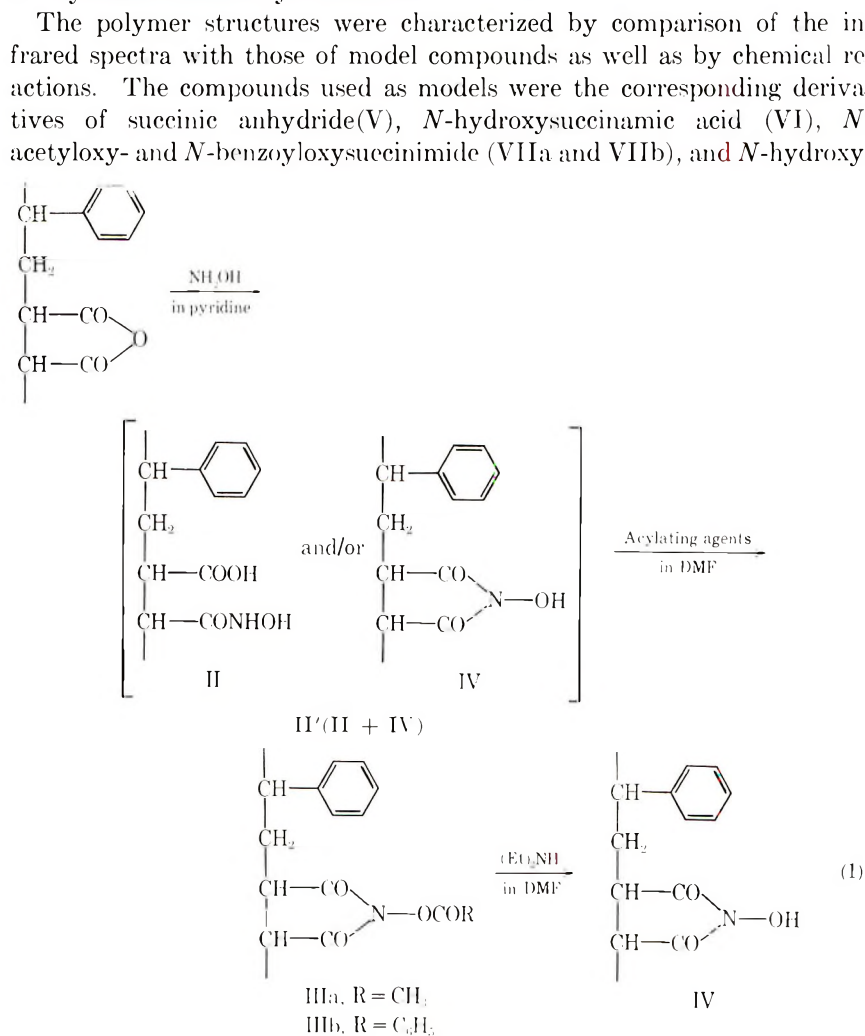
The polymer structures were characterized by comparison of the infrared spectra with those of model compounds as well as by chemical reactions. The compounds used as models were the corresponding derivatives of succinic anhydride(V), N-hydroxysuccinamic acid (VI), N-acetyloxy- and N-benzoyloxysuccinimide (VIIa and VIIb), and N-hydroxy-

succinimide(VIII). Major infrared absorption bands of the polymers obtained are listed in Table I and those of the model compounds are given in Table II.

TABLE I

Characteristic Infrared Absorptions of the Polymers (KBr Disk)

Poly- mer	Infrared absorptions,[a] cm^{-1}		
	—OH	>C=O	Others
II'	3500–2700s	1780m, 1705s, 1650sh	1600w, 1230s, 1060m
IIIa		1815m, 1785m, 1740s	1385m, 1220s, 1170s, 1060m, 830s
IIIb		1770s, 1735s	1360m, 1240s, 1060m, 995s, 840w
IV	3500–2700s	1780m, 1705s, 1655sh	1230s, 1060m

[a] Absorption intensity: s = strong, m = medium, w = weak, sh = shoulder.

TABLE II

Characteristic Infrared Absorptions of the Model Compounds (KBr Disk)

Com- pound	Infrared absorptions, cm^{-1}		
	—OH	>C=O	Others
VI	3300–2500s	1700s, 1660m, 1620m	1570w, 1220m, 1100m, 890s
VIIa		1815m, 1790m, 1750s	1385m, 1220s, 1160m, 1060m, 835s
VIIb		1770m, 1735s	1365m, 1235s, 1070m, 995s, 840w
VIII	3500–2700s	1780m, 1705s, 1650sh	1225s, 1080m, 815w

The reaction of I with hydroxylamine was conducted in dry pyridine at room temperature for a few days in order to convert I to II. However, the colorless product obtained was not II, since its infrared absorptions were not in good agreement with those of VI, but rather similar to that of VIII. The differences were noted in the hydroxyl and carbonyl regions. The similarity and the presence of absorption at 1 780 cm^{-1} indicated that the reaction was primarily formation of the hydroxyimide structure which was favorable for later modifications. This is tentatively denoted II', which means that the product might be a mixture of II and IV, although it was found to be mainly N-hydroxymaleimide copolymer(IV) after transformation of IIIa into IV. The elemental analysis showed that II' was rich in hydrogen as compared with the pure alternating copolymer of styrene and N-hydroxymaleimide, and water and maleic acid group were present. The extent of reaction was roughly estimated to be more than 90% imide structure based on nitrogen analysis, indicating the ease of the cyclization process.

In connection with the polymer reaction, treatment of V with hydroxylamine in pyridine below 40°C gave an oily substance (VI') whose infrared spectrum showed that it mainly consisted of VIII. Treatment of VI' with acetic anhydride or benzoyl chloride at room temperature in dimethyl-

formamide gave VIIa or VIIb, respectively. The structures of VIIa and VIIb were confirmed by the NMR spectra.

To attain complete cyclization with simultaneous esterification of the N-hydroxyl group of the polymer, II′ was treated with acetic anhydride or benzoyl chloride in dimethylformamide at room temperature. An N-acyloxymaleimide–styrene copolymer (IIIa or IIIb) was obtained as a colorless powder. The infrared spectrum of IIIa exhibited characteristic absorptions similar to those of VIIa, though very minor differences in the 1740–1750 cm^{-1} region were observed. The absorption bands of IIIb were consistent with those of VIIb. These show that the maleic acid moiety of the polymer has the correct N-acyloxyimide structure based on the model compounds. When the cyclization was conducted at elevated temperature, colored products with lower purity were obtained. The acyl content of the polymers was roughly determined by the crude yield of N-cyclohexylacetamide obtained in the reaction with excess cyclohexylamine. The contents thus determined chemically agreed with the values obtained by the elemental analysis of polymers. The conversion from II′ to IIIa or IIIb was more than 90%.

In order to test the utility of IIIa and IIIb, acylation of several primary amines was carried out in dimethylformamide at room temperature, with the use of an excess of polymer agents. The consumed polymer agent was removed by precipitation in methanol, affording residual acylated products easily isolated by evaporation of solvent. Table III shows the yield and melting points of the crude products obtained in the acylation reaction.

TABLE III

Crude Products in Acylation of Amines with N-Acyloxyimide Polymers (IIIa and IIIb)

	Acetylation with IIIa			Benzoylation with IIIb		
Amine	Yield, %	mp, °C	Lit. mp, °C	Yield, %	mp, °C	Lit. mp, °C
Benzylamine	81	59–60	61[12a]	55	102–104	106[13a]
Cyclohexylamine	85	102–103	104[13b]	91	139–143	147[13b]
Aniline	25	94–104	115[13c]	10	~90	161[12b]
p-Toluidine	66	142–144	146[13d]	15	140–148	158[13e]
Ethyl glycinate[a]	84	43–45	48[13f]	85	54–57	67[13g]
Ethyl DL-leucinate[a]	90	Oil		59	61–64	79[12c]

[a] The hydrochloride was used in the presence of equimolar triethylamine.

Aliphatic amines were easily acylated, whereas aromatic amines generally gave low-melting products in poor yields. The effect was marked in benzoylation with IIIb, suggesting that the phenyl group in the polymer chain might hinder sterically the aminolysis reaction. These acylations demonstrate transfer of the acyl group from polymers to amines, affording acylated products and the N-hydroxysuccinimide unit in the polymer chain.

Formation of the ammonium salt of VIII was noted in the reaction of VIIa with alcoholic ammonia.[14] The pK_a value of VIII was 6.0,[15] making

it a weaker acid than acetic acid. Treatment of IIIa with a slight excess of diethylamine in dimethylformamide at room temperature, followed by addition of acetic acid gave a clear solution, from which N-hydroxyimide type copolymer (IV) was precipitated as a colorless powder from water. The infrared spectrum exhibited absorptions which were consistent with those of VIII and similar to those of II'. The difference between II' and IV was observed in solubility; II' was partially soluble in dioxane, whereas IV was not.

To confirm the structure of IV and also to check the possibility of the convenient transformations into the N-acyloxyimide type polymer, IV was treated with acetic acid in the presence of dicyclohexylcarbodiimide in dimethylformamide at room temperature. IIIa was again obtained as colorless product; similarly II' afforded IIIa.

These experiments show that simple treatment of maleic anhydride copolymer with hydroxylamine in pyridine gives N-hydroxyimide-type copolymer easily. As compared to the described polymer,[11] all the polymers obtained in the polymer transformation were colorless products; therefore, the process appears to be useful.

EXPERIMENTAL

Melting points were uncorrected. Infrared spectra were run on a Hitachi infrared photometer, Model EPI-S2, and NMR spectra were obtained on a Japan Electron Optics 60 Mc spectrophotometer in chloroform solutions, tetramethylsilane being used as an internal standard. The chemical shift was expressed in δ.

Styrene–Maleic Anhydride Copolymer (I)

This copolymer was supplied by Arakawarinsan Co., Ltd., Osaka, Japan. It had an average molecular weight of 56 000. The anhydride content was determined to be 50 mole-% by titration with sodium methoxide.[16]

Model Compounds

N-Hydroxysuccinamic acid (VI) was obtained by Ames's procedure,[15] mp 102–103° C (Lit. mp, 103° C). N-Hydroxysuccinimide(VIII) was prepared according to Anderson,[9] mp 100–101° C (Lit. mp, 99° C). The oil-(VI')* was obtained as follows. A mixture of 4.0 g of succinic anhydride and 2.8 g of hydroxylamine hydrochloride in 33 ml of pyridine was kept at room temperature for 18 hr. Pyridine was removed below 40°C under vacuum to give a residue. The aqueous solution of the residue was made alkaline with sodium carbonate and again evaporated. The residue was made acidic with dilute hydrochloric acid, concentrated to dryness, and extracted with methanol. Evaporation of methanol gave the oil(VI').

Treatment of VI' with excess acetic anhydride or benzoyl chloride at room temperature gave N-acetoxy- or benzoyloxysuccinimide, VIIa or

* The oily product of VI was reported.[14]

VIIb, respectively. Recrystallization from ethanol yielded VIIa, mp 132–133°C (Lit.[16] mp, 131–132°C) and VIIb, mp 135–136°C (Lit.[17] mp, 136°C). The NMR peaks were at 2.80δ ($-CH_2-$) and 2.30δ ($-CH_3$) for VIIa, and 2.85δ ($-CH_2-$) and 7.20–8.30δ ($-C_6H_5$) for VIIb. The methylene peak of both VIIa and VIIb was a singlet, showing the symmetrical structure.

Copolymer of *N*-Hydroxymaleamic Acid and/or *N*-Hydroxymaleimide with Styrene (II′)

To a suspension of 32.0 g of hydroxylamine hydrochloride in 640 ml of dry pyridine was added 63.6 g of I. The mixture was kept at room temperature until all of I went into solution (6 days). After dilution with 500 ml of dimethylformamide, the resulting solution was poured dropwise into a large volume of water which contained a sufficient amount of hydrochloric acid to neutralize pyridine, yielding II′ as a colorless product. It was filtered and washed with water and dried under vacuum at room temperature. The yield was 69.0 g. Reprecipitation twice from dioxane to water and drying at 56°C under vacuum gave an analytical sample. Drastic drying of the sample was avoided to prevent cyclization into the imide structure at this stage. The ratio of hydroxyimide group to hydroxamic group was not determined.

ANAL. Calcd for $[(C_8H_8)_{50}:(C_4H_3O_3N)_{46}:(C_4H_4O_4)_4:60 . H_2O]_n$: C, 60.30%; H, 5.66%; N, 5.38 (assuming nitrogen came from the *N*-hydroxyimide structure). The degree of hydroxylamination was roughly estimated to be 92% in this calculation. Found: C, 60.56%; H, 6.06%; N, 5.57%.

Copolymer of *N*-Acetoxymaleimide with Styrene (IIIa)

To a solution of 20.0 g of II′ in 200 ml of dimethylformamide was added 100 ml of acetic anhydride in one portion. The mixture was kept at room temperature with stirring for 10 hr and added dropwise into a large volume of methanol to give IIIa as a colorless product. The residue filtered and washed with methanol, redissolved in dioxane, and precipitated in methanol, yielding 22.4 g of IIIa. This procedure was repeated twice more affording an analytical sample.

ANAL. Calcd for $[(C_8H_8)_{50}:(C_6H_5O_4N)_{43}:(C_4H_4O_4)_7:4 . CH_4O]_n$: C, 64.64%; H, 5.18%; N, 4.70%. The conversion from II′ into IIIa was calculated to be nearly 90%. Found: C, 64.43%; H, 5.75%; N, 4.60%.

The found value for nitrogen of 4.60% corresponded to 3.28 mmole/g. A value of 3.1 mmole/g was obtained by a chemical reaction which was based on treatment of 1.00 g of cyclohexylamine in dimethylformamide to give 0.44 g of crude *N*-cyclohexylacetamide.

Copolymer of *N*-Benzoyloxymaleimide with Styrene (IIIb)

A similar treatment of 10.0 g of II′ in 100 ml of dimethylformamide with 50 ml of benzoyl chloride as in IIIa gave 13.4 g of IIIb as a colorless product.

ANAL. Calcd for $[(C_8H_8)_{50}:(C_{11}H_7O_4N)_{44}:(C_4H_4O_4)_6:20.CH_4O]_n$: C, 69.22%; H, 5.07%; N, 3.83%. The conversion was estimated to be more than 90%.

Found: C, 69.04%; H, 4.98%; N, 3.68%.

The nitrogen content of 3.68% corresponded to 2.62 mmole/g. Treatment of 1.00 g of IIIb with 0.80 g of cyclohexylamine in dimethylformamide gave 0.50 g of crude N-cyclohexylbenzamide (2.5 mmole/g).

Copolymer of N-Hydroxymaleimide with Styrene(IV)

To a solution of 10.0 g of IIIa in 160 ml of dimethylformamide was gradually added 3.5 g of diethylamine in 40 ml of dimethylformamide. The gel-like solution resulting was kept at room temperature for 3.0 hr under stirring. By addition of 5 ml of acetic acid, the gel turned to a clear solution. The solution was poured dropwise into a large volume of water, yielding 8.0 g of IV as colorless precipitate. Reprecipitations from dimethylformamide to water gave an analytical sample.

ANAL. Calcd for $[(C_8H_8)_{50}:(C_4H_3O_3N)_{41}:(C_4H_4O_4)_9:32.H_2O]_n$: C, 62.84%; H, 5.47% N, 5.01%. The conversion of IIIa into IV was estimated to be nearly 90%. Found C, 62.87%; H, 5.64%; N, 4.80%.

Acylations of Amines

To a solution of 1.0 g of IIIa or IIIb in 15 ml of dimethylformamide was added 2.0 mmole of an amine in 5 ml of dimethylformamide; the solution was stirred for 2.0 hr at room temperature and then poured into 400 ml of ether. The consumed polymer was removed as insoluble product. After evaporation of ether and dimethylformamide under reduced pressure, 30 ml of methanol was added to the residue to separate a small amount of polymer. A clear methanol solution obtained was evaporated to give an acylated amine as oil or crystals. In the benzoylation of aromatic amines, the residue thus obtained was dissolved in ether, washed with dilute hydrochloric acid, and dried; evaporation of ether gave products. Acylation of amino acid ethyl esters was performed by using their hydrochlorides in the presence of equimolar triethylamine. The yields and melting points of the crude products are listed in Table III. Recrystallizations of the crude products afforded pure compounds.

Conversions of II′ and IV into IIIa

To a chilled mixture of 1.0 g of II′ or IV and 0.50 g of acetic acid in 10 ml of dimethylformamide was added 2.20 g of dicyclohexylcarbodiimide. The mixture was kept at room temperature for 20 hr and filtered to remove the N,N'-dicylohexylurea produced. The clear dimethylformamide solution obtained was poured into 150 ml of methanol to separate a white precipitate. Reprecipitation from dioxane to methanol gave 1.10 g of a colorless product having an infrared spectrum identical with that of IIIa.

References

1. M. Okawara, *Yuki Gosei Kagaku Kyokaishi*, **24**, 293 (1966).

2. H. Morawetz and W. R. Song, *J. Amer. Chem. Soc.*, **88**, 5714 (1966).

3. R. B. Merrifield, *Science*, **150**, 178 (1965).

4. H. Hayatsu and H. G. Khorana, *J. Amer. Chem. Soc.*, **89**, 3880 (1967).

5. M. Fridkin, A. Patchornik, and E. Katchalski, *J. Amer. Chem. Soc.*, **87**, 4646 (1965); *ibid.*, **88**, 3164 (1966).

6. Th. Wieland and Ch.Birr, *Angew. Chem. Intern. Ed.*, **5**, 310 (1965).

7. Y. Wolman, S. Kivity, and M. Frankel, *Chem. Commun.*, **1967**, 629.

8. M. Okawara and H. Shinohara, *Kogyo Kagaku Zasshi*, **60**, 75 (1957).

9. G. W. Anderson, J. E. Zimmerman, and F. M. Callahan, *J. Amer. Chem. Soc.*, **86**, 1839 (1964).

10. G. W. Anderson, F. M. Callahan, and J. E. Zimmerman, *J. Amer. Chem. Soc.*, **89**, 178 (1967).

11. P. A. Laufer, D. I. Marlborough, T. M. Chapman, V. M. Vaidya, and E. R. Blout, *J. Amer. Chem. Soc.*, **90**, 2696 (1968).

12. Beilsteins, Handbuch der organischen chemie, Julius Springer, Berlin, 4th Ed., Hauptwerk, (a) Vol. 12, p. 1045; (b) Vol. 12, p. 262; (c) Vol. 9, p. 253.

13. J. R. A. Pollock, Ed., *Dictionary of Organic Compounds*, Eyre and Spottiswoode, London, 4th Ed., 1965 (a) p. 370; (b) p. 790; (c) p. 8; (d) p. 15; (e) p. 3077; (f) p. 21; (g) p. 1622.

14. G. Errera, *Gazz. chim. ital.*, **25**[II], 26 (1895); *Chem. Zentr.*, **1895** [II], 862.

15. D. E. Ames and T. F. Grey, *J. Chem. Soc.*, **1955**, 631.

16. J. S. Fritz and W. M. Lisicki, *Anal. Chem.*, **23**, 589 (1951).

17. C. D. Hurd, C. M. Buss, and L. Bauer, *J. Org. Chem.*, **19**, 1140 (1954).

Kinetics of Polymerization of *N-tert*-Butylacrylamide. Part II.

E. A. S. CAVELL and I. T. GILSON, *Department of Chemistry, The University, Southampton, England*

Synopsis

The effect of ferric chloride on the kinetics of the radical polymerization of *N-tert*-butylacrylamide has been investigated in methanol solution at 25°C, with the use of 4,4'-dicyano-4,4'-azodipentanoic acid as initiator. A shrinkage factor of 0.193 mmole polymerized for 1 mm contraction in a capillary of 1 mm diameter has been obtained from density measurements. In the absence of ferric chloride, rates of polymerization were found to be proportional to the concentration of monomer and to the square root of the initiator concentration. With ferric chloride present, the rate of polymerization becomes directly proportional to the initiator concentration and inversely proportional to the concentration of ferric salt. From measurements of the rates of production of ferrous iron, the specific rate constant of the initiation reaction has been found to be $(1.8 \pm 0.4) \times 10^{-6} \sec^{-1}$ at 25°C, compared with a value of $7.63 \times 10^{-8} \sec^{-1}$ calculated from the kinetic data obtained with no ferric salt present. The value of the ratio k_p/k_4, where k_p is the propagation coefficient and k_4 is the velocity coefficient for termination by ferric chloride, has been calculated to be 6.0×10^{-4} at 25°C, which is considerably smaller than the value found for the ferric chloride-terminated polymerization of acrylamide in water. This markedly lower value of k_p/k_4 has been attributed principally to the steric effect of the *tert*-butyl group on the magnitude of k_p.

INTRODUCTION

The mechanism of polymerization of *N-tert*-butylacrylamide (NTBA) appears to be similar in most respects to that of the unsubstituted monomer acrylamide, although its overall rate of polymerization is about an order of magnitude smaller.[1] The reduced rate of polymerization of NTBA probably reflects principally the net steric effect of the *tert*-butyl substituent on the magnitudes of the propagation and termination rate coefficients. In the case of electron-transfer reactions, such as those which are known to occur between polymeric radicals and salts of transitional metals,[2] steric effects are likely to be less significant than in reactions involving two radicals. In the presence of transitional metal salts, therefore, the difference between the rates of polymerization of NTBA and acrylamide should be larger than that observed when such salts are absent.[1]

Ferric chloride is particularly suitable as an effective linear terminator of radical polymerization by an electron transfer mechanism and has been widely used for this purpose.[3] In a previous investigation with acrylamide

as monomer,[4] water was used as solvent.   In the present study, it has been necessary to carry out kinetic measurements in methanol, owing to the insolubility of poly-NTBA in water, although the monomer itself is appreciably soluble in water.   As in previous investigations into the effects of transitional metal salts on rates of polymerization, 4,4'-dicyano-4,4'-azodipentanoic acid (ACV) was used to initiate polymerization.

EXPERIMENTAL

Materials

Commercial N-tert-butylacrylamide was purified by a series of crystallizations from benzene solution followed by drying in vacuo at room temperature: mp 128–130°C.   Purified NTBA was stored in a vacuum desiccator under reduced pressure.   The initiator ACV was prepared and purified as described in a previous paper.[5]   Analar grade methanol was used as solvent in kinetic measurements without further purification, since it was found that the presence of up to 10% water in the solvent had no detectable effect on the rate of polymerization.   If the concentration of water exceeded 20%, however, then polymer was precipitated during the course of the reaction, although initial rates of contraction were unaffected.

Stock solutions of ferric chloride were prepared by dissolving freshly precipitated ferric hydroxide in methanolic hydrochloric acid.   These were analyzed both gravimetrically and volumetrically for iron and were diluted to an appropriate concentration as and when required.   The concentration of hydrochloric acid was adjusted to be decimolar throughout.   Diluted solutions of ferric chloride were allowed to stand for several days before use to ensure that ionic equilibration processes were complete.

Measurements

Rates of polymerization were measured either by precipitating and weighing the polymer produced during a known interval of time or by measuring the contraction in volume which occurs during polymerization in a suitable dilatometer.   Liquid oxygen was used to freeze the solutions during deaeration cycles, but otherwise the details of the procedures adopted were similar to those outlined previously.[5]   Water was found to be a satisfactory precipitant for the polymer in the gravimetric determinations of reaction rate, the monomer itself being appreciably soluble in water.

It has been observed that in the presence of ferric chloride, the rate of polymerization of NTBA, employing ACV as initiator, is dependent upon the intensity of the incident light.   In all kinetic experiments, therefore, care was taken to exclude all light as far as possible from the polymerizing solution.   Details of the precautions taken have been outlined elsewhere.[6]   In the present investigation, reproducible linear plots of contraction against time were obtained in replicate dilatometric experiments.   It was therefore concluded that the precautions taken were adequate to ensure that photochemical effects were negligible.

The increase in the concentration of ferrous iron, which occurs during polymerization with ferric salts present, was followed spectrophotometrically as described in a previous paper.[4] o-Phenanthroline was used as the complexing agent and measurements of optical absorption were made at 504 mμ.

RESULTS AND DISCUSSION

Rates of Polymerization with Ferric Chloride absent

In order to evaluate rates of polymerization from measured rates of contraction, a shrinkage factor of 0.193 mmole polymerized per millimeter contraction in a 1-mm diameter capillary was employed. This value was initially calculated from the appropriate density measurements of monomer and polymer. The general agreement between values for the rates of polymerization obtained by the gravimetric and dilatometric procedures for

TABLE I
Comparison of Rates of Polymerization R_p Obtained by Dilatometric and Gravimetric Methods at 25°C

[NTBA], mole/l.	[ACV] $\times$ 10⁴, mole/l.	$R_p \times 10^6$, mole/l.-sec	
		Dilatometric	Gravimetric
0.253	17.3	1.90	1.86
0.253	17.3	1.70	1.75
0.253	56.4	3.19	3.19
0.253	46.3	2.86	2.98
0.253	8.92	1.31	1.28
0.452	6.72	1.92	1.88
0.313	9.34	1.75	1.61

identical reaction conditions and summarized in Table I provides a satisfactory confirmation for the value of the shrinkage factor used.

The variation of the rate of polymerization R_p with monomer concentration $[M_1]$ is illustrated in Figure 1; in Figure 2, R_p has been plotted against the square root of the initiator concentration used $[ACV]^{1/2}$. Both plots are linear within the limits of experimental error and the mean value of the ratio $R_p/[M_1][ACV]^{1/2}$ estimated from their slopes is $(1.74 \pm 0.07) \times 10^{-4}$ $l.^{1/2}$-mole$^{-1/2}$-sec^{-1} at 25°C. An alternative analysis of the kinetic data summarized in Figures 1 and 2 by the method of least squares has shown the rate of polymerization to be proportional to $[M_1]^{1.02}$ and to $[ACV]^{0.48}$ for conversions of up to 10%.

The linearity of the plots shown in Figures 1 and 2 indicates that primary radical termination is not a significant feature under the experimental conditions employed in the present investigation. This conclusion is confirmed by the value of 1.90×10^{-4} $l.^{1/2}$-mole$^{-1/2}$-sec^{-1} estimated from a plot[7] of the reciprocal of the rate of polymerization against $[ACV]^{-1/2}$, for the ratio $k_p(f_i k_i/k_t)^{1/2}$, where $f_i k_i$, k_p, and k_t are the velocity coefficients for

initiation, propagation, and termination respectively. Within the limits of experimental error, this result is not distinguishable from the value quoted above, for the ratio $R_p/[\mathrm{M_1}][\mathrm{ACV}]^{1/2}$, which can of course be equated
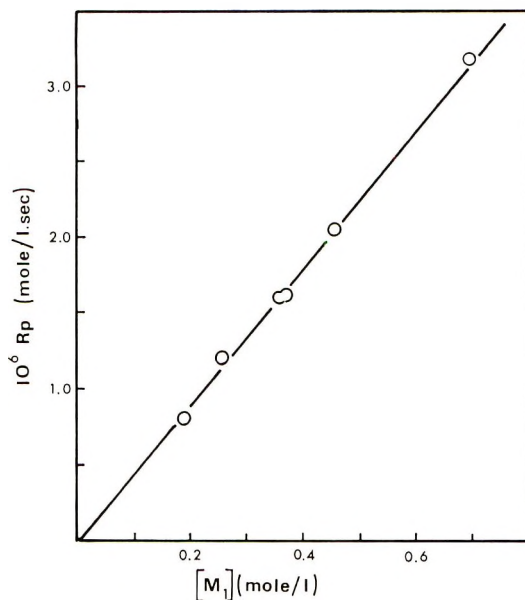

Fig. 1. Variation of rate of polymerization $R\rho$ with monomer concentration $[\mathrm{M_1}]$ at 25°C. Initiator concentration, $6.72 \times 10^{-4}M$.
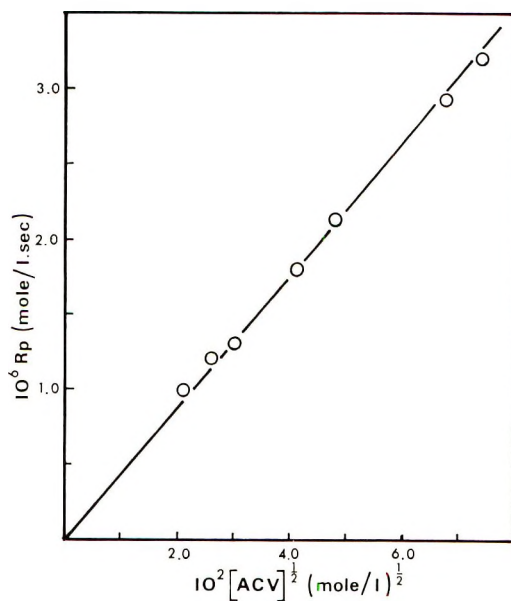

Fig. 2. Plot of rate of polymerization $R\rho$ against the square root of initiator concentration $[\mathrm{ACV}]^{1/2}$ at 25°C in absence of ferric chloride. Monomer concentration, $0.253M$.

to $k_p(f_i k_i/k_t)^{1/2}$ when the effects of primary radical termination are negligible.

In the calculation of the initiation coefficient $f_i k_i$, i.e., $2f_i k_d$, where k_d is the velocity coefficient for the decomposition of the initiator, $k_p(f_i k_i/k_t)^{1/2}$ has been taken as 1.74×10^{-4} l.$^{1/2}$-mole$^{-1/2}$-sec^{-1} and $k_p/k_t^{1/2}$ as 0.63 l.$^{1/2}$-mole$^{-1/2}$-sec$^{-1/2}$, as reported previously.[1] The value of $f_i k_i$ so obtained is 7.63×10^{-8} sec.$^{-1}$ at 25°C., which is somewhat smaller than that obtained in aqueous solution with acrylamide as monomer,[5] i.e. $(12.9 \pm 2.9) \times 10^{-8}$ sec.$^{-1}$. In the case of the related initiator, azobisisobutyronitrile, variations in the specific rate of decomposition of up to 40% have been observed in different solvents,[8] and it is possible therefore that with the present initiator, ACV, similar variations in rate constant may occur with changes in solvent.

Effect of Ferric Chloride on Kinetics

In the presence of a fixed concentration of ferric chloride of about $10^{-5} M$, the rate of polymerization of NTBA becomes directly proportional to the concentration of ACV as shown by the linear plot illustrated in Figure 3. A plot of R_p against the reciprocal of the concentration of ferric chloride with constant initiator concentration is also linear within the limits of experimental error as shown in Figure 4. Both observations indicate that linear termination by the ferric salt is the predominant mechanism of chain termination under these experimental conditions. An analysis of the relevant kinetic data by the method of least squares has shown the overall rate of polymerization to be proportional to $[ACV]^{1.01}$ and inversely proportional to $[FeCl_3]^{1.04}$.

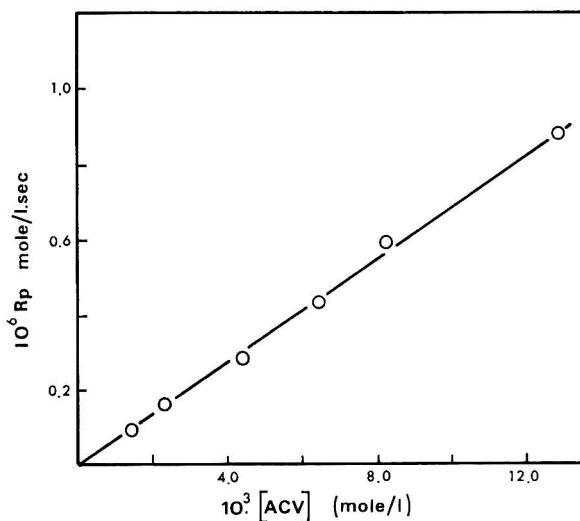Fig. 3. Variation of rate of polymerization R_p with initiator concentration ($[ACV]$) at 25°C in the presence of $8.0 \times 10^{-6} M$ FeCl$_3$. Monomer concentration, $0.50M$; HCl concentration, $0.100M$.
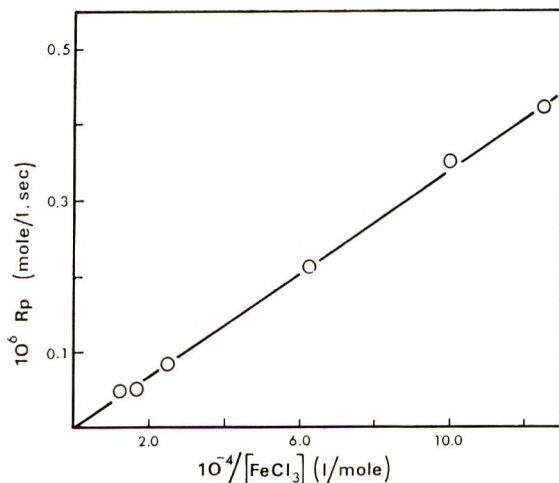
Fig. 4. Plot of rate of polymerization R_p against the reciprocal of the concentration of ferric chloride at 25°C. Initiator concentration, $6.4 \times 10^{-3}M$; monomer concentration, $0.50M$; HCl concentration, $0.100M$.

Owing to the sensitivity of the rate of polymerization to light when ferric chloride was present, the kinetic results summarized in Figures 3 and 4 were obtained under conditions in which light was excluded as far as possible from the polymerizing system. It was found, however, that if the initiator ACV was absent, then no detectable polymerization occurred in methanolic solutions of NTBA containing ferric chloride and hydrochloric acid, when these were exposed to daylight at 30°C. These observations suggest that in methanol solution ferric chloride can act as a photosensitizer for the decomposition of ACV. Increased rates of initiation by ACV in the presence of ferric salts have previously been found to occur in the polymerization of acrylamide in aqueous solution.[4] It now appears that a similar process can also take place in methanol solution, although in the latter case the process is apparently photosensitive. In the absence of ferric chloride, variation in the intensity of the incident light has no detectable effect on the rate of polymerization of NTBA with ACV as initiator.

Rate of Formation of Ferrous Iron

If the concentration of ferric chloride is such that polymer chains are exclusively terminated by a reaction which is first order with respect to both the ferric salt and polymer radicals, then in present circumstances the rate of production of ferrous iron can be equated to the rate of initiation of polymerization by ACV. The manner in which the concentration of the ferrous salt increases with time during the polymerization of NTBA is illustrated in Figure 5, which summarizes the measurements made in a typical experiment, from which light was excluded as far as possible. The average value of the initiation rate coefficient $(f_i k_i)$ calculated from the results of a number of replicate experiments of this kind was found to be
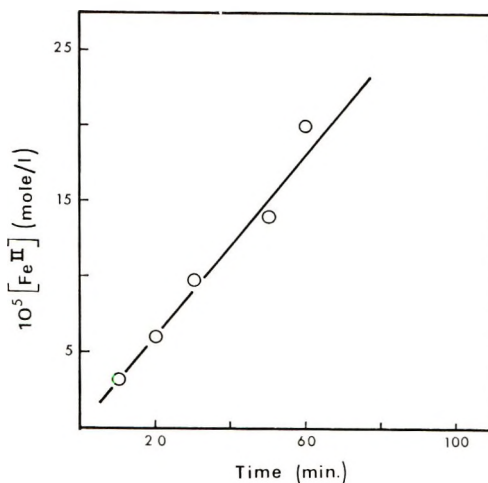
Fig. 5. Plot showing rate of production of ferrous iron ([Fe^{II}]) with initiator concentration of $2.28 \times 10^{-2}M$. Monomer concentration, $0.50M$; HCl concentration, $0.100M$; temperature, 25°C.

$(1.8 \pm 0.4) \times 10^{-6}$sec^{-1}. Although the experimental uncertainty is larger than that for other kinetic measurements in this investigation, it is evident that the effect of ferric chloride is to facilitate the decomposition of ACV into radicals and that the proportionate increase in the specific rate of initiation is similar in magnitude to that observed in aqueous solutions with acrylamide as monomer.[4]

Comparison of Polymerization of NTBA and Acrylamide

The mean value of the ratio $R_p[\text{Fe(III)}]/[\text{M}_1][\text{ACV}]$ estimated from the rate measurements summarized in Figures 3 and 4 is $(1.08 \pm 0.06) \times 10^{-9}$ sec^{-1} which for the experimental conditions employed in this investigation can be equated to $k_p f_i k_i / k_4$, where k_4 is the velocity coefficient for the linear termination reaction with ferric chloride. With $f_i k_i$ equal to the value calculated from the measured rates of formation of ferrous iron, k_p/k_4 becomes 6.0×10^{-4}. This is considerably smaller than the value of the corresponding ratio of rate coefficients found in the ferric chloride terminated polymerization of acrylamide in water as solvent,[4] for which k_p/k_4 equals 0.23 at 25°C.

The magnitude of the termination coefficient (k_4) would be expected to show a marked increase if a substituent having a large capacity for electron release is introduced into an appropriate position in the parent monomer. The replacement of hydrogen in the acid amido group of the acrylamide molecule by a tert-butyl group is unlikely to increase the electron availability to the extent required to account completely for the observed reduction in the value of k_p/k_4. It is also possible that the change in solvent from water to methanol increases the relative reactivity of the ferric salt as a chain terminating agent, although experiments were conducted in decimo-

lar hydrochloric acid in order to minimize the degree of solvolysis of the ferric ions. The principal reason for the marked reduction in the value of k_p/k_4 is more likely to be a significantly smaller propagation constant arising from the steric effect of the bulky *tert*-butyl substituent.

References

1. E. A. S. Cavell and I. T. Gilson, *Makromol. Chem.*, in press.

2. E. Collinson, F. S. Dainton, D. R. Smith, B. Mile, and S. Tazuke, *Nature*, **198,** 26 (1963).

3. C. H. Bamford, A. D. Jenkins, and R. Johnston, *Proc. Roy. Soc.* (London), **A239,** 214 (1957); *J. Polym. Sci.*, **29,** 355 (1958).

4. E. A. S. Cavell and I. T. Gilson, *J. Polym. Sci. A-1*, **4,** 541 (1966).

5. E. A. S. Cavell, *Makromol. Chem.*, **54,** 70 (1962).

6. E. A. S. Cavell and A. C. Meeks, *Polymer*, **8,** 79 (1967).

7. C. H. Bamford, A. D. Jenkins, and R. Johnston, *Trans. Faraday Soc.*, **55,** 1451 (1959); *ibid.*, **58,** 1212 (1962).

8. A. F. Moroni, *Makromol. Chem.*, **105,** 43 (1967).

.

Vinyl Polymerization Photosensitized by Anthraquinone Sulfonates in Aqueous Solutions

Q. ANWARUDDIN and M. SANTAPPA, *Department of Physical Chemistry, University of Madras, Madras, India*

Synopsis

The kinetics of the photopolymerization of the vinyl monomers MMA and MA sensitized by anthraquinone sulfonate–NaCl–HClO$_4$ systems have been studied systematically. The wavelength 365 mμ was used for irradiation. Sodium anthraquinone-2-sulfonate and disodium anthraquinone-2,6-disulfonate were used as sensitizers, and all experiments were conducted in deaerated conditions. The polymerization was followed by the measurement of monomer disappearance (gravimetrically), rate of sensitizer disappearance (spectrophotometrically) and the chainlength of the polymer formed (viscometrically). Monomer concentration, k_e, [NaCl], and I were varied. In the light of the experimental results a *prima facie* kinetic scheme was proposed. The specific rate constants for the various steps have been evaluated.

INTRODUCTION

Photosensitized oxidation of ethyl and isopropyl alcohols by anthraquinone β-sulfonates was elaborately studied by Wells[1] and Bolland and Cooper.[2] The oxidation products as well as the anthrahydroquinols were identified, a detailed mechanism was suggested and the reactive state of the sensitizer was proved to be a triplet by quenching reactions[3] and by flash photolytic studies.[4] The quantum yields with respect to the production of anthrahydroquinols or acetone in case of isopropanol were almost unity within the limits of experimental accuracy for the anthraquinone β-sulfonate sensitizers. Grafting[5] of a vinyl monomer on cellulose backbone by using disodium anthraquinone-2,7-disulfonate as sensitizer by ultraviolet light was studied and hydrogen abstraction by the excited sensitizer to produce radical ends in cellulose and the addition of this radical to the vinyl monomer was inferred. Egerton et al.[6] used aminoanthraquinones for the phototendering of cellulose at wavelengths $\lambda < 300$ mμ. Not much work except a few patents were reported regarding the vinyl polymerization by anthraquinone β-sulfonates. Dainton and Tordoff[7] conducted photopolymerization of acrylamide using disodium anthraquinone-2,6-disulfonate, but no detailed kinetic studies were given. A regular detailed study of the photochemical polymerization of vinyl monomers in aqueous solution by anthraquinone β-sulfonates was undertaken.

In this paper the results of the photopolymerization of methyl acrylate (MA) and methyl methacrylate (MMA) by sodium anthraquinone-2-sulfonate and by disodium anthraquinone-2,6-disulfonate at $\lambda = 365$ mμ are given and discussed. With the anthraquinone β-sulfonates alone in the presence of monomer in aqueous solution, polymerization did not start even under deaerated conditions for long times (of the order of about 2–3 hr).

A reducing agent like chloride ion in combination with the sensitizer was found necessary. Some qualitative experiments were also done using sodium bromide or a phosphate–citrate buffer in place of sodium chloride. Light of $\lambda = 365$ mμ was employed for irradiation of the system. From the experimental results obtained with the use of monomer concentration, light absorption fraction k_t, sodium chloride concentration, and light intensity I as variables we have attempted to throw light on the nature of initiation and termination reactions in the photopolymerization.

EXPERIMENTAL

Optical Arrangement

The light source used was a 125-W bulb type ultraviolet lamp (B.T.H. Mazda, MBW/U) which gave almost 98% of $\lambda = 3650$ Å light. The lamp was connected to the mains through the necessary choke. The light beam from the lamp was collimated by means of a quartz condenser lens, and the parallel beam of the monochromatic light was allowed to fall on the quartz window of a metal thermostat inside which the reaction cell was mounted. The reaction cell (length 4.6 cm in the direction of the beam and 5 cm in diameter, capacity about 75 ml) fused at both ends with flat Pyrex plates, is fitted with two outlet tubes, of standard B-14 cones on the top.

Reagents

All the chemicals used in the preparation of solutions were B.D.H., AnalaR, E.Merck, G.R. or M & B reagent grade. Water doubly distilled (over alkaline permanganate) in an all-glass quickfit apparatus and then passed through Biodeminrolit (Permutit, London) resin was used throughout for the preparation of solutions. Sodium anthraquinone-2-sulfonate (AnalaR, B.D.H.) and disodium anthraquinone-2,6-disulfonate (Fluka) were recrystallized from ethanol-water mixtures. The monomers, methyl methacrylate and methyl acrylate (Rohm and Haas Co., U.S.A.), were washed free of inhibitor with a solution of sodium hydroxide (5%), then with water, and finally distilled under reduced pressure in an atmosphere of nitrogen. The monomers were distilled frequently before use and stored at 5°C. The sodium chloride (AnalaR, B.D.H.) was used without further purification.

Estimations

The system consisting of anthraquinone sulfonate–NaCl–HClO$_4$ (pH = 2–5), and methyl acrylate or methyl methacrylate in aqueous solution at μ = 0.2 in the reaction cell (capacity 80 ml) was deaerated by passing through the former oxygen-free nitrogen (Fieser's solution[8]). To prevent loss of monomer in the deaeration process, nitrogen was first passed through a blank wash bottle containing the same concentration of monomer as the reaction solution and then through the reaction system. The reaction cell was then placed in the cell holder inside a thermostat maintained at 35 ± 0.1°C by use of a toluene regulator and a hot wire vacuum switch relay (Gallenkamp) in the path of the light beam and then irradiated for about 45 min in the case of both the monomers. The precipitated polymer was then filtered off, dried and weighed. Almost all experiments were conducted under deaerated conditions.
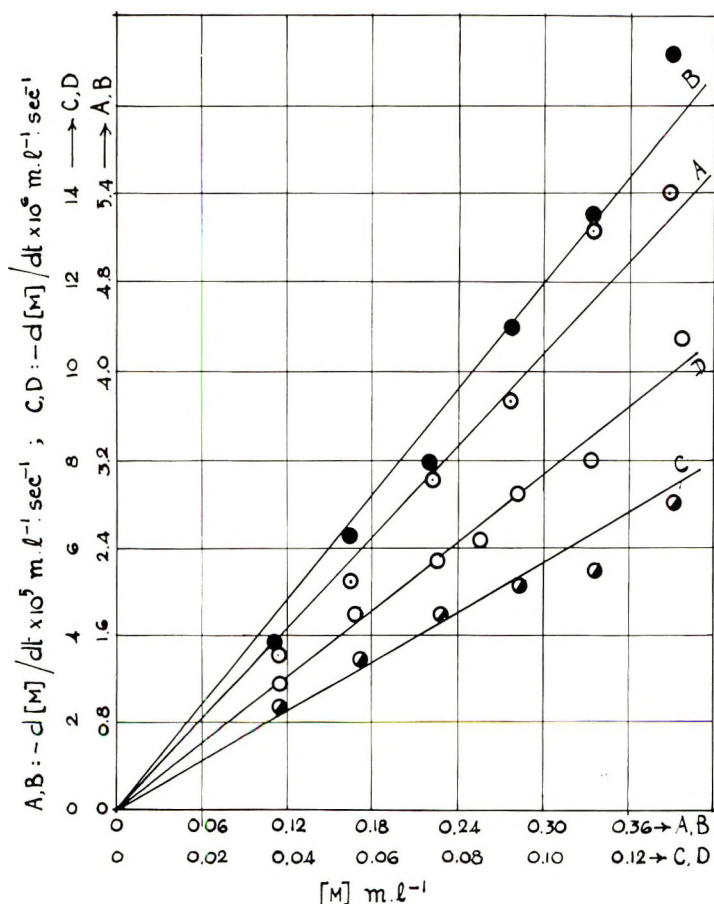
Fig. 1. $-d[M]/dt$ vs. $[M]$ (λ = 365 mμ): (A) AQ-2-SO$_3$Na–NaCl–MA system; (B) AQ-2,6-diSO$_3$Na–NaCl–MA system; (C) AQ-2-SO$_3$Na–NaCl–MMA system; (D) AQ-2,6-diSO$_3$Na–NaCl–MMA system.
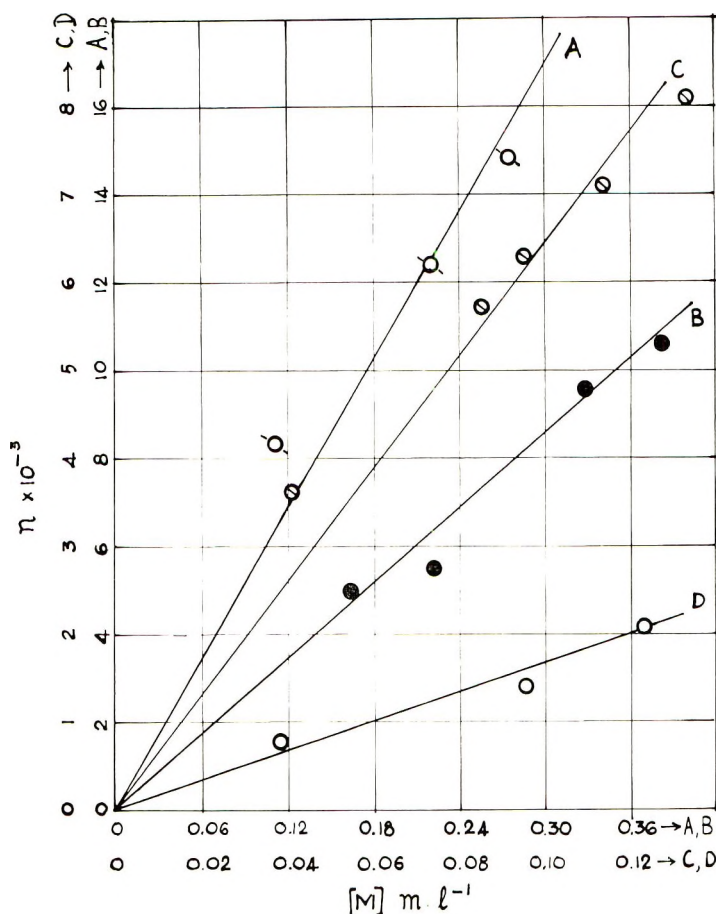
Fig. 2. Chainlength n vs. [M] ($\lambda = 365$ mμ): (A) AQ-2-SO$_3$Na–NaCl–MA system; (B) AQ-2,6-diSO$_3$Na–NaCl–MA system; (C) AQ-2-SO$_3$Na–NaCl–MMA system; (D) AQ-2,6-diSO$_3$Na–NaCl–MMA system.

The rate of monomer disappearance ($-d[M]/dt$) was computed from the weight of polymer obtained (gravimetrically). In the case of poly-(methyl acrylate) the polymer was a colloidal suspension and so was coagulated by addition of ammonium nitrate before filtration. Poly(methyl methacrylate) was precipitated as a fine flocculent precipitate.

The rate of sensitizer (anthraquinone sulfonate) disappearance was followed by measuring the optical density of the reaction solution initially and of the filtrate obtained after irradiation of the system and filtering of the polymer. A calibration curve at $\lambda = 365$ mμ for sensitizer concentration versus optical density was constructed for the two sensitizers (2- and 2,6-sulfonated, and all absorptiometric measurements were made in a Uvispek Spectrophotometer (Hilger-Watts, H-700 type) with matched Corex silica cells. For measuring the chainlengths the polymers were purified by reprecipitation with methanol from their benzene solutions and
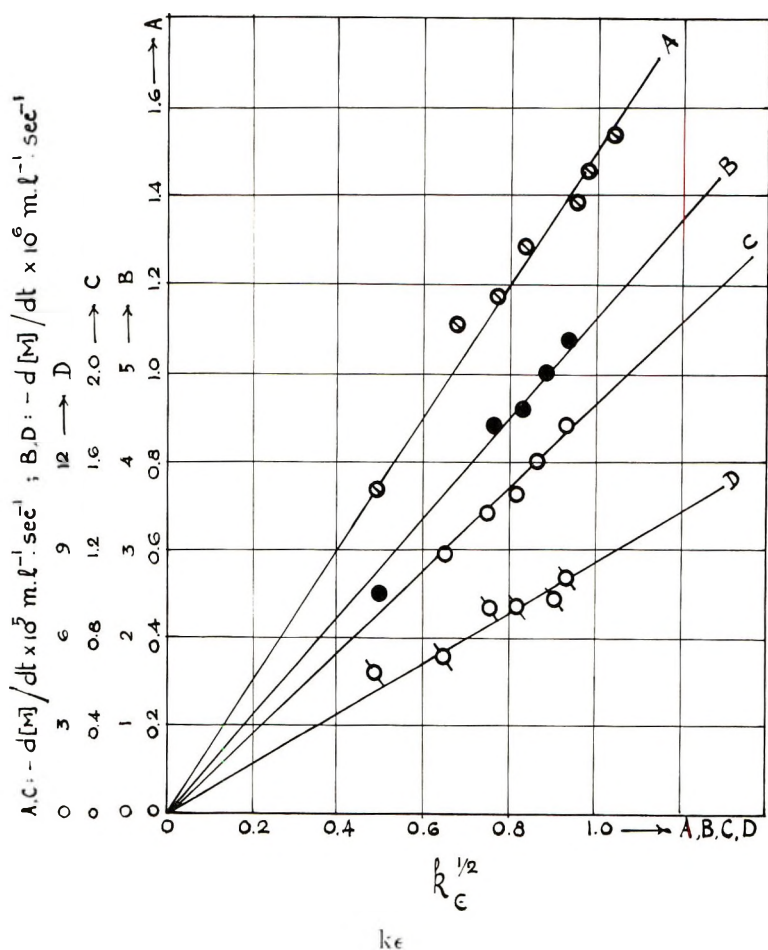
Fig. 3. $-d[M]/dt$ vs. $k_\epsilon^{1/2}$ ($\lambda = 365$ mμ): (A) AQ-2-SO$_3$Na–NaCl–MA system; (B) AQ-2-SO$_3$Na–NaCl–MMA system; (C) AQ-2,6-diSO$_3$Na–NaCl–MA system; (D) AQ-2,6-diSO$_3$Na–NaCl–MMA system.

dried. The viscosities of solutions of the PMMA (0.1%) and PMA in benzene were measured in a viscometer (PCL Ubbelohde type, ASTM specification D445-46T) thermostated to $\pm$ 0.01°C in a viscometric bath designed for precision viscometry (Krebs Electrical and Manufacturing Co., New York). From the viscosity measurements chainlengths were evaluated by using the Mark-Houwink type relationships of eq. (1)

$$n = 2.81 \times 10^3 [\eta]^{1.32} \tag{1}$$

at 25°C for poly(methyl methacrylate), due to Baxendale et al.,[9] and eq. (2)

$$[\eta] = 1.282 \times 10^{-4} M^{0.7143} \tag{2}$$

at 35°C for poly(methyl acrylate) due to Sen, et al.[10]

The light absorption fraction k_ϵ for the sensitizer for 4.6 cm thickness was calculated from optical density (OD) values for 1 cm cell thickness (OD for 1 cm of $1 \times 10^{-4} M$ sodium anthraquinone-2-sulfonate $= 0.121$). As an example, $k_\epsilon (= I_0 - I/I_0)$ for $1 \times 10^{-4} M$ of sodium anthraquinone-2-sulfonate was calculated to be 0.2775. The light absorption fraction was varied from about 0.25 to 0.85. We would like to emphasize that under conditions of strong absorption ($k_\epsilon \simeq 0.85$) the data on photochemical
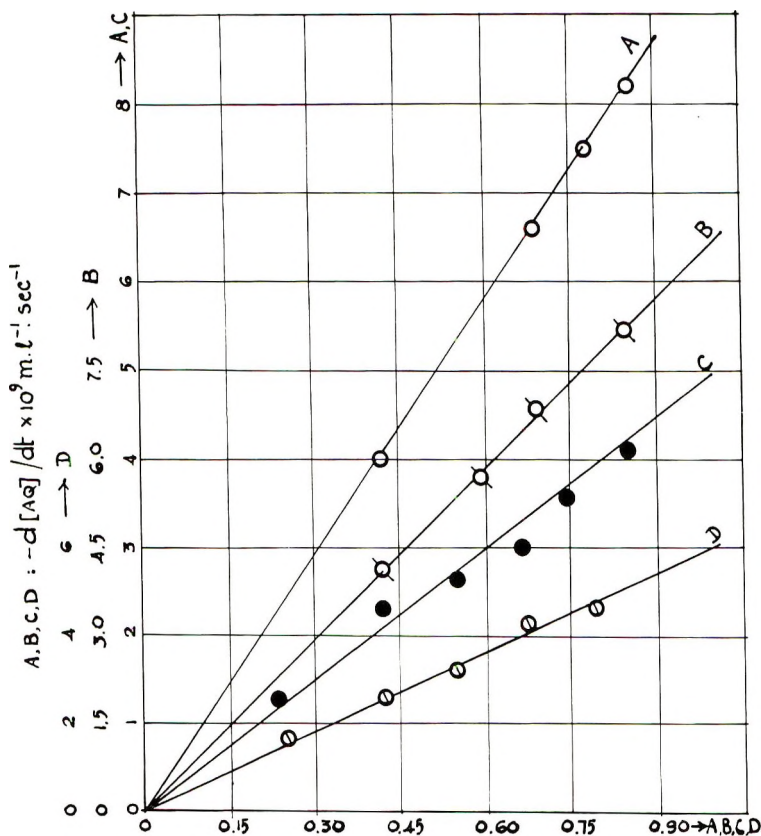
Fig. 4. $-d[AQ]/dt$ vs. k_ϵ ($\lambda = 365$ mμ): (A) AQ-2-SO$_3$Na–NaCl–MA system; (B) AQ-2-SO$_3$Na–NaCl–MMA system; (C) AQ-2,6-diSO$_3$Na–NaCl–MA system; (D) AQ-2,6-diSO$_3$Na–NaCl–MMA system.

rates would be complicated by nonuniform rates, diffusion of active species etc., and should be taken with caution.

Potassium ferrioxalate actinometry[11] was used throughout to determine the light intensities. This method was particularly useful for the measurement of low light intensities (2×10^{-7} to 7×10^{-7} $Nh\nu$ l.$^{-1}$ sec^{-1}). The amount of ferrous ion produced was estimated colorimetrically by forming a colored complex with o-phenanthroline and making absorption measurements at 510 mμ in a Hilger-Watts ultraviolet spectrophotometer (H-700).

KINETIC RESULTS

With the anthraquinone sulfonates alone and no Cl⁻ in the system, no polymerization of the monomer took place under deaerated or undeaerated conditions. With the anthraquinone sulfonate plus Cl⁻ or buffer (phosphate–citric acid, pH 6) polymerization was initiated without an induction period. Br⁻ was less effective, and no polymerization took place when I⁻ was used. No thermal polymerization took place (30–80°C). In the pH range of 1–3 the rate of polymerization increased and then decreased for pH 4 and 5 in $HClO_4$ acid medium. It was therefore obvious that initia-
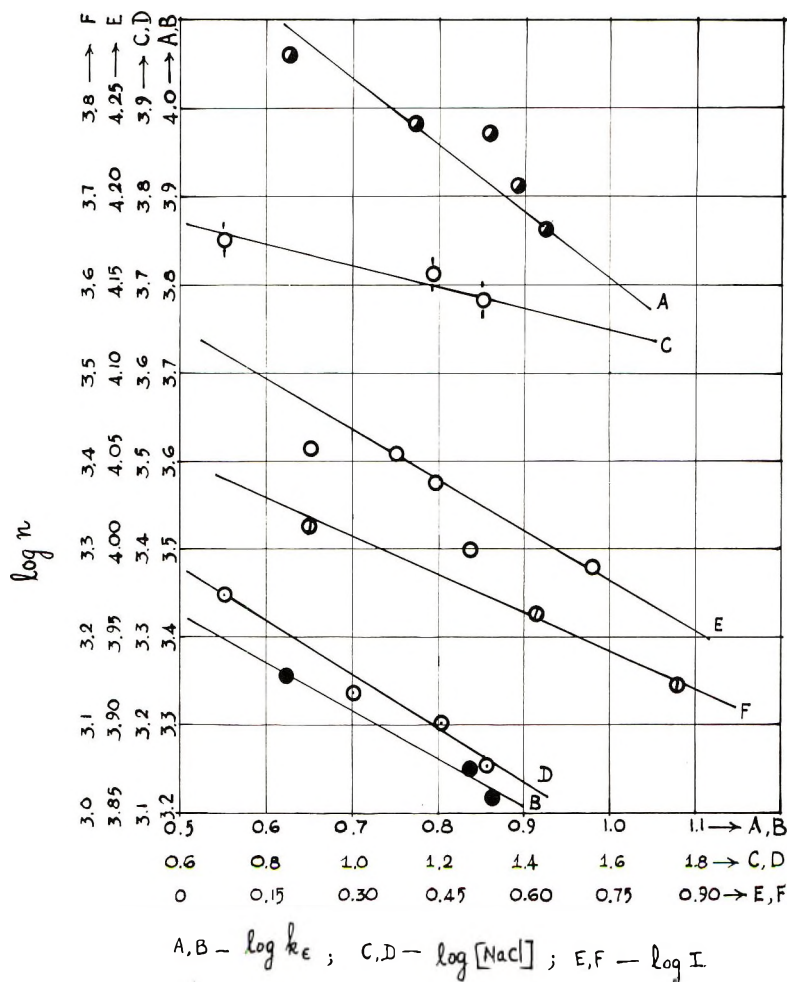
Fig. 5. Plots of log n (λ = 365 mμ): (*A*) log n vs. log k_ϵ, AQ-2-SO₃Na–NaCl–MA system; (*B*) log n vs. log k_ϵ, AQ-2,6-diSO₃Na–NaCl–MA system; (*C*) log n vs. log[NaCl], AQ-2-SO₃Na–NaCl–MA system; (*D*) log n vs. log [NaCl], AQ-2,6-diSO₃Na–NaCl–MA system; (*E*) log n vs. log I, AQ-2-SO₃Na–NaCl–MA system; (*F*) log n vs. log I, AQ-2,6-diSO₃Na–NaCl–MA system.
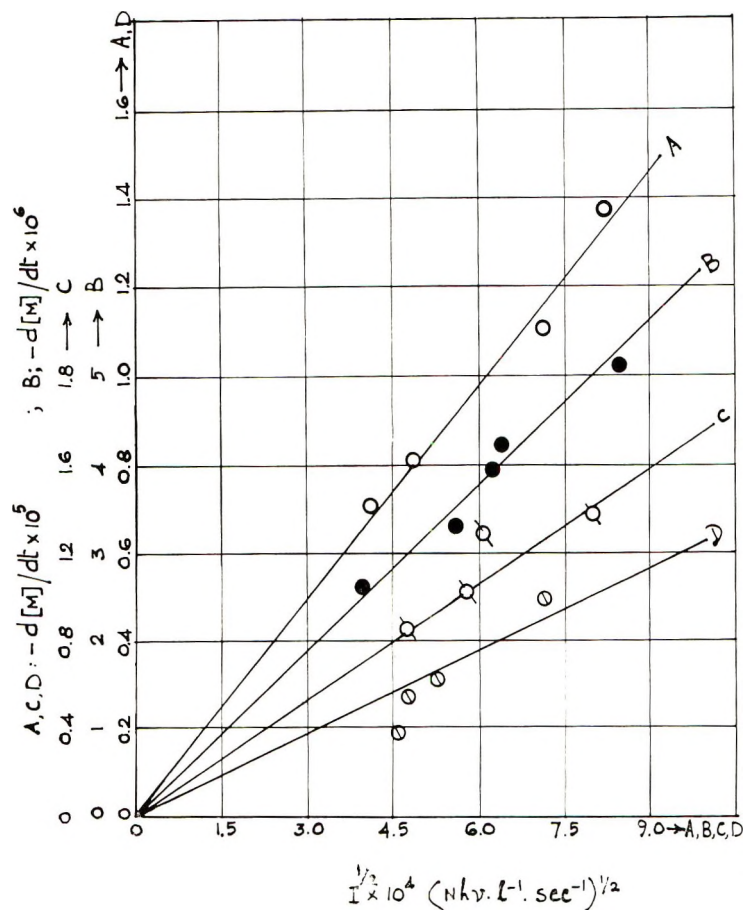
Fig. 6. $-d[\mathrm{M}]/dt$ vs. $I^{1/2}$ ($\lambda = 365$ mμ): (A) AQ-2-SO$_3$Na–NaCl–MA system; (B) AQ-2-SO$_3$Na–NaCl–MMA system; (C) AQ-2,6-diSO$_3$Na–NaCl–MA system; (D) AQ-2,6-diSO$_3$Na–NaCl–MMA system.

tion of polymerization was free radical in nature and probably that Cl atoms were initiators; slow or no initiation by Br and I atoms (fast terminators) under corresponding conditions would therefore be understandable.

The effects of the variables, viz, monomer concentration, k_c, [NaCl], and I on the rates of monomer disappearance ($-d[\mathrm{M}]/dt$), sensitizer disappearance ($-d[\mathrm{AQ}]/dt$), and chainlength n were investigated in detail.

Effect of Varying Monomer Concentration

The rate of monomer disappearance was found to be proportional to the first power of monomer concentration in the cases of both MA and MMA (Fig. 1). The chainlengths evaluated were directly proportional to the first power of monomer concentration (Fig. 2).

Effect of Varying k_ϵ

k_ϵ was varied from ~ 0.2 to ~ 0.85 and $-d[\mathrm{M}]/dt$ was directly proportional to square root of k_ϵ (Fig. 3), $-d[\mathrm{AQ}]/dt$ was directly proportional to k_ϵ itself (Fig. 4). The chainlengths were found to be inversely proportional to $k_\epsilon^{0.5}$ (Fig. 5).
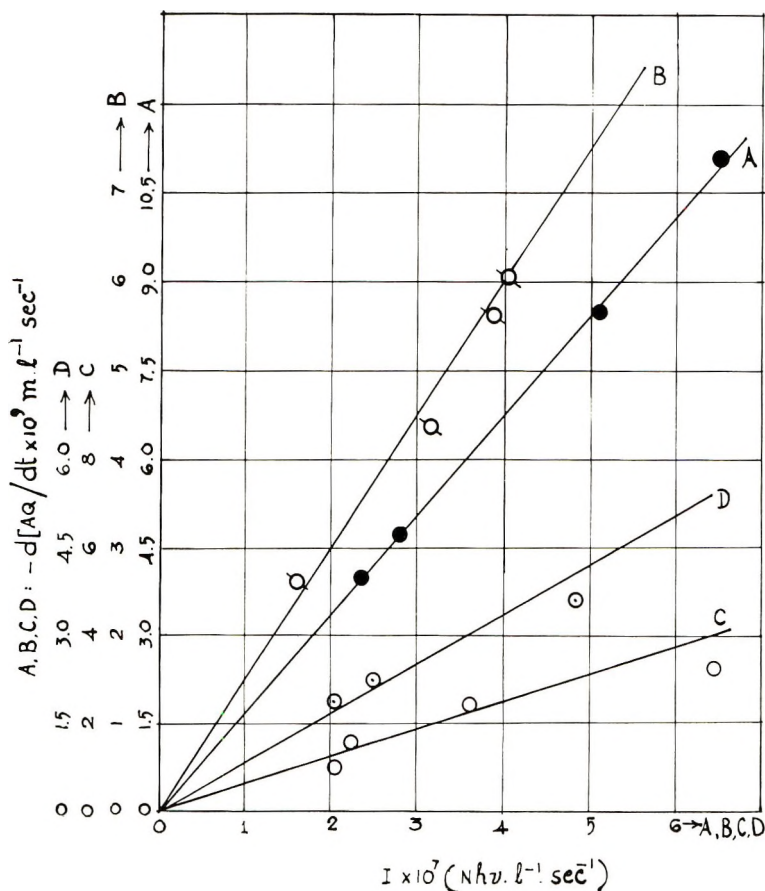
Fig. 7. $-d[\mathrm{AQ}]/dt$ vs. I ($\lambda = 365$ mμ): (A) AQ-2-SO$_3$Na–NaCl–MA system; (B) AQ-2-SO$_3$Na–NaCl–MMA system; (C) AQ-2,6-diSO$_3$Na–NaCl–MA system; (D) AQ-2,6-diSO$_3$Na–NaCl–MMA system.

Effect of Varying Light Intensity I

The light intensity I was varied by interposing diaphragms in the light path. $-d[\mathrm{M}]/dt$ and $-d[\mathrm{AQ}]/dt$ were found to vary directly with the square root and first power of light intensity, respectively, with MA and MMA (Figs. 6 and 7). The chainlengths depended inversely on $I^{0.5}$ (Fig. 5).

Effect of Varying Sodium Chloride Concentration

The optimum concentration of sodium chloride chosen for the majority of the experiments was 0.1 M. $-d[M]/dt$ was proportional to the square root of sodium chloride concentration and $-d[AQ]/dt$ was proportional
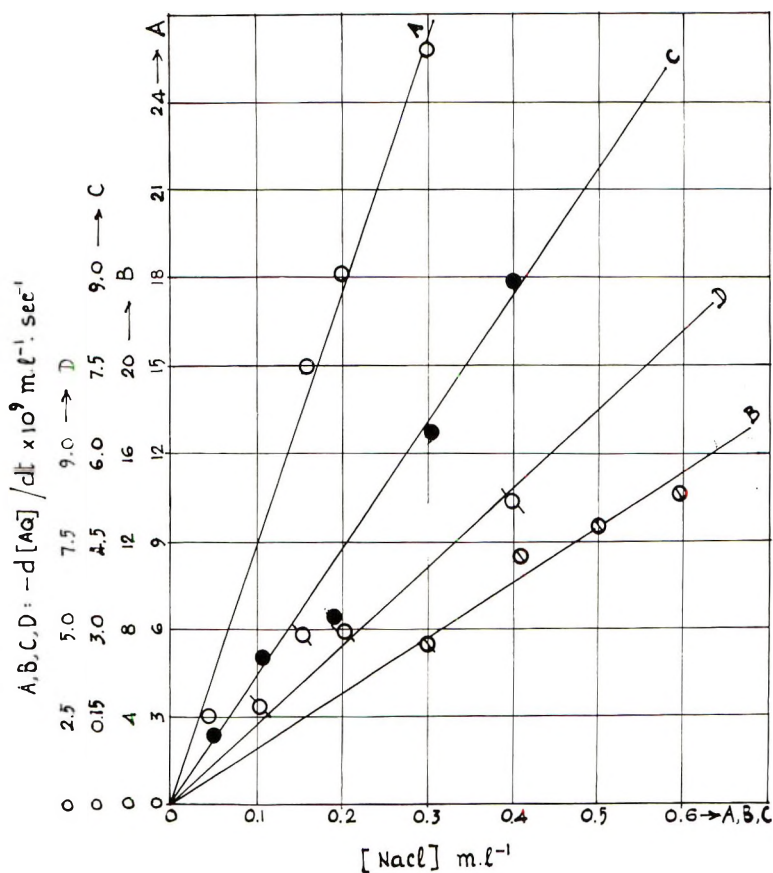
Fig. 8. $-d[AQ]/dt$ vs. [NaCl] (λ = 365 mμ): (A) AQ-2-SO$_3$Na–NaCl–MA system; (B) AQ-2-SO$_3$Na–NaCl–MMA system; (C) AQ-2,6-diSO$_3$Na–NaCl–MA system; (D) AQ-2,6-diSO$_3$Na–NaCl–MMA system.

to the first power of sodium chloride concentration (Fig. 8). The chain-lengths varied inversely with the square root of sodium chloride concentration (Fig. 5).

KINETIC SCHEME AND DISCUSSION

Mechanism 1

Steps (1) to (7) shown in the reaction scheme embody the possible reactions.

The first step is excitation of the transient complex between the anthra-quinone sulfonate sensitizer and sodium chloride:

$$(AQ \cdots HCl) \underset{k_d}{\overset{k_\epsilon \text{ (complex) } I}{\rightleftharpoons}} (AQ \cdots HCl)^* \tag{1}$$
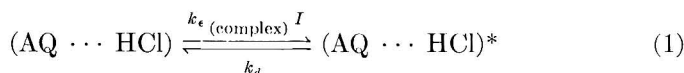
k_d is the rate constant for the dark deactivation reaction in which complex may lose the extra energy.

Step (2) is radical formation:

$$(AQ \cdots HCl)^* \xrightarrow{k_r} AQH^\cdot + Cl \tag{2}$$
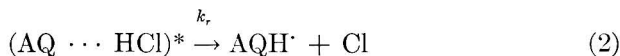
The chlorine atom may attack AQ to form $AQ^\cdot$:

$$Cl^\cdot + AQ \xrightarrow{K_1} HCl + AQ^\cdot \tag{3}$$
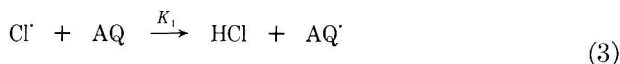
where AQ is
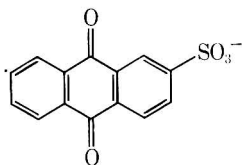
in the case of sodium anthraquinone-2-sulfonate.

The fourth step is initiation of polymerization:

$$Cl^\cdot + M \xrightarrow{k_i} M_1^\cdot \tag{4a}$$

$$AQ^\cdot + M \xrightarrow{k_i} M_1^\cdot \tag{4b}$$

This is followed by propagation as shown in eqs. (5):

$$M_1^\cdot + M \xrightarrow{k_p} M_2^\cdot$$

$$M_2^\cdot + M \xrightarrow{k_p} M_3^\cdot$$

$$\cdot$$
$$\cdot$$
$$\cdot$$

$$M_{(n-1)}^\cdot + M \xrightarrow{k_p} M_n^\cdot \tag{5}$$
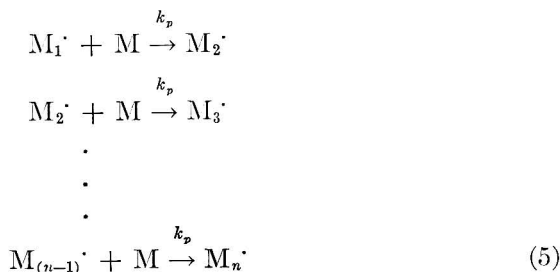
Termination may be of the mutual type [eq. (6a)], by the Cl atom, [eq. (6b)] or by the sensitizer [eq. (6c)].

$$M_n^\cdot + M_m^\cdot \xrightarrow{k_t} M_{n+m} \text{ or } M_n + M_m \text{ (polymer)} \tag{6a}$$

$$M_n^\cdot + Cl^\cdot \xrightarrow{k_{t_1}} \text{Polymer} \tag{6b}$$

$$M_n^\cdot + AQ \xrightarrow{k_{t_2}} \text{Polymer} \tag{6c}$$
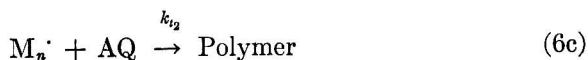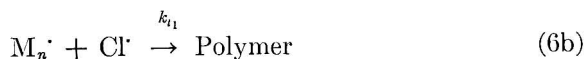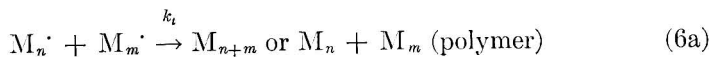
The final step is given by eq. (7).

$$2AQH^{\cdot} \xrightarrow{K_S} AQ + AQH_2 \tag{7}$$
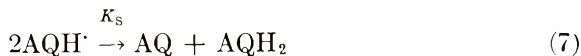
The light absorption fraction involved in the reaction scheme is actually that due to photosensitive complex $k_{\epsilon(complex)}$. It can be shown that

$$k_{\epsilon(complex)} = k_{\epsilon(total)}\, K[Cl^-]/(1 + K[Cl^-]) \tag{8a}$$

where $[Cl^-]$ denotes concentration of sodium chloride, if the equilibrium of eq. (9) is assumed:

$$AQ + HCl \xrightleftharpoons{K} (AQ \cdots HCl) \tag{9}$$

The extinction coefficients for the complex and free sensitizer are assumed to be same because the absorption spectrum of the sensitizer is not altered by the presence of a large excess of sodium chloride. Since under the experimental conditions $K[Cl^-] \ll 1$ equation: (8) becomes,

$$k_{\epsilon(complex)} = k_{\epsilon(total)}\, K[Cl^-] \tag{8b}$$

$k_{\epsilon(total)} \approx k_{\epsilon(sensitizer)} = k_{\epsilon}$, since sensitizer is the only absorbing species. The possibility of direct interaction of the excited anthraquinone sulfonate and monomer leading to monomer radical was excluded because there was no polymerization at long times in aqueous solution without the aid of a reducing agent. Bolland and Cooper[2] studied the photosensitized oxidation of ethanol by disodium anthraquinone-2,6-disulfonate and suggested a cyclic mechanism. The excited singlet of the sensitizer was assumed to be the reactive state for the hydrogen abstraction from alcohol. The primary act was interpreted in terms of the formation of a pair of radicals, one being semiquinone and the other a substrate radical:

$$Q \rightarrow Q^*(S) \tag{10}$$

$$Q^*(S) + CH_3CH_2OH \rightarrow QH^{\cdot} + CH_3\dot{C}HOH \tag{11}$$
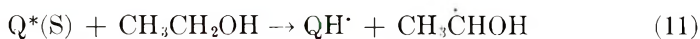
Wilkinson[3] noticed that acceptors with lower triplet levels retarded the photooxidation of isopropyl alcohol and so the excited triplet state was assumed to be the reactive state in the case of anthraquinone derivatives. Cooper[12] described the retarding action of halide ions in the photooxidation of ethyl alcohol by anthraquinone sulfonates as probably due to the chemical quenching of the excited triplet by electron transfer. The primary step of the photochemical reaction in the present investigation probably comprises the excitation of the weak (or loose) complex (the anthraquinone sulfonate–sodium chloride) which then decomposes by the oxidative electron transfer from halogen anion to the anthraquinone sulfonate sensitizer, forming semiquinone and halogen atom. The chlorine atom so produced initiates the polymerization of MA or MMA. Analysis by the dye-partition test[13,14] indicated the presence of chlorine in polymer, which supports initiation by Cl.

Assuming steady-state kinetics for the radicals involved, the rate expressions under conditions of initiation by Cl atom and termination of mutual type are

$$-d[\text{M}]/dt = \frac{k_p}{k_t^{1/2}} \left\{ \frac{k_r k_\epsilon K[\text{Cl}^-]I}{(k_r + k_d)} \right\}^{1/2} [\text{M}] \tag{12}$$

$$-d[\text{AQ}]/dt = \left\{ \frac{k_r}{(k_r + k_d)} \right\} K k_\epsilon [\text{Cl}^-]I \tag{13}$$

$$n = \frac{k_p}{k_t^{1/2}} \left\{ \frac{(k_r + k_d)}{k_r k_\epsilon K[\text{Cl}^-]I} \right\}^{1/2} [\text{M}] \tag{14}$$

Mechanism 2

Steps (3)–(7) may be considered identical with mechanism 1. The primary process not involving sensitizer–halide ion, complex is also possible when steps (1) and (2) of the reaction scheme are replaced by (1a) and (2a), respectively:

$$\text{AQ} \underset{k_d'}{\overset{k_\epsilon I}{\rightleftharpoons}} \text{AQ*(S)} \tag{1a}$$

$$\text{AQ*(S)} \to \text{AQ*(T)}$$

$$\text{AQ*(T)} + \text{HCl} \overset{k_t'}{\to} \text{AQH}^\cdot + \text{Cl} \tag{2a}$$
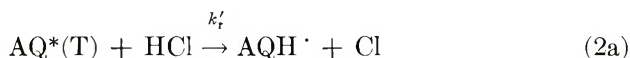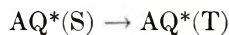
The anthraquinone sulfonate sensitizer may itself pass to an excited singlet, AQ*(S), on light absorption which is then converted to the AQ*(T) triplet by intersystem crossing. The AQ*(T) interacts with chlorine anion by an electron-transfer mechanism to produce chlorine atom, which initiates polymerization. The rate expressions for this second possibility coupled with mutual termination under conditions of $k_d' \gg k_r'[\text{Cl}^-]$ could be:

$$-d[\text{M}]/dt = \frac{k_p}{k_t^{1/2}} \left[\frac{k_r' k_\epsilon I[\text{Cl}^-]}{k_d'} \right]^{1/2} [\text{M}] \tag{15}$$

$$-d[\text{AQ}]/dt = (k_r'/k_d')k_\epsilon I[\text{Cl}^-] \tag{16}$$

$$n = \frac{k_p}{k_t^{1/2}} \left\{ \frac{k_d'}{k_r' k_\epsilon [\text{Cl}^-]I} \right\}^{1/2} [\text{M}] \tag{17}$$

It may be seen from eqs. (12)–(17) that it is not possible to distinguish between these two possible primary processes by kinetics alone. The fact that there is no change in optical absorption of the sensitizer with increased [Cl⁻] and that constant K values could not be obtained from the data go against the mechanism 1; mechanism 2 must indeed be the correct one.

The square root dependence of the rate of polymerization on the incident light intensity indicates that the termination was of the mutual type. The $-d[\text{AQ}]/dt$ was found to be directly proportional to the first powers of the

TABLE I
Values of K, k'_d/k'_r and $k_p/k_t^{1/2}$

Wave-length, mμ	Sensitizer	Monomer	$k_p/k_{p_l t}^{1/2}$, 1.$^{1/2}$ mole$^{-1/2}$-sec$^{-1/2}$				Average $k_p/k_t^{1/2}$, 1.$^{1/2}$ mole$^{-1/2}$-sec$^{-1/2}$	k'_d/k'_r
			$-d[M]/dt$ vs. [M]	$-d[M]/dt$ vs. $k_\epsilon^{1/2}$	$-d[M]/dt$ vs. $[Cl^-]^{1/2}$	$-d[M]/dt$ vs. $I^{1/2}$		
365	AQ-2-SO₃Na	MMA	1.171	1.193	1.257	1.389	1.253	5.9
365	AQ-2-SO₃Na	MA	1.37	1.12	0.85	1.23	1.140	5.7
365	AQ-2,6-diSO₃Na	MMA	1.161	1.234	1.385	0.869	1.162	12.0
365	AQ-2,6-diSO₃Na	MA	1.399	1.398	0.785	1.126	1.177	13.7

concentration of sodium chloride, k_e, and I. Toppet et al.[15] observed similar dependences of the rate of dye disappearance on variables in the polymerization of acrylamide sensitized by eosin. The other modes of termination, e.g., by Cl or AQ itself do not agree with the proportionalities observed with respect to variables. For termination by Cl there will be square dependence of $-d[M]/dt$ over [M] and no dependences on k_e and I. For termination by AQ itself, $-d[M]/dt$ will be proportional to the first powers of k_e and I. Since no such proportionalities have been observed, termination by Cl or AQ will have to be discounted.

Rate and Equilibrium Parameters

It may be mentioned that k_r'/k_d' of mechanism 2 is equal to $K[k_r/(k_r + k_d)]$ of mechanism 1, while $k_p/k_t^{1/2}$ by both mechanisms will be identical. From the slopes of the plots of $-d[AQ]/dt$ versus k_e, [Cl$^-$], and I, k_r'/k_d' was calculated. By plotting $-d[M]/dt$ versus [M], $k_e^{1/2}$, Cl$^{-1/2}$, and $I^{1/2}$ (Figs. 1, 3, 6) and substituting the average value of k_r'/k_d' into the slopes, $k_p/k_t^{1/2}$ values were obtained; the average values are given (Table I). For $k_p/k_t^{1/2}$ in the dye-sensitized polymerization Sheriff and Santappa[16] got the values 1.19 and 1.56 for MA and MMA, respectively; Subramanian and Santappa,[17] using a ceric redox system obtained the values 1.2 and 1.2 for MA and MMA. In the photopolymerization by cobalt complexes Natarajan and Santappa[18] reported the values 1.221 and 1.188 for MA and MMA, respectively. Mahadevan and Santappa,[19] using uranyl ion sensitizer got the values 0.374 and 0.3009 for MA and MMA, respectively. Atkinson and Cotton[20] obtained a value of 0.5591 for MMA. The literature values agree with the other values obtained in our laboratory. The values for the precipitating media are higher than the values for homogeneous media in the cases of both MA and MMA.

The overall quantum yields for monomer disappearance γ_m

$$\gamma_m = \frac{-d[M]/dt}{k_e I}$$

increased with increasing monomer concentration and decreased with increasing k_e, [Cl$^-$], and I. For monomer variation at $\lambda = 365$ mμ the γ_m varied in the range of 30–120 for MA and 5–15 for MMA. The quantum yields were found to be in the order of reactivity of monomers, i.e., MA > MMA. The quantum yields with respect to the sensitizer $\phi_{AQ} = (-d[AQ]/dt)/k_e I$ did not vary much with the variations carried out. The value of ϕ_{AQ} ranged from 0.01 to 0.015 for MA and 0.01 to 0.02 for MMA for k_e variation at $\lambda = 365$ mμ. The low ϕ_{AQ} may be explained on the basis of probable deactivation of the excited sensitizer.

References

1. C. F. Wells, *Trans. Faraday Soc.*, **57**, 1703 (1961).

2. J. L. Bolland and H. R. Cooper, *Proc. Roy. Soc.* (London), **A225**, 405 (1954).

3. F. Wilkinson, *J. Phys. Chem.*, **66**, 2569 (1962).

4. N. K. Bridge and G. Porter, *Proc. Roy. Soc.* (London), **A244**, 259 (1958).

5. N. Geacintov, V. Stannett, E. W. Abrahamson, and J. J. Hermans, *J. Appl. Polym. Sci.* **3**, 54 (1960).

6. G. S. Egerton and A. G. Roach, *J. Soc. Dyers Colourists*, **74**, 408 (1958).

7. F. S. Dainton and M. Tordoff, *Trans. Faraday Soc.*, **53**, 499 (1957).

8. L. F. Fieser, *J. Amer. Chem. Soc.*, **46**, 2639 (1924).

9. J. H. Baxendale, S. Bywater, and M. G. Evans, *J. Polym. Sci.*, **1**, 237 (1946).

10. J. Sen, S. R. Bannerjee, and S. R. Palit, *J. Sci. Ind. Research* (India), **11B**, 90 (1952).

11. C. A. Parker and C. G. Hatchard, *Proc. Roy. Soc.* (London), **A235**, 518 (1956).

12. H. R.Cooper, *Trans. Faraday Soc.*, **62**, 2865 (1966).

13. P. Ghosh, P. K. Sengupta, and A. Pramanik, *J. Polym. Sci. A*, **3**, 1725 (1965).

14. M. K. Saha, P. Ghosh, and S. R. Palit, *J. Polym. Sci. A*, **2**, 1365 (1964).

15. S. Toppet, G. Delzenne, and G. Smets, *J. Polym. Sci. A*, **2**, 1539 (1964).

16. A. I. Sheriff and M. Santappa, *J. Polym. Sci. A*, **3**, 3131 (1965).

17. S. V. Subramanian, Thesis, Madras University, 1967.

18. L. V. Natarajan, Thesis, Madras University, 1968.

19. V. Mahadevan and M. Santappa, *J. Polym. Sci.* **50**, 361 (1961).

20. B. Atkinson and G. R. Cotton, *Trans. Faraday Soc.*, **54**, 877 (1958).

Polymerization of β-Cyanopropionaldehyde.
V. Anionic Polymerization Initiated by
Benzophenone–Alkali Metal Complexes

HIROSHI SUMITOMO and KAZUHIKO HASHIMOTO,
Faculty of Agriculture, Nagoya University, Chikusa, Nagoya, Japan

Synopsis

Anionic polymerization of β-cyanopropionaldehyde was studied with use of benzo-phenone–monosodium, -disodium, and -dilithium complexes as initiators. The resulting poly(cyanoethyl)oxymethylene was compared with that obtained by cationic and coordinated initiators previously reported. Polymer of higher stereoregularity but lower molecular weight was formed in the present system. The marked influence of the initiator concentration on the polymer yield and stereoregularity is explained on the basis of the difference in the degree of association of the alcoholate ion pair, i.e., the associated ion pair may form stereoregular polymer and the nonassociated or less-associated ion pair may form a large amount of amorphous atactic polymer. The initiation with benzophenone–dialkali metal complex was found to be bond-formation type. Chain transfer with active hydrogen of β-cyanopropionaldehyde frequently occurs.

INTRODUCTION

In the preceding studies,[1-4] β-cyanopropionaldehyde (β-CPA) was poly-merized by using ionic initiators, e.g., boron trifluoride etherate, diethyl-zinc, triethylaluminum, and triethylaluminum–titanium chloride com-plexes at low temperature to give high molecular weight poly(cyanoethyl)-oxymethylene (I).

$$n\,NC\!-\!CH_2\!-\!CH_2\!-\!CHO \longrightarrow \left[\begin{matrix} CH\!-\!O \\ | \\ CH_2\!-\!CH_2\!-\!CN \end{matrix}\right]_n$$

I
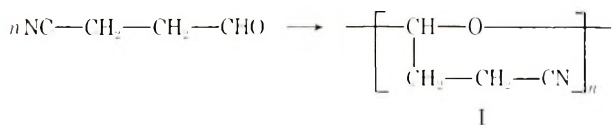
The present investigation is concerned with the anionic polymerization of β-CPA initiated by benzophenone–monosodium, –disodium, and –dilith-ium complexes, in comparison with the results obtained in the cationic and coordinated polymerization.

EXPERIMENTAL

All the procedures, including purification of materials, preparation of initiators, and polymerization, were carried out in a high-vacuum system

($<10^{-5}$ mm Hg). General experimental techniques of a homogeneous anionic polymerization developed by Szwarc[5] and Morton et al.[6] were employed with some modification.[7-9]

Materials

β-Cyanopropionaldehyde (β-CPA) prepared as already described[1] was distilled *in vacuo* after drying over molecular sieves.

Tetrahydrofuran (THF) and toluene used as solvents were distilled after refluxing in the presence of sodium and drying over the mixture of sodium and benzophenone in a high-vacuum system until a reddish-violet color appeared. Benzophenone was purified by recrystallization from ethanol.

Preparation of Initiators

Benzophenone–disodium complex (Na_2–BzPh) was prepared by treating benzophenone–THF solution at 0°C with excess of sodium freshly distilled. After 1 or 2 days the reddish-violet solution was filtered prior to use. The formation of the complex was confirmed by the measurement of its ultra-violet and visible absorption spectra. The concentration of initiator solution was determined by acid titration. Commercial lithium metal was used for the preparation of benzophenone–dilithium complex (Li_2–BzPh). Benzophenone–monosodium complex (Na–BzPh) solution was prepared by adding an equivalent amount of benzophenone to the Na_2–BzPh solution prepared previously.

Polymerization

Cold solution of β-CPA was added to cold initiator solution with stirring under high vacuum. Polymerization was stopped by the addition of acetic anhydride following by the addition of a large amount of cold methanol. Polymer obtained was washed with methanol and dried under reduced pressure.

Fractional extraction and measurements of melting point, solution vis-cosity, and optical density of polymer were conducted by the same methods as previously described.[1-4]

RESULTS AND DISCUSSION

Polymerization was initiated, accompanied by the fading of the color of the initiator immediately after the addition of β-CPA solution to the initiator solution. The results of polymerization with use of Na_2–BzPh, Li_2–BzPh and Na–BzPh are given in Tables I and II.

In the tables are listed also the values of D_{1258}/D_{1270}, i.e. the ratio of optical density of the stereoregular band (1 258 cm^{-1}) to that of the amor-phous band (1 270 cm^{-1}) in the infrared absorption spectrum of polymer, as a semiquantitative measure of stereoregularity of polymer.[3]

TABLE I
Polymerization of β-Cyanopropionaldehyde with
Benzophenone–Dialkali Metal Complexes[a]

Run no.	β-CPA, g	Initiator	Initiator concn., mole-% (based on monomer)	Volume ratio of solvent to monomer	Time, days	Polymer Yield, %	$\dfrac{D_{1255}}{D_{1270}}$
14	10.4	Na₂–BzPh	0.01	2	2	17.6	0.81
42	7.8	"	0.02	5	1	49.2	0.87
43	3.1	"	0.10	"	"	63.6	0.87
37	3.9	"	0.20	"	"	58.1	<1.00
39	4.1	"	0.49	"	"	24.5	1.75
29	4.2	"	1.01	"	"	12.3	2.97
41	2.5	"	1.48	"	"	4.8	2.37
15	10.1	Li₂–BzPh	0.05	2	2	16.7	<1.00
30	16.3	"	1.00	5	1	4.7	2.41

[a] At <10⁻⁵ mm Hg; −78°C; solvent, THF.

TABLE II
Benzophenone–Monosodium Complex Initiated Polymerization
of β-Cyanopropionaldehyde[a]

Run no.	β-CPA, g	Na–BzPh, mole-% (based on monomer)	Volume ratio of solvent to monomer	Time, days	Polymer yield, %	$\dfrac{D_{1255}}{D_{1270}}$
35	10.2	0.05	5	1	45.0	0.82
33	10.7	0.19	"	"	71.9	<1.00
36	2.0	0.54	"	"	44.2	<1.00
32	10.3	0.94	"	"	24.0	1.68
31	10.3	1.97	"	"	15.7	2.44
34	5.7	2.96	"	"	17.1	2.50
28[b]	10.3	0.10	"	"	4.1	1.61
25[b]	10.4	1.00	"	"	14.0	1.67

[a] At <10⁻⁵ mm Hg; −78°C; solvent, THF.
[b] Solvent, toluene.

It is interesting to note that the polymerization starts even at extremely low concentration of initiator, such as a mole ratio of initiator to monomer of 1/10 000 (run 14 in Table I).

The polymer obtained here is also found to be poly(cyanoethyl)oxymethylene from the comparison of its infrared absorption spectrum with that obtained previously. No absorption at 700 cm⁻¹ based on monosubstituted phenyl group appears in the infrared spectrum of polymer prepared from Na–BzPh, but does in those from Na₂–BzPh and Li₂–BzPh. The NMR spectra of the latter also show a peak due to phenyl protons at a τ value of about 2.6.

It was mentioned by Vogl[10] that Na–BzPh dimerized to benzopinacolate, and these alcoholate anions initiated the polymerization of aliphatic aldehydes [eq. (1)].

$$2 \ \cdot \overset{|}{\underset{|}{C}}{-}O^- \ Na^+ \ \longrightarrow \ Na^+ \ {}^-O{-}\overset{|}{\underset{|}{C}}{-}\overset{|}{\underset{|}{C}}{-}O^- \ Na^+ \tag{1}$$
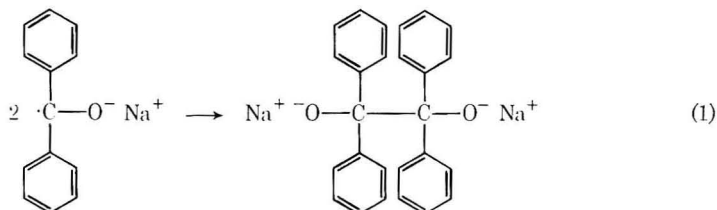
It was also considered by Takida and Noro[11] that the initiation induced by Na–BzPh might involve bond formation through the alcoholate anion. The initiation mechanism in the present system might also be of the bond formation type. No confirmation on this point, however, was still obtained here, since no initiator residue was detected in the polymerization product obtained with Na–BzPh. The occurrence of the chain-transfer reaction and of degradation of polyacetal produced make confirmation difficult. Takida et al.[11] described the initiation mechanism with Na_2–BzPh including the electron-transfer step shown in eq. (2).

$$Na^+ \ {}^-\overset{|}{\underset{|}{C}}{-}O^- \ Na^+ \ + \ \underset{R}{\overset{|}{C}H{=}O} \ \longrightarrow \ \cdot\overset{|}{\underset{|}{C}}{-}O^- \ Na^+ \ + \ \underset{R}{\overset{|}{\cdot C}H{-}O^- \ Na^+} \tag{2}$$
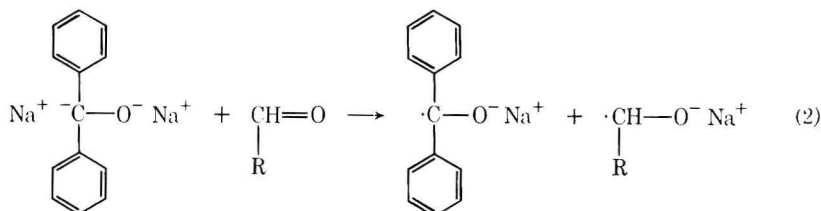
This mechanism seems improbable by virtue of the fact that the monomer radical anion must be too unstable to form, though the Na–BzPh simultaneously formed would start the polymerization.

From the fact that the initiator residue was detected in Na_2–BzPh-initiated polymer but not in Na–BzPh polymer in the present investigation, it is suggested that the initiator residue is more stably incorporated in the chain derived from Na_2–BzPh than that from Na–BzPh and that it is also

Fig. 1. Influence of initiator concentration. Initiator, Na_2–BzPh; solvent, THF; volume ratio of solvent to monomer, 5; time, 1 day; temperature, $-78°C$.

possible to initiate by bond formation with the carbanion of the dialkali metal complexes [eq. (3)].

$$Na^+ \ ^-C-O^- \ Na^+ \ + \ 2 \ CH=O \longrightarrow$$
$$CH_2-CH_2-CN$$

$$Na^+ \ ^-O-CH-C-O-CH-O^- \ Na^+ \quad (3)$$
$$NC-CH_2-CH_2 \qquad CH_2-CH_2-CN$$

Figures 1 and 2 show that the concentration of initiators (Na₂–BzPh and Na–BzPh) has a marked influence on the yield and stereoregularity of polymer. The polymer yield has a maximum at a certain initiator concentration, and the optical density ratio, in index of stereoregularity of polymer, increases with decreasing polymer yield. It should be noticed that there may be a main difference between Figures 1 and 2 in an initiator concentration scale, namely the concentration of Na₂–BzPh corresponds to twice of that of Na–BzPh. This suggests that the concentration of the active species plays a more important role than the kind of initiator in these polymerization systems. A simplification of this tendency is made in Figure 3. A larger amount of amorphous atactic polymer is produced at lower initiator concentration, and the content of stereoregular polymer increases with the initiator concentration.

Two kinds of growing species may be presumed to be present here. The one is an associated ion pair which may form a stereoregular polymer, and the other species is a non- or less-associated one which may form an amorphous atactic polymer. Higher initiator concentration results in higher concentration of an alcoholate-type ion pair as growing species, and the
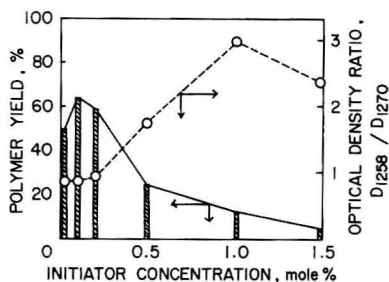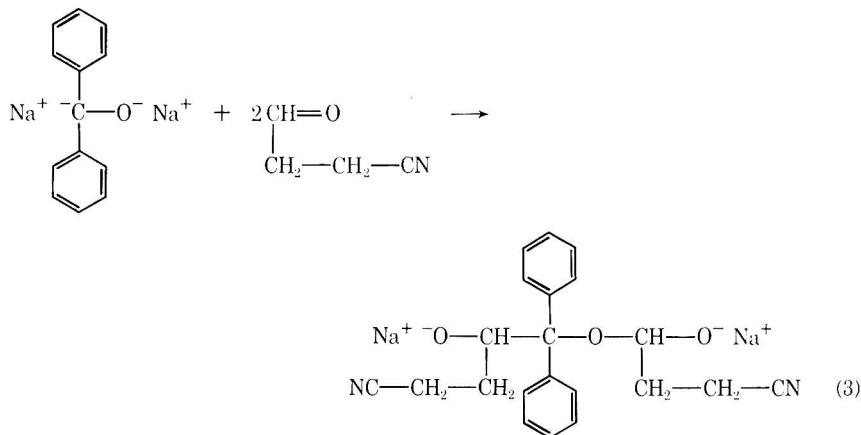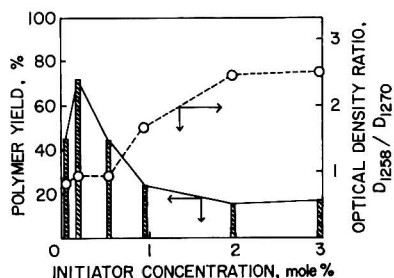

Fig. 2. Influence of initiator concentration. Initiator, Na–BzPh; solvent, THF; volume ratio of solvent to monomer, 5; time, 1 day; temperature, −78°C.
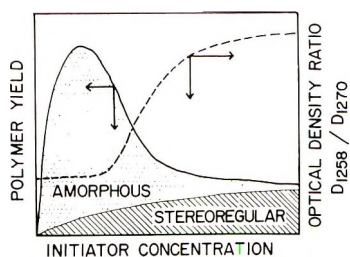
Fig. 3. Simplification of the influence of initiator concentration.
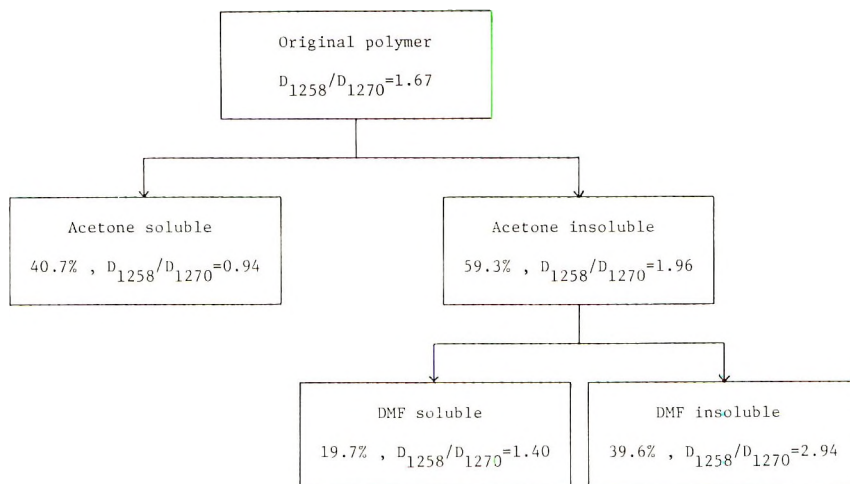
Fig. 4. Effect of elution farcmentation of polymer on optical density ratio (polymer sample, from run 25 in Table II).

species may be associated enough to form stereoregular polymer and to decrease polymer yield. At lower initiator concentration, the growing chain is assumed to be not associated or less highly associated, leading to the formation of a larger amount of amorphous atactic polymer. It was mentioned by Richards and Szwarc[12] that the alcoholate-type ion pair was associated. Such marked effects of initiator concentration on the polymer yield and on the stereoregularity have never been observed in the vinyl polymerization with a carbanion-type ion pair. It seems, therefore, that these phenomena may be characteristic of associative alcoholate-type ion pair. Further investigation of the effect of solvents on the active species will be needed.

Polymer was elution-fractionated with use of acetone and dimethyl-formamide (DMF) as solvents. The effect of the fractionation on the optical density ratio, D_{1258}/D_{1270}, is shown in Figure 4.

In general, the solubility of polymer depends upon its average molecular weight and stereoregularity when the chemical structure is the same. In the present system it may depend mainly upon the stereoregularity.

TABLE III
Results of Elution Fractionation of Produced Polymers[a]

Run no.	Original polymer				DMF-soluble			DMF-insoluble	
	Na–BzPh, mole-%	Solvent	$\dfrac{D_{1258}}{D_{1270}}$		%	$\dfrac{D_{1258}}{D_{1270}}$	%		$\dfrac{D_{1258}}{D_{1270}}$
28	0.10	Toluene	1.61		18.5	1.11	81.5		2.11
25	1.00	"	1.67		60.4	1.08	39.6		2.94
33	0.19	THF	<1.00		<99.5	<1.00	< 0.5		—
32	0.94	"	1.68		96.9	1.59	3.1		2.15
34	2.96	"	2.50		96.6	1.95	3.4		—

[a] At $<10^{-5}$ mm Hg; $-78°C$; 1 day; volume ratio of solvent to monomer, 5.

In Table III are given some results of the elution fractionation with the use of DMF as solvent for the polymer samples prepared in toluene and in THF.

The content of DMF-insoluble fraction of polymer prepared in toluene is much higher than that in THF. Some of the polymers obtained in THF give a large amount of DMF-soluble fractions having relatively high values of D_{1258}/D_{1270}. This means that low molecular weight stereoregular polymer is produced in THF.

TABLE IV
Properties of Polymer

Properties	Polymer prepared with Na₂–BzPh	Polymer prepared with triethylaluminum[a]
Melting point, °C	120–125.5	162–172
Reduced viscosity, η_{sp}/c[b]	0.015–0.065	0.76
Solubility in γ-butyrolactone	Almost soluble at room temperature	Partially insoluble at high temperature
Optical density ratio D_{1258}/D_{1270}		
Amorphous	<1.0	<1.0
Stereoregular	2.5	1.84

[a] Unpublished data.
[b] DMF soluble fraction, DMF, 25°C, c = 0.3 g/100 ml.

Table IV shows a comparison between the properties of polymer obtained from benzophenone–alkali metal complexes and that obtained with triethylaluminum. Marked differences were observed with respect to melting point, solution viscosity, and solubility in γ-butyrolactone. It appears that anionic polymerization of β-CPA with use of alkali metal complexes may result in the formation of polymer of lower molecular weight but higher stereoregularity than polymer obtained by cationic and coordinated ionic polymerization.

A chain-transfer reaction may be thought to occur frequently in the polymerization, in view of the fact that the molecular weight of the polymer is lower than expected and also independent of the initiator concentration.

It must be accompanied by the migration of one of the hydrogens of β-CPA, but which hydrogen participates in the reaction is still not clear, since both α- and β-hydrogens of the monomer are quite active. Chain transfer to polymer may also be possible, but this point must be the subject of future research.

References

1. H. Sumitomo and K. Kobayashi, *J. Polym. Sci. A-1*, **4**, 907 (1966).

2. H. Sumitomo and K. Kobayashi, paper presented at the International Symposium on Macromolecular Chemistry, Tokyo and Kyoto, 1966; *Preprints of Scientific Papers*, I-197 (1966).

3. H. Sumitomo and K. Kobayashi, *J. Polym. Sci. A-1*, **5**, 2247 (1967).

4. K. Kobayashi and H. Sumitomo, *J. Polym. Sci.*, in press.

5. R. Milkovich, M. Szwarc, and M. Levy, *J. Amer. Chem. Soc.*, **78**, 2656 (1956).

6. M. Morton and R. Milkovich, *J. Polym. Sci. A*, **1**, 443 (1963).

7. H. Sumitomo, K. Nobutoki, and Y. Hachihama, *Kogyo Kagaku Zasshi*, **67**, 260 (1966).

8. K. Nobutoki and H. Sumitomo, *Bull. Chem. Soc. Japan*, **40**, 1741 (1967).

9. K. Nobutoki and H. Sumitomo, *Bull. Chem. Soc. Japan*, **40**, 2725 (1967).

10. O. Vogl, *J. Polym. Sci. A*, **2**, 4607 (1964).

11. H. Takida and K. Noro, *Kobunshi Kagaku*, **22**, 724 (1965).

12. D. H. Richards and M. Szwarc, *Trans. Faraday Soc.*, **55**, 1644 (1959).

Synthesis of Difunctional Polystyrenes and Their Incorporation in Block Copolymers with Bisphenol A Polycarbonate

M. N. BERGER, J. J. K. BOULTON, and B. W. BROOKS,*

Shell Research Limited, Urmston, Manchester, England

Synopsis

Block polymers of polystyrene and bisphenol A polycarbonate have been prepared and their bulk viscosities studied as functions of both shear stress and polystyrene block length. The polystyrene blocks were α,ω-diacid chlorides prepared from the reaction of "living" polystyrenes with diacid chlorides. These reactions were studied in order to discover the most effective way of preparing the polystyrene diacid chlorides. The polystyrene diacid chlorides are best prepared by reaction of disodiopolystyrene with phosgene. The flow properties of the block copolymers depend on the composition of the polymers but do not depend on the length of the polystyrene blocks.

INTRODUCTION

The preparation of block copolymers presents a number of problems. When the copolymers are prepared by condensation reactions of presynthesized blocks it is essential that the blocks should have a high degree of α,ω difunctionality. Various techniques such as chain-transfer processes, ozonolysis, and the use of "living" polymers have been used by previous workers[1-4] to prepare difunctional blocks.

In our work, we have presynthesized polystyrene α,ω-diacid chlorides from "living" polystyrene. After a careful investigation of various processes (described below) for preparing this material, we found that the best product was obtained by reaction of α,ω-disodiopolystyrene with excess phosgene. Dilithiopolystyrene also reacted with phosgene to produce a polystyrene acid chloride, but in the presence of tetrahydrofuran (THF) (solvent for the initiator) coupling of polystyrene blocks was unavoidable. The polystyrene was incorporated into block copolymers with bisphenol A polycarbonate by condensation reactions (described below).

Molten bisphenol A polycarbonate exhibits[5] Newtonian flow at temperatures around 250°C, i.e., the viscosity of the melt does not change with applied stress, and the output of a molding machine is proportional to the

* Present address: Chemical Engineering Department, Loughborough University of Technology, England.

load applied.   Other polymers such as polystyrene show non-Newtonian behavior, so that the viscosity of the melt decreases with increasing stress. This aids the fabrication process at high loads.   Polystyrene is, therefore, easier to process than polycarbonate.   It was considered desirable to examine this aspect of the rheological behavior of block copolymers of styrene and polycarbonate.   The properties might depend on many factors including overall composition, final average molecular weight and block lengths. In the experiments described we were able to control the overall composition and polystyrene block length.   The polystyrene blocks were randomly distributed along the polymer chains.

RESULTS AND DISCUSSION

Preparation of polystyrene diacid chloride

α,ω-Disodiopolystyrene was prepared by reaction of styrene (in toluene solution) with the disodio tetramer of α-methylstyrene (in THF solution). This reaction was carried out at 0°C to avoid chain transfer.[6]   The polymer solution was added to a 500 molar excess of liquid phosgene at 0°C.   The color of the living polystyrene was immediately discharged. After reaction the excess phosgene was displaced with nitrogen at room temperature and samples were quickly extracted for viscometric molecular weight determination.   A living polymer of molecular weight 19 000 gave a product of molecular weight 18 000.   We concluded that no significant coupling took place but that a simple end-tipping reaction occurred:

$$Na^+ \ ^-PS^- \ Na^+ + 2COCl_2 \rightarrow ClCO-PS-COCl + 2NaCl \tag{1}$$
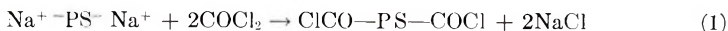
Finaz et al.[3] obtained coupling with much smaller amounts of phosgene.

Polystyrene diacid chlorides prepared in this manner were used in the synthesis of the block copolymers.   These blocks would probably have a higher percentage difunctionality than the polystyrene blocks used by Merrill[7] in his preparations.

Preparation of Block Copolymers

A typical block copolymer was prepared as follows.   A solution of polystyrene diacid chloride in toluene was added over 2 hr to a solution of a large molar excess of bisphenol A in dry pyridine; the mixture was then refluxed for 2 hr.   Thus, the polystyrene molecules became end-tipped with phenolic hydroxy groups having the same chemical reactivity as the hydroxyl groups in bisphenol A.

$$2HO-C_6H_4-\underset{\underset{CH_3}{|}}{\overset{\overset{CH_3}{|}}{C}}-C_6H_4-OH + ClCO-PS-COCl \rightarrow$$

$$HO-C_6H_4-\underset{\underset{CH_3}{|}}{\overset{\overset{CH_3}{|}}{C}}-C_6H_4-OCO-PS-COO-C_6H_4-\underset{\underset{CH_3}{|}}{\overset{\overset{CH_3}{|}}{C}}-C_6H_4-OH + 2 HCl \tag{2}$$
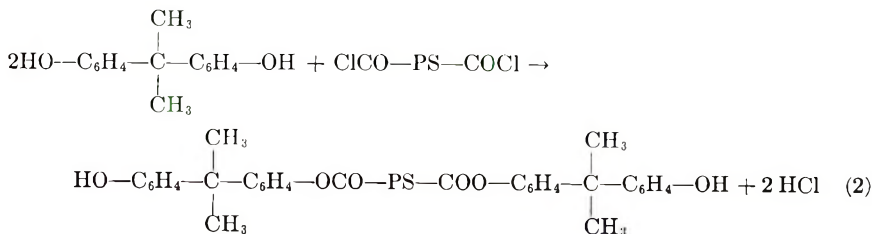
The molecular weight of the polymer did not increase during this process. The resultant mixture was cooled to 0°C and pure phosgene was passed through it. Orange-red colors developed as the phosgene complexed with the pyridine which marked the end of the reaction. Excess phosgene was displaced with nitrogen and a small quantity of bisphenol A was added to end-tip the polymer with hydroxyl groups. The polymers were precipitated in methanol and the unreacted polystyrene ($< 1\%$ of original) was extracted with boiling cyclohexane. Copolymer yields were $>95\%$. Solutions of the polymers in dichloromethane were washed with aqueous hydrochloric acid to remove pyridine.

Table II gives the results. The polystyrene blocks having been made as "living" anionic polymers should have a very narrow molecular weight distribution. The copolymers were all made by condensation reation under very similar conditions. The final intrinsic viscosity values are all similar, and the distributions can be expected to be typical of linear condensation polymers, with

$$\frac{\mathrm{Mw}}{\mathrm{Mn}} 2$$

Flow Properties of Block Copolymers

The shear stress–shear rate relations for the materials were examined with a melt index grader at 250°C with the use of various loads. The throughly dried copolymers showed no significant breakdown at 250°C.

Shear rates (Table I) were found from the equation

$$\text{shear rate (sec}^{-1}) = 4W/\pi\rho r^3$$

where W is the weight of extrudate (in grams/second), ρ is the density (in grams/cubic centimeter), r is the radius of die (in centimeters). For the copolymers we took each density as the arithmetic mean of the densities of molten polystyrene[8] and molten bisphenol A polycarbonate[5] at 250°C; thus

$$\rho_{\mathrm{cp}} = f_{\mathrm{ps}}\rho_{\mathrm{ps}} + (1 - f_{\mathrm{ps}})\rho_{\mathrm{pc}}$$

where f_{ps} denotes the weight fraction of polystyrene and ρ_{cp}, ρ_{ps}, ρ_{pc} are the densities of the copolymer, polystyrene, and polycarbonate, respectively.

(The pure bisphenol A polycarbonate was prepared as above but without the polystyrene.) Intrinsic viscosities of the polymers in tetrachloroethane at 25°C were also measured.

Figure 1 shows plots of shear stress against shear rate at 250°C (the copolymers were unstable at higher temperatures). In all cases the viscosities of the copolymers were considerably lower than the viscosity of bisphenol A polycarbonate. As the polystyrene content increased the deviation from Newtonian flow became more pronounced.

The copolymers which had almost equal polystyrene contents (19 and 22%, respectively), had similar flow properties even though the polystyrene block lengths in these two polymers were decidedly different (2 900 and

TABLE I

Preparation and Shear Sensitivity of Polycarbonate–Polystyrene Copolymers at 250°C

Intrinsic viscosity of polystyrene diacid chloride, dl/g[a]	Weight of bisphenol A used, g	Weight of polystyrene used, g	Intrinsic viscosity of block copolymer, dl/g[b]	Block-bound polystyrene, wt-%	Molecular wt of polystyrene blocks	Density at 250°C, g/cm³[c,e]	Shear stress, dyne/cm² × 10^{-5}	Shear rate, sec × 10^{-1}
—	60	—	0.65	0	—	1.09[d]	1.97	0.454
							4.56	1.07
							9.12	2.13
							19.7	4.54
0.052	60	17.5	0.65	19	2 900	1.06	1.97	2.41
							3.46	4.61
							4.56	6.81
							9.12	17.2
0.106	60	21.0	0.65	22	9 300	1.06	1.97	2.46
							3.46	5.84
							4.56	8.14
							9.12	24.1
0.064	60	30.0	0.52	29	4 100	1.05	1.97	3.14
							3.46	6.15
							4.56	11.2
							9.12	58.0

[a] In benzene at 25°C.
[b] In tetrachloroethane at 25°C.
[c] Density of polystyrene at 250°C = 0.940 g/cm³.
[d] Data of Schnel.[5]
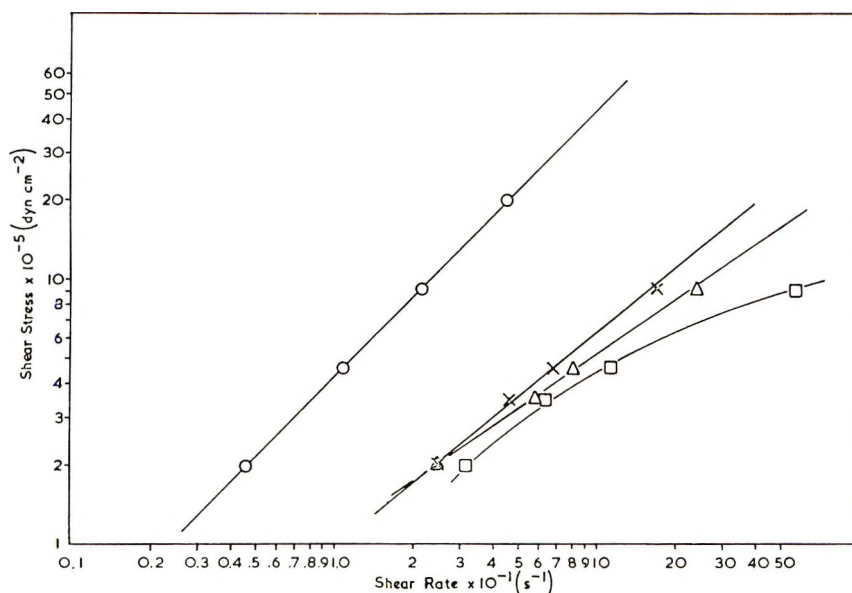
Fig. 1. Shear sensitivity of polycarbonate–polystyrene block copolymers. (O: 0% polystyrene; ×: 19% polystyrene; △: 22% polystyrene; □: 29% polystyrene).

9 300, respectively). These results indicated that the total proportion of polystyrene in the copolymers had a greater effect on flow properties than had the block length of the polystyrene segments.

Reactions of Lithiopolystyrene with Phosgene

In addition to the method described above we attempted to prepare polystyrene α,ω-diacid chlorides from reactions of lithiopolystyrenes with various diacid chlorides, including phosgene.

Solutions of α,ω-dilithiopolystyrene in toluene (containing small amounts of THF) were prepared using dilithiostilbene as an initiator. These solutions were treated with phosgene as described above for disodiopolystyrene. Table II shows that the phosgenation reaction did not lead to a molecular

TABLE II
Reaction of α,ω-Dilithiopolystyrene with Phosgene at 0°C

Concentration of polystyrene living ends, mole/l. $\times 10^2$	THF, vol-%	Molecular wt of living polymer[a]	Molecular wt of phosgenated polymer[a]
3.70	1.0	30 000	60 000
2.47	0.67	45 000	85 000
1.11	0.3	120 000	130 000
0.986	0.027	152 000	163 000
0.952	0.026	210 000	205 000

[a] Determined viscometrically.

weight increase for polymers of high molecular weight, but as the initial molecular weight was lowered (i.e., the amount of original initiator solution was raised), coupling reactions occurred.

It seems reasonable to assume that once the benzylic acid chloride is formed, the coupling results from the reaction, (3):

$$PS-CH_2CHCOCl + PS^- Li^+ \rightarrow PS-CHCO-PS + LiCl$$
$$\underset{C_6H_5}{\big|} \qquad\qquad \underset{C_6H_5}{\big|}$$
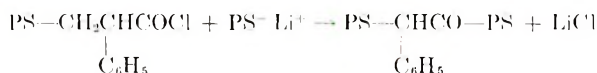
and that in the presence of THF this reaction is faster than reaction (4):

$$PS^- Li^+ + COCl_2 \rightarrow PS-COCl + LiCl \tag{4}$$

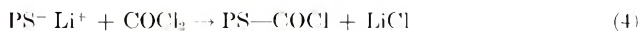THF could be excluded from the system only by preparing monolithium polystyrene with butyl lithium as an initiator in an all-hydrocarbon solvent. A solution of monolithium polystyrene was prepared in this manner (molecular weight 38 000) with the use of cyclohexane as a solvent. The initiator was sec-butyllithium dissolved in n-heptane. After treatment with phosgene a sample of polymer solution was estimated for acid chloride content by hydrolysis with excess standard aqueous alkali followed by titration with standard aqueous hydrochloric acid. The number-average molecular weight for the final polymer was calculated to be 32 000, on assuming one acid chloride group per molecule. The remaining reaction solution was poured into excess methanol; the precipitated polymer had a molecular weight of 38 400 as determined viscometrically.

Thus, it seems that under the conditions used, one acid chloride group is deposited on one end of each polymer molecule without any substantial coupling,

$$PS^- Li^+ + Cl-CO-Cl \rightarrow PS-COCl + LiCl \tag{5}$$
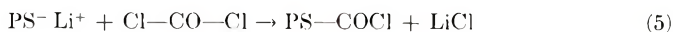
Since coupling does occur with dilithiopolystyrene, we may assume that the presence of THF (used to dissolve the dilithiostilbene) greatly accelerates the coupling reaction. At high initiator concentrations (i.e., higher amounts of THF in the reaction mixture) coupling is quite pronounced.

To obtain some indication of the nature of the coupling reaction the following model reactions were carried out.

Monolithium polystyrene (molecular weight about 500; 2×10^{-2} mole) in a heptane–toluene mixture was added in two aliquots to a solution of 1.0 $\times 10^{-2}$ mole of acetyl chloride in THF solution. Addition of the first aliquot produced a pale yellow solution containing a white precipitate. After stirring for 5 min the second aliquot was added rapidly, giving a noticeable exotherm and a dark brown solution. After 1.5 hr the solution was quenched with water. An infrared spectrum of the recovered polymer showed no carbonyl absorption in the 5.9 μ region. In a similar two-stage experiment with lithium polystyrene of molecular weight 6700, the molecular weight of the polymer was found to be 9000 after the addition of the first aliquot and 14 000 after the addition of the second aliquot.

These two experiments indicate that one mole of acetyl chloride will couple two moles of lithium polystyrene. The reaction sequence may be either reaction (6) followed by reaction (7),

$$PS^- Li^+ + CH_3COCl \rightarrow CH_3CO—PS + LiCl \tag{6}$$

$$PS^- Li^+ + CH_3CO—PS \rightarrow CH_3—\overset{\displaystyle PS}{\underset{\displaystyle PS}{\overset{|}{\underset{|}{C}}}}—OLi \tag{7}$$
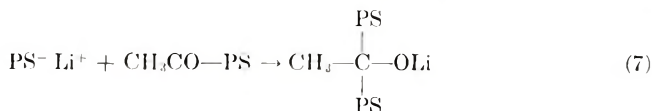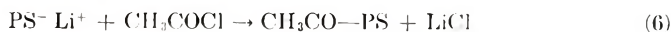
with reaction (7) competing with reaction (6) even in the presence of excess acetyl chloride. An alternative sequence might be reaction (8) followed by reaction (9), or (10),

$$PS^- Li^+ + CH_3COCl \rightarrow CH_3—\overset{\displaystyle Cl}{\underset{\displaystyle PS}{\overset{|}{\underset{|}{C}}}}—OLi \tag{8}$$

$$CH_3—\overset{\displaystyle Cl}{\underset{\displaystyle PS}{\overset{|}{\underset{|}{C}}}}—OLi \rightarrow CH_3—\overset{}{\underset{\displaystyle PS}{\underset{|}{C}}}{=}O + LiCl \tag{9}$$

$$CH_3—\overset{\displaystyle Cl}{\underset{\displaystyle PS}{\overset{|}{\underset{|}{C}}}}—OLi + PS^- Li^+ \rightarrow CH_3—\overset{\displaystyle PS}{\underset{\displaystyle PS}{\overset{|}{\underset{|}{C}}}}—OLi + LiCl \tag{10}$$
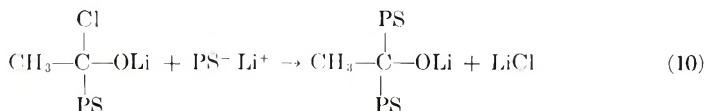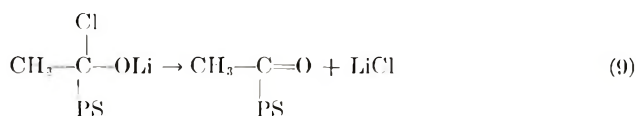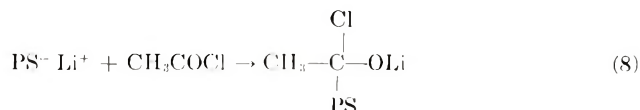
with reaction (10) competing with reaction (9).

It may be that similar addition reactions of the carbonyl group feature in the reaction of dilithiostyrene with phosgene. However, the formation of appreciable amounts of $(PS)_3COLi$ would result in crosslinking. No evidence for crosslinking was obtained.

Further Routes to Difunctional Polystyrene

The reaction of adipyl or terephthaloyl chloride with α,ω-dilithiopolystyrene might be expected to produce polymer molecules tipped with acid chloride groups of a reactivity similar to that of the acid chloride originally added [eq. (11)].

$$Li^+ \ ^- PS^- Li^+ + ClCO—R—COCl \rightarrow Li^+ \ ^- PS—CO—R—COCl + LiCl \tag{11}$$

Therefore, we added solutions of α,ω-dilithiopolystyrene to an excess of adipyl chloride and terephthaloyl chloride respectively in toluene solution at room temperature. As with phosgene, the color of living polystyrene was immediately discharged. The polymer solutions were boiled with water, filtered (to remove terephthalic acid), and then poured into methanol. Table III shows the molecular weights of the polymers before and after reaction with the acid chlorides.

No coupling occurred in these reactions. However, the polystyrene diacid chlorides prepared by these methods were not used for the prepara-

TABLE III
Reaction of α,ω-Dilithiopolystyrene with Acid Chlorides

Acid chloride	Concentration of living ends of polystyrene, mole/l. $\times 10^4$	Molecular wt of living polymer[a]	Molecular wt of polymer after reaction[a]
Terephthaloyl	2.88	69 400	68 100
Terephthaloyl	8.51	23 500	26 200[b]
Adipyl	2.99	66 900	55 900
Adipyl	5.88	34 000	34 000[c]

[a] Determined viscometrically.
[b] $\bar{M}_n$ by endgroup analysis = 13 100.
[c] $\bar{M}_n$ by endgroup analysis = 33 000.

tion of block copolymers because of the difficulties encountered in removing excess tipping reagents.

EXPERIMENTAL

All starting materials were purified and stored in a dry nitrogen atmosphere. All the experimental procedures involving these materials (except polymer precipitation and molecular weight determinations) were also conducted in dry nitrogen atmospheres. The nitrogen was purified by passing it through columns of manganous oxide and Lindé molecular sieves, type 4A. This procedure reduced the water content to 1 ppm and oxygen to < 2 ppm. The nitrogen was passed to the reaction vessels, etc., through thick-walled high-density polyethylene tubing.

Materials

Tetrahydrofuran (THF) was refluxed for 8 hr over molten potassium; the appearance of a red color on addition of a few drops of α-methylstyrene indicated the absence of impurities which could react with benzylic anions. The THF was then fractionally distilled and used within two days.

Toluene was refluxed over sodium then fractionally distilled. Cyclohexane (spectroscopic grade) was fractionally distilled. Styrene (inhibitor free) was stirred over Lindé molecular sieves for 8 hr, fractionally distilled at reduced pressure, and stored at $-10°C$. α-Methylstyrene was treated similarly. Pyridine was dried over molecular sieves before use.

Acetyl chloride and terephthaloyl chloride were fractionally distilled, the latter under reduced pressure. Adipyl chloride was synthesized from thionyl chloride and adipic acid, then doubly distilled. Phosgene from a cylinder was condensed at $-15°C$, purged with nitrogen for 1 hr to remove CO_2 and HCl and used within 2 hr.

Stilbene (BDH laboratory grade) was used as supplied. Sodium and lithium were freed of oxide layers and washed with toluene. The sodium was then dispersed in hot toluene and filtered off for use. Solutions of

dilithiostilbene (1:2 dilithio 1:2 diphenyl ethylene) were prepared by refluxing solutions of stilbene in THF over lithium turnings for 2 hr. Solutions of α,ω-disodio α-methylstyrene tetramer were prepared by reaction of α-methylstyrene in THF with a sodium dispersion at 0°C for 1 hr. Both of these metal alkyls were filtered (to remove excess metal) and standardized with aqueous hydrochloric acid.

sec-Butyllithium was supplied as a solution in n-heptane by Pfizer Ltd., it was filtered and standardized with aqueous hydrochloric acid.

Preparation of Living Polymers

The techniques used in preparing the "living" polystyrenes have been described previously.[6] Polystyrene molecular weights (unless otherwise stated) were calculated from intrinsic viscosities measured in benzene solution at 25°C by the equations of Krigbaum and Flory.[9]

References

1. C. H. Bamford and E. F. T. White, *Trans. Faraday Soc.*, **52**, 716 (1956).
2. E. B. Jones and C. S. Marvel, *J. Polym. Sci. A*, **2**, 5313 (1964).
3. G. Finaz, Y. Gallot, J. Parrod, and P. Rempp, *J. Polym. Sci.*, **58**, 1363 (1962).
4. J. C. Galin, P. Rempp, and J. Parrod, *Compt. Rend.*, **260**, 5558 (1965).
5. H. Schnell, *Chemistry and Physics of Polycarbonate*, Interscience, New York, 1962.
6. B. W. Brooks, *Chem. Commun.*, **1967**, 68.
7. S. H. Merrill, *J. Polym. Sci.*, **55**, 343 (1961).
8. T. G. Fox and P. J. Flory, *J. Polym. Sci.*, **14**, 315 (1954).
9. W. R. Krigbaum and P. J. Flory, *J. Polym. Sci.*, **11**, 37 (1953).

Polymers of 2-Vinyl-1,3-Dioxolanes

J. DAVID NORDSTROM,[*] *Ashland Chemical Company,*
Research Center, Bloomington, Minnesota 55420

Synopsis

Lewis acid-initiated polymerizations of 2-vinyl-1,3-dioxolanes have been studied. Evidence is presented showing at least three types of structural units in the polymer. Polymerization is propagated by 1,2 addition, by acetal ring opening, and by rearrangement, ring opening mechanisms. Polymerization is accompanied by the formation of a dimer consisting of a 1,4-dioxepane and 1,3-dioxolane ring. Film formers from methacrylate esters of vinyl dioxolane compounds are also described.

INTRODUCTION

This work was part of a program to prepare film formers which could be applied in liquid form and be cured without the loss of inert volatile materials (solvent). The materials under investigation were multifunctional so that crosslinked, chemically resistant films could be prepared.

A monomeric material with a vinyldioxolane portion and an acrylic ester portion (I) was prepolymerized with Lewis acids to a viscous liquid. This was convertible to a crosslinked, insoluble film by free-radical sources. The conversion was accomplished by heat or at room temperature under ultraviolet light radiation or with a redox initiator system.

I, R_2 = H, CH_3 II, R_3 = H, CH_3
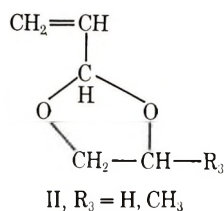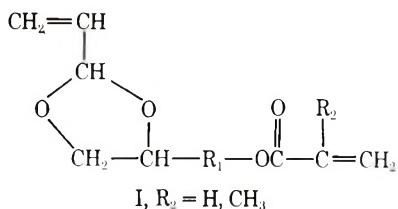
While attempting to optimize prepolymerization conditions, the cationic polymerization of model vinyldioxolanes were studied. During the course of the study an interesting phenomenon was discovered. The infrared spectrum of the polymerized material exhibited an absorption in the carbonyl region. This suggested the possibility of the rearrangement, ring opening polymerization shown in reaction (1). Recently, Tada et al.[1] published results of Lewis acid-initiated polymerization of 2-vinyl-1,3-

dioxolane (2VD) which showed evidence for this mechanism.   The present work shows a number of other interesting events occurring in this polymerization reaction, including ring-opening polymerization and dimer formation.

(1)
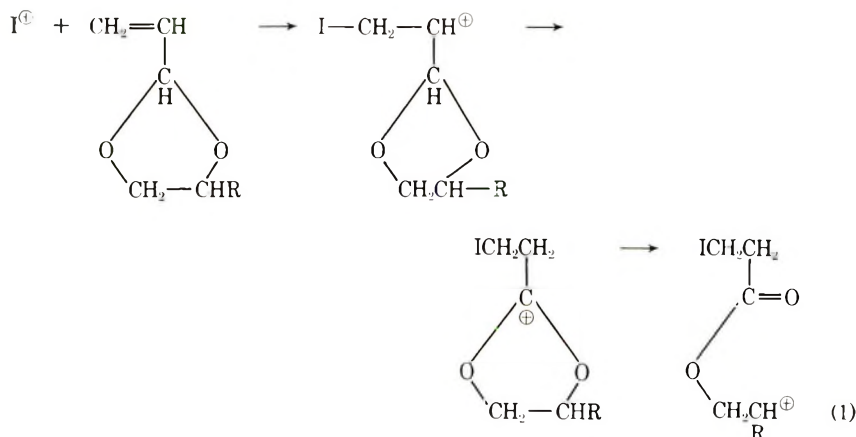
Two types of products are isolated from the reaction mixture.   A polymer of relatively high molecular weight is precipitated from aliphatic hydrocarbons and a liquid material containing a vinyldioxolane dimer is obtained from the precipitation solvent.

This report describes the film formation from the acrylate–dioxolanes, presents evidence for the structure of the dimer, and discusses the polymerization of 2-vinyldioxolanes and the polymer structure.

EXPERIMENTAL

The spectroscopic investigations were performed with a Perkin-Elmer Infracord infrared spectrometer and a Varian A60 NMR spectrometer. Elemental analysis were done with an F & M carbon–hydrogen–nitrogen analyzer (Model 185) and molecular weights with the Mechrolab vapor-pressure osmometer (Model 301A).

Synthesis of Cyclic Acetals

The vinyldioxolanes were all prepared according to the procedure of Fischer and Smith.[2]

Synthesis of Methacrylate Functional Vinyl Dioxolanes

The esters were prepared by transesterification of methyl methacrylate or methyl acrylate in the presence of sodium methoxide.[3]   The dioxolane containing alcohols used were 2-vinyl-4-(4-hydroxy butyl)-1,3-dioxolane, 2-vinyl-5-ethyl-5-hydroxymethyl-1,3-dioxane, 2 - vinyl- 4-hydroxymethyl-1,3-dioxolane, and 2-(1-propenyl)-4-(4-hydroxybutyl)-1,3-dioxolane.

Polymerization Procedure for Model Compounds

The monomers were distilled just prior to use and dried by chromatography through alumina. In the cases where methylene chloride was used as solvent, it was redistilled in glass at atmospheric pressure. The boron trifluoride etherate was redistilled prior to use. The monomer, cocatalyst, and solvent (if used) were sealed in a serum-capped bottle containing a magnetic stirrer. The solution was cooled at 0°C in an ice-water bath. The initiator was added dropwise with stirring over a 60-sec period. The solution was kept at 0°C for 30 min and then allowed to warm to room temperature. The mixture was stirred at room temperature overnight and then worked up. The initiator was inactivated by addition of a slight excess of 30% ammonium hydroxide. The solvent was removed by reduced pressure distillation and the polymer isolated by precipitation into hexane. After reprecipitation the polymer was dried under vacuum (1 mm Hg). The liquid product was isolated by reduced pressure distillation of the hexane solvent. The reactants, reaction conditions, yields, and molecular weights of products are shown in Table I.

Polymerization of Methacrylate-Functional Vinyldioxolane

4-(4'-Methacryloxybutyl)-2-vinyl-1,3-dioxolane I [R_1=(CH$_2$)$_4$-, R_2=CH$_3$] was treated as described above. Boron trifluoride etherate (2 wt-%) was added to the neat monomer containing 2 wt-% hydroquinone. The product was worked up by dissolving it in benzene and washing with 10% sodium hydroxide solution and then saturated brine. After drying the benzene solution over MgSO$_4$, the benzene was stripped, leaving a light yellow syrup having a viscosity of 2.5 S.

Film Formation from Polymer of I

To 10 g of the resinous product described above was added 0.083 g cobalt naphthenate and 0.10 g of methyl ethyl ketone peroxides. A 0.003-in. thick film was drawn on glass plate by a doctor blade. The film was nontacky after 6 hr and resistant to attack by methyl ethyl ketone after 24 hr. The Sward hardness was 60.

Isolation of the Dimers

The liquid product from the polymerization of 2-vinyl-4-methyldioxolane was distilled under reduced pressure; 58% of the material distilled at 115–132°C at 0.01 mm Hg. The residue was solid at room temperature but still soluble in acetone.

The distillate exhibited the following infrared absorptions: 3070, 1640 cm⁻¹ (weak, C=C); 2960, 2920, 2860 cm⁻¹ (strong, C—H); 1460, 1370 cm⁻¹ (strong, C—H); 1410, 930 cm⁻¹ (medium, C=C); 1165, 1090 cm⁻¹ (strong, C—O—C).

The molecular weight (Mechrolab vapor-phase osometer, benzene solvent) was 232. (Calculated molecular for $C_{12}H_{20}O_4$ is 228.)

TABLE I

Polymerization of 2-vinyl-1,3-cyclic Acetals

Run	Monomer[a]	Catalyst	Catalyst, %	Temp, °C	Cocat-alyst[b]	Cocatalyst Catalyst	Polymer yield, %	Molecular wt	Yield dimer fraction, %	Molecular wt	Comments
N	2V4MD	$BF_3 \cdot Et_2O$	2	−78	—	—	0.2	—	5.3	—	—
T	2V4MD	$BF_3 \cdot Et_2O$	2	25	—	—	2.9	—	32.8	287	
O	2V4MD	$BF_3 \cdot Et_2O$	2	−78	H_2O	1	0.1	—	5.3	—	
S	2V4MD	$BF_3 \cdot Et_2O$	2	25	H_2O	1	10.3	4752	42.3	332	
C	2V4MD	$BF_3 \cdot Et_2O$	2	25	H_2O	2.3	20.2	3200	42.0	339	
E	2V4MD	$BF_3 \cdot Et_2O$	2	25	H_2O	3.9	24.5	2870	46.8	—	
H	2V4MD	$BF_3 \cdot Et_2O$	2	25	C_2H_5OH	1	6.2	—	34.0	—	
V	2V4MD	$BF_3 \cdot Et_2O$	0.5	25	HQ	1	4.2	4320	18.8	324	
W	2V4MD	$BF_3 \cdot Et_2O$	1.0	25	HQ	1	8.8	5110	21.9	—	
K	2V4MD	$BF_3 \cdot Et_2O$	2.0	25	HQ	1	18.0	4838	25.7	—	
X	2V4MD	$BF_3 \cdot Et_2O$	5.0	25	HQ	1	18.5	3740	33.8	—	59 wt-% CH_2Cl_2
AA	2V4MD	$BF_3 \cdot Et_2O$	2.0	25	HQ	1	13.7	3870	34.8	—	
AC	2V4MD	$BF_3 \cdot Et_2O$	2.0	25	HQ	1	8.7	2712	36.0	—	81 wt-% CH_2Cl_2
AH	2V4MD	$SnCl_4$	2.0	25	HQ	1	5.0	—	5.0	—	
BA	2VD	$BF_3 \cdot Et_2O$	2.0	25	HQ	1	Insol.	—	—	—	
BB	2VD	$BF_3 \cdot Et_2O$	2.0	25	None	—	Insol.	—	—	—	
BC	2VD	$BF_3 \cdot Et_2O$	2.0	−78	None	—	26	—	5	—	63 wt-% CH_2Cl_2
BD	2VD	$BF_3 \cdot Et_2O$	2.0	−78	HQ	1	21	—	3	—	63 wt-% CH_2Cl_2
BE	2VD	$BF_3 \cdot Et_2O$	2.0	25	HQ	1	51	2280	21	—	63 wt-% CH_2Cl_2
CA	2V DOX	$BF_3 \cdot Et_2O$	2.0	25	HQ	1	50	—	10	—	67 wt-% CH_2Cl_2

[a] 2V4MD = 2-vinyl-4-methyl-1,3-dioxolane; 2VD = 2-vinyl-1,3-dioxolane; 2V DOX = 2-vinyl-1,3-dioxane.

[b] HQ = hydroquinone.

TABLE II
Nuclear Magnetic Resonance Absorptions

Absorption (vs. TMS), ppm	Description	Relative area, %	Assignment
1.15	double triplet	30	C—CH₃ of dioxolane and dioxepane rings
1.95	multiplet	5	C—CH—C of dioxepane
3.0–4.5	many overlapping patterns	45	O—CH—C in both rings
4.95	singlet	5	vinyl hydrogen
5.1	doublet	5	O—CH—O in dioxolane
5.4	singlet	5	vinyl hydrogen
5.6–6.4	octet	5	vinyl hydrogen

Elemental analysis showed C = 63.37% and H = 8.97%. (Calculated values for $C_{12}H_{20}O_4$ are C = 63.11%, H = 8.83%.)

Nuclear magnetic resonance absorptions as determined on a (Varian A-60) are listed in Table II.

Distillation of the liquid product from 2-vinyl-1,3-dioxolane polymerization gave 75% recovery of a liquid distillate (bp 80–83°C/0.1 mm Hg). The molecular weight was 207 (calcd for $C_{10}H_{16}O_4$ = 200). Elemental analysis showed C = 59.40%, H = 7.74% (calcd for $C_{10}H_{16}O_4$: C = 59.99%, H = 8.05%). The features of the infrared and nuclear magnetic resonance spectra were similar to those of the 2-vinyl-4-methyl-1,3-dioxolane dimer except for the methyl group features.

RESULTS

Film Formation from Difunctional Materials

Early work resulted in a wide variance in viscosity when the methacrylate-dioxolanes were treated with boron trifluoride etherate. It was discovered that hydroquinone, used as an inhibitor in synthesis, codistilled with the monomer and acted as a cocatalyst for the cationic polymerization. Controlled levels of this or other hydrogen donating cocatalysts resulted in reproducible viscosities.

Several methods were used to convert the methacrylate functional prepolymers to crosslinked films. The use of a peroxide–metal redox system at room temperature resulted in films which were nontacky after several hours and resistant to solvent attack after one day. The films developed Sward hardnesses of 50–70. Puddles of ketonic solvents standing on the fully cured films for several hours did not soften the film surface. Weight loss measurements on the films at room temperature during cure showed that a minimum of 93% of the original weight was reached after 30 min and then a small weight increase occurred. Peroxide development upon vinyl dioxolanes have been described,[4] and this is likely an important process in the development of a hard surface.

Polymerization of the Model Compounds

Table I shows the results of a variety of conditions for the polymerization of 2-vinyl-4-methyl-1,3-dioxolane (2V4MD). The effects of initiator levels and cocatalyst concentrations are those expected for a chain process. The presence of a hydrogen-donating cocatalyst is necessary for significant conversion of monomer to product. Hydroquinone was especially convenient, since it is easily handled and weighed in small quantities. It was valuable in the methacrylate functional dioxolane polymerization, as it prevented premature gelation during polymerization and storage. Polymerizations attempted at 35°C or higher resulted in runaway polymerizations and yielded insoluble products. The polymerization described in Table I had to be cooled in an ice bath for the initial 30 min due to an exothermic reaction when the initiator was added.

The unsubstituted 2-vinyl-1,3-dioxolane (2VD) was more reactive toward $BF_3 \cdot Et_2O$-initiated polymerization, requiring the presence of cocatalyst and solvent to moderate the reaction so that soluble polymer was obtained. A higher ratio of polymer to dimer resulted from the polymerization of 2-VD.

Other Cyclic Acetals

Attempts to polymerize 4-methyl-1,3-dioxolane and 2-ethyl-4-methyl-1,3-dioxolane under conditions which cause 2V4MD and 2VD to polymerize resulted in no polymer or dimer. The dimethyl acetal of acrolein gave no nonvolatile products under these polymerization conditions. Both type of reactive species, cyclic acetal and vinyl unsaturation, appear to be necessary for polymerization to occur.

2-Vinyl-1,3-dioxane (2VDOX) was polymerized in a similar manner. A vigorous exotherm occurred, and slow initiator addition to a cold solution was necessary to prevent local gel formation. A low molecular weight product was isolated from the dioxane polymerization which was very similar to the dimer from the dioxolanes, but it was not characterized.

Characterization of the Dimer

In every case where polymerization occurred, a low molecular weight material was isolated by removing the precipitable polymer. The molecular weight of the liquid product from 2V4MD was always in the 280–340 range. Gas chromatography showed that the major portion was a single compound. Upon vacuum distillation about 60% was recovered and was shown to be a single compound by gas chromatography. The compound was identified as III by elemental analysis, molecular weight and nuclear magnetic resonance. The position of the methyl group on the dioxepane ring of III has not been established. Distillation of the liquid product of 2VD polymerization gave 75% yield of product IV. The elemental analysis, nuclear magnetic resonance spectrum, and molecular weight established the structure of IV. The position of the dioxolane substituent on the

III   IV
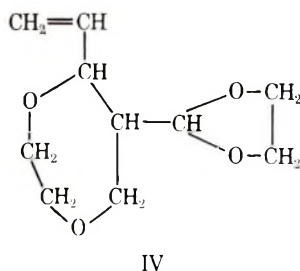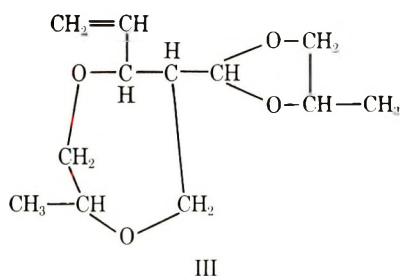
dioxepane ring is shown by the presence of just one proton in the 2 ppm region of the NMR spectra of the two compounds.

Compound III was refluxed in methanol for 72 hr with a trace of acid catalyst, and the new compound isolated was the dimethyl acetal of III (identification by nuclear magnetic resonance).

Rearrangement Polymerization

Saponification of four separate polymers of 2V4MD in $1N$ methanolic potassium hydroxide indicated ester equivalent weights of 1 200–1 400. Apparently 8–10% of the units are the result of the rearrangement, ring-opening mechanism outlined by Tada et al.[1]

DISCUSSION

The study of the polymerization of model vinyldioxolanes show that the methacrylate functional syrups produced by the cationic polymerization of type I compounds are mixtures of monomer, dimer, and higher molecular weight species.   The monomer and dimer are capable of participation in the free-radical crosslinking of the polymer and provide the fluidity necessary for making films under ambient conditions.

TABLE III
Relative Nuclear Magnetic Resonance Absorption of Vinyl Dioxolane Polymers

| Polymer	0–3.0 ppm	3.0–4.5 ppm	4.5 ppm
C—CH$_2$—CH—C $\quad$C O H O CH$_2$—CH—CH$_3$	0.60	0.30	0.10
Run S	0.53	0.36	0.11
C—CH$_2$—CH—C $\quad$C O H O CH$_2$—CH$_2$	0.375	0.50	0.125
Run BE	0.26	0.59	0.15

The isolated polymers of 2V4MD and 2VD have been studied by nuclear magnetic resonance and apparently are not simply 1,2-addition polymers with a few units resulting from the rearrangement ring opening mechanism. The fact that neither noncyclic vinyl acetals or dioxolanes without the 2-vinyl group undergo significant polymerization under the conditions described above indicates that the propagation steps must involve both the vinyl group and the cyclic acetal portion. Previous reports indicate that 2-substituted dioxolanes will not undergo cationic polymerization.[5,6]

Table III compares the absorption regions of the nuclear magnetic resonance spectra of the 2VD and 2V4MD polymers with theoretical absorptions if 1,2-addition were the sole propagating mechanism. Units of the

type $-C-\overset{\overset{\displaystyle H}{|}}{C}-C$ or $C-CH_3$ will absorb in the 0–3 ppm range, those with

$-O-\overset{\overset{\displaystyle H}{|}}{C}-C-$ units in the 3–4.5 ppm region, and protons on unsaturated carbons or acetal protons absorb higher than 4.5 ppm. Studies of model compounds verify these assumptions. The spectra of the 2V4MD polymer exhibits a large C-methyl absorption at 1.3 ppm, a low broad absorption peaked at 1.7 ppm, two broad maxima centered at 3.5 and 4.05 ppm, a small broad absorption at 5.05 ppm, and very weak absorption features of the vinyl group in the 5.2–6.3 ppm region. The noteable features are the increased absorption in the 3–4.5 ppm region with an accompanying decrease in the 0–3 ppm region. There is an increase in absorptions above 4.5 ppm. The rearrangement mechanism [reaction (1)] does not explain these features since that propagation step would yield a repeating unit with increased absorption in the 0–3 ppm region.

The increased absorption in the 3–4.5 ppm region indicates more ether-like structure in the polymer. The new absorption appears primarily at 3.5 ppm. This is the region where poly(ethylene oxide) shows strong absorption. The infrared spectra of the polymers exhibit a larger, broader absorption than do the monomers in the C—O—C region (1 100 cm^{-1}). This evidence supports a propagation mechanism involving ring opening as well as 1,2 vinyl addition polymerization. Electrophilic attack of the propagating species on an acetal oxygen would produce a species of carbonium ion, stabilized by resonance into the vinyl portion and by the neighboring oxygen. Okada[5] reported evidence for bond scission between the O—C$_2$ bond in the polymerization of unsubstituted cyclic acetals.
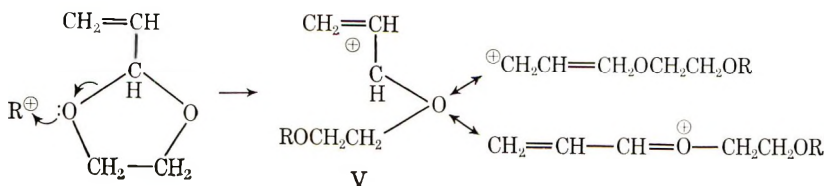
The intermediate species V would be capable of propagating the polymerization through a vinyl group or ring oxygen of another monomer. This unit introduces unsaturation onto the polymer backbone and replaces a carbon-carbon backbone unit of the 1,2 vinyl polymer with an oxygen-carbon-containing backbone unit. Units from ring opening polymerization would increase the nuclear magnetic resonance absorption in the 3.0–4.5 ppm regions. This evidence along with that of Tada et al. supports the presence of at least three types of repeating units in the backbone. A polymer of structure VI, with 70% of x units,
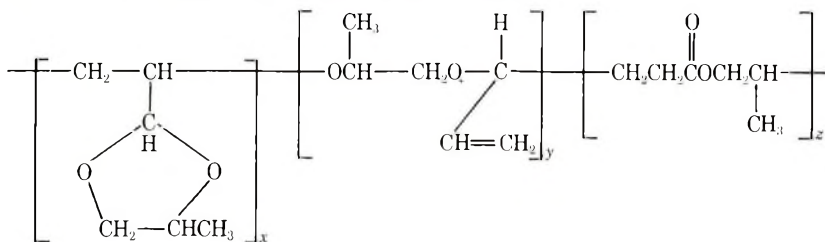
VI

20% y units, and 10% z units, would have a ratio of NMR absorptions in the three regions discussed above of 0.54: 0.33:0.13 compared to the actual ratio of 0.53: 0.36: 0.11 (Table III). Tada presented quantitative evidence for the amount of glycol produced by acid hydrolysis of the polymer. Both units, x and y, would yield glycol, and only unit z would be a non-glycol-producing unit.

Dimers and other low molecular weight species are often isolated in cationic polymerizations of cyclic ethers and acetals and in copolymers of vinyl compounds with cyclic ethers.[7–10] Much evidence has been presented to describe their formation by a depolymerization or back-biting mechanism. If a dimer of structure III were to be produced by back-biting, the unit involved must be one introduced by a 1,2 addition mechanism where the α carbon was the entering position. Tada could find no evidence for
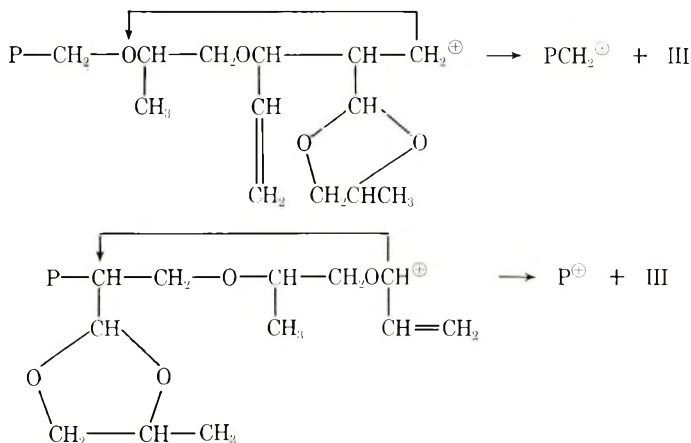
attack at the α carbon during chain propagation. This attack would probably introduce C—CH$_3$ groups by isomerization or in the rearrangement ring opening step. There is no absorption in the C—CH$_3$ region of the nuclear magnetic resonance spectrum of the 2VD polymer.

It seems more likely that the dimer is formed by a direct process of some type. Dietrich et al.[9] showed that dimers were formed directly in the copolymerization of dioxolane and chloral. If dimer formation is in competition with polymerization, then more dimer should form from a monomer which polymerizes with difficulty. Table I shows that dimer formation is considerably more prevalent with 2V4MD than with the 2VD monomer. Prior studies[5,6] indicated that 4-substituted dioxolanes do not polymerize as well as unsubstituted dioxolanes due to steric hindrance.

The processes occurring in the cationic polymerization of vinyldioxolanes are complicated. Besides the variety of reaction steps that can occur in ionic polymerizations of simple materials, the multiplicity of propagation steps with this type of monomer makes a very complex process.

References

1. K. Tada, T. Saegusa, and J. Furakawa, *Makromol. Chem.*, **95**, 168 (1966).

2. R. F. Fischer and C. W. Smith, *J. Org. Chem.*, **25**, 319 (1960).

3. J. D. Nordstrom (to Archer-Daniels-Midland Company), U. S. Pat. 3,291,860 (1965).

4. C. K. Ikeda, R. A. Braun, and B. E. Sorenson, *J. Org. Chem.*, **29**, 287 (1964).

5. M. Okada, Y. Yamashita, and Y. Ishii, *Makromol. Chem.*, **80**, 196 (1964).

6. T. Kugiya, M. Hatta, T. Shimizu, and K. Fukeii, *Kogyo Kagaku Zasshi*, **66**, 1890 (1963).

7. D. J. Worsfold and A. M. Eastham, *J. Amer. Chem. Soc.*, **79**, 900 (1957).

8. T. Miki, T. Higashimura, and S. Okamura, *J. Polym. Sci. B*, **5**, 583 (1967).

9. H. J. Dietrich, J. V. Karabinos, and M. C. Raes, *J. Polym. Sci. A-1*, **5**, 1395 (1967).

10. V. Jaacks, *Makromol. Chem.*, **101**, 33 (1967).

Graft Polymerization of Styrene on Lithiated Poly(2,6-Dimethyl-1,4-Phenylene Ether)

A. J. CHALK and T. J. HOOGEBOOM, *General Electric Research and Development Center, Schenectady, New York 12301*

Synopsis

Styrene has been grafted onto poly(2,6-dimethyl-1,4-phenylene ether) (I) with the use of lithiated I as an initiator. In benzene solution, solvent metalation resulted in some polystyrene homopolymer. In tetrahydrofuran, however, only graft copolymer was formed. By forming a derivative with trimethylchlorosilane and examining by NMR, it was possible to establish the proportion of lithium scavenged by impurities, the amount of polymeric lithium which reacted with styrene, and the amount which did not. The chain length of the grafted polystyrene was also calculated. No cross-linking was found, except where a high ratio of lithium to styrene resulted in some unreacted ring-metalated polymer. In this case only, reaction with trimethylchlorosilane causes some crosslinking.

INTRODUCTION

Earlier papers describe the direct metalation of poly(2,6-dimethyl-1,4-phenylene ether) (I) with alkali metals and its use for the synthesis of graft copolymers by reaction with vinyl monomers.[1,2] This paper in the series reports the results obtained in further investigating the graft polymerization of styrene onto lithiated I and the synthesis of graft copolymers of controlled dimensions.

Anionic polymerization offers one of the most versatile methods of polymer synthesis. It allows the formation of living polymers capable of building successive blocks, and the carbanions are capable of undergoing all the varied reactions of Grignard or organolithium reagents. Correspondingly the use of polymeric polyanions offers one of the most versatile methods of graft polymer synthesis. In a clean system, the ratio of the monomer concentration to the number of metalated sites directly determines the chain length of the grafted polymer, and this fact may be checked by terminating the reaction with a suitable marker such as trimethylchlorosilane. Trimethylsilyl groups are readily identified by NMR which provides a sensitive measure of their concentration and chemical environment.[1,2]

Reviews on block and graft copolymerization[3–7] reveal that anionic graft polymerization has, however, received little attention. A number of papers have recently appeared on the subject,[8–16] but the systems used have

suffered from a variety of problems,[8] including chain scission during metalation[13,14] and crosslinking.[12,15] On the contrary, the metalation of I can be accomplished without chain scission or crosslinking.[1,2] The reaction of lithiated I with trimethylchlorosilane can result in crosslinking, but this appears to be related to the presence of ring-metalated sites[2] which would not be present if completely reacted with a monomer such as styrene.

The choice of solvent is an important consideration, since even though butyllithium may have completely disappeared by reaction with I, solvent metalation can still give species capable of initiating styrene homopolymerization. For this reason, results in benzene and tetrahydrofuran are discussed separately.

EXPERIMENTAL

Materials

The materials are described in the previous paper.[2] The styrene was stirred overnight with calcium hydride and distilled *in vacuo* immediately prior to use.

Graft Polymerization of Styrene

Lithiated I was prepared with butyllithium as described previously[2] with the use of solvents degassed under nitrogen. Unless otherwise noted, I was left 1 hr at room temperature after addition of butyllithium to ensure complete reaction before adding styrene. Styrene addition was made at room temperature when benzene was employed as solvent and at $-40°C$ when tetrahydrofuran was used as a solvent. After varying times, the reaction was terminated with methanol or trimethylchlorosilane, the polymer recovered by precipitation in methanol, and dried *in vacuo* at 70°C for 18 hr.

Samples were examined by NMR (Varian A60 CDCl$_3$ solution, dioxane standard), gel-permeation chromatography, automatic osmometer (Hallikainen model 1361), capillary viscometer, and light-scattering photometer (Brice-Phoenix). Except for NMR, all measurements were made in benzene solution.

Determination of the Ratio of Polystyrene to I

The NMR spectra of polystyrene and (I) overlap in both the aromatic and aliphatic regions (see Fig. 2). For this reason, the only ratio of areas which can be obtained accurately is R (total aromatic/total aliphatic) = $5n + 2m/3n + 6m$, where n/m = molar ratio of polystyrene/I. Unfortunately, a 5% error in R results in a 15% error in n/m.

A somewhat more accurate determination can be made from infrared measurements by using a band at 695 cm^{-1} in polystyrene and a band at 1185 cm^{-1} in I.[17]

RESULTS AND DISCUSSION

On adding styrene to the lithiated polymer, the deep red color of the styryl anion was observed. The polymerization was accompanied by a noticeable exotherm and increase in viscosity. At the higher concentrations of lithium, the metalated polymer precipitates from solution to some extent,[2] so that the styrene polymerization becomes a heterogeneous reaction. In Table I samples 1, 2, and 3 gave homogeneous polymerizations

TABLE I
Effect of Varying the Amount of Lithium (Solvent Benzene)

Sample	Yield, %	[Li]/[I] (added), mole BuLi/120 g I[a]	[Polystyrene]/[I] (found), mole/ mole monomer[b]	Molecular weight[c]	
				Graft	Homopolymer
1	55	0.05	0.26	10^4	None
2	85	0.10	0.68	10^4	5000
3	86	0.20	0.88	10^4	2000
4	86	0.50	1.03	10^4	None
5	80	1.0	0.78	10^4	5000

[a] Initial values.

[b] Determined by NMR, added ratio = 1.0.

[c] Maximum in gel-permeation chromatograph. These compare to a value of 40,000 found for initial I.

(benzene solvent). When tetrahydrofuran was used as solvent, somewhat higher levels of lithium could be used in a homogeneous system (samples 22–31). The results will be discussed in terms of the solvent used.

Benzene Solution

The formation of graft copolymers was clearly shown by the molecular weight distribution curves obtained from gel-permeation chromatography.* Figure 1 shows a typical curve revealing the presence of both styrene homopolymer and graft copolymer. Styrene homopolymer presumably resulted from solvent metalation to form phenyllithium.[2] The styrene homopolymer usually coprecipitated with the graft copolymer except when large ratios of lithium to styrene were used. In such cases the molecular weight of the polystyrene was often low enough for it to remain in solution in the precipitating solvent. No unreacted I was found.

The amount of polystyrene homopolymer cannot be obtained accurately from gel-permeation chromatographs such as Figure 1, since the different fractions vary in composition and structure. Further, the abscissa is not

* Maxima in gel-permeation chromatograms (GPC) occur at approximately M_w for the most probable distribution of linear polymers ($M_w/M_n = 2$).[18] The GPC appearance volumes depend on the hydrodynamic volumes of the polymer molecules.[19,20] For graft copolymers of the type discussed here, maxima should occur at molecular weights somewhat lower than $\overline{M}_w$, since the masses of the molecules are increased by grafting without a proportional increase in the hydrodynamic volumes (see Table VI).
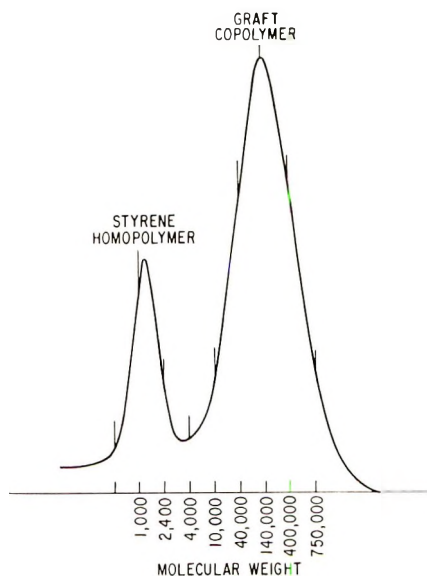
Fig. 1. Styrene polymerization on lithiated I. Formation of styrene homopolymer with benzene as solvent.

linear in log molecular weight. In spite of this the areas were found to be approximately proportional to weight fractions partly because of the similar refractive indices for (I) and polystyrene. The amount of styrene which grafted onto (I) was generally in excess of 50%.

Table I shows the effect of varying the amount of butyllithium used. All samples were left one hour at room temperature after addition of styrene before quenching with methanol. Although graft polymerization occurred in all cases, the low values of the ratio of polystyrene to I for

TABLE II
Effect of Varying the Time of Styrene Polymerization (Benzene Solvent)

Sample	Time, min[a]	Yield, %	[Li]/[I] (added)	[Styrene]/[I] (Added)	(Found)	Molecular weight Graft	Molecular weight Homo-polymer
6	0.08	37	0.1	2.0	<0.1	100000	None
7	1	39	0.1	2.0	<0.1	100000	None
8	2	40	0.1	2.0	0.07	100000	None
9	10	55	0.1	2.0	0.6	100000	2200
10	20	80	0.1	2.0	1.3	100000	5000
11	60	85	0.1	2.0	2.3	110000	8000
12	120	91	0.1	2.0	2.5	110000	9000
13	180	98	0.1	2.0	2.0	110000	9000
14	480	96	0.1	2.0	2.6	130000	10000
15	4320	96	0.1	2.0	2.1	130000	8500

[a] Time allowed for the styrene to react with lithiated polymer before quenching with trimethylchlorosilane.
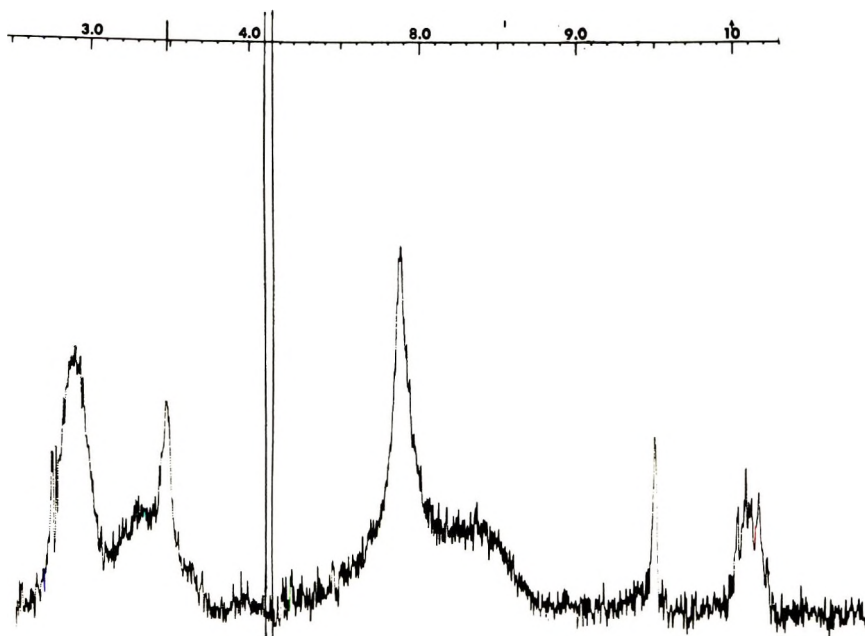
Fig. 2. NMR of I-Polystyrene graft copolymer (sample 19).

samples 1 and 2 indicated incomplete reaction. The amount of lithium was then kept constant, and the length of time allowed for the styrene polymerization varied (Table II). Here several factors can be used to judge completion of reaction, namely a high yield, a constant maximum value for the molecular weights, or the ratio of polystyrene to I found.

When the styrene polymerization was terminated by trimethylchlorosilane, information was obtained both on the amount of lithium and whether or not it initiated polymerization. Figure 2 shows relevant parts of the NMR spectrum of sample 19, Table III, which was typical of samples 17–21. Absorption at 9.53τ is typical of I substituted on the ring position with $Si(CH_3)_3$.[2] A broad absorption from 10.06 to 10.27τ was similar to that found for low molecular weight polystyrene terminated with trimethylchlorosilane (10.13–10.27τ). Unfortunately the latter absorption is contiguous to the value expected for $Si(CH_3)_3$ on the side chain of I (10.05τ).[2] This makes it difficult to know whether such an absorption is present. However, the bulk of the absorption from 10.06 to 10.27τ would seem to be due to $Si(CH_3)_3$ on polystyrene. From the areas of these two absorptions, the corresponding amounts of silicon were calculated and expressed as a percentage of the amount of butyllithium added (Table III). Included in Table III are data for sample 16, which gives the values expected at 9.53 and 10.05τ for I in the absence of styrene. These values are the average for a number of samples.[2] From the values at 9.53τ it is apparent that a considerable amount (generally $> 50\%$) of the lithium on the ring position of I, initiated styrene polymerization. If $Si(CH_3)_3$ substituted on

TABLE III
Identification of Lithium on Graft Copolymer by Trimethylchlorosilane
Quench (Benzene Solvent)

Sample	Time, min	[Styrene]/[I]		Si found, %[a]	
		Added	Found	9.53 τ	10.06–10.27 τ
16	0	0		48[b]	28[b]
17	10	2	2.1	30	48
18	20	2	2.0	30	48
19	30	2	1.8	16	38
20	40	2	1.6	18	38
21	60	2	1.9	12	42
6	0.08	2	<0.1	8	12
7	1	2	<0.1	16	14
8	2	2	0.07	8	16
9	10	2	0.6	4	16
15	4320	2	2.1	0	40

[a] 100% would correspond to the amount of butyllithium added, which for samples 16–21 was 1 mole per 2 equivalents of I (240 g) and for samples 6–15 was 1 mole per 10 equivalents of I.

[b] These are the values expected for I at 9.53 and 10.05 τ in the absence of any styrene (for 1 mole butyllithium per 240 g I).

the methyl group of I is assumed to absorb only at 10.05 τ, it can also be said that a considerable amount of the lithium in this position also initiated styrene polymerization. The absorption corresponding to low molecular weight polystyrene (10.06–10.27 τ) includes a fraction due to styrene homopolymer. The homopolymer was removed experimentally in some cases by reprecipitation of the graft copolymer in octane. The NMR spectra of the resulting pure graft copolymers gave slightly lower values than those in the fourth and sixth columns of Table III. The shape and range of the absorptions from 10.06 to 10.27 τ were unchanged, however, showing that these truly represented $Si(CH_3)_3$ on grafted polystyrene.

At the low level of butyllithium used in Table II the $Si(CH_3)_3$ absorptions were so weak that they were only clearly evident in some cases. These are included in the latter half of Table III. Styrene polymerization was slow in this case but appears to be complete for sample 15, since it had the expected [polystyrene]/[I] ratio. It showed only a single absorption at 10.06 τ in the $Si(CH_3)_3$ region. This was accordingly attributed to silicon at the end of a longer polystyrene chain than was present in samples 17–21.

From the results of Table III it appears that it is possible to react all the lithium on I with styrene only if the amount of lithium is quite small, at least in comparison to the amount of styrene.

An average value for the chain length of the polystyrene present as both homopolymer and graft copolymer was obtained by assuming the sixth column of Table III represented only lithium at the end of polystyrene chains. The corresponding molecular weights agree quite well with molecular weight values for the homopolymer obtained from gel-permeation

TABLE IV
Molecular Weights

Sample	Graft (I–polystyrene)[a]	Molecular weight Polystyrene homopolymer[a]	Polystyrene (average)[b]
17	80000	1050	910
18	80000	1000	940
19	80000	1020	960
20	80000	1100	870
21	80000	1030	920
9	100000	2200	3900
15	130000	8500	5300

[a] From gel-permeation chromatography (GPC).
[b] Calculated average value for homopolymer and graft (see text).

chromatography (Table IV). To a first approximation then it appears that the polystyrene grows to a similar length regardless of whether it is initiated by lithium on I or phenyllithium. Table IV also includes data for the two samples (9 and 15) where a smaller amount of butyllithium was used, resulting in higher molecular weights.

Tetrahydrofuran Solution

No homopolymer was found in any of the samples. Presumably this is due to further reaction of the metalated tetrahydrofuran to produce lithium alkoxides incapable of initiating styrene polymerization.

Table V gives the results for varying polymerization times for two butyllithium concentrations. Figure 3 shows the relevant parts of the NMR spectrum of sample 27. As in the earlier results, there were NMR absorptions at both 9.53τ and 10.06–10.27τ. As before, in the absence of styrene, one would expect absorptions at 9.53 and 10.05τ with areas in the approximate ratio $2/1$. Clearly with these large amounts of lithium on the polymer, the styrene polymerization in tetrahydrofuran is so fast,

TABLE V
Polymerization of Styrene on Lithiated I in Tetrahydrofuran

Sample	Time, min	Yield, %	[Styrene]/[I] Added	[Styrene]/[I] Found[a]	Si found, %[b] 9.53 τ	Si found, %[b] 10.06–10.27 τ	Mol. wt. of graft
22	2	27	2	2.4	33	22	150000
23	5	42	2	2.5	35	28	170000
24	10	84	2	3.8	36	29	160000
25	60	90	2	2.3	35	29	100000
26	10	38	2	2.5	32	18	100000
27	60	36	2	2.1	34	18	130000

[a] Calculated from infrared measurements.
[b] 100% corresponds to the amount of butyllithium added, which for samples 22–25 was 0.4 mole per equivalent of I and for samples 26 and 27 was 1.0 moles per equivalent of I.

TABLE VI
Polymerization of Styrene on (I) Lithiated to Various Extents (Tetrahydrofuran Solvent)[a]

Sample	Yield, %	[Styrene]/[I] found[b]	[Li]/[I], mole Li/120 g I		Found[c]		Molecular weight × 10⁻³			[η][g]
			Added	9.53τ	$10.06\text{-}10.27 \tau$	From GPC maximum[d]	From light scattering[e]	Osmometric[f]	
28	76	2.9	0.1	0	0.062	140	238	60	0.59
29	73	2.5	0.1			120	222	51	0.61
30	79	2.6	0.2	0	0.141	100	191	49.2	0.53
31	85	2.5	0.2			100	180	46	0.54
32	55	2.9	1.0	0.23	0.36	110[h]	2470	50	0.67
33	86	2.5	1.0			100	206	47.7	0.50

[a] Styrene polymerization was terminated after 18 hours, samples 28, 30 and 32 with trimethylchlorosilane, samples 29, 31 and 33 with methanol.

[b] Added ratio 2·1. Results from NMR measurements.

[c] From NMR measurements on silylated polymer.

[d] Molecular weight corresponding to maximum in the gel-permeation chromatograph. (These values correspond to a value of 40000 for I.)

[e] M_w from light scattering (chloroform) (I had a value of 37200).

[f] M_n from osmotic measurements in chloroform (I had a value of 18500).

[g] Intrinsic viscosity in chloroform (I had a value of 0.50).
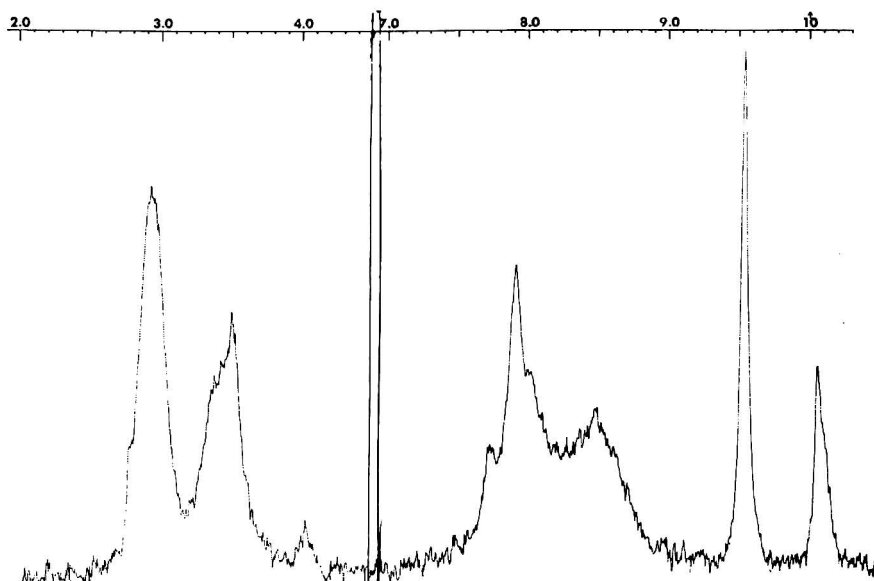
[h] Shoulder at 2×10^6.

Fig. 3. NMR of I-Polystyrene graft copolymer (sample 27).

even at −40°C, that much of the lithium on the ring position remains unreacted.

Table VI shows some results of varying the lithium concentration for a constant ratio of the two polymers. The length of time allowed for styrene polymerization was 18 hr to ensure complete reaction at the lower lithium concentrations. Surprisingly, even at the higher concentrations a much higher fraction of the lithium turned up at the end of polystyrene chains (e.g., samples 30 and 32). This would seem to indicate a slow polystyrene depolymerization followed by reaction with metalated sites on I. At the lowest levels of butyllithium, e.g., [Li]/[I] = 0.02, no polymerization took place. This probably resulted from a scavenging of such small amounts of butyllithium rather than slowness of reaction. At the lower concentrations of butyllithium, a trimethylsilyl absorption appeared only at 10.06 τ; this was attributed to silicon on polystyrene. From these values a polystyrene chain length was calculated and assumed to be correct

TABLE VII
Variation of T_g with Polystyrene Chain Length

| Sample | Chain length[a] | T_g (from DSC), °C | |
		At 40°C/min	At 80°C/min
29	46	122.1	123.6
31	18	121.9	123.4
33	8	121.8	122.3

[a] Calculated from the ratio of styrene found to lithium found on polystyrene for the trimethylchlorosilane terminated samples.

also for the corresponding methanol terminated samples which were assumed to be identical except for the lack of a silicon end group. The latter samples (29, 31, and 33) thus had identical I/polystyrene compositions and varied only in the number and chain length of the polystyrene grafts. They were examined by differential scanning calorimetry (DSC); the results are reported in Table VII.

The effect of increasing the number of chain ends is seen to result in a decreasing value of T_g, but the effect is small. All the samples have significantly lower values of T_g than a physical mixture of high molecular weight polystyrene with I of the same composition ($T_g = 126°C$).[21]

No crosslinking was found except for sample 32, a sample where ring-metalated I was terminated by trimethylchlorosilane. This confirms earlier evidence that crosslinking is associated with these two factors. The crosslinking is clearly evident from the reduced yield and the molecular weights from GPC and light scattering for this sample. The values for $\overline{M}_n$ and $\overline{M}_w$ for the grafts agree quite well with the expected values for a mole ratio of polystyrene/I of 2.5 [$\overline{M}_n = 18\,500 + 2.5(104/120) = 58\,500$].

In conclusion it may be said that the results confirm that the system is capable of "tailor-making" graft copolymers if allowance is made for the amount of lithium lost due to solvent metalation. Measurement of the average chain length is possible by forming a derivative with a suitable reagent. A limitation here is the sensitivity with which the trimethylsilyl group can be detected. The range over which chain lengths can be usefully measured could doubtless be increased by more sensitive techniques, e.g., by using computer methods to eliminate NMR background noise (CAT).

Details concerning the synthesis of a wide variety of other graft copolymers will be reported in a subsequent paper.

References

1. A. S. Hay and A. J. Chalk, *J. Polym. Sci. B*, **6**, 105 (1968).

2. A. J. Chalk and A. S. Hay, *J. Polym. Sci. A-1*, in press.

3. W. J. Burlant and A. S. Hoffman, *Block and Graft Polymers*, Reinhold, New York, 1960.

4. R. J. Ceresa, *Block and Graft Copolymers*, Butterworths, Washington, 1962.

5. G. S. Kolesnikov and T. Han-ming, *Russ. Chem. Revs.*, **31**, 485 (1962).

6. G. Smets and R. Hart, *Fortschr. Hochpolymer. Forsch.*, **2**, 173 (1960).

7. N. G. Gaylord and F. S. Ang, in *Chemical Reactions of Polymers*, E. M. Fettes, Ed., Interscience, New York, 1964, p. 831.

8. D. Braun and I. Löflund, *Makromol. Chem.*, **53**, 219 (1962).

9. A. Dondos, *Bull. Soc. Chim. France*, **1963**, 2762.

10. G. Greber, *Makromol. Chem.*, **54**, 136 (1962).

11. P. Rempp, J. Golé, and G. Goutière, *Compt. Rend.*, **254**, 3867 (1962).

12. P. Rempp and A. Dondos, *Compt. Rend.*, **258**, 4045 (1964).

13. P. Rempp and A. Dondos, *Compt. Rend.*, **254**, 1426 (1962).

14. P. Rempp and A. Dondos, *Bull. Soc. Chim. France*, **1962**, 2313.

15. K. Shiina and Y. Minoura, *J. Polym. Sci. A-1*, **4**, 1069 (1966).

16. M. A. Yampol'skaya, O. Yu. Okhlobystin, S. L. Davydova, and N. A. Plate, *Vysokomol. Soedin.*, **8**, 771 (1966).

17. J. E. Sheridan, private communication.

18. H. L. Berger and A. R. Shultz, *J. Polym. Sci. A*, **3**, 4227 (1965).

19. Z. Grubisic, P. Rempp, and H. Benoit, *J. Polym. Sci. B*, **5**, 753 (1967).

20. M. J. R. Cantow, R. S. Porter, and J. F. Johnson, *J. Polym. Sci. A-1*, **5**, 987 (1967).

21. J. M. O'Reilly, private communication.

NOTES

Macrocyclic Neopentyl Adipate

Recently, several papers[1-3] have appeared in the literature on cyclic oligomers which are found in fiber-forming and film-forming condensation polymers. These oligomers, although present in small amounts, can affect product quality and lead to processing problems. This paper describes the isolation and characterization of an interesting cyclic oligomer from polyneopentyl adipate.

The oligomer was obtained by liquid–liquid extraction with hexane from a hydroxyl-terminated poly(neopentyl adipate) ester ($\overline{M}_n = 2000$), which was made by well known methods.[4] About 2% of colorless crystalline solid (recrystallized from alcohol) melting at 127–128°C was isolated. This oligomer was found to have a 22-membered ring structure:
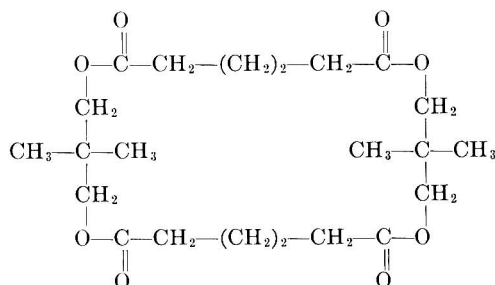
This was shown by the results of analyses and determinations of neutralization equivalent and molecular weight.

ANAL. Calcd: C, 61.66%; H, 8.47%; neutralization equivalent, 107; molecular weight, 428. Found: C, 61.59%; H, 8.58%; neutralization equivalent, 107; molecular weight (by vapor pressure osmometry in benzene), 435.

The NMR spectrum in CDCl$_3$ had singlets at 6.1 τ (R$_3$C—CH$_2$—O—), 9.0 τ

$$\text{(CH}_3\text{—}\overset{\overset{\displaystyle O}{\|}}{\text{C}}\text{—CH}_3\text{)}$$

and multiplets at 7.7 τ (—CH$_2$—CH$_2$—C), 8.3 τ (R—CH$_2$—CH$_2$—R) in the ratio 2:3:2:2 which agreed with the proposed structure. The infrared spectrum (Nujol) showed a strong, sharp peak at 1728 cm^{-1} and no hydroxyl peak in the 3300 cm^{-1} region.

According to Carothers and other workers,[5] the 11-membered ring would not be likely to form because of nonbonded interactions, although 11-membered cyclic esters can be made under special conditions.[6] Only the 22-membered macrocyclic ester was found in the polyester poly(neopentyl adipate). It is interesting to note that macrocyclic neopentyl adipate and neopentyl glycol have identical melting points and both sublime. This may explain why the cyclic ester has escaped detection in these polyesters.

References

1. I. Goodman and B. F. Nesbitt, *Polymer*, **1**, 384 (1960); *J. Polym. Sci.*, **48**, 423 (1960).
2. H. Zahn, J. Kunde, and G. Heidemann, *Makromol. Chem.*, **43**, 220 (1961).
3. R. Okada, T. Fukumura, and H. Tanzawa, *J. Polym. Sci. B*, **4**, 971 (1966).
4. J. B. Boylan, *Mod. Plastics*, **44**, No. 9, 143 (1967).

5. P. J. Flory, *Principles of Polymer Chemistry*, Cornell Univ. Press, Ithaca, N. Y., 1953, pp. 95–99.

6. W. J. Bailey and W. R. Sorenson, *J. Amer. Chem. Soc.*, **78**, 2287 (1956).

I. S. Megna
A. Koroscil

Rubber Chemicals Research Laboratory
American Cyanamid Company
Bound Brook, New Jersey 08805

Reinvestigation of the Reaction of Piperazine with Aldehydes

In our continuing investigations of the reaction of formaldehyde with nitrogen hetero-cycles and other active hydrogen-containing materials to produce thermosetting materials it was of interest to investigate piperazine.

The literature reveals few data concerning the products of the reaction of aldehydes with piperazine. Herz[1] reported that the reaction of piperazine with an excess of aqueous formaldehyde at 70°C gave a substance which analyzed for the structure $C_4H_{10}N_2 \cdot 2CH_2O$ and was insoluble in all solvents. Forsee and Pollard[2] and later Butler[3] reported that formaldehyde reacted with piperazine to give a material assumed to be polymethylene-piperazine based only on its elemental analysis. In addition, the later product was similar to the product obtained from methylene iodide and piperazine. More recently Burns and Moss[4] described the preparation of dimethylpiperazine by the hydrogenation of the intermediate, but not isolated, dimethylolpiperazine. Forsee and Pollard[2] also reported that acetaldehyde and n-butyraldehyde reacted with piperazine to give products of undetermined structure.

Reacting two or more moles of formaldehyde (37%) with one mole of piperazine at temperatures ranging from 15 to 85° gave a white solid which was readily soluble in water and had a molecular weight of 168. The NMR spectrum of this material was consistent with the 1,4-dimethylolpiperazine structure, as described in the Experimental Section of this report. The elemental analysis and infrared spectral data were also consistent with this structural assignment.

When equimolar amounts of piperazine and formaldehyde were reacted, poly-methylenepiperazine was obtained as described in Tables I and II. This polymer was insoluble in all solvents (DMF, DMSO, THF, etc.) except acids.

Under the same conditions, acetaldehyde was found to undergo a polycondensation reaction even in the presence of trace amounts of piperazine to give nitrogen-containing oligomers. Diethylamine gave similar results.[5]

Excess n-butyraldehyde in the presence of piperazine unexpectedly gave a 79% yield of the mono-N-1-butenylpiperazine and a mixture of 2-ethyl-2-hexenal with higher molecular weight products. These results suggest that N-piperazinyl-1-butanol was
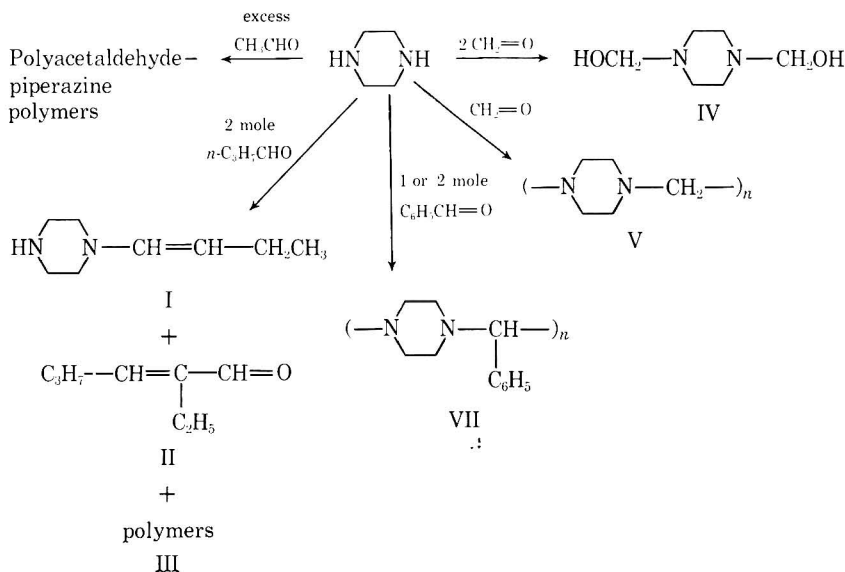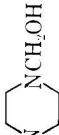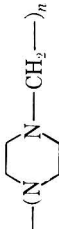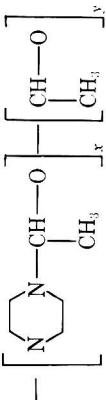
Scheme 1.
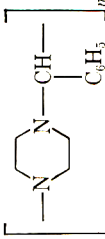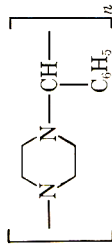
TABLE I
Reaction of Piperazine with Aldehydes

Expt no.	Piperazine, mole	Aldehyde Type	Aldehyde Amt, mole	Solvent Type	Solvent Amt, mole	Temp, °C	Product	Yield, %	Mp, °C
1	0.3	Formaldehyde (37%)	0.6	H₂O	5.83	15–20	HOCH₂N⌷NCH₂OH (IV)	66	360
2	0.3	"	0.6	H₂O	5.83	0	"	97	360
3	1.0	"	2.0	—		85	"	89	360
4	0.5	"	1.0	H₂O	9.72	0–10	"	88	360
5	0.5	"	0.5	Dioxane / H₂O	1.14 / 16.6	80–90	—(N⌷N—CH₂—)ₙ (V)	97	360
6	0.5	"	0.5	Dioxane / H₂O	1.14 / 16.6	10	"	78	360
7	0.6	"	0.6	H₂O	11.7	5–15	"	78	360
8	0.55	Acetaldehyde	3.0	THF	3.0	10–15	VI (polymer structure)	96	—

Product 1: HOCH_2N⌷NCH_2OH (IV)

Product 5: $-(\text{N}$⌷$\text{N}-\text{CH}_2-)_n$ (V)

Product 8: polymer VI
$$\left[\text{N}⌷\text{N}-\overset{\text{CH}_3}{\underset{}{\text{CH}}}-\text{O}\right]_x \left[\overset{}{\underset{\text{CH}_3}{\text{CH}}}-\text{O}\right]_y$$
VI

NOTES 1375

9	0.5	"	1.0	THF	14.0	0.5		66	—
10	2.0	n-Butyraldehyde	4.0	THF	3.1	−20	$C_2H_5CH=C(C_2H_5)—CH=O$ (I)	22ᵃ / 79ᶜ	83–85
11	0.05	+ alc. KOH (1N)	2.0		—	−20	$C_3H_7CH=C(C_2H_5)—CH=O$ (I)	100 (crude) / 61 (distilled)ᵈ	
12	0.3	Benzaldehyde	0.3	THF	3.0	−20	VII	95	218–220
13	0.1	"	0.2	THF	3.0	−20	VII	80	"

(Row 10 product / related structures)

HN⟨piperazine⟩$N—CH=CH—C_2H_5$ (III)

Higher boiling materials and polymers (II)

VII structures (rows 12, 13):

$\big[\,N\langle\text{piperazine}\rangle N—CH(C_6H_5)\,\big]_n$ VII

ᵃ Based on butyraldehyde reacted.
ᵇ Bp, 33–35°C/(0.4 mm); N_D 1.4560 (21°C.)
ᶜ Yield based on piperazine reacted.
ᵈ Bp, 33–34°C/(0.4 mm); N_D 1.4542 (18°C.)

probably an intermediate which dehydrated under the reaction conditions. Another example exists in the recorded literature which indicates that this type of reaction occurs with isobutyraldehyde to give di-n-isobutenylpiperazine under refluxing conditions.[6] The isolation of 2-ethyl-2-hexenal also suggests that some of the n-butyraldehyde undergoes a base catalyzed condensation to its aldol which subsequently dehydrates. The latter was also found to be true when potassium hydroxide was used in place of piperazine under the same experimental conditions[7] as described in Tables I and II.

Benzaldehyde (1–2 mole) reacted with 1 mole of piperazine at 0–10°C in THF to give polymers instead of the expected monomeric piperazinyl phenylcarbinols. These polymers were high-melting and were insoluble in all solvents except acids.[2]

The data of our investigation are briefly summarized in Scheme 1.

TABLE II

Elemental Analysis and Molecular Weights of the Reaction Products
of Piperazine With Aldehydes

Expt no.	Analysis						Molecular weight[a]
	Calcd			Found			
	C, %	H, %	N, %	C, %	H, %	N, %	
1	49.24	9.58	19.18	49.39	9.61	19.05	168
2	49.24	9.58	19.18	48.92	9.74	19.14	160
3	49.24	9.58	19.18	49.15	9.80	19.01	
4	49.24	9.58	19.18	49.13	9.80	19.00	
5	61.23	10.20	28.58	58.93	10.24	27.84	b
6	61.23	10.20	28.58	60.02	10.45	27.95	
7	61.23	10.20	28.58	59.47	10.62	27.85	
8				67.89	9.11	8.01	1025
9				65.75	10.89	17.63	450
10 (I)	76.20	11.12	—	75.65	11.11		—
10 (III)	68.58	11.42	20.00	68.40	11.36	19.75	140
11	76.20	11.12	—	75.95	11.11	—	—
12	75.80	8.10	16.10	75.45	8.50	15.67	b
13	75.80	8.10	16.10	75.66	8.03	16.00	b

[a] Determined at Galbraith Laboratories, Knoxville, Tenn., by vapor-pressure osmometry.

[b] These compounds were highly insoluble in all solvents (H_2O, THF, C_2H_5OH, C_6H_6, DMF) except acids.

The intrinsic viscosities for experiments 6, 12, and 13 in glacial acetic acid were 0.145, 0.093, 0.092 dl/g, respectively, determined at 30.0°C.

EXPERIMENTAL

General Procedure Followed for the Reaction of Piperazine with Aldehydes

The aldehydes and piperazine were obtained commercially and were not further purified.

To a resin kettle was added the aldehyde and brought to the appropriate temperature. Piperazine was slowly added, the temperature being kept within the desired range. After 16–24 hr, the contents were filtered and the filtrate concentrated under reduced pressure. Two typical procedures are described below. The more detailed data are given in Tables I and II.

The NMR spectra were recorded on a Varian Associates A60A or HA100 spectrometer, and the δ values are in parts per million against tetramethylsilane. The infrared spectra were recorded on a Perkin-Elmer Model 21 spectrophotometer.

1,4-Dimethylolpiperazine

As an example illustrating the general procedure, 49 g (0.5 mole) of 37% formaldehyde was added to a resin kettle. The pH was adjusted to 8.0–8.5 with 50% sodium hydroxide. The flask was cooled to 0–5°C, and 25.9 g (0.3 mole) of piperazine dissolved in 105 g water was slowly added, the temperature being kept at 15–20°C. The clear solution was stirred for 1 hr at 0–5°C and then kept at room temperature for 16 hr. On concentration of the clear solution under reduced pressure a white solid, soluble in water, was obtained in 66% yield. The melting point was 360°C. The analysis of the product is shown in Table II. The NMR spectrum in D_2O showed a singlet at 2.63 δ (157 cps) and another singlet at 4.16 δ (249 cps) in the ratio of 8:4. Some of the major infrared absorption bands are: 2.9 (—OH), 3.20 (—N—CH_2), 3.52, 8.70, 9.80, 10.10, and 12.52 μ.

Reaction of Piperazine with *n*-Butyraldehyde

To a flask with 288 g (4.0 mole) of *n*-butyraldehyde cooled to −20°C was slowly added a suspension of 172 g (2.0 mole) of piperazine in 300 ml of THF over a period of 1 hr. The reaction was exothermic, and the highest temperature reached in the flask was 35°C. The reaction mixture was stirred for an additional hour at 0°C, and then 200 ml of THF was added. The flask was then stirred at room temperature for 16 hr, filtered, washed, and dried. The solid product of *N*-1-butenylpiperazine (I) was obtained in 79% yield, mp 83–85°C. The analytical data are summarized in Table II.

The major infrared absorption bands (KBr disk) were at 3.4, 3.57, 6.05 (C=C),

8.65, and 10.08 μ.

NMR ($CDCl_3$) showed a triplet at 0.98 δ (—CH_3), multiplet at 1.98 δ (CH), mul-

tiplet at 2.98 δ (N—C—C—N—C—C), multiplet at 4.5 δ (=CH—CH_2), and a doublet

at 5.7 δ, 5.9 δ (—N—CH=).

This material appears to polymerize on standing in chloroform to give a red solution, as seen by the disappearance of the vinyl protons in the NMR.

The residue was vacuum-distilled to yield 2-ethyl-2-hexenal and a high boiling residue as described in Table I. The 2-ethyl-2-hexenal had an infrared spectrum identical to an authentic sample made by the reaction of *n*-butyraldehyde and potassium hydroxide (Table I). Some of the major infrared absorption bands were as follows: 3.37,

5.90 (C=O), 6.07 (C=C), 6.85, 9.25, 9.42, and 12.53 μ.

The NMR showed a multiplet at 0.95 δ (—CH_3), multiplet at 1.5 δ (CH_2), multiplet

at 2.25 δ (CH_2), triplet at 6.15 δ (—CH=), and singlet at 9.0 δ (—CH=O).

The analytical data are given in Table II. The elemental analysis was obtained by Dr. Stephen M. Nagy, 78 Oliver Rd., Belmont, Mass. The molecular weight determinations were carried out at Galbraith Laboratories, Knoxville, Tenn.

References

1. W. Herz, *Ber.*, **30**, 1587 (1897).
2. W. T. Forsee, Jr., and C. B. Pollard, *J. Amer. Chem. Soc.*, **57**, 2363 (1935).
3. G. B. Butler, *J. Amer. Chem. Soc.*, **78**, 482 (1956).

4. S. P. Burns and P. H. Moss, U. S. Pat. 3,249,613 (May 3, 1966).
5. W. Frankenburger and H. Hammerschmid, U. S. Pat. 2,190,184 (Feb. 13, 1940).
6. E. Benzing, *Angew. Chem.*, **71,** 521 (1959).
7. S. G. Powell and A. T. Nielsen, *J. Amer. Chem. Soc.*, **70,** 3627 (1948).

STANLEY R. SANDLER
MARIA L. DELGADO

Central Research Laboratory
Borden Inc., Chemical Division
Philadelphia, Pennsylvania 19124